

Fluturë Novakazi

Institut für Resistenzforschung und Stresstoleranz

Identification of QTL for
resistance against two fungal
pathogens, *Pyrenophora teres* f.
teres and *Bipolaris sorokiniana*,
in a barley (*Hordeum vulgare* L.)
diversity set



Dissertationen aus dem Julius Kühn-Institut

Kontakt | Contact:

Fluturë Novakazi
Beethovenstraße 24
18069 Rostock

Die Schriftenreihe „Dissertationen aus dem Julius Kühn-Institut“ veröffentlicht Doktorarbeiten, die in enger Zusammenarbeit mit Universitäten an Instituten des Julius Kühn-Instituts entstanden sind.

The publication series „Dissertationen aus dem Julius Kühn-Institut“ publishes doctoral dissertations originating from research doctorates and completed at the Julius Kühn-Institut (JKI) either in close collaboration with universities or as an outstanding independent work in the JKI research fields.

Der Vertrieb dieser Monographien erfolgt über den Buchhandel (Nachweis im Verzeichnis lieferbarer Bücher - VLB) und OPEN ACCESS unter:

https://www.openagrar.de/receive/openagrar_mods_00005667

The monographs are distributed through the book trade (listed in German Books in Print - VLB) and OPEN ACCESS here:

https://www.openagrar.de/receive/openagrar_mods_00005667

Wir unterstützen den offenen Zugang zu wissenschaftlichem Wissen.

Die Dissertationen aus dem Julius Kühn-Institut erscheinen daher OPEN ACCESS.

Alle Ausgaben stehen kostenfrei im Internet zur Verfügung:

http://www.julius-kuehn.de/Bereich_Veroeffentlichungen.

We advocate open access to scientific knowledge. Dissertations from the Julius Kühn-Institut are therefore published open access. All issues are available free of charge under

<http://www.julius-kuehn.de> (see Publications).

Bibliografische Information der Deutschen Nationalbibliothek

Die Deutsche Nationalbibliothek verzeichnet diese Publikation

In der Deutschen Nationalbibliografie: detaillierte bibliografische

Daten sind im Internet über <http://dnb.d-nb.de> abrufbar.

Bibliographic information published by the Deutsche Nationalbibliothek (German National Library)

The Deutsche Nationalbibliothek lists this publication in the Deutsche Nationalbibliografie; detailed bibliographic data are available in the Internet at <http://dnb.dnb.de>.

ISBN 978-3-95547-097-5

DOI 10.5073/dissjki.2020.006

Herausgeber | Editor

Julius Kühn-Institut, Bundesforschungsinstitut für Kulturpflanzen, Quedlinburg, Deutschland

Julius Kühn-Institut, Federal Research Centre for Cultivated Plants, Quedlinburg, Germany

© Der Autor/ Die Autorin 2020.

Dieses Werk wird unter den Bedingungen der Creative Commons Namensnennung 4.0 International Lizenz (CC BY 4.0) zur Verfügung gestellt (<https://creativecommons.org/licenses/by/4.0/deed.de>).



© The Author(s) 2020.

This work is distributed under the terms of the Creative Commons Attribution 4.0 International License (<https://creativecommons.org/licenses/by/4.0/deed.en>).

Institute of Agronomy and Plant Breeding I, Department of Plant Breeding,
Justus Liebig University, Giessen

and

Institute for Resistance Research and Stress Tolerance, Julius Kühn-Institute,
Federal Research Centre for Cultivated Plants, Quedlinburg

**Identification of QTL for resistance against two fungal pathogens,
Pyrenophora teres f. teres and *Bipolaris sorokiniana*,
in a barley (*Hordeum vulgare* L.) diversity set**

Inaugural Dissertation

for a Doctorate Degree in Agricultural Sciences

- Dr. agr -

In the Faculty Agricultural Sciences, Nutritional Sciences and
Environmental Management

Submitted by

Fluturë Novakazi

born in Prishtina, Kosovo

Giessen 2020

Approved by the Faculty Agricultural Sciences,
Nutritional Sciences and Environmental Management,
Justus Liebig University Giessen

Examining Committee:

First Reviewer: Prof. Dr. Rod Snowdon

Second Reviewer: Prof. Dr. Frank Ordon

Examiner: Prof. Dr. Matthias Frisch

Examiner: PD Dr. Annaliese Mason

Chair of the Examining Committee: Prof. Dr. Gesine Lühken

Date of Defence: May 11th, 2020

“So long, and thanks for all the fish.”

Douglas Adams

Contents

List of abbreviations	II
List of publications	V
1 Summary	1
2 Introduction	3
2.1 Barley	3
2.2 Net Blotch of Barley	7
2.3 Spot Blotch of Barley	12
2.4 Marker systems and genome-wide association studies	14
3 Aims	20
4 Genetic analysis of a worldwide barley collection for resistance to net form of net blotch disease (<i>Pyrenophora teres</i> f. <i>teres</i>)	21
5 Genome-wide association studies in a barley diversity set reveal a limited number of loci for resistance to spot blotch	40
6 Discussion	56
6.1 Candidate genes located in regions identified for net blotch resistance	56
6.2 Resistant accessions	66
References	71
Appendix	VII
Contributions to meetings and conferences	XLVI
Acknowledgement	XLVIII
Erklärung	XLIX

List of abbreviations

List of abbreviations

°C	degree Celsius
AFLP	amplified fragment length polymorphism
apaf	apoptotic protease-activating factor
<i>Avr</i> gene	avirulence gene
bp	base pairs
<i>Bs</i>	<i>Bipolaris sorokiniana</i>
<i>Btr1/2</i>	brittle rachis gene
CC-NBS-LRR/ CNL	coiled-coil nucleotide binding site LRR
DNA	deoxyribonucleic acid
<i>Eam8</i>	early maturity 8 gene
ET	ethylene
ETI	effector triggered immunity
GBS	genotyping-by-sequencing
GWAS	genome-wide association studies
h	hours
HC gene	high-confidence gene
HR	hypersensitive response
HSP	heat shock protein
IBSC	International Barley genome Sequencing Consortium
JA	jasmonic acid
K	kinship
LC gene	low-confidence gene
LD	linkage disequilibrium
LRR	leucine-rich repeat

List of abbreviations

MAGIC	multi-parent advanced generation inter-cross
MAMPs	microbe-associated molecular patterns
MAPK	mitogen-activated protein kinase
MAS	marker-assisted selection
<i>Mat-a</i>	Praematurum-a gene
Mbp	mega base pairs
<i>Mlo</i>	mildew resistance locus o
MTA	marker-trait association
NADPH	nicotinamide adenine dinucleotide phosphate
NAM	nested association mapping
NB	nucleotide-binding
NETS	necrotrophic effector-triggered susceptibility
NFNB	net form of net blotch
NGS	next generation sequencing
NO	nitric oxide
NPR1	non-expressor of pathogen-related
<i>nud</i>	nudum/ naked kernel gene
PAMPs	pathogen-associated molecular patterns
PCA	principle component analysis
PCD	programmed cell death
PCR	polymerase chain reaction
<i>Ppd-H1</i>	Photoperiod-H1 gene
PR proteins	pathogenesis-related proteins
PRR	pattern recognition receptors
PTI	pattern triggered immunity
<i>Ptm</i>	<i>Pyrenophora teres</i> f. <i>maculata</i>

List of abbreviations

<i>Ptt</i>	<i>Pyrenophora teres</i> f. <i>teres</i>
Q-matrix	population structure matrix
qPCR	quantitative PCR
QTL	quantitative trait locus
<i>R</i> gene	resistance gene
R protein	disease resistance protein
RAPD	randomly amplified polymorphic DNA
RFLP	restriction fragment length polymorphism
ROS	reactive oxygen species
RT-PCR	real time PCR
SA	salicylic acid
SAR	systemic acquired resistance
SFNB	spot form of net blotch
SNP	single nucleotide polymorphism
SSR	simple sequence repeats
TF	transcription factor
<i>thresh-1</i>	threshability gene
TIR-NBS-LRR/ TNL	toll interleukin receptor nucleotide binding site LRR
<i>Vrn</i>	vernalisation gene
<i>Vrs1</i>	six-rowed spike gene

List of publications

This thesis is based on the following peer-reviewed publications:

Novakazi F, Afanasenko O, Anisimova A, Platz GJ, Snowdon R, Kovaleva O, Zubkovich A, Ordon F, 2019. **Genetic analysis of a worldwide barley collection for resistance to net form of net blotch disease (*Pyrenophora teres* f. *teres*).** *Theoretical and Applied Genetics*, 132 (9): 2633-2650, <https://doi.org/10.1007/s00122-019-03378-1>.

Novakazi F, Afanasenko O, Lashina N, Platz GJ, Snowdon R, Loskutov I, Ordon F, 2019. **Genome-wide association studies in a barley (*Hordeum vulgare*) diversity set reveal a limited number of loci for resistance to spot blotch (*Bipolaris sorokiniana*).** *Plant Breeding*, 00: 1-15, <https://doi.org/10.1111/pbr.12792>.

List of publications

1 Summary

Barley is worldwide the fourth most important cereal crop and is cultivated in near desert to sub-arctic conditions. The majority of production, around 70 %, is used for animal feed, 20 % are used for malting and the rest for human consumption, with regional differences.

Pests and diseases constantly result in high yield losses. Two worldwide important fungal foliar diseases of barley are *Pyrenophora teres* f. *teres* (*Ptt*) and *Bipolaris sorokiniana* (*Bs*), the causal agents of net blotch and spot blotch, respectively. Yield losses are on average around 40 % and can amount to over 70 % in years with epidemics. Both pathogens are highly variable and the occurrence of new pathogenic strains demands for breeding of resistant cultivars.

In order to identify new resistance sources, a diverse barley set comprising 449 accessions originating from over 50 different regions all over the world, expressing different levels of resistance against both pathogens, was screened. Seedling resistance was tested under controlled greenhouse conditions with three isolates of each pathogen. Adult plant resistance was tested in field trials at three and two locations for *Ptt* and *Bs*, respectively. Phenotypic results showed a wide range of the level of resistance and significant differences between accessions were observed in all trials. The set was genotyped using the Illumina iSelect 50k barley SNP chip. After filtering for quality control parameters, i.e. failure rates < 10%, heterozygous calls < 12.5% and minor allele frequency > 5%, 33,318 polymorphic, mapped SNPs were left for further genome-wide association studies (GWAS). Markers were mapped against the barley reference sequence. GWAS was conducted using a compressed mixed linear model (CMLM) including population structure and kinship matrix. GWAS for *Ptt* revealed 254 significant marker-trait associations (MTAs) located on chromosomes 3H, 4H, 5H, 6H, and 7H and corresponding to 15 quantitative trait loci (QTL). Four of these loci are putatively new and were not previously described. In nine out of the 15 regions, 63 high-confidence genes that are directly involved in pathogen defence are located and represent putative candidate genes. GWAS for *Bs* revealed 38 significant MTAs corresponding to two major QTL on chromosomes 1H and 7H and a putative new minor QTL on chromosome 7H. In the major QTL regions, 10 and 14 high-confidence genes were identified, respectively. Based on haplotypes and phenotypic reactions it was possible to identify accessions with enhanced resistance against *Ptt* and *Bs*.

Summary

2 Introduction

2.1 Barley

Cereal crops are grown all over the world and are the main sources for calorie and protein intake in human diets (McKevith 2004). The most important cereals are wheat (*Triticum aestivum* L.), maize (*Zea mays* L.), rice (*Oryza sativa* L.), and barley (*Hordeum vulgare* L.), with annual global productions of 771 million tons, 1.1 billion tons, 769 million tons and 147 million tons, respectively (FAOSTAT 2019). In 2017, barley was cultivated on 47 million hectares. The largest producer of barley is the Russian Federation, with a barley acreage of 7.8 million hectares and 20 million tons of produced barley. The second largest producer is Australia with 13.5 million tons, followed by Germany and France with roughly 10 million tons of barley produced in 2017 (FAOSTAT 2019). While production quantity in the Russian Federation, Germany and France has remained steady over the years, production in Australia has almost doubled since 2010, from 7.6 to 13.5 million tons (FAOSTAT 2019). Even though, whole-grain barley has higher contents of beta-glucans, calcium, iron and zinc compared to whole-grain wheat, and might therefore be considered healthier, its use in human diet plays only a minor role (Langridge 2018; Zhou 2009). The majority of barley production is used as animal feed and about 20 % are used for malting (Langridge 2018).

Barley is a diploid, inbreeding species of the *Poaceae* family with a genome size of 5.1 Gb and $2n=14$ chromosomes (IBSC 2012). In 2006 the International Barley Genome Sequencing Consortium (IBSC) was founded with the goal to develop a reference sequence for the barley genome, which at that time seemed like a mammoth task considering the relatively large genome size and the high number in repetitive elements (Stein and Mascher 2018). Nonetheless, in 2012 a first partly ordered version was released and in 2017 a comprehensively ordered reference sequence was published (IBSC 2012; Mascher et al. 2017).

The oldest remains of cultivated barley (*Hordeum vulgare* subsp. *vulgare*) were discovered in the Fertile Crescent, today's Iran, Iraq, Israel, Jordan, Lebanon, Syria and Turkey, and date back to over 10,000 years ago (von Bothmer et al. 2003). Since then, barley cultivation spread from near-desert areas (Langridge 2018) to areas with sub-arctic conditions (Hilmarsson et al. 2017). Cultivated barley belongs

Introduction

to the genus *Hordeum*, which comprises 33 grass species (Blattner 2018). The wild progenitor of cultivated barley is *Hordeum vulgare* subsp. *spontaneum* and originated from South-West Asia (Blattner 2018). Wild barley belongs to the primary gene pool and is easily crossed with cultivated barley. Bulbous barley (*Hordeum bulbosum*), the closest relative, belongs to the secondary gene pool and crosses with cultivated barley usually lead to offspring with low fertility (Blattner 2018). However, the production of double haploid plants employing the *Hordeum bulbosum* method is a reliable technique for generating fertile double-haploid plants (Devaux 2003). All other species belong to the tertiary gene pool and crosses lead to sterile hybrids (Blattner 2018).

Hordeum vulgare and *Hordeum spontaneum* share several morphological traits, however, the difference in their phenotype is the non-brittle rachis. In wild barley, when seeds are mature the spike gets fragile, in order for seeds to be dispersed more easily. In cultivated barley, mutations occurred which lead to a non-brittle rachis and enabled early farmers to harvest the grain more comfortably. This phenotype is the result of two independent mutations of two tightly linked genes on chromosome 3H, namely *Non-brittle rachis 1 (btr1)* and *Non-brittle rachis 2 (btr2)*. The genotype for a non-brittle rachis is either *Btr1/btr2* or *btr1/Btr2* and is only found in cultivated barleys. In wild barley the wild allele of both genes is necessary for a brittle rachis (Pourkheirandish et al. 2015). Since these two mutations arose independently from each other, it is believed that barley was domesticated twice, first in the southern Levant (Syria) where the *btr1* mutation occurred, and later in the northern Levant, where the *btr2* mutation occurred (Pourkheirandish et al. 2015). Qingke barley, a six-rowed naked barley, has been cultivated for over 3,500 years in Tibet and for a long time this area was discussed as another domestication site, based on findings of six-rowed wild barleys (*Hordeum agriocrithon*) and barleys with intermediate phenotypes between *Hordeum spontaneum* and qingke. However, recently 437 Tibetan accessions were analysed and compared to a global barley set based on three major domestication genes (brittleness, row type and hullless/ naked grain). It was shown that qingke barley most probably was derived from the Fertile Crescent and introduced into Tibet through India and Nepal around 4,500 to 3,500 years ago, clearly rejecting the hypothesis of Tibet as a centre of domestication (Zeng et al. 2018).

Introduction

Another distinct feature of cultivated barley is the row type, which can be distinguished into two- and six-rowed forms. Wild barley shows the two-rowed phenotype, with one central spikelet at each rachis node and two rudimentary, lateral spikelets. Through a loss of function mutation at the *Six-rowed spike 1* (*Vrs1*) locus on chromosome 2H, the two lateral spikelets are transformed into fertile spikelets (Komatsuda et al. 2007). Komatsuda et al. (2007) were able to clone the *Vrs1* gene and showed that it encodes for a homeodomain-leucine zipper motif, which is only expressed in the lateral spikelets and suppresses the development of these. This gene shows multiple alleles and is considered to have arisen independently at several mutation events (Haas et al. 2019; Komatsuda et al. 2007). Another gene controlling row-type is the INTERMEDIUM-C gene located on chromosome 4H (Ramsay et al. 2011). This gene interacts with *Vrs1* and influences spikelet fertility. Two-rowed barley have the *Vrs1.b/int-c.b* and six-rowed the *vrs1.a/int-c.a* genotype (Haas et al. 2019; Ramsay et al. 2011).

Barley in general has hulled seeds, which are preferred in the malting industry as they serve as seed protection and filtration medium, but are not desired in human consumption. Hence, a mutation that appeared around 8,000 years ago and led to hullless or naked barley was preferred for human consumption. The strong adhesion of the hull to the seed is based on a sticky substance that is expressed in hulled barleys only in the caryopsis about two weeks after flowering (Taketa et al. 2008). The underlying gene is located on the long arm of chromosome 7H and referred to as *Nud* (nudum – naked) (Taketa et al. 2008). This gene codes for an ethylene response factor, which interacts with a lipid biosynthesis pathway and leads to adhesion of the hull to the caryopsis. Taketa et al. (2008) showed that in all naked barleys they studied a 17-kb deletion is present at the *nud* locus and proposed the trait to be of monophyletic origin. A further gene named *thresh-1* was fine-mapped by Schmalenbach et al. (2011) to the long arm of chromosome 1H located between BOPA markers 1_0433 and 2_0959, which are located at 508,780,593 bp and 533,223,592 bp on the physical map of barley, respectively (Bayer et al. 2017). The *thresh-1* gene influences the separation of the awn and rachis from the grain and facilitates threshing (Haas et al. 2019).

One of the reasons for barley's successful migration to higher altitudes and latitudes is the adaptation to a range of day lengths and the absence of vernalisation requirement. These traits are based on a number of well-characterized genes. One major flowering gene controlled by photoperiod is

Introduction

Photoperiod-H1 (*Ppd-H1*), which encodes for *PSEUDO-RESPONSE REGULATOR 7* and is located on chromosome 2H (Turner et al. 2005). The wild-type allele (*Ppd-H1*), that is present in winter and wild barley, shows a strong response to long days for inducing flowering. Through a recessive mutation, the response to photoperiod is reduced and flowering in barleys with the mutated *ppd-H1* gene is delayed under long days. This is particularly useful in regions with long growing seasons as found in Western Europe and North America, since it enables spring-sown barleys to prolong the vegetative growth phase in order to accumulate more biomass, which in return benefits yields (Turner et al. 2005).

In order to induce flowering, wild and winter barley require a cold period extending over several weeks, i.e. vernalisation. Flowering in this case is regulated by the interaction of three vernalisation genes, namely *Vrn-H1*, *Vrn-H2* and *Vrn-H3* (*HvFT*), located on chromosomes 5H, 4H and 7H, respectively (von Zitzewitz et al. 2005; Yan et al. 2006). *Vrn-H1* induces the transmission from the vegetative growth phase to the reproductive growth phase by inducing flowering. Vernalisation upregulates *Vrn-H1*, which subsequently upregulates *Vrn-H3*. Without vernalisation, *Vrn-H1* is repressed by *Vrn-H2*, which on the other hand is downregulated by vernalisation (von Zitzewitz et al. 2005; Yan et al. 2006; Yan et al. 2004). The spring growth habit of barley can be explained by the deletion of an intron in *HvBM5A* and the complete deletion of *ZCCT-H*, the candidate genes of *Vrn-H1* and *Vrn-H2*, respectively. In facultative barley only the deletion of *Vrn-H2* is present (von Zitzewitz et al. 2005). *Vrn-H3* is an orthologue of the *FLOWERING LOCUS T* in *Arabidopsis thaliana* (Yan et al. 2006). It is influenced by vernalisation and photoperiod, i.e. the expression is upregulated under long days. The dominant (*Vrn-H3*) and recessive (*vrn-H3*) alleles lead to early and late flowering, respectively (Yan et al. 2006). The interaction of the vernalisation genes (*Vrn-H1* and *Vrn-H2*) results in the differentiation into winter and spring growth habit. The interplay of the vernalisation and photoperiod sensitive genes (*Ppd-H1* and *Vrn-H3*) determines when an individual will flower.

In regions like Scandinavia, it is important that plants reach maturity within the short growing season; one prerequisite for this is early flowering. In 1961 the first cultivar (Mari) with early maturity was released (Zakhrabekova et al. 2012). Mari had an X-ray induced mutation at the *Praematurum-a* (*Mat-a*), also called *early maturity 8* (*eam8*), locus (Faure et al. 2012; Zakhrabekova et al. 2012). *Mat-a* is an orthologue of the *EARLY FLOWERING 3* gene in *Arabidopsis thaliana* and insensitive to

photoperiod, thus enabling plants to flower early in long as well as short days (Faure et al. 2012; Zakhrabekova et al. 2012). Zakhrabekova et al. (2012) identified more than 20 *mat-a* alleles, which result in a disturbed flowering pathway due to deletions, nonsense mutations, splice-site mutations or point mutations. They were able to map the *mat-a* locus to the long arm of chromosome 1H between markers 1_0590 and 3_1081 located between 555 to 558 Mbp on the physical map (Bayer et al. 2017; Zakhrabekova et al. 2012).

Traits like the above-mentioned enabled early farmers to select for individuals that were most suitable for cultivation and to expand the barley growing area. Since then barley was constantly improved by selection and breeding efforts. Nonetheless, it remains an on-going task, since cultivation and yield are threatened by abiotic stresses like temperature, drought, soil acidity and salinity, or nutrient deficiency, as well as biotic stresses, like insect pests, viruses and pathogenic fungi (Elmore et al. 2018; Saade et al. 2018).

2.2 Net Blotch of Barley

Net blotch is one of the most important foliar disease in barley (Mathre 1997). The underlying pathogen is the ascomycete *Pyrenophora teres* Drechsler, which exists in two forms, namely *Pyrenophora teres* f. *teres* (*Ptt*) and *Pyrenophora teres* f. *maculata* (*Ptm*). *Ptt* induces the net form of net blotch (NFNB), after which the disease was named, *Ptm* induces the spot form of net blotch (SFNB) (Smedegård-Petersen 1971). Symptoms appear on the leaves, leaf sheaths, stems, and seeds. Infections

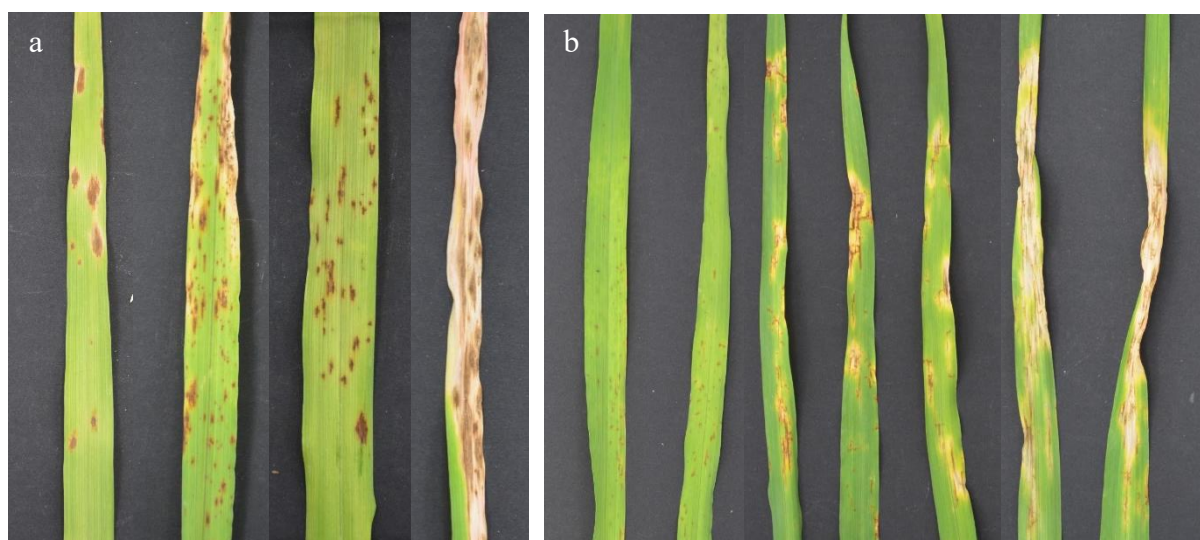


Figure 2.1 Symptoms on barley leaves after infection with a) *Pyrenophora teres* f. *maculata* and b) *Pyrenophora teres* f. *teres*.

Introduction

with *Ptm* lead to dark brown elliptical, necrotic lesions surrounded by chloroses (Smedegård-Petersen 1971) (Fig. 2.1a). Initially, *Ptt* symptoms are small spots that grow into dark brown lesions with longitudinal and transverse streaks, resulting in a net-like pattern (Fig. 2.1b). The affected tissue is surrounded by a chlorotic area (Mathre 1997; Smedegård-Petersen 1971). The anamorph *Drechslera teres* (Sacc.) Shoemaker produces light brown conidiophores that are found in groups of up to three (Fig. 2.2a). The conidia have a straight cylindrical form with round ends, 1-10 pseudosepta and are hyaline to light yellow-brown in colour (Mathre 1997; Smedegård-Petersen 1971) (Fig. 2.2b). If two opposite, compatible mating types are present, the teleomorph *Pyrenophora teres* Drechsler produces dark brown globose pseudothecia, which contain asci. The light brown asci are bitunicate with a hyaline

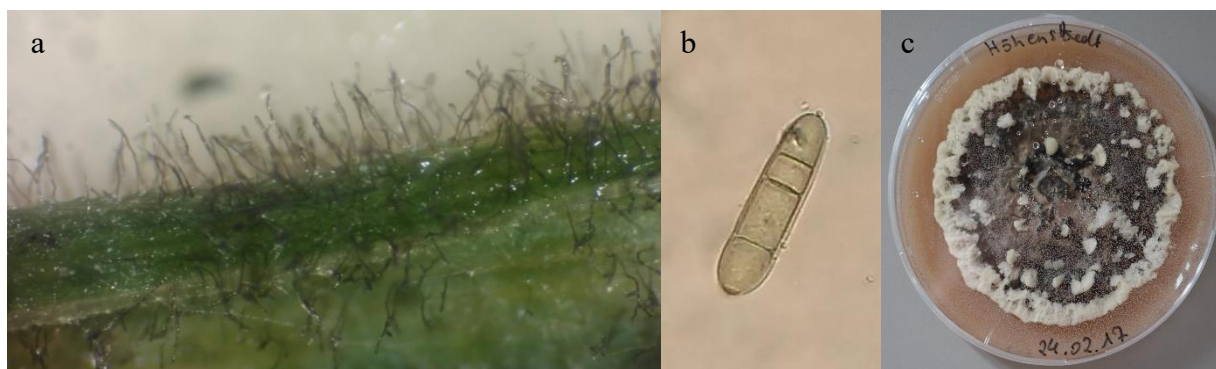


Figure 2.2 a) Conidiophores with conidia on infected barley leaf and b) single conidium of *Pyrenophora teres* f. *teres* the causal agent of net form of net blotch. c) Characteristic mycelial fan-like structures of *Pyrenophora teres* f. *teres* in culture on V8-medium.

wall and club-shaped with up to eight ascospores. Ascospores are ellipsoidal with round ends with one longitudinal and three transverse septa (Mathre 1997; McLean et al. 2009; Smedegård-Petersen 1971). In culture, isolates may show high variation with respect to mycelium structure and formation, colour, and sporulation ability. However, Smedegård-Petersen (1971) observed that most *Ptt* and *Ptm* isolates produce fan-like mycelial tufts (Fig. 2.2c). He also stated that the ability to produce these structures is often lost after several cycles of mycelial transfer in culture without re-isolation from fresh plant tissue. Based solely on morphological features, it is not possible to distinguish the two forms (Lightfoot and Able 2010; Smedegård-Petersen 1971). However, reliable polymerase chain reaction (PCR) assays have been developed in order to distinguish *Ptt* and *Ptm* from each another on the molecular level (Leisova et al. 2005; Williams et al. 2001).

Introduction

P. teres prefers temperate and humid conditions. Temperatures between 10 and 15°C are optimal for primary infections. Conidia develop at temperatures between 15 to 25°C and sufficient humidity, where the optimal temperature is 20°C. Nonetheless, this fungal pathogen may also occur in regions outside this temperature range and is, therefore, prevalent in barley-growing regions all over the world (Mathre 1997; Obst and Gehring 2002).

P. teres overwinters as pseudothecia on plant debris that is left on fields after harvest or as mycelium on seeds (Fig. 2.3). In spring when ascospores are mature, they are actively released from asci and dispersed by wind onto young barley plants. Conidia overwintering on plant residue can also serve as primary inoculum (Liu et al. 2011). Ascospores and conidia germinate within 6 h and hyphae grow on the leaf surface before forming appressoria (24 h), which are at least five epidermal cells apart from the spore (Lightfoot and Able 2010). *Ptt* rarely penetrates directly into epidermal cells, but rather between epidermal cells. The fungus then continues growing under the epidermis and in the mesophyll. In susceptible genotypes, the first symptoms appear after 72 h (Lightfoot and Able 2010; Sarpeleh et al. 2007). By this time, cells in contact with fungal hyphae become necrotic. After 120 h also cells not directly in contact with the fungus show necroses surrounded by chloroses (Lightfoot and Able 2010). The hyphae thicken and eventually disrupt the leaf tissue. By 168 h new conidiophores carrying conidia can be observed on the leaf surface (Lightfoot and Able 2010). These conidia are dispersed by rain and carried up the canopy to younger leaves where they serve as secondary inoculum (Fig. 2.3). As long as conditions are favourable new infection cycles occur (Deadman and Cooke 1989). Lightfoot and Able (2010) showed that *Ptt* and *Ptm* grow differently *in planta*. In contrast to *Ptt*, hyphae of *Ptm* grow less before forming an appressorium and penetrate directly into epidermis cells. They also showed that *Ptm* only induced necroses in cells directly adjoin to fungal hyphae in contrast to *Ptt* (Keon and Hargreaves 1983; Lightfoot and Able 2010). *Ptt* grows mainly necrotrophic, whereas *Ptm* shows a prolonged biotrophic growth before transitioning to necrotrophic growth (Lightfoot and Able 2010). The authors concluded differences in *in planta* growth and lifestyle between the two forms to be the reason for the different symptom development. Additionally, it was shown that *Ptt* and *Ptm* produce several toxins that act as virulence factors and induce chlorosis and necrosis. These toxins are L,L-N-(2-amino-2carboxyethyl) aspartic acid (toxin A), anhydroaspergillomarasmine A (toxin B) and

Introduction

aspergillomarasmine A (toxin C) (Friis et al. 1991; Liu et al. 2011; Sarpeleh et al. 2007; Smedegård-Petersen 1977; Weiergang et al. 2002).

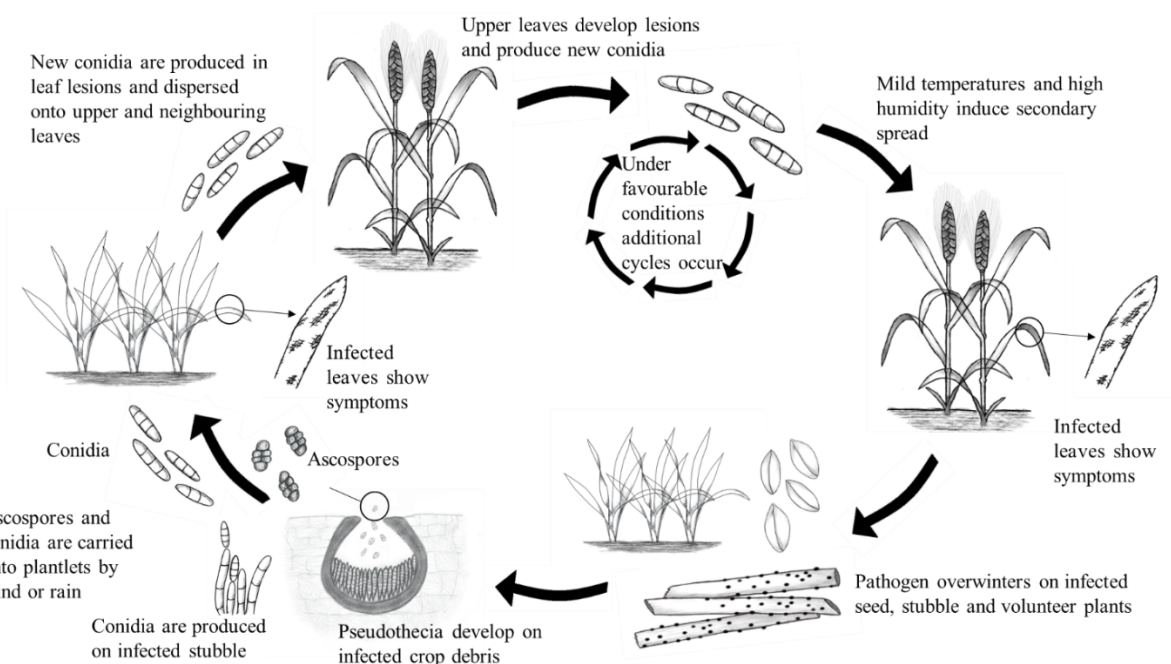


Figure 2.3 Life cycle of *Pyrenophora teres f. teres* according to Liu et al. 2011. Illustration by Fluturë Novakazi.

The ability to reproduce sexually leads to a high variability within *Pyrenophora teres* populations. The occurrence of physiological races or pathotypes was first described in 1969 (Khan and Boyd 1969). Since then, many studies on pathotype diversity and the genetic structure of the pathogen have been conducted (Arabi et al. 2003; Brandl and Hoffmann 1991; Fowler et al. 2017; Jonsson et al. 1997; Rau et al. 2003; Robinson and Jalli 1996; Statkevičiūtė et al. 2010; Stefansson et al. 2012; Steffenson and Webster 1992a; Tekauz 1990; Tuohy et al. 2006; Wu et al. 2003). Identification of major qualitative resistance genes is a difficult task due to the high pathogenic variation. So far, only a few major resistance genes against *Ptt* have been identified. *Rpt3d* on chromosome 2H (Bockelman et al. 1977), *Rpt1a*, *Rpt1b* (Bockelman et al. 1977) and *Pt_{1,a}* on chromosome 3H (Graner et al. 1996), *Rpt2c* on chromosome 5H (Bockelman et al. 1977), and *Rpt5* (Manninen et al. 2006) and *rpt.r/rpt.k* on chromosome 6H (Abu Qamar et al. 2008). Barley chromosome 6H was identified in many studies for harbouring several major resistance genes. Two of these genes have recently been fine-mapped. Liu et al. (2015) were able to map the sensitivity locus *SPN1* to chromosome 6H at 47,261,684 to 91,140,417 bp. This region was also identified employing genome-wide association studies by

Introduction

Amezrou et al. (2018), Novakazi et al. (2019a), Richards et al. (2017), Vatter et al. (2017), and Wonneberger et al. (2017a). Many studies identified resistance loci located close to the resistance gene *rpt.r/rpt.k* initially identified by Abu Qamar et al. (2008) (Amezrou et al. 2018; Islamovic et al. 2017; Koladia et al. 2017; Martin et al. 2018; Novakazi et al. 2019a; Richards et al. 2017; Vatter et al. 2017; Wonneberger et al. 2017a) and which was fine-mapped by Richards et al. (2016). They located it on chromosome 6H at 370,429,069 to 384,412,678 bp and renamed it *Spt1* (susceptibility to *P. teres* f. *teres*).

Quantitative resistance in barley against *Ptt* was described by Steffenson and Webster (1992b) and quantitative trait loci (QTL) for resistance have been identified on all seven barley chromosomes (Afanasenko et al. 2015; Berger et al. 2013; Cakir et al. 2011; Cakir et al. 2003; Graner et al. 1996; Grewal et al. 2008; Grewal et al. 2012; Koladia et al. 2017; König et al. 2013; König et al. 2014; Ma et al. 2004; Manninen et al. 2006; O'Boyle et al. 2014; Raman et al. 2003; Richards et al. 2017; Richter et al. 1998; Steffenson et al. 1996; Wonneberger et al. 2017a; Wonneberger et al. 2017b).

Yield losses due to *Ptt* are reported to be between 10 and 45%, with losses of up to 70% in years with severe infection pressures (Afonin et al. 2008; Mathre 1997; Murray and Brennan 2010; Wallwork et al. 2016). Yield losses are the result of a reduced photosynthesis rate due to necrotic leaf tissue, leading to a reduced 1,000-kernel weight, reduced number of seeds and ears, reduced kernel size and to loss of seed quality (Burleigh et al. 1988). The latter is of high importance for the malting industry (Mathre 1997). Control of *Ptt* can be achieved with fungicides as foliar applications or as seed coatings (Liu et al. 2011). However, since the use of fungicides is not always desirable or economic and resistances have been reported (Sierotzki et al. 2007), their use should preferably be limited. Agricultural control measurements involve implementation of extended and diversified crop rotations, ploughing under of left-behind crop debris and volunteer barley, and the use of healthy and pathogen-free seeds (Liu et al. 2011). Resistant cultivars are the best mean to control infection and subsequent yield loss. Nonetheless, the high variability of *Ptt* and its high number of pathotypes makes the breeding of cultivars with broad resistances a difficult task.

2.3 Spot Blotch of Barley

The ascomycete *Bipolaris sorokiniana* (Sacc.) Shoem. (teleomorph: *Cochliobolus sativus* (Ito & Kurib.) Drechs. ex Dastur) is a hemi-biotrophic fungal plant pathogen. It can be found in cereal growing regions worldwide, but prefers warm and humid conditions (Gupta et al. 2018). Over 100 grass species are described as possible hosts for *B. sorokiniana* (Sprague 1950), including crops like bread and durum wheat, barley, triticale, rye, maize, rice, pearl and fox millet (Acharya et al. 2011; Gupta et al. 2018; Kumar et al. 2002). *B. sorokiniana* is seed and stubble-borne and causes a number of diseases like common root rot, seedling blight, black point and spot blotch (Kumar et al. 2002; Manamgoda et al. 2014). In barley production the foliar disease referred to as spot blotch, is economically the most important one. The symptoms start as small chocolate-coloured necrotic lesions surrounded by chlorotic halos. In susceptible reactions, the spots



Figure 2.4 Symptoms on Barley leaves after infection with *Bipolaris sorokiniana*, the causal agent of spot blotch

grow into bigger blotches that eventually coalesce and cover large proportions of the leaf area (Fig. 2.4) (Acharya et al. 2011). The symptoms can easily be confounded with the spot form of net blotch (*Pyrenophora teres* f. *maculata*) (Mathre 1997). However, the two pathogens can easily be distinguished based on morphological features. The brown to olive-brown conidiophores of *B. sorokiniana* grow out of the stoma or wounds. They are erect, unbranched, septate, and grow in groups of up to three (Acharya et al. 2011; Manamgoda et al. 2014; Sprague 1950). The fusiform conidia are dark brown, straight or boomerang-shaped with a smooth surface and three to twelve pseudosepta (Acharya et al. 2011; Gupta et al. 2018; Manamgoda et al. 2014; Sprague 1950). A special characteristic is that conidia germinate bipolar, i.e. from both ends, thus, inspiring the genus name *Bipolaris* (Kumar et al. 2002; Manamgoda et al. 2014). The bitunicate asci are cylindrical, straight or slightly curved and contain up to eight ascospores. The hyaline ascospores have a fili- or flagelli-form shape and 6-14 septa (Manamgoda et al. 2014).

Introduction

The fungus overwinters as mycelium in soil or as conidia on seeds, crop debris or volunteer plants (Fig. 2.5). When temperatures increase, the conidia germinate and infect young seedlings. The fungus affects the leaves and roots, which may lead to the death of the seedlings. New conidia are produced on infected plant tissue and dispersed by wind and rain, thereby serving as secondary inoculum (Fig. 2.5). This way, several infection cycles can be produced during one growing season and increase the potential for epidemics (Acharya et al. 2011). Temperatures between 20 to 25°C promote foliar spot blotch symptoms, however, the higher the temperature the higher the damage will be. The highest yield losses are to be expected when infection appears on the flag leaf or during anthesis (Nutter et al. 1985).

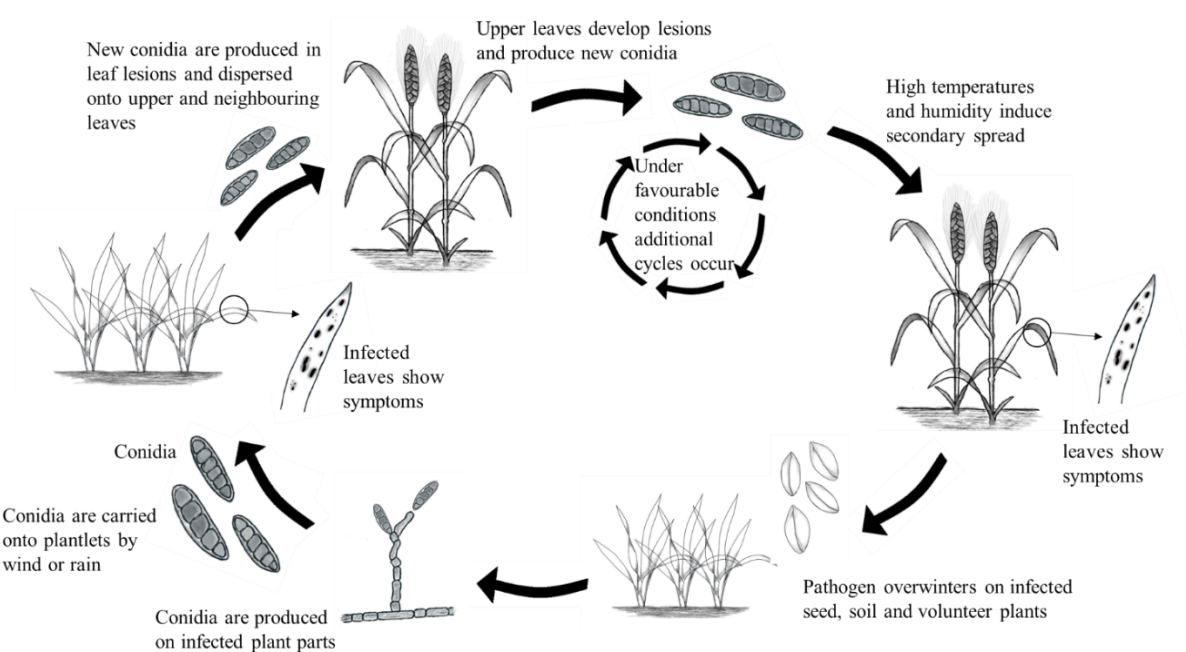


Figure 2.5 Life cycle of *Bipolaris sorokiniana* according to Acharya et al. 2011. Illustration by Fluturë Novakazi.

Even though the sexual stage (*Cochliobolus sativus*) plays no important role in the infection cycle, it can develop on dead plant material or in culture (Hrushovetz 1956; Shoemaker 1955) and two opposite mating types (*A* and *a*) do exist (Tinline 1951), leading to comparably high variability in *B. sorokiniana* populations (Gupta et al. 2018). Valjavec-Gratian and Steffenson (1997) were the first to classify pathotypes and many other studies with isolates from all over the world have followed since (Arabi and Jawhar 2002; Arabi and Jawhar 2004; Ghazvini and Tekauz 2007; Leng et al. 2016; Meldrum et al. 2004).

Introduction

B. sorokiniana produces sesquiterpenes, which act as phytotoxins and virulence factors. Prehelminthosporol was proposed to be predominantly produced (Åkesson and Jansson 1996; Carlson et al. 1991). The toxin was shown to be non-host-specific and cause lesions resembling fungal infection (Åkesson and Jansson 1996). It disrupts the cell membranes leading to leakage (Olbe et al. 1995) and may be involved in dissolving the wax layer of leaves (Åkesson and Jansson 1996). Apoga et al. (2002) demonstrated a positive correlation between the virulence of isolates and the amount of toxins produced. Another phytotoxic metabolite, sorokinianin, was shown to inhibit seed germination (Nakajima et al. 1994). Recently, a host-specific necrotrophic effector, ToxA, was reported to be metabolised by *B. sorokiniana* isolates in Australia and the U.S. (Friesen et al. 2018; McDonald et al. 2018). This proteinaceous toxin is also produced by *Pyrenophora tritici-repentis* and *Parastagonospora nodorum* strains and is known to induce disease like symptoms on wheat (Friesen et al. 2006b; Tuori et al. 1995).

Major and minor QTL for resistance against *B. sorokiniana* have been identified across the barley genome on all seven chromosomes (Berger et al. 2013; Bilgic et al. 2005; Bilgic et al. 2006; Bovill et al. 2010; Bykova et al. 2017; Grewal et al. 2012; Gutiérrez et al. 2015; Gyawali et al. 2018; Haas et al. 2016; Novakazi et al. 2019b; Roy et al. 2010; Steffenson et al. 1996; Wang et al. 2017; Yun et al. 2006; Yun et al. 2005; Zhou and Steffenson 2013). To date three major genes for resistance have been mapped. *Rcs 5* on chromosome 7H (Drader et al. 2009; Steffenson et al. 1996), *Rcs 6/ Scs 6* on chromosome 1H between 63,571 and 192,067 bp (Bilgic et al. 2005; Leng et al. 2018), and *Rbs 7* on chromosome 6H between 13,136,710 and 13,370,566 bp (Wang et al. 2017; Wang et al. 2019).

The identification of resistant cultivars and accessions is an on-going and difficult task, but represent the most effective and sound measure to control the disease. Yield losses are mainly the result of reduction of 1,000 kernel weight, number of kernels per ear and kernel size, which also leads to a decrease in malting quality (Agostinetto et al. 2015; Nutter et al. 1985). Reported yield losses range between 30 and 70 % (Agostinetto et al. 2015; Bengyella et al. 2018; Karov et al. 2009), with the possibility for epidemics every few years (Lashina and Afanasenko 2019).

2.4 Marker systems and genome-wide association studies

The identification and mapping of genes requires phenotypic variation. For a long time, these phenotypic variations were limited to morphological markers that were easily observable, like the

Introduction

colour of seeds and flowers, plant height or blood type in humans. The development of molecular markers enables the identification of markers for phenotype variations on the DNA level. Today, several marker systems exist, which have different advantages and disadvantages depending on the performed analysis and crop investigated.

Restriction Fragment Length Polymorphism (RFLP) markers detect variations in restriction sites between individuals that occurred through point mutations, deletions or insertions. The DNA is digested with restriction endonucleases and the DNA-fragments are sorted according to their length by gel electrophoresis. The DNA fragments are then transferred to a membrane (nitrocellulose or nylon) and the membrane is exposed to labelled DNA probes, which hybridize with complementary DNA fragments (Beckmann and Soller 1983). RFLPs are co-dominant, can be used for gene mapping, QTL analysis and genetic fingerprinting. Nevertheless, they have considerable disadvantages, i.e. a large amount of DNA is required, the information content is only low to medium, and it is a quite laborious approach (Beckmann and Soller 1983). Randomly Amplified Polymorphic DNA (RAPD) markers are a fast, simple and cheap alternative. Several arbitrary, short primers (8-12 nucleotides) are used to amplify random DNA segments using PCR. Sequence knowledge is not necessary and a small amount of DNA is sufficient. The big drawback of RAPD markers is the bad reproducibility (Waugh and Power 1992). Amplified Fragment Length Polymorphism (AFLP) markers detect variations in the restriction site of DNA sequences. The DNA is digested with restriction endonucleases, adapters are ligated to the sticky end of the restriction fragments and a subset of fragments is amplified with primers complementary to the adapter sequence using PCR. AFLP require no prior sequence knowledge and are suitable for every species. Only a small amount of DNA is needed, while offering high information content and high reproducibility. The drawbacks, however, are the many enzymatic steps necessary and the laborious protocol and evaluation of the results (Vos et al. 1995).

Simple Sequence Repeats (SSR) or microsatellites are short (1 to 10 nucleotides), tandemly repeated DNA sequences. They are highly polymorphic between individuals and due to their high mutation rate occur mostly in non-coding regions (Vieira et al. 2016). The primer hybridises on each site of the SSR, the sequences are amplified and the length of the products is determined by high-resolution gel or capillary electrophoresis. The development of SSR markers is costly, yet, the

Introduction

advantages overcome this drawback. SRR analysis requires only a small amount of DNA and even unpurified material can be used, the amplification is robust, reproducible, and can be automated. Additionally, in contrast to AFLPs and RAPDs, SSR markers are co-dominant. The system is suitable for mapping and widely used for population genetic analyses. Single Nucleotide Polymorphisms (SNPs) are variations between individuals of a population that occurred through point mutations of single nucleotides. SNPs occur in high frequencies throughout the genome of every species and, hence, allow the construction of high-density maps that are needed for gene identification and mapping. SNP markers are usually bi-allelic, and knowledge of the sequence is necessary in order to develop new markers, which can be costly. Nonetheless, SNPs are very suitable for high throughput analyses, since it is easy to automate the process and data analysis. Additionally, once developed they can be used for every individual within a species (Khlestkina and Salina 2006).

The development of SNP markers enabled the development of whole-genome genotyping with SNP microarrays or chips, like the Illumina Infinium™ assay (Imelfort et al. 2009). One microarray holds hundreds of thousands of beads. These beads are covered with strands of DNA (SNP primers) that extend just to the SNP in question without including it. The beads are then incubated with amplified DNA fragments, which bind to the primers. Further incubation with nucleotides (A, T, C, G) labelled with different fluorescent colours and DNA polymerase, leads to elongation of the DNA fragment. Depending on the SNP variant of the individual the respective nucleotide is incorporated into the DNA strand and a specific colour signal can be detected. The efforts and costs to develop these kind of arrays are very high, however, once they are available it is a moderately cost-effective method that is suitable for high-throughput of large sample sizes and generates large marker data sets with high information content (Mason et al. 2017). One of the first chips developed was for the human genome. The current human SNP array contains one million SNPs (Marenne et al. 2011). However, genotyping SNP arrays are available, amongst others for livestock genomes like cattle (Matukumalli et al. 2009), apple (Chagné et al. 2012), sunflower (Bachlava et al. 2012), cherry (Peace et al. 2012), peach (Verde et al. 2012), tomato (Sim et al. 2012), maize (Ganal et al. 2011), oilseed rape (Clarke et al. 2016), and wheat (Wang et al. 2014). For barley the 9k Illumina SNP chip (Comadran et al. 2012), containing roughly 8,000 SNPs, and the advanced 50k Illumina SNP chip, containing 44,000 SNPs, including 6,200 SNPs from

the 9k platform, are available (Bayer et al. 2017). The 50k array provides a very good coverage of the genome and is based on the physical map of barley, which is based on the fully annotated reference genome sequence of cultivar ‘Morex’ (Mascher et al. 2017).

In the case that SNP chips and/or reference sequences are not available genotyping-by-sequencing (GBS) is a simple, fast and cheap alternative for genotyping large sample sets (Elshire et al. 2011; Voss-Fels and Snowdon 2016). First, a DNA library has to be constructed. For this, the DNA is digested with one or two restriction enzymes to reduce the complexity of the genome and a barcode adapter is ligated to the DNA. Each sample DNA is amplified using PCR and pooled afterwards. The amplified and pooled samples are then sequenced with next generation sequencing (NGS) technologies (He et al. 2014). The big advantages of GBS are (i) the barcoding system, which allows to assign a particular read to a particular sample, (ii) that marker discovery and genotyping is conducted simultaneously and the more diverse samples are genotyped, the more markers can be discovered, and (iii) that a reference genome is not necessary, because it can be constructed based on the genotyping output. The drawback, however, is that the sequence data and discovered markers only apply to the genotyped set and cannot be transferred or compared to other studies (Elshire et al. 2011).

The advances in genotyping and genotyping platforms, combined with decreasing costs for whole-genome sequencing and the publication of physical maps, facilitates the high throughput genotyping of large sets of species and the identification of QTL for traits of interest (Alqudah et al. 2019). A popular approach for identifying complex traits in recent years has become genome-wide association studies (GWAS). Basically, the association between a trait of interest and molecular markers is calculated. GWAS has several advantages compared to traditional bi-parental QTL mapping. In GWAS, a higher proportion of the allelic diversity and a higher number of recombination events can be exploited since the analysed set consists of unrelated individuals, thereby better explaining the genetic architecture of complex traits (Huang and Han 2014; Rafalski 2010). Because consensus or physical maps can be used for mapping, GWAS does not require the construction of segregating populations and genetic linkage maps; this saves time and facilitates the comparison of results among studies. Therefore, GWAS can offer higher mapping resolution, especially in combination with the advanced SNP chips that provide ten to hundreds of thousands SNPs per analysis.

Introduction

There are also some limitations to GWAS, which can be controlled to some extent. A very important factor is the population size. The population size should be at least 100 individuals, but in order to detect rare alleles, and robust and statistically sound marker-trait associations (MTAs) the size should best be several hundred (Alqudah et al. 2019; Wang et al. 2012). The population size also affects the possibility to detect rare alleles, the explained phenotypic effect and linkage disequilibrium (LD) decay, which is especially important with regard to mapping resolution. When performing GWAS it is also very important to account for relatedness between the individuals. Some individuals will be closer related to each other than to other individuals, this can lead to spurious associations (Alqudah et al. 2019). This can be controlled by accounting for population structure (Pritchard et al. 2000) and kinship (Yu et al. 2006). The population structure factors in the admixture and historical structure of a population in order to calculate the relatedness among individuals and clusters the population into subgroups according to, e.g. geographic origin, row-type or growth habit (Alqudah et al. 2019). This can be controlled either with a Q-matrix, calculated with the software STRUCTURE (Earl and vonHoldt 2012; Pritchard et al. 2000), or with a principle component analysis (PCA) (Price et al. 2006). The kinship (K) also accounts for the relatedness, but the output is a $n \times n$ (with n = number of individuals) matrix that shows the probability of relatedness between each pair of individuals (Yu et al. 2006). The need to account for population structure and kinship can be discarded, when the advantages of both QTL-mapping and GWAS populations are combined. This is the case for so-called 'Nested Association Mapping' (NAM) and 'Multi-parent Advanced Generation Inter-Cross' (MAGIC) populations (Huang et al. 2015; Maurer et al. 2015; Sannemann et al. 2015).

GWAS is a powerful tool to identify QTL that are associated with a phenotypic trait of interest. Nevertheless, it is also possible to identify genes and allelic variation of genes. Genes and allelic variations identified using GWAS have been carefully reviewed by Alqudah et al. (2019).

QTL identified with GWAS should be verified for their reliability and transferability into other populations. The combination of SNP chips and physical consensus maps facilitates the verification and comparison of results across populations and studies. This will also accelerate the identification and development of markers suitable for marker-assisted selection (MAS). MAS requires markers that are tightly and reliably linked with the gene of interest, polymorphic and cost-effective (Collard and

Introduction

Mackill 2008). With the use of MAS it is possible to speed up selection in the breeding process, since single plants can be rapidly screened in the seedling stage without having to conduct phenotypic assessments (Collard and Mackill 2008).

In summary, it can be stated that genotyping SNP chips or combination with other marker systems and GWAS are useful advances for basic research questions but also for the practical breeding process.

3 Aims

As described above, barley yields are constantly threatened by fungal diseases, two very important ones being net blotch (*Pyrenophora teres* f. *teres*) and spot blotch (*Bipolaris sorokiniana*). Both fungi can be very damaging and are highly variable, which increases the possibility for new pathotypes that overcome known resistances. Thus, the search for new resistance sources and the breeding of new resistant cultivars is an on-going task. The developments and advances in the field of molecular markers and genotyping techniques constantly facilitate the identification of QTL of interest and associated markers.

Based on the hypothesis that a worldwide set of barley may contain new QTL for resistance to *P. teres* f. *teres* and *B. sorokiniana* the aims of this study were (i) to screen a diverse set of barley accessions for resistance against *P. teres* f. *teres* and *B. sorokiniana* under controlled and greenhouse conditions, (ii) to genotype this set with the 50 k iSelect barley SNP chip, (iii) identify QTL for resistance employing GWAS, (iv) compare the identified QTL with previously described ones to identify putatively new resistance loci and closely linked markers, (v) identify putative candidate genes located in the identified QTL regions and (vi) identify resistant accessions as potential new resistance sources for future breeding programmes.

- 4 Genetic analysis of a worldwide barley collection for resistance to net form of net blotch disease (*Pyrenophora teres* f. *teres*)

Novakazi F, Afanasenko O, Anisimova A, Platz GJ, Snowdon R, Kovaleva O, Zubkovich A, Ordon F.

Theoretical and Applied Genetics, 132 (9), 2633-2650

<https://doi.org/10.1007/s00122-019-03378-1>



Genetic analysis of a worldwide barley collection for resistance to net form of net blotch disease (*Pyrenophora teres* f. *teres*)

Fluturë Novakazi¹ · Olga Afanasenko² · Anna Anisimova² · Gregory J. Platz³ · Rod Snowdon⁴ · Olga Kovaleva⁵ · Alexandr Zubkovich⁶ · Frank Ordon¹

Received: 4 December 2018 / Accepted: 9 June 2019 / Published online: 17 June 2019
© Springer-Verlag GmbH Germany, part of Springer Nature 2019

Abstract

Key message A total of 449 barley accessions were phenotyped for *Pyrenophora teres* f. *teres* resistance at three locations and in greenhouse trials. Genome-wide association studies identified 254 marker–trait associations corresponding to 15 QTLs.

Abstract Net form of net blotch is one of the most important diseases of barley and is present in all barley growing regions. Under optimal conditions, it causes high yield losses of 10–40% and reduces grain quality. The most cost-effective and environmentally friendly way to prevent losses is growing resistant cultivars, and markers linked to effective resistance factors can accelerate the breeding process. Here, 449 barley accessions expressing different levels of resistance comprising landraces and commercial cultivars from the centres of diversity were selected. The set was phenotyped for seedling resistance to three isolates in controlled-environment tests and for adult plant resistance at three field locations (Belarus, Germany and Australia) and genotyped with the 50 k iSelect chip. Genome-wide association studies using 33,818 markers and a compressed mixed linear model to account for population structure and kinship revealed 254 significant marker–trait associations corresponding to 15 distinct QTL regions. Four of these regions were new QTL that were not described in previous studies, while a total of seven regions influenced resistance in both seedlings and adult plants.

Communicated by Kevin Smith.

Electronic supplementary material The online version of this article (<https://doi.org/10.1007/s00122-019-03378-1>) contains supplementary material, which is available to authorized users.

✉ Frank Ordon
frank.ordon@julius-kuehn.de

- ¹ Institute for Resistance Research and Stress Tolerance, Julius Kuehn-Institute, Erwin Baur-Straße 27, 06484 Quedlinburg, Germany
- ² All-Russian Research Institute of Plant Protection, 196608 shosse Podbelski 3, Saint Petersburg, Russia
- ³ Queensland Department of Agriculture and Fisheries, Hermitage Research Facility, Warwick, QLD 4370, Australia
- ⁴ Department of Plant Breeding, IFZ Research Centre for Biosystems, Land Use and Nutrition, Justus Liebig University, Heinrich-Buff-Ring 26, 35392 Giessen, Germany
- ⁵ Federal Research Center the N. I. Vavilov All-Russian Institute of Plant Genetic Resources, 42–44, B. Morskaya Street, Saint Petersburg, Russia 190000
- ⁶ Republican Unitary Enterprise, The Research and Practical Center of the National Academy of Sciences of Belarus for Arable Farming, Timiriazeva Street 1, 222160 Zhodino, Belarus

Introduction

Net blotch caused by *Pyrenophora teres* Drechsler is one of the most important, damaging and widely distributed diseases of barley (Mathre 1997). *Pyrenophora teres* exists in two forms: *Pyrenophora teres* f. *teres* and *P. teres* f. *maculata*, causing ‘net form’ net blotch (NFNB) and ‘spot form’ net blotch (SFNB), respectively. These two forms are similar in morphology during the sexual and asexual stages and only differ in the symptoms they cause (Lightfoot and Able 2010; Smedegård-Petersen 1971). NFNB produces brown netted lesions containing longitudinal and transverse striations, while SFNB produces brown spotted lesions (Smedegård-Petersen 1976). Under favourable conditions, NFNB causes significant reductions in both yield (Brandl and Hoffmann 1991; Kangas et al. 2005; Mathre 1997) and quality (Burleigh et al. 1988). Yield losses caused by NFNB on susceptible barley cultivars can reach up to 40% under favourable epidemic conditions (Steffenson et al. 1996). In the Northern Caucasus, the North-West and Central regions of the Non-Chernozem region, the South Ural, in the far east of Russia and in Belarus *P. teres* f. *teres* is the most

important disease in barley. In these regions, an epidemic appears every 4–5 years. Yield losses due to epidemics are estimated to be at 36–45% (Afonin et al. 2008). In Australia, *P. teres* f. *teres* is considered a major disease in barley and is estimated to cause average annual losses of \$AUD 19 million (Murray and Brennan 2009). Conservation tillage is standard practice in Australian farming systems resulting in a plentiful bank of over-seasoning inoculum. Losses of up to 70% with severe lodging were recorded in 2009 in South Australia on barley cultivar ‘Maritime’ (Wallwork et al. 2016). Resistance to *P. teres* f. *teres* is a major priority of all barley breeding programs in Australia.

Pyrenophora teres f. *teres* is a highly variable pathogen (Khan 1982; Liu et al. 2011; Serenius 2006; Steffenson and Webster 1992; Tekauz 1990). As a result of global virulence studies, 153 pathotypes among 1162 isolates were identified in different geographic populations of *P. teres* f. *teres* originating from Europe, Syria and Canada on a set of 9 barley differential lines (Anisimova et al. 2017). One of the reasons for the high diversity of *P. teres* f. *teres* populations is the ability to reproduce both sexually and asexually (Mathre 1997). This high heterogeneity concerning virulence of the pathogen implies high genetic diversity in host resistance. In several studies, the complexity of the *P. teres* f. *teres*–barley interaction was shown to be controlled by major qualitative genes (Afanasenko et al. 1999; Cakir et al. 2003; Friesen et al. 2006; Grewal et al. 2012; Ma et al. 2004; Manninen et al. 2006) and quantitative trait loci (QTL) (Douglas and Gordon 1985; König et al. 2013, 2014; Robinson and Jalli 1997; Steffenson et al. 1996; Vatter et al. 2017).

Resistance genes and QTL against NFNB were identified on all seven barley chromosomes in bi-parental mapping populations and by association genetics studies (Afanasenko et al. 2015; Berger et al. 2013; Cakir et al. 2011; Cakir et al. 2003; Graner et al. 1996; Grewal et al. 2008, 2012; Gupta et al. 2004; Koladia et al. 2017; König et al. 2013, 2014; Ma et al. 2004; Manninen et al. 2006; O’Boyle et al. 2014; Raman et al. 2003; Richards et al. 2017; Richter et al. 1998; Steffenson et al. 1996; Wonneberger et al. 2017a, b). Several studies report that resistance genes identified in adult plants are often different from genes conferring NFNB resistance at the seedling stage (Cakir et al. 2003; Grewal et al. 2012; Steffenson et al. 1996; Wonneberger et al. 2017a). Pathotype-specific resistance QTL were found when different *P. teres* f. *teres* isolates were used for phenotyping different mapping populations (Afanasenko et al. 2015; Grewal et al. 2012; Koladia et al. 2017; Richards et al. 2017).

In recent years, genome-wide association studies (GWAS) have become popular for mapping QTL and major genes for several reasons: (1) segregating populations and the construction of own genetic linkage maps are not needed for GWAS, (2) It enables discovery of useful genetic variation in a broader portion of the genetic diversity present in a species

than bi-parental mapping approaches, and (3) it exploits historic recombination events, and by using populations including breeding lines and commercial cultivars, there is a higher probability that markers are directly transferable into current breeding programmes. Nevertheless, a limiting factor in GWAS can be population size. As shown by Wang et al. (2012), population size in GWAS approaches should be at least around 380 individuals to ensure statistically sound and consistently detectable marker–trait associations (MTAs). Another limitation is the presence of extensive linkage disequilibrium (LD) associated with natural or artificial selection, particularly in crop species, which have been subject to intense breeding. LD is the non-random association between two alleles at different loci and is affected by population size and mutation rate, but mostly by recombination rate (Flint-Garcia et al. 2003; Rafalski and Morgante 2004). In out-crossing species, such as maize, recombination rates are high and LD therefore decays within hundreds to a few thousands of base pairs (Remington et al. 2001; Yan et al. 2009). In contrast, in selfing species, which are usually homozygous, recombination is less effective (Flint-Garcia et al. 2003). The highly inbreeding model species *Arabidopsis thaliana*, for example, displays an average genome-wide LD decay of around 250 kilobases, corresponding to about 1 cM (Nordborg et al. 2002). Thus, compared to its very small genome size of roughly 130 Mb, LD extends over large blocks. In barley GWAS panels, LD was reported to be between 18 and 1.3 cM, depending on the diversity of the evaluated materials (Bellucci et al. 2017; Bengtsson et al. 2017; Burlakoti et al. 2017; Gyawali et al. 2017; Massman et al. 2010; Mitterbauer et al. 2017; Tamang et al. 2015; Vatter et al. 2017; Wehner et al. 2015; Wonneberger et al. 2017a). It was shown that LD decays faster in global populations. In other words, genetically and geographically diverse GWAS sets, which include *inter alia* landraces, have a comparatively low LD (Mohammadi et al. 2015; Nordborg et al. 2002). Low LD has the advantage of higher mapping resolution, narrowing the intervals of interesting QTL. However, this also means that a higher marker density is required (Zhu et al. 2008). Recently developed genotyping methods for barley, like the 50 k Barley iSelect SNP Chip (Bayer et al. 2017) or genotyping-by-sequencing (GBS) (Poland et al. 2012), reduce genotyping costs and ensure high marker density and coverage of the barley genome and overcome some of the limitations outlined. Based on these considerations, the main objectives of this study were (1) to screen a diverse set of barley accessions for resistance against *Pyrenophora teres* f. *teres* under greenhouse and field conditions, (2) to genotype this set with the 50 k iSelect chip, (3) to identify QTL for resistance against NFNB and (4) to compare these with previously known QTL in order to identify potentially new resistance loci along with associated markers for resistance breeding.

Materials and methods

Germplasm set

For GWAS, a set of 277 barley landraces and 172 commercial cultivars (total 449 accessions) from the N. I. Vavilov Research Institute of Plant Genetic Resources (VIR) collection were studied (Online Resource 1). This set was the result of a long-term joint research project between the All-Russian Institute of Plant Protection (VIZR), the VIR and the Institute of Resistance Research and Stress Tolerance of the Federal Research Centre for Cultivated Plants (JKI). A total of 12,000 barley accessions from different centres of barley diversity and commercial cultivars were screened for resistance to *Pyrenophora teres* f. *teres* and *Cochliobolus sativus* under greenhouse conditions and in detached leaf assays at the JKI and VIZR (Afanasenko 1995; Silvar et al. 2010; Trofimovskaya et al. 1983). Out of these, about 300 and 150 accessions with different levels of resistance to *P. teres* f. *teres* and *C. sativus* were identified, respectively, and investigated in the present study. With respect to the landraces, the set comprises 31 accessions from Ethiopia and Sudan, 56 from the Middle East (Turkey, Syria, Israel, Palestine), 20 from the Mediterranean Region (Cyprus, Italy, Spain, Crete, Greece), 59 from Central Asia (Tajikistan, Turkmenistan, Kyrgyzstan, Uzbekistan, Kazakhstan), 33 from China, Japan and Mongolia, 37 from South America (Peru, Ecuador, Bolivia), 4 from India, Korea, and Pakistan, 2 from Tunisia and Egypt, 8 from the Caucasus region (Georgia, Armenia, Dagestan) and 6 from the USA. With regard to commercial cultivars, the set includes one cultivar each from Austria, Denmark, Finland, Italy, Kyrgyzstan, Manchuria, Sardinia, Tunisia, Turkey, Turkmenistan, Uruguay and Yugoslavia. Mexico, the Netherlands, Poland, Portugal and Sweden are represented with two cultivars each, India with three and Germany and Ethiopia with four cultivars each. Six cultivars each are from China, France and Kazakhstan, eight and nine from the Czech Republic and Ukraine, respectively. Canada, and the USA and Japan are represented with 11, 12 and 18 cultivars, respectively. Thirty-one cultivars are from Australia and 33 from Russia.

Some of the landrace accessions date back to Nikolai I. Vavilov, who collected them on different expeditions. Accession VIR CI 3175 dates back to his first expedition in Pamir during 1916. Accessions VIR CI 7687–8378 were collected in Syria, Tunis and Cyprus during 1926, and accessions VIR CI 8515–8877 were collected in Italy, Spain and Ethiopia in 1927.

The set represents 31 morphological forms of *Hordeum vulgare* (Online Resource 1). It includes 178 two-rowed and 271 six-rowed accessions. Out of 449 accessions, 20

are winter types, 28 have black kernels, and 51 have naked kernels.

Single plant selections were made for each accession, and these selections were self-pollinated by bagging in 2013 and 2014 under field conditions at VIR (Pushkin, Russia) and in Zhodino (Belarus).

Fungal isolates

Five single-spore-derived *P. teres* f. *teres* isolates were used in this study. They were selected based on their origin, virulence and sporulation ability. Isolate *No 13* was collected in 2014 near Volosovo in the Leningrad Region, Russia, and isolate *Hoehnstedt* was collected in 2016 on infected fields close to the village of Hoehnstedt in Saxony-Anhalt (Germany). The three isolates *NFNB 50*, *NFNB 73* and *NFNB 85* are Australian isolates from Queensland, each with different virulence profiles. *NFNB 50* and *NFNB 85* were from the Gatton area, while *NFNB 73* was collected from Tansey in the South Burnett region. *NFNB 50* was used in both greenhouse and field trials, but *NFNB 73* and *NFNB 85* were used in field trials only.

Pyrenophora teres isolates *No 13* and *Hoehnstedt* were grown on V8-agar medium containing 150 ml V8 juice, 10.0 g Difco PDA, 3.0 g CaCO₃, 10.0 g agar and 850 ml distilled water. Petri dishes were placed in a dark chamber at room temperature for 5 to 7 days, exposed to light for 24 h and placed again in a dark chamber at 13 °C for 24 h. Conidia were then harvested by adding sterile water to the Petri dish and scraping conidia off with a sterile spatula. Conidia were counted with a haemocytometer, and the concentration was adjusted to 5000 conidia/ml. Australian isolates were grown as described by Martin et al. (2018).

In the Australian field trials, single isolates were used for inoculation. For this, isolated blocks of highly susceptible varieties were sown in early to mid-April. Inoculum for these blocks was multiplied in the laboratory and applied to the blocks at the 4–5 leaf stage. Epidemics in these blocks were promoted by sprinkler irrigation at least twice a week when conditions for infection were favourable. These blocks provided the inoculum for the subsequent field screening (Martin et al. 2018).

Greenhouse trials

Greenhouse trials were performed at the Julius Kuehn-Institute in Quedlinburg, Germany, in 2015 and 2017 with isolates *No 13* and *Hoehnstedt*, respectively. Three seeds per accession were grown in plastic pots (8×8×8 cm) for 2–3 weeks at 16–18 °C with alternating 12 h periods of light/darkness (exposure min 5000 lx). The experiment was set up in four replications in a complete randomized block design. The NFNB differential set proposed by Afanasenko

et al. (2009) was included in each replication as a standard. When the second leaf was fully developed (BBCH 12–13), plants were spray-inoculated with the spore suspension until the inoculum was at the point of running off (approximately 0.35 mL/plant). Plants were then covered with plastic foil for 48 h to ensure 100% humidity and grown for another 10–14 days at 20–22 °C and 70% humidity until symptoms were clearly visible.

Isolate *NFNB 50* was tested at the Hermitage Research Facility in Warwick, Queensland, Australia, in 2017. Plants were grown in commercial potting mix (Searles Premium Potting Mix) in plastic maxipots (10 cm in diameter, 17 cm tall). Four to five seeds were sown at 0°, 120° and 240° around the circumference of each pot. The experiment was set up in two replications in an incomplete block design, where pots corresponded to blocks and there were three lines per block. Pots were maintained in the greenhouse at 15/27 °C for 2 weeks until the second leaf was fully expanded. Field-collected conidia were suspended in water at 3000 conidia/mL and applied from four directions using a WallWick® commercial spray gun delivering an average 3 mL/pot. Immediately after inoculation, pots were placed into a fogging chamber for 20 h at 19 °C with 14 h in the dark. After incubation, pots were returned to the greenhouse, double-spaced and bottom watered, and grown for another 8 days. Pots were fertilized twice weekly after emergence with a soluble complete fertilizer (Grow Force EX7) until notes were taken.

Infection response type was assessed on the second leaf of each plant following the scale of Tekauz (1985).

Field trials

Field trials were conducted at three locations, Belarus, Germany and Australia, during the years 2015, 2016 and 2017.

Trials in Belarus were conducted at the Research and Practical Centre of the National Academy of Sciences of Belarus for Arable Farming (Zhodino, Belarus) in 2016 and 2017. Accessions were sown in rows of 1 m with 15–20 seeds per row and a spacing of 0.3 m between rows. The trial was set up in a complete randomized block design with two replications. The cultivar ‘Thorgal’, susceptible to net blotch and resistant to powdery mildew, was sown around the trial as a border and after every 10th accession to support net blotch and reduce powdery mildew development in the nurseries. Additionally, ‘Thorgal’ was used as a spreader for net blotch. To increase infection, infected barley straw was spread in the rows of ‘Thorgal’ after sowing. The infected straw was harvested in the previous year at the same location. The percentage of leaf area infected was assessed at early-dough to mid-dough stages (BBCH 83–85) on the three upper leaves of the plants.

In Germany, the field trials were conducted at the Julius Kuehn-Institute (Quedlinburg, Germany) in 2015 and 2016 using the Summer Hill design developed by König et al. (2013). Accessions were sown at the beginning of August in hills with 25 seeds/hill and a spacing of 0.5 m between hills. The susceptible varieties ‘Candesse’ and ‘Stamm 4046’ were used as spreader rows and sown in rows between the hills, spacing 1.0 m between rows as described in Vatter et al. (2017). The trials were set up in two replications in a complete randomized block design. Infected barley straw was used as inoculum and was incorporated into the soil prior to sowing. Phenotyping started when symptoms were clearly visible on the susceptible standards. The percentage of leaf area infected (Moll et al. 2010) and the infection response type (Tekauz 1985) were assessed at three different time points with a period of 2 weeks between scoring dates. The area under disease progress curve (AUDPC) was calculated and used to calculate the average ordinate (AO) as described by Vatter et al. (2017).

Field trials in Australia were conducted at the Hermitage Research Facility in Warwick, Queensland in 2017 with three distinct isolates. Trials were sown as hill plots with an in-row spacing of 0.5 m and between-row spacing of 0.76 m. Two rows of datum plots were sown between five rows of spreader (0.19 m spacing). Spreaders were sown 11–19 days before the plots and were inoculated by spreading infected green plant material cut from inoculum increase blocks when the spreaders were at about BBCH 30. Epidemics were promoted with overhead sprinkler irrigation applied in the late afternoon and/or early evening so that the nurseries remained wet overnight. In the absence of rainfall, irrigation was applied two or more nights per week when conditions were favourable for infection. Infection responses were taken on a whole plot basis using a 0 to 9 scale at BBCH stages 70–73. The scale is a variant of the scale by Saari and Prescott (1975). It takes into account the plant response (infection type; IT) and the amount of disease in a plot and therefore correlates very well with the host response and the leaf area diseased (Martin et al. 2018).

Statistical analysis

Statistical analyses and analysis of variance (ANOVA) were performed using the software package SAS 9.4 (SAS Institute Inc. Cary, NC, USA) using *proc mixed* and *proc glimmix* for greenhouse trials and field trials in Australia. For field trials, the least square means (lsmeans) and for greenhouse trials the means of the infection response type were calculated and used for genome-wide association studies (GWAS). Broad sense heritability across years was calculated using the formula $h^2 = V_G / (V_G + V_{GY} + V_R)$ as described by Vatter et al. (2017), where V_G is genotypic variance, V_{GY} is genotype \times year variance, V_R is residual

variance, and y and r are the number of years and replicates, respectively.

Genotyping, population structure, kinship and linkage disequilibrium

Genomic DNA was extracted from 14-day-old plants according to Stein et al. (2001). The accessions were genotyped on the Illumina iSelect 50 k Barley SNP Chip (Illumina) at Trait Genetics GmbH (Gatersleben, Germany). Physical positions of markers were taken from Bayer et al. (2017), which is based on the barley pseudo-molecule assembly by Mascher et al. (2017). SNPs having failure rates > 10%, heterozygous calls > 12.5% and a minor allele frequency (MAF) < 5% were excluded from the analyses, as well as unmapped SNPs. Thus, 33,818 SNPs were left for subsequent GWAS. In order to calculate the kinship matrix and the population structure, the markers were further filtered with the software PLINK 1.9 (www.cog-genomics.org/plink/1.9/) (Chang et al. 2015). The tool *LD prune* was used with the following parameters: indep pairwise window size 50, step 5 and an r^2 threshold 0.5 (Campoy et al. 2016). This resulted in 8533 markers for calculating the kinship and population structure. Kinship was calculated with the web-based platform Galaxy (Afgan et al. 2016) using the tool *Kinship* and the modified Roger's distance (Reif et al. 2005). Population structure was determined with the software STRUCTURE v2.3.4 (Pritchard et al. 2000). In order to identify the optimal subpopulations, an admixture model was used with a burn-in of 50,000, followed by 50,000 Monte Carlo Markov chain (MCMC) replications for $k = 1$ to $k = 10$ with 10 iterations. STRUCTURE HARVESTER (Earl and vonHoldt 2012) was used to identify the optimal k . Following this, a new STRUCTURE analysis was performed with a burn-in of 100,000 and 100,000 MCMC iterations at the optimal k value. Accessions were considered as admixed, when their membership probabilities were < 80% (Richards et al. 2017). Linkage disequilibrium (LD) was calculated as squared allele frequency correlations (R^2) between all intra-chromosomal marker pairs using the tool *linkage disequilibrium* in the web-based platform Galaxy. Genome-wide LD decay was plotted as R^2 of a marker against the corresponding genetic distance, and a Loess regression was computed. For R^2 , the default settings were used (Sannemann et al. 2015).

Genome-wide association studies

Genome-wide association studies (GWAS) were performed using the Galaxy implemented tool *GAPIT*, which uses the *R* package GAPIT (Lipka et al. 2012). The model used was a compressed mixed linear model (CMLM) (Zhang et al. 2010) including the population structure (Q) and kinship (K). In order to detect significant marker–trait associations,

a Bonferroni correction was employed. For this, the reduced marker set of 8533 markers, which was used for calculating population structure and kinship, and a significance level of $P = 0.2$ was used (Muqaddasi et al. 2017; Storey and Tibshirani 2003). This resulted in a threshold of $-\log_{10}(P) \geq 4.63$. GWAS for greenhouse trials, and field trials in Australia were conducted for each isolate separately. For field trials in Zhodino and Quedlinburg, GWAS were conducted across years for each location. Manhattan plots were generated with the *R* v.3.4.4 package *qqman*.

In order to compare previously described QTL with QTL identified in the present study, the databases GrainGenes (<https://wheat.pw.usda.gov/GG3/>) and BARLEX (<https://apex.ipk-gatersleben.de/apex/f?p=284:10>) were used to obtain marker information and identify physical positions of previously published QTL studies. Where previously described QTL were identified based on iSelect markers, the physical positions were obtained from Bayer et al. (2017).

Results

Phenotypic evaluation of greenhouse trials

Phenotyping in the greenhouse with three different isolates showed a wide range of variability in the infection response type (1–10 scale) for all three isolates tested. The average infection response type (IRT) for isolate *Hoehnstedt* ranged from 1 to 9 (mean 3.96), for *No 13* from 1 to 10 (mean 5.28) and for *NFNB 50* from 1 to 10 (mean 3.6) (Fig. 1). Analysis of variance showed significant differences among the barley accessions for seedling resistance to NFNB for all isolates (Table 1). In trials with isolates *No 13* and *Hoehnstedt*, the proposed differential set by Afanasenko et al. (2009) was used as a reference. The infection scores for the differential lines can be seen in Table 2. For isolate *No 13*, the infection scores ranged from 0.75 (CI 5791) to 8 (Harrington). For *Hoehnstedt*, the lines showed less variance and the scores ranged from 2.63 (Harbin) to 4.89 (CLS 25282). For isolate *NFNB 50*, the lines used as references and their respective infection scores can be obtained from Table 3. The scores ranged from 0.8 (Beecher) to 9.1 (Grimmett).

Phenotypic evaluation of field trials

A wide range of disease severity was observed for all three locations (Fig. 2; Table 1).

In Germany in both years, infection pressure for NFNB was high in Summer Hill trials. Disease severity scores ranged on average between 4.1 and 31.5% (mean 11.5%). The frequency distribution was slightly right skewed with 184 accessions showing disease severity of < 10% and 7

Fig. 1 Frequency distribution for *Pyrenophora teres* f. *teres* reaction after inoculation with isolates Hoehnstedt, No 13 and NFNB 50

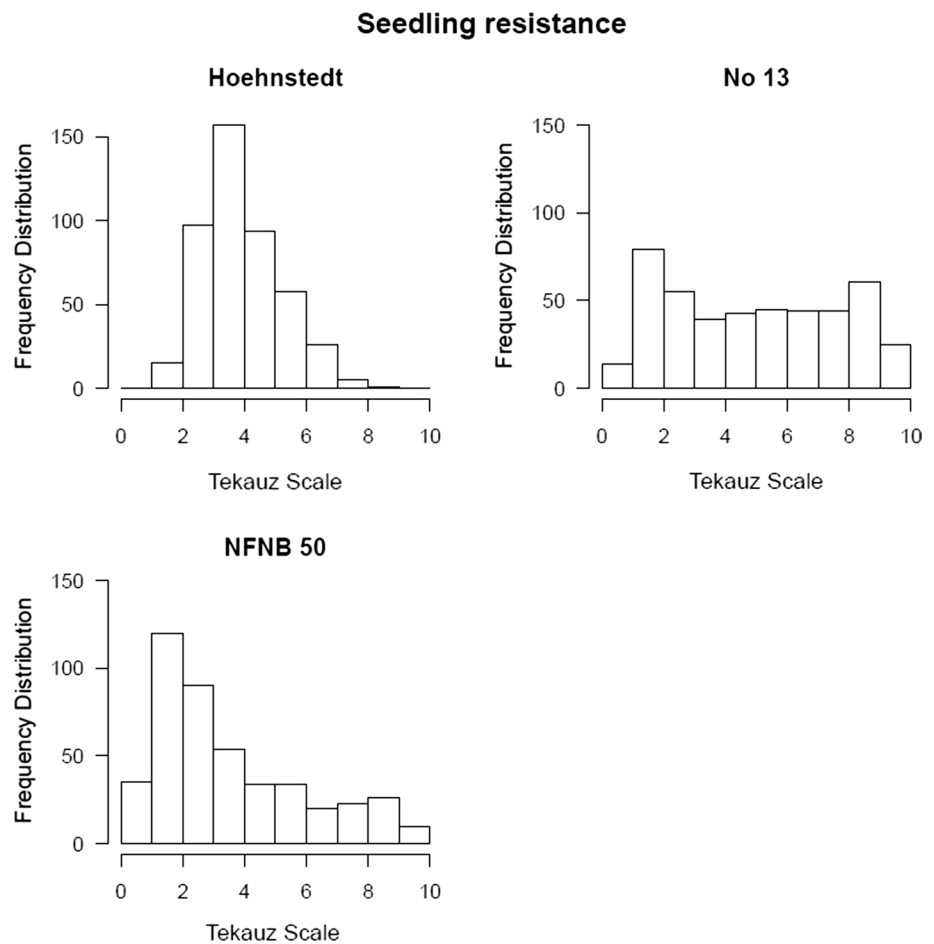


Table 1 Analysis of variance (ANOVA) for net form of net blotch (NFNB) severity for 449 barley genotypes evaluated under greenhouse and field conditions

Isolate/location	Effect	F value	P value
Hoehnstedt	Genotype	4.66	<0.0001
No 13	Genotype	19.12	<0.0001
NFNB 50 (greenhouse)	Genotype	22.15	<0.0001
Quedlinburg	Genotype	3.68	<0.0001
Zhodino	Genotype	4.63	<0.0001
NFNB 50 (field)	Genotype	11.9	<0.0001
NFNB 73	Genotype	12.29	<0.0001
NFNB 85	Genotype	12.61	<0.0001

accessions showing scores of > 25%. The heritability for this location was estimated at $h^2=0.73$.

In Belarus in 2017, conditions were unfavourable for NFNB yet favourable for powdery mildew, which did not allow any more than two assessments of net blotch. Hence, for this location the disease score based on the respective last scoring date was used to calculate the mean disease severity across years. Disease severity scores ranged on

Table 2 Disease severities of differential lines (Afanasenko et al. 2009) used in field trials in Belarus and Germany, and in greenhouse trials with isolates No 13 and Hoehnstedt

Differential line	Trial			
	Belarus ^a	Germany ^a	No 13 ^b	Hoehnstedt ^b
Harrington	19.75	12.20	8.00	4.75
Skiff	13.5	7.49	6.13	3.22
Prior	3	5.52	7.63	–
CI 9825	1.5	10.27	1.56	2.44
Harbin	3	11.79	1.38	2.63
K 20019	3	10.19	1.63	2.89
CI 5791	0.75	14.51	0.75	2.86
CLS 25282	0.75	14.11	1.17	4.89
K 8755	1	14.06	1.88	3.38

^a% of leaf area infected

^binfection response type based on Tekauz (1985), 1 to 9 scale

average between 0.1 and 60% (mean 7.7%). The frequency distribution for this location is right-skewed with 201 accessions showing a disease severity of < 5% and 5 accessions showing scores of 40% and higher. Heritability for

Table 3 Disease severity of reference lines used in Australian field trials and in greenhouse trials with isolate *NFNB50* (0 to 9 scale based on Saari and Prescott 1975)

Reference line	Trial				
		NFNB50 (GH)	NFNB50	NFNB73	NFNB85
Commander			4.9	5.3	6.6
Beecher	0.8				
BS89-4-3		8.8	8.6	7.6	
Corvette		4.7	5.2	8.0	
Fleet	3.7				
Grimmett	9.1				
Kaputar	4.8				
Prior	2.7	2.6	2.2	8.8	
QB15127		7.7	6.0	5.2	
Rajo		2.1	2.0	2.3	
Schooner		5.1	4.0	3.8	
Shepherd	4.0	4.9	7.9	4.5	
Skiff	8.0	8.7	5.7	3.1	
WPG8412-9-2-1	2.2	2.2	1.5	1.7	

field trials in Belarus was $h^2=0.79$. In field trials in Germany and Belarus again the differential set by Afanasenko et al. (2009) was scored as a reference (Table 2). In Germany, the disease severity among the differentials ranged from 5.52 (Prior) to 14.51% (CI 5791). In Belarus, the disease severity ranged from 0.75 (CI 5791, CLS 25282) to 19.75% (Harrington).

In Australia, three individual isolates were tested in the field. For all three isolates, disease scores from 1 to 9 were observed. Frequency distributions for isolates *NFNB 50* and *NFNB 73* were right-skewed towards resistance with 316 and 292 accessions showing disease scores ≤ 3 , respectively. For isolate *NFNB 85* only 149 accessions showed disease scores ≤ 3 . The reference lines used in field trials in Australia are shown in Table 3. The infection scores ranged from 1.5 (WPG8412-9-2-1) to 8.8 (BS89-4-3). Line WPG8412-9-2-1 was resistant against all isolates used. So far no isolate found in Australia has been virulent on this line.

Population structure and linkage disequilibrium

STRUCTURE analysis identified an optimal k value of 3, with 58, 139 and 91 individuals belonging to subpopulation one, two and three, respectively (Online Resource 2; Online Resource 3). Out of the 449 accessions, 161 showed membership probabilities of less than 0.8 and were considered as admixed. Accessions belonging to subpopulations one and two were mainly 6-rowed types, population three comprised mainly 2-rowed accessions. Genome-wide linkage disequilibrium (LD) decay was estimated at 167 kb.

Genome-wide association mapping

Seedling resistance

For isolate *Hoehnstedt*, eight significant marker–trait associations (MTAs) were detected on chromosome 6H (Fig. 3). Their $-\log_{10}(p)$ ranged from 4.63 to 6.3 (Table 4, Online Resource 4). The MTAs corresponded to two regions. The first region spanned from 128 to 165 Mbp (53.52 cM), including seven markers, with the peak marker at 140 Mbp with a $-\log_{10}(p)=6.3$ (JHI-Hv50 k-2016-391848), which explained 4.9% of the phenotypic variance. In addition, a second region comprising one significant marker (JHI-Hv50 k-2016-399702) was identified at 370 Mbp with a $-\log_{10}(p)=5.2$ and an R^2 of 3.9%.

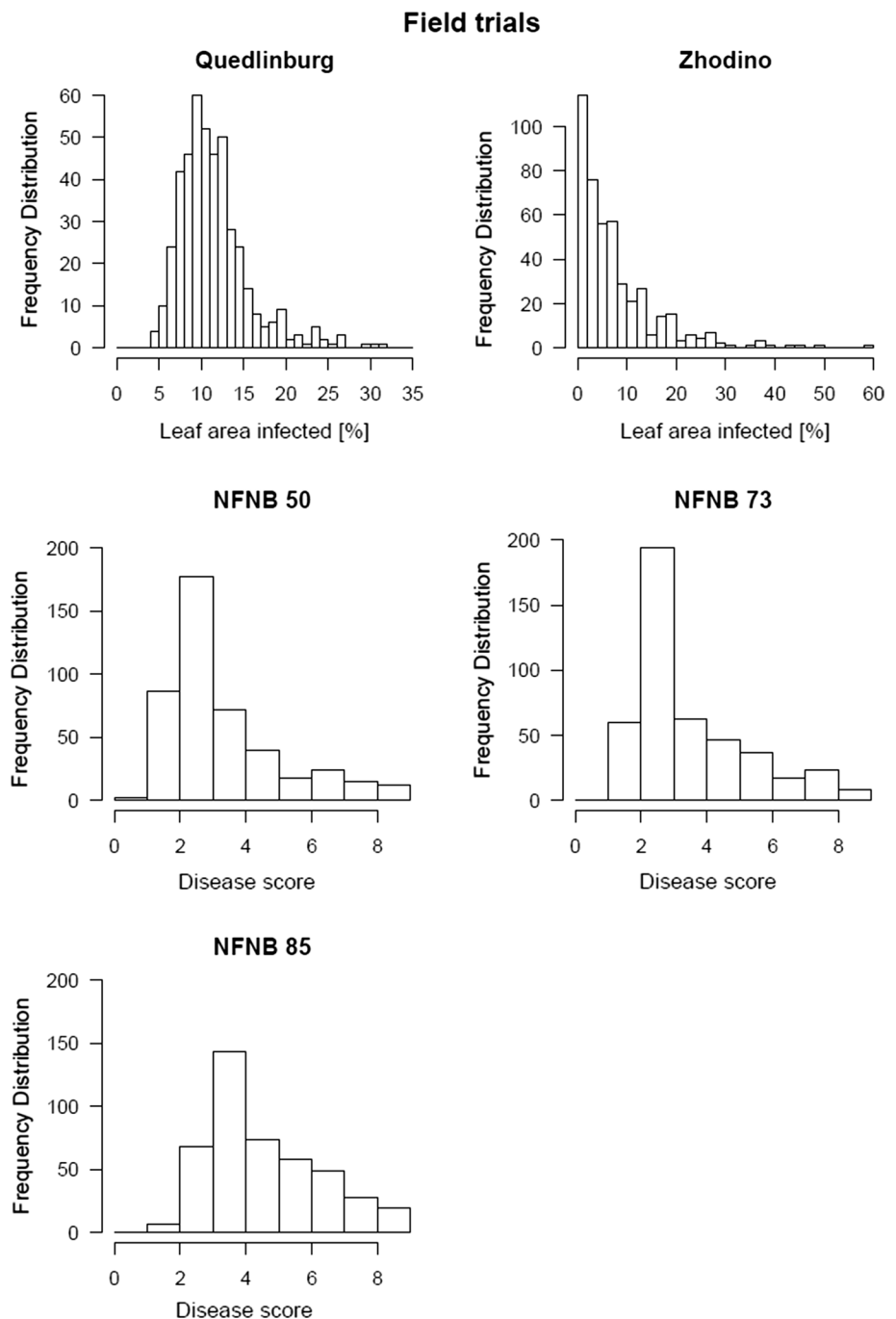
GWAS for isolate *No 13* revealed 12 significant MTAs with $-\log_{10}(p)$ from 4.71 to 6.92 (Table 4; Fig. 3). Five markers associated with resistance were located on chromosome 4H between 64 and 70 Mbp with a peak marker at 70 Mbp with a $-\log_{10}(p)=6.92$ (JHI-Hv50 k-2016-237924), explaining 2.8% of the phenotypic variance. Additional MTAs were detected on chromosomes 4H (JHI-Hv50 k-2016-241935) and 6H (SCRI_RS_176650) at 352 Mbp and 373 Mbp, respectively. In addition, five MTAs were detected on chromosome 7H at 645 Mbp explaining 1.8–2.2% of the phenotypic variance.

For isolate *NFNB 50 32*, significant MTAs were detected (Fig. 3). The $-\log_{10}(p)$ ranged from 4.64 to 9.24 (Table 4). On chromosome 3H, 15 MTAs were detected, corresponding to three regions. One marker was located at 73 Mbp (46.29 cM, $R^2=2.0\%$) (JHI-Hv50 k-2016-165152), and three were located between 119 and 138 Mbp (46.68 cM), explaining 2.2–2.6% of the phenotypic variance (Online Resource 4). The third region spanned from 490 to 492 Mbp (48.44–48.63 cM) and included 11 markers, with the peak marker (JHI-Hv50 k-2016-183207) located at 490 Mbp ($-\log_{10}(p)=9.24$), which explained 4.4% of the phenotypic variance. On chromosome 6H, MTAs were detected in three regions, i.e. eight MTAs between 64 and 72 Mbp (52.73 cM, $R^2=2.0$ to 2.6%), six MTAs between 133 and 140 Mbp (53.52 cM, $R^2=2.1\%$ per marker) and two MTAs at 373 Mbp (SCRI_RS_188243 and SCRI_RS_195914), each explaining 2.1% of the phenotypic variance. One single MTA was detected on chromosome 7H (JHI-Hv50 k-2016-440870) at 5 Mbp with an R^2 of 2.4%.

Adult plant resistance

GWAS based on the data of the field trials in Quedlinburg revealed nine MTAs on chromosome 6H with $-\log_{10}(p)$ between 4.78 and 6.62 (Table 4; Fig. 4, Online Resource 5). Five markers were located between 44 and 47 Mbp with three peak markers at 47 Mbp ($-\log_{10}(p)=4.95$), explaining

Fig. 2 Frequency distribution of resistance to *Pyrenophora teres f. teres* for field trials in Quedlinburg (Germany), Zhodino (Belarus) and Warwick (Australia) with isolates NFNB 50, NFNB 73 and NFNB 85



2.8% of the phenotypic variance, each. The remaining four markers were located at 406–410 Mbp with the peak marker (JHI-Hv50 k-2016-403424) at 406 Mbp explaining 3.9% of the phenotypic variance.

For the location Zhodino, a total of 61 significant MTAs were detected; 58 of these were located on chromosome 3H (Fig. 4, Online Resource 5). The 58 markers can be divided into five regions based on the physical map, and genetically these regions are less than 1 cM apart (Table 4). The first region comprised two markers located at 58 (46.29 cM)

(JHI-Hv50 k-2016-164734) and 101 Mbp (46.29 cM) (JHI-Hv50 k-2016-166000) with $-\log_{10}(p) = 4.81$ and 4.74, respectively. The second region comprised two markers located at 119 (46.68 cM) (JHI-Hv50 k-2016-166356) and 130 Mbp (46.68 cM) (JHI-Hv50 k-2016-166392) with $-\log_{10}(p) = 5.84$. The third region spanned from 233 to 350 Mbp and included 50 markers with $-\log_{10}(p) = 4.83$ to 5.24. The explained phenotypic variance ranged between 2.3 and 2.6% per marker. One marker mapped at 428 Mbp (47.07 cM), and the remaining three markers mapped

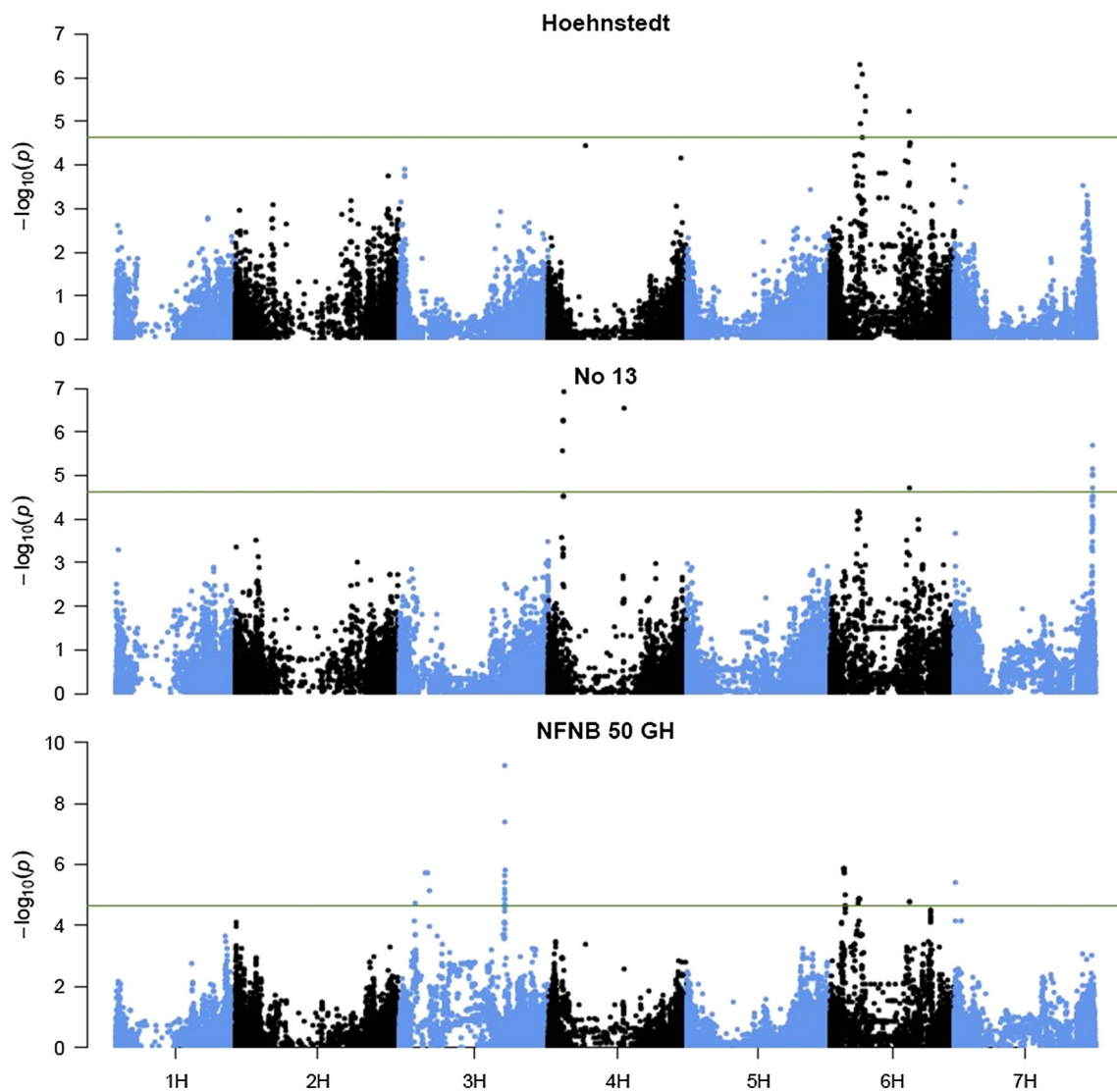


Fig. 3 Genome-wide association analyses of resistance to *Pyrenophora teres* f. *teres* isolates Hoehnstedt, No 13 and NFNB 50 tested under greenhouse conditions. The x-axis shows the seven bar-

ley chromosomes, positions are based on the physical map, and the $-\log_{10}(p)$ value is displayed on the y-axis. The green horizontal line represents the significance threshold of $-\log_{10}(p)=4.63$

to 621 Mbp. On chromosomes 4H, 5H and 6H one MTA was identified on each, located at 33, 634 and 140 Mbp, respectively.

For field trials conducted with isolate *NFNB 50*, eleven MTAs were detected (Fig. 5), four of which were located on chromosome 3H at 446 to 490 Mbp (47.46–48.44 cM) with the peak marker located at 490 Mbp ($-\log_{10}(p)=6.08$; JHI-Hv50 k-2016-183351) explaining 3.4% of the phenotypic variance. The remaining MTAs were located on chromosome 6H in the interval 133–135 Mbp (53.52 cM), 368 and 373 Mbp, R^2 values ranged between 2.5 and 4% (Table 4, Online Resource 6).

GWAS for isolate *NFNB 73* revealed 65 significant MTAs (Fig. 5, Online Resource 6). One marker was located on chromosome 5H at 579 Mbp ($-\log_{10}(p)=4.65$;

JHI-Hv50 k-2016-326506) and one on chromosome 6H at 72 Mbp (JHI-Hv50 k-2016-388677). 51 MTAs mapped to chromosome 6H between 123 and 344 Mbp (53.52–53.91 cM) with $-\log_{10}(p)$ between 4.8 and 8.18, explaining 2.3 to 4% of the phenotypic variance (Table 4). The remaining 12 MTAs were also located on chromosome 6H in an interval from 356 to 373 Mbp with the peak marker at 373 Mbp with a $-\log_{10}(p)=20.07$ and a R^2 value of 11.1% (SCRI_RS_188243).

A total of 56 markers, all located on chromosome 6H, were detected for isolate *NFNB 85*, corresponding to two regions (Fig. 5, Online Resource 6). The first region spanned from 37 to 76 Mbp with three peak markers at 47 Mbp ($-\log_{10}(p)=10.22$), explaining 6.8% per marker (JHI-Hv50 k-2016-385826, JHI-Hv50 k-2016-385857,

Table 4 Chromosomal regions significantly associated with disease resistance/susceptibility towards *Pyrenophora teres* f. *teres*. Seedling resistance was tested using isolates *Hoehnstedt*, *No 13* and *NFNB 50*. Adult plant resistance was tested under field conditions

in Quedlinburg (Germany), Zhodino (Belarus) and Warwick (Australia, with isolates *NFNB 50*, *NFNB 73* and *NFNB 85*). The complete lists of significant marker–trait associations can be found in Online Resources 4, 5 and 6

Isolate/location	Chr	Position (MB) ^a	cM ^b	–log 10 (<i>p</i> value)	<i>R</i> ^{2c}	Peak marker
Hoehnstedt	6H	128.978649–165.696981	53.52	4.629–6.314	0.034–0.049	JHI-Hv50 k-2016-391848
	6H	370.400702	N/A	5.223	0.039	JHI-Hv50 k-2016-399702
No 13	4H	64.213185–70.916854	N/A	5.565–6.921	0.022–0.028	JHI-Hv50 k-2016-237924
	4H	352.904766	N/A	6.530	0.026	JHI-Hv50 k-2016-241935
	6H	373.424916	N/A	4.726	0.018	SCRI_RS_176650
	7H	645.343981–645.821472	N/A	4.714–5.674	0.018–0.022	JHI-Hv50 k-2016-514022
NFNB 50 (seedling)	3H	73.225203	46.29	4.724	0.020	JHI-Hv50 k-2016-165152
	3H	119.62783–138.756589	46.68	5.122–5.735	0.022–0.026	JHI-Hv50 k-2016-166356
Quedlinburg						JHI-Hv50 k-2016-166392
	3H	490.244247–492.773583	48.44–48.63	4.633–9.243	0.020–0.044	JHI-Hv50 k-2016-183207
	6H	64.21999–72.704287	52.73	4.640–5.848	0.020–0.026	JHI-Hv50 k-2016-387864
						JHI-Hv50 k-2016-387926
						JHI-Hv50 k-2016-388164
	6H	133.169988–140.843412	53.52	4.740–4.851	0.021	JHI-Hv50 k-2016-391664
						JHI-Hv50 k-2016-391711
						JHI-Hv50 k-2016-391719
						JHI-Hv50 k-2016-391721
	6H	373.423645–373.61703	N/A	4.772–4.796	0.021	SCRI_RS_188243
	7H	5.165127	N/A	5.416	0.024	JHI-Hv50 k-2016-440870
	6H	44.246648–47.371815	N/A	4.775–4.947	0.027–0.028	JHI-Hv50 k-2016-385826
						JHI-Hv50 k-2016-385857
						JHI-Hv50 k-2016-385944
	6H	406.693351–410.500947	N/A	5.007–6.620	0.029–0.039	JHI-Hv50 k-2016-403424
Zhodino	3H	58.922007–101.184493	46.29	4.742–4.812	0.023	JHI-Hv50 k-2016-164734
	3H	119.62783–130.79036	46.68	5.839	0.029	JHI-Hv50 k-2016-166356
						JHI-Hv50 k-2016-166392
	3H	233.011291–350.511777	N/A	4.827–5.243	0.023–0.026	SCRI_RS_160464
NFNB 50 (adult plant)						JHI-Hv50 k-2016-173670
						JHI-Hv50 k-2016-174303
	3H	428.370730	47.07	4.695	0.023	JHI-Hv50 k-2016-179690
	3H	621.113001–621.116747	N/A	4.654	0.022	JHI-Hv50 k-2016-202195
	4H	33.367057	47.27	4.836	0.024	JHI-Hv50 k-2016-233404
	5H	634.732801	N/A	4.733	0.023	SCRI_RS_236545
	6H	140.843412	53.52	5.726	0.029	JHI-Hv50 k-2016-391848
	3H	446.058505–490.798579	47.46–48.44	4.703–6.077	0.025–0.034	JHI-Hv50 k-2016-183351
	6H	133.169988–135.378543	53.52	4.728–5.250	0.025–0.029	JHI-Hv50 k-2016-391636
	6H	368.968887–373.423645	N/A	4.921–7.121	0.026–0.040	SCRI_RS_188243
NFNB 73	5H	579.069274	N/A	4.646	0.021	JHI-Hv50 k-2016-326506
	6H	72.039115	N/A	4.924	0.023	JHI-Hv50 k-2016-388677
	6H	123.046959–344.799609	53.52–53.91	4.796–8.181	0.022–0.040	JHI-Hv50 k-2016-394438
NFNB 85						JHI-Hv50 k-2016-394846
						JHI-Hv50 k-2016-395883
						JHI-Hv50 k-2016-397733
	6H	356.025431–373.424916	N/A	4.738–20.065	0.022–0.111	SCRI_RS_188243
	6H	37.571424–76.621753	N/A	4.629–10.221	0.028–0.068	JHI-Hv50 k-2016-385826
						JHI-Hv50 k-2016-385857
						JHI-Hv50 k-2016-385944
	6H	355.018439–379.784111	N/A	4.688–8.710	0.028–0.057	JHI-Hv50 k-2016-399838

^aphysical positions based on Bayer et al. (2017)

^bgenetic positions based on RIL population of Golden Promise × Morex by Bayer et al. (2017)

^cexplained phenotypic variance per marker

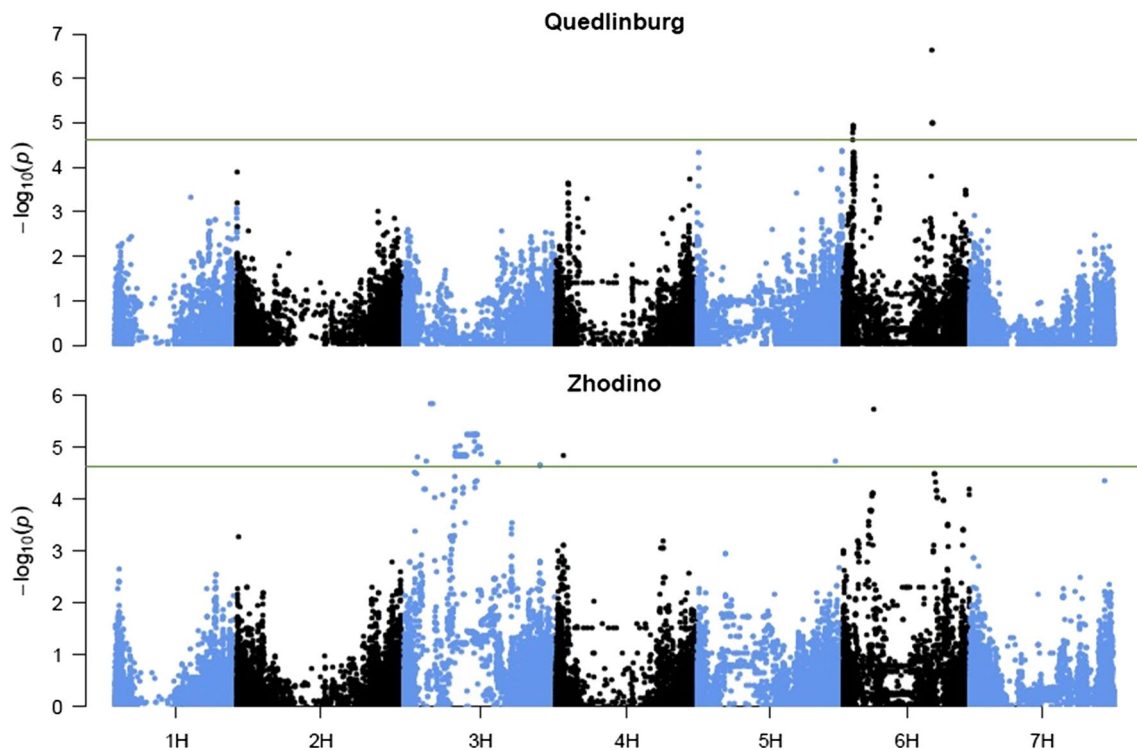


Fig. 4 Genome-wide association analyses of resistance to *Pyrenophora teres* f. *teres* under field conditions in Quedlinburg (Germany) and Zhodino (Belarus). The *x*-axis shows the seven barley

chromosomes, positions are based on the physical map, and the $-\log_{10}(p)$ value is displayed on the *y*-axis. The green horizontal line represents the significance threshold of $-\log_{10}(p)=4.63$

JHI-Hv50 k-2016-385944) (Table 4). The second region was located at 355 to 379 Mbp with the peak marker at 373 Mbp and a $-\log_{10}(p)=8.71$ (JHI-Hv50 k-2016-399838), which explained 5.7% of the phenotypic variance.

Discussion

The net form of net blotch (NFNB) is a threat to barley producing regions all over the world. The high variability of this pathogen (Khan 1982; Liu et al. 2011; Serenius 2006; Steffenson and Webster 1992; Tekauz 1990) makes it a difficult task for breeders to identify and successfully introduce new resistance genes and QTL into current breeding material. Via bi-parental mapping approaches, several QTL for resistance on all seven barley chromosomes have been identified (König et al. 2014; Liu et al. 2011; Martin et al. 2018; Vatter et al. 2017). In recent years, GWAS has become a prominent approach to identify QTL and major genes for agronomically important traits, e.g. yield, abiotic and biotic stress (Gurung et al. 2011; Lex et al. 2014; Rode et al. 2011; Simmonds et al. 2014; Wehner et al. 2015). So far, only three studies were published showing the use of GWAS to identify NFNB resistance in barley (Amezrou et al. 2018; Richards et al.

2017; Wonneberger et al. 2017a) along with one study using nested association mapping (NAM)(Vatter et al. 2017). All of these previous studies used the low-density 9 k iSelect SNP Chip as a genotyping platform and applied genetic linkage maps for approximation of QTL positions. To our knowledge, the present study represents the first study on NFNB in barley to employ the 50 k iSelect barley SNP chip in association with physical marker positions (Bayer et al. 2017) based on the pseudo-molecule genome assembly of Mascher et al. (2017).

Phenotypic results of all experiments showed a high variability of the accessions towards the pathogen. Heritability ranged from $h^2=0.67$ to 0.79 and was in good accordance with previously published studies, reporting on h^2 for this trait ranging between 0.62 and 0.99 (Grewal et al. 2012; König et al. 2013; Richards et al. 2017; Vatter et al. 2017; Wonneberger et al. 2017a).

Overall, 254 significant marker–trait associations (MTAs) were detected, which corresponded to 15 distinct regions. Three of them were identified conferring seedling resistance, five conferring adult plant resistance and seven were active at both growth stages. The regions were located on barley chromosomes 3H, 4H, 5H, 6H and 7H.

On chromosome 3H, five regions were identified associated with NFNB resistance (Fig. 6). The first two regions

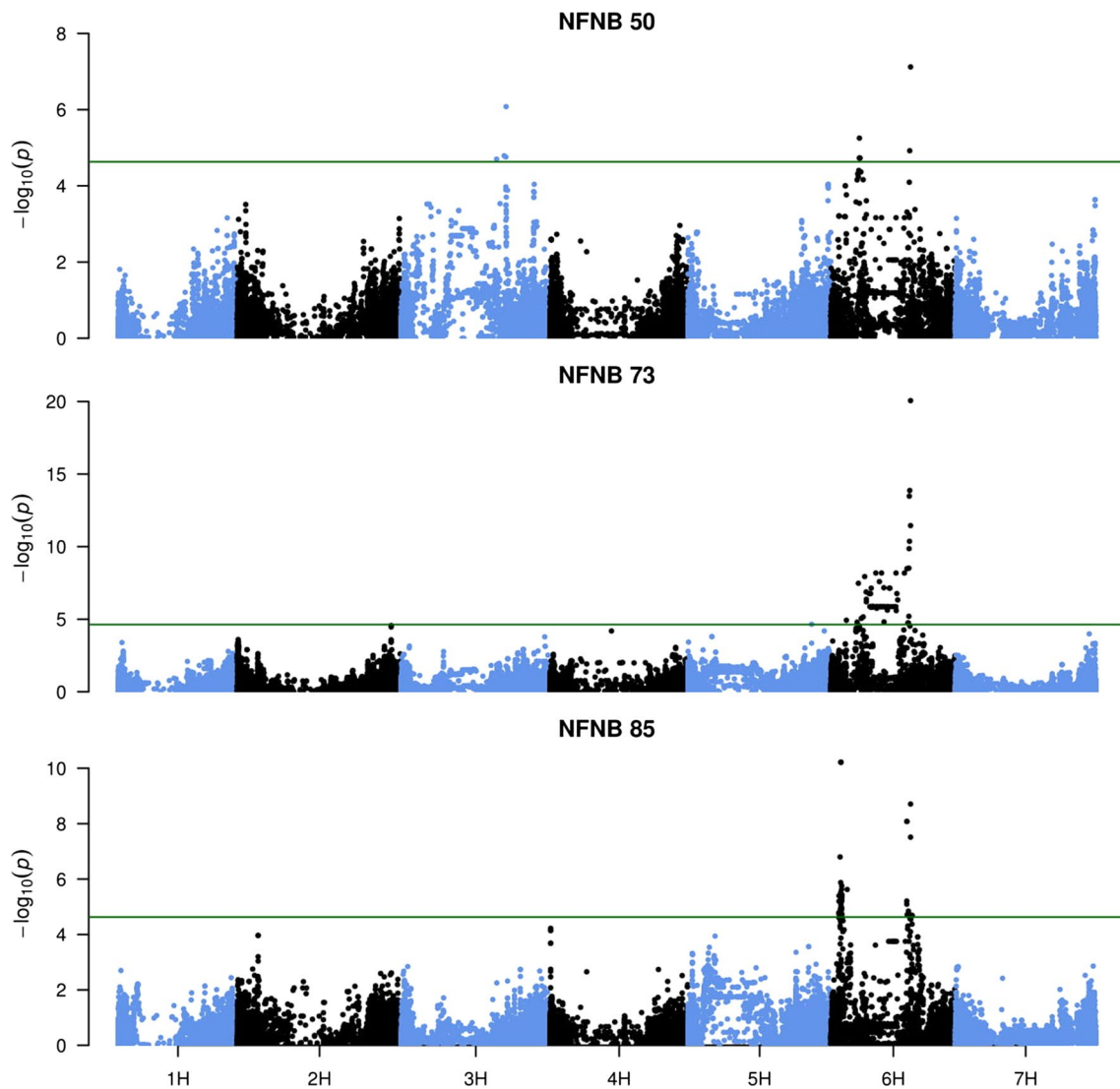


Fig. 5 Genome-wide association analyses of resistance to *Pyrenophora teres* f. *teres* isolates NFNB 50, NFNB 73 and NFNB 85 tested under field conditions in Warwick (Australia). The *x*-axis shows the seven barley chromosomes, positions are based on the

physical map, and the $-\log_{10}(p)$ value is displayed on the *y*-axis. The green horizontal line represents the significance threshold of $-\log_{10}(p)=4.63$

identified based on phenotypic data from the field trials at Zhodino and greenhouse trials using isolate *NFNB 50*, were located at 58–101 Mbp and 119–130 Mbp corresponding genetically to 46.29 and 46.68 cM, respectively. These MTAs are assumed to contribute resistance at seedling and adult plant stages. König et al. (2014) identified several regions on the short arm of chromosome 3H (QTLuHS-3H, QTLuHS-3H-1 and QTLuHS-3H-2), but with the data available it is not possible to determine whether it corresponds to our regions. The third region on chromosome 3H was mapped to 233–350 Mbp for data based on field trials in Zhodino. Physically, this appears to be a large interval, and Bayer et al. (2017) were not able to anchor markers located in this interval into a genetic map of their

RIL population. Physically, there is a gap between the two markers JHI-Hv50 k-2016-169770 (222.344564 Mbp) and JHI-Hv50 k-2016-175163 (352.146586 Mbp); however, genetically both markers are located at 47.07 cM (Bayer et al. 2017). The region is located near or in the centromere, where little recombination occurs, which explains the large physical interval. Graner et al. (1996) identified a gene on the long arm of chromosome 3H conferring resistance to *NFNB* designated *Pt.a*. In our study, two regions on chromosome 3HL were identified. The first spanned from 428 to 492 Mbp and was based on data from the field trials in Zhodino and the field and greenhouse trials with isolate *NFNB 50*, hence contributing to seedling and adult plant resistance. One of the significant associated markers in our studies was

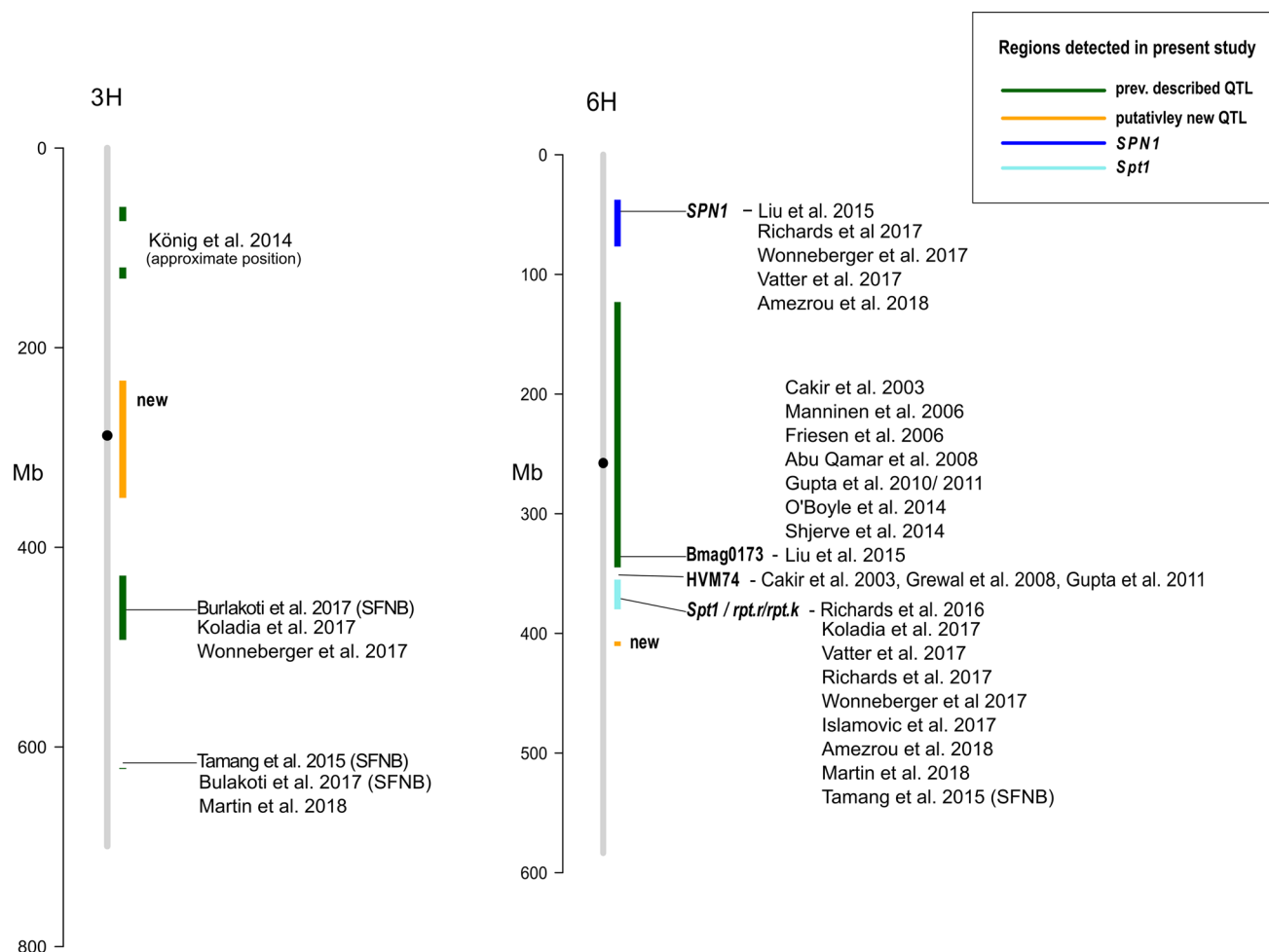


Fig. 6 QTLs for *P. teres* f. *teres* resistance in barley on chromosomes 3H and 6H. QTLs detected in the present study are represented by vertical bars. Previous studies reporting overlapping QTLs are shown next to the respective region

SCRI_RS_152172, which was also significantly associated with NFNB resistance in the study by Wonneberger et al. (2017a). Koladia et al. (2017) evaluated nine NFNB isolates and detected a QTL, which was significant for all these isolates, located at 490 Mbp with the peak marker being SCRI_RS_221644. Burlakoti et al. (2017) also found a QTL, which corresponds to our region. Interestingly, they conducted GWAS on resistance for the SFNB, indicating that even though both forms are genetically distinct, this region harbours resistance against both forms and is not isolate specific. The same holds true for the second region identified on chromosome 3HL located at 621 Mbp and identified from field data from Zhodino. Burlakoti et al. (2017) and Tamang et al. (2015), who both worked with SFNB, identified QTL on chromosome 3HL at 625 Mbp and 616–619 Mbp, respectively. Martin et al. (2018), also detected a QTL for NFNB resistance located at 622 Mbp by mapping a DH-population (UVC8 x SABBI Erica) and developed a PCR-based KASP marker (USQ3_1329) for use in breeding programmes.

On chromosome 4H, two regions harbouring NFNB resistance were identified. The first was located on the short arm of chromosome 4H at 33–70 Mbp and was detected from field trials at Zhodino and greenhouse trials with isolate *No 13*. This region corresponded to a QTL found by Islamovic et al. (2017), which was flanked by markers 4544–461 (46 Mbp) and 1944–1901 (76 Mbp) and was significantly associated with resistance for all four isolates tested. One of the isolates they used was *NFNB 50*, which was also tested in our study, but did not reveal any marker–trait association at this chromosomal region. The second region on chromosome 4H was located near the centromere at 352 Mbp. This region was found for seedling tests using isolate *No 13*. Wonneberger et al. (2017a) detected a QTL at 350 Mbp for seedling resistance and Steffenson et al. (1996) located a major QTL on chromosome 4H near the centromere for seedling resistance, which explained 31% of the phenotypic variance.

Two regions for NFNB resistance at the adult plant stage were detected on chromosome 5HL. The first region was detected using isolate *NFNB 73* and was located at 579 Mb. For this region, no overlap with previously published QTL was found. Based on the data from field trials in Zhodino, an association located at 634 Mbp was detected. The resistance locus *AL_QRptt5-2*, identified in a study using a DH-population of the cross Arve x Lavrans, and in a GWA study (Wonneberger et al. 2017a, b), is located in the same region (648–652 Mbp). In addition, Amezrou et al. (2018) detected a MTA at 624–629 Mbp and Grewal et al. (2012) mapped a QTL to the telomeric region of chromosome 5HL (199.4–206.3 cM).

Chromosome 6H is widely known to harbour several QTL for resistance/susceptibility to NFNB. In this study, four regions associated with resistance were detected (Fig. 6). The first region is located on chromosome 6HS between 37 and 76 Mbp and was detected for field trials in Quedlinburg, field trials using isolates *NFNB 73* and *NFNB 85* and for greenhouse trials using isolate *NFNB 50*. This region mapped to the sensitivity locus *SPN1*, which is flanked by the markers 4191-268 (47.261684 Mbp) and ABC08769-1-1-205 (91.140417 Mbp) (Liu et al. 2015). In that study, Liu et al. screened a RIL-population of Hector x NDB 112. The latter is a highly resistant, North American landrace, which was also included in our study and showed low infection responses for all experiments. Vatter et al. (2017) and Wonneberger et al. (2017a) both found associations at 46 Mbp, while Richards et al. (2017) identified MTAs for all isolates tested at between 42 and 66 Mbp. Interestingly, five of the markers identified in their study (SCRI_RS_162581, SCRI_RS_119674, SCRI_RS_142506, SCRI_RS_168111 and 12_30658), also revealed a significant MTA in our study. Finally, Amezrou et al. (2018) also identified a MTA at 66 Mbp. Furthermore, a large region spanning from 123 to 344 Mbp was detected based on the data for field trials in Zhodino, field trials using isolates *NFNB 50* and *NFNB 73*, and greenhouse trials using isolates *NFNB 50* and *Hoehnstedt*. Genetically, this region spanned from 53.52 to 53.91 cM (Bayer et al. 2017). Wonneberger et al. (2017a) and Islamovic et al. (2017) detected significant QTL at 120–164 Mbp and 340 Mbp (marker 5497-661), respectively. Martin et al. (2018) developed several PCR-based KASP markers for the identification of NFNB resistance QTL. Their marker USQ2_0799 is located at 335.741625 Mbp (Anke Martin, Centre for Crop Health, University of Southern Queensland, Toowoomba, QLD 4350, Australia, unpublished data) and co-located with the microsatellite marker Bmag0173 (67.4 cM). This microsatellite marker has long been associated with NFNB resistance and was used in several studies in the past (Abu Qamar et al. 2008; Cakir et al. 2003; Friesen et al. 2006; Gupta et al. 2010; Gupta et al. 2011; Liu et al. 2015; Manninen et al. 2006; O'Boyle et al. 2014;

Shjerve et al. 2014). The third region on chromosome 6H is located near the centromere at 355–379 Mbp and turned out to be significantly associated with NFNB resistance in all experiments, except field trials in Germany and Zhodino. Markers located in this interval could not be anchored genetically in the RIL population by Bayer et al. (2017). Similar to chromosome 3H, there is a gap on chromosome 6H in the region between markers JHI-Hv50 k-2016-397733 (344.799609 Mbp) and JHI-Hv50 k-2016-401495 (387.092035 Mbp). Genetically, they are located at 53.91 and 54.30 cM, respectively (Bayer et al. 2017). Nevertheless, this region corresponds to the major susceptibility locus *Spt1*, formerly named *rpt.r/ rpt.k* (Abu Qamar et al. 2008), and was fine-mapped by Richards et al. (2016). In their study, the markers rpt-M12, rpt-M13 and rpt-M20 co-segregated with the *Spt1* locus and corresponded to the Morex WGS contigs morex_contig_43862, morex_contig_64570 and morex_contig_37494, respectively. The contig morex_contig_64570 includes the iSelect marker SCRI_RS_176650, which is positioned at 373.424916 Mbp and significantly associated with resistance to isolates *No 13*, *NFNB 73* and *NFNB 85*. The gene is flanked by the markers rpt-M8 and SCRI_RS_165041 (384.412678 Mbp). Rpt-M8 corresponds to morex_contig_1573477, which includes the SNP markers SCRI_RS_171997 (370.428440 Mbp) and SCRI_RS_186193 (370.429069 Mbp). Hence, the locus is positioned between 370 and 384 Mbp. According to Richards et al. (2016) *Spt1* is delimited to 0.24 cM. This region contains 49 genes including 39 high-confidence genes with 6 genes encoding immunity receptor-like proteins. Moreover, this region was also identified via GWAS by Richards et al. (2017), Wonneberger et al. (2017a), Vatter et al. (2017) and Martin et al. (2018). In the latter study, PCR-based KASP markers were developed, namely USQ1_1140 (352 Mbp) and USQ3_0144 (384 Mb). The marker USQ1_1140 co-located with the microsatellite marker HVM 74 (68.0 cM), which was reported in several previous studies to be associated with resistance to NFNB (Cakir et al. 2003; Grewal et al. 2008; Gupta et al. 2011). In a study with SFNB, Tamang et al. (2015) identified significant MTAs at 370–373 Mbp for all isolates tested. One of the significant markers was the above-mentioned iSelect marker SCRI_RS_176650 (373.424916 Mbp). This suggests that *Spt1* does not only confer susceptibility to NFNB but also to SFNB and that this SNP (SCRI_RS_176650) can be very valuable for identifying resistant or susceptible genotypes. The last region on 6H is located at 406–410 Mbp and was identified from field trials in Quedlinburg. Amezrou et al. (2018) and Koladia et al. (2017) both reported a QTL at 390 Mbp and in both studies the marker SCRI_RS_140091 was one of the peak markers. Using the genetic map of Bayer et al. (2017), our region is located at 54.69 cM, while the region reported in the other two studies is located at 54.3 cM. Based on the

available data, it is not possible to determine whether the regions belong to one QTL or if they have to be considered as individual QTLs.

On chromosome 7H, two regions contributing to seedling resistance were identified. The first region was identified from greenhouse trials using isolate *NFNB 50* and was located on chromosome 7HS at 5 Mbp and consisted of one MTA (marker JHI_Hv50 k-2016-440870). Vatter et al. (2017) found significant associations at 2 Mbp. The second region was located on the long arm of chromosome 7H, consisted of five MTAs at 645 Mbp, and was based on greenhouse trials with isolate *No 13*. Richards et al. (2017) reported a QTL at 643 Mbp against all isolates tested. In a study by Martin et al. (2018), a QTL at 655 Mbp was reported from field trials using isolates *NFNB 50* and *NFNB 85*. These isolates were used in the present study as well, yet we did not detect any significant associations from our trials using these two isolates.

The set of barley accessions used in this study showed a genome-wide LD decay of 167 kb. Notably, for an inbreeding crop such as barley, this can be considered comparably low. LD decay in previous GWA studies in barley were estimated at 18 to 1.3 cM (Bellucci et al. 2017; Bengtsson et al. 2017; Burlakoti et al. 2017; Gyawali et al. 2017; Massman et al. 2010; Mitterbauer et al. 2017; Tamang et al. 2015; Vatter et al. 2017; Wehner et al. 2015; Wonneberger et al. 2017a). Burlakoti et al. (2017) evaluated a barley set of 376 advanced breeding lines from four breeding programmes from the Upper Midwest and reported LD decays between 10 and 18 cM. Wonneberger et al. (2017a) used a set comprising landraces and breeding lines predominantly originated from Norway, Sweden, Denmark and Finland and reported LD decay to be 13 cM. Vatter et al. (2017) used a nested association mapping (NAM) population (Maurer et al. 2015), where the spring barley cultivar Barke was crossed with 25 wild barley accessions originated from the Fertile Crescent. This population showed a LD decay of 8 cM. LD decays between 4 and 8 cM were also reported by Massman et al. (2010), Bellucci et al. (2017) and Tamang et al. (2015), who evaluated 768 advanced breeding lines from the Upper Midwest, 112 cultivated winter barleys from eleven European countries and 2062 geographically diverse barley cultivars, breeding lines and landraces, respectively. Mitterbauer et al. (2017) evaluated a set of 98 winter barleys comprising gene bank accessions and European cultivars released in different years and estimated LD decay at 1.3 cM. This shows that LD varies greatly between studies and is highly dependent on the material investigated. However, it gives an insight into the diversity of the genotypes involved. The barley accessions in the present study originated from almost

50 different countries from all over the world. The high diversity of the set was observed in the phenotypic reactions towards infection with *NFNB*, but is also reflected in the low LD. A low LD enables a high mapping resolution, which requires a high marker saturation (Zhu et al. 2008). With the 50 k iSelect chip (Bayer et al. 2017), this hurdle can be overcome. The chip comprises 44,040 SNP markers, of which 33,818 SNP markers were informative for the barley set investigated in the present study. This means, with a genome size of 5.1 Gb in barley, there was on average a marker every 150 kb. In combination with the physical map, it will enable researchers to define QTL more accurately. The centromeric region of chromosome 6H is a good example for this. This region has long been known to harbour several resistance/susceptibility QTL and has been described in many studies (Abu Qamar et al. 2008; Friesen et al. 2006; Gupta et al. 2010; Gupta et al. 2011; Liu et al. 2015; Martin et al. 2018; O'Boyle et al. 2014; Richards et al. 2016, 2017; Shjerve et al. 2014; Vatter et al. 2017; Wonneberger et al. 2017a). Two markers located in this region are the SSR markers Bmag0173 and HVM 74. These two markers were repeatedly reported to map to the same region. Martin et al. (2018) mapped them only 0.6 cM apart (Bmag0173: 67.4 cM, HVM 74: 68 cM). However, in the present study it was shown that they can be assigned to two different regions, located at 123–344 Mbp and 356–379 Mbp.

The aim of this study was to identify QTL for resistance against *NFNB* in a diverse barley set. The MTAs detected corresponded to 15 distinct regions and were located on barley chromosomes 3H, 4H, 5H, 6H and 7H. Eleven of these regions corresponded to QTL already described in previous studies, and seven regions were identified at the seedling and adult plant stage. The four putatively new QTL were located on chromosomes 3H at 233 to 350 Mbp, 5H at 579 Mbp, 6H at 406 to 410 Mbp and on chromosome 7H at 5 Mbp. Most regions were identified across several isolates and/or locations tested, which makes them interesting for breeding purposes, since they do not seem to be race-specific.

Author contribution statement OA and FO planned and managed the project. OK provided and characterized all accessions. AZ identified varieties and was involved in the resistance screening in field trials in Belarus. AA conducted the field screening in Russia. GJP was in charge of the screenings conducted in Australia (field and greenhouse). OA, FO, GJP and RS contributed to the interpretation and discussion of the results. FN conducted the field and greenhouse screenings in Germany, analysed the data and wrote the manuscript. OA contributed to the introduction and the material and methods parts of the manuscript.

Acknowledgements This research was supported by the German Research Society (DFG) (OR 72/11-1) and the Russian Foundation for Basic Research (RFBR) (No 15-54-12365 NNIO_a).

Compliance with ethical standards

Conflict of interest The authors declare that they have no conflicts of interest.

References

- Abu Qamar M et al (2008) A region of barley chromosome 6H harbors multiple major genes associated with net type net blotch resistance. *Theor Appl Genet* 117:1261–1270. <https://doi.org/10.1007/s00122-008-0860-x>
- Afanasenkov O (1995) Characteristics of resistance of barley accessions to different *Pyrenophora teres* populations. *Mycol Phytopathol* 29:27–32
- Afanasenkov O, Makarova I, Zubkovich A (1999) The number of genes controlling resistance to *Pyrenophora teres* Drechs. strains in barley. *Russ J Genet C/C Genet* 35:274–283
- Afanasenkov O, Jalli M, Pinnschmidt H, Filatova O, Platz G (2009) Development of an international standard set of barley differential genotypes for *Pyrenophora teres* f. *teres*. *Plant Pathol* 58:665–676
- Afanasenkov O et al (2015) Mapping of the loci controlling the resistance to *Pyrenophora teres* f. *teres* and *Cochliobolus sativus* in two double haploid barley populations. *Russ J Genet Appl Res* 5:242–253
- Afgan E et al (2016) The Galaxy platform for accessible, reproducible and collaborative biomedical analyses: 2016 update. *Nucleic Acids Res* 44:W3–W10. <https://doi.org/10.1093/nar/gkw343>
- Afonin A, Greene S, Dzyubenko N, Frolov A (2008) Interactive Agricultural ecological Atlas of Russia and Neighboring Countries. Economic Plants and their Diseases, Pests and Weeds. <http://www.agroatlas.ru/>. Accessed 26 Mar 2019
- Amezrou R et al (2018) Genome-wide association studies of net form of net blotch resistance at seedling and adult plant stages in spring barley collection. *Mol Breed* 38:1–14. <https://doi.org/10.1007/s11032-018-0813-2>
- Anisimova A, Novikova L, Novakazi F, Kopahnke D, Zubkovich A, Afanasenkov O (2017) Polymorphism on virulence and specificity of microevolution processes in populations of causal agent of barley net blotch *Pyrenophora teres* f. *teres*. *Mikol I Fitopatol* 51:229–240
- Bayer MM et al (2017) Development and evaluation of a barley 50 k iSelect SNP. *Array Front Plant Sci* 8:1792. <https://doi.org/10.3389/fpls.2017.01792>
- Bellucci A et al (2017) Genome-wide association mapping in winter barley for grain yield and culm cell wall polymer content using the high-throughput CoMPP technique. *PLoS ONE* 12:e0173313. <https://doi.org/10.1371/journal.pone.0173313>
- Bengtsson T, Manninen O, Jahoor A, Orabi J (2017) Genetic diversity, population structure and linkage disequilibrium in Nordic spring barley (*Hordeum vulgare* L. subsp. *vulgare*). *Genet Resour Crop Evolut* 64:2021–2033. <https://doi.org/10.1007/s10722-017-0493-5>
- Berger GL et al (2013) Marker-trait associations in Virginia Tech winter barley identified using genome-wide mapping. *Theor Appl Genet* 126:693–710
- Brandl F, Hoffmann G (1991) Differentiation of physiological races of *Drechslera teres* (Sacc.) Shoem., pathogen net blotch of barley. *Zeitschrift fuer Pflanzenkrankheiten und Pflanzenschutz*
- Burlakoti RR et al (2017) Genome-Wide Association Study of spot form of net blotch resistance in the upper midwest barley breeding programs. *Phytopathology* 107:100–108. <https://doi.org/10.1094/PHYTO-03-16-0136-R>
- Burleigh J, Tajani M, Seck M (1988) Effects of *Pyrenophora teres* and weeds on barley yield and yield components. *Phytopathology* 78:295–299
- Cakir M et al (2003) Mapping and validation of the genes for resistance to *Pyrenophora teres* f. *teres* in barley (*Hordeum vulgare* L.). *Aust J Agric Res* 54:1369–1377
- Cakir M et al (2011) Genetic mapping and QTL analysis of disease resistance traits in the barley population Baudin × AC Metcalfe. *Crop Pasture Sci* 62:152–161
- Campoy JA et al (2016) Genetic diversity, linkage disequilibrium, population structure and construction of a core collection of *Prunus avium* L. landraces and bred cultivars. *BMC Plant Biol* 16:49. <https://doi.org/10.1186/s12870-016-0712-9>
- Chang CC, Chow CC, Tellier LC, Vattikuti S, Purcell SM, Lee JJ (2015) Second-generation PLINK: rising to the challenge of larger and richer datasets. *Gigascience* 4:7. <https://doi.org/10.1186/s13742-015-0047-8>
- Douglas G, Gordon I (1985) Quantitative genetics of net blotch resistance in barley. *N Z J Agric Res* 28:157–164
- Earl DA, vonHoldt BM (2012) Structure harvester: a website and program for visualizing structure output and implementing the Evanno method. *Conserv Genet Resour* 4:359–361. <https://doi.org/10.1007/s12686-011-9548-7>
- Flint-Garcia SA, Thornsberry JM, Buckler ESt (2003) Structure of linkage disequilibrium in plants. *Annu Rev Plant Biol* 54:357–374. <https://doi.org/10.1146/annurev.arplant.54.031902.134907>
- Friesen TL, Faris JD, Lai Z, Steffenson BJ (2006) Identification and chromosomal location of major genes for resistance to *Pyrenophora teres* in a doubled-haploid barley population. *Genome* 49:855–859. <https://doi.org/10.1139/g06-024>
- Graner A, Foroughi-Wehr B, Tekauz A (1996) RFLP mapping of a gene in barley conferring resistance to net blotch (*Pyrenophora teres*). *Euphytica* 91:229–234
- Grewal TS, Rossmagel BG, Pozniak CJ, Scoles GJ (2008) Mapping quantitative trait loci associated with barley net blotch resistance. *Theor Appl Genet* 116:529–539. <https://doi.org/10.1007/s00122-007-0688-9>
- Grewal TS, Rossmagel BG, Scoles GJ (2012) Mapping quantitative trait loci associated with spot blotch and net blotch resistance in a doubled-haploid barley population. *Mol Breed* 30:267–279
- Gupta S et al (2004) Gene distribution and SSR markers linked with net type net blotch resistance in barley. In: 9th International Barley Genetics Symposium, 20–26 June. Czech Republic, Brno, pp 668–673
- Gupta S et al (2010) Quantitative trait loci and epistatic interactions in barley conferring resistance to net type net blotch (*Pyrenophora teres* f. *teres*) isolates. *Plant Breed* 129:362–368
- Gupta S, Li C, Loughman R, Cakir M, Westcott S, Lance R (2011) Identifying genetic complexity of 6H locus in barley conferring resistance to *Pyrenophora teres* f. *teres*. *Plant Breed* 130:423–429. <https://doi.org/10.1111/j.1439-0523.2011.01854.x>
- Gurung S et al (2011) Identification of novel genomic regions associated with resistance to *Pyrenophora tritici-repentis* races 1 and 5 in spring wheat landraces using association analysis. *Theor Appl Genet* 123:1029–1041. <https://doi.org/10.1007/s00122-011-1645-1>
- Gyawali S, Otte ML, Chao S, Jilal A, Jacob DL, Amezrou R, Verma RPS (2017) Genome wide association studies (GWAS) of element contents in grain with a special focus on zinc and iron in a world collection of barley (*Hordeum vulgare* L.). *J Cereal Sci* 77:266–274. <https://doi.org/10.1016/j.jcs.2017.08.019>

- Islamovic E, Bregitzer P, Friesen TL (2017) Barley 4H QTL confers NFNb resistance to a global set of *P. teres* f. *teres* isolates. Mol Breed 37:29. <https://doi.org/10.1007/s11032-017-0621-0>
- Kangas A, Jalli M, Kedonperä A, Laine A, Niskanen M, Salo Y, Vuorinen M, Jauhiainen L, Ramstad E 2005 Viljalajikkeiden herkkyyt tautitartunnoille virallisissa lajikekokeissa 1998–2005. Disease susceptibility of cereals in Finnish official variety trials. [English summary and titles] Agrifood Res Rep, MTT:n selvityksiä 96: 33
- Khan T (1982) Occurrence and pathogenicity of *Drechslera teres* isolates causing spot-type symptoms on barley in Western Australia. Plant Dis 66:423–425
- Koladia V, Faris J, Richards J, Brueggeman R, Chao S, Friesen T (2017) Genetic analysis of net form net blotch resistance in barley lines CIho 5791 and Tifang against a global collection of *P. teres* f. *teres* isolates. Theor Appl Genet 130:163–173
- König J, Perovic D, Kopahnke D, Ordon F (2013) Development of an efficient method for assessing resistance to the net type of net blotch (*Pyrenophora teres* f. *teres*) in winter barley and mapping of quantitative trait loci for resistance. Mol Breed 32:641–650. <https://doi.org/10.1007/s11032-013-9897-x>
- König J, Perovic D, Kopahnke D, Ordon F, Léon J (2014) Mapping seedling resistance to net form of net blotch (*Pyrenophora teres* f. *teres*) in barley using detached leaf assay. Plant Breed 133:356–365. <https://doi.org/10.1111/pbr.12147>
- Lex J, Ahlemeyer J, Friedt W, Ordon FJ (2014) Genome-wide association studies of agronomic and quality traits in a set of German winter barley (*Hordeum vulgare* L.) cultivars using Diversity Arrays Technology (DART). J Appl Genet 55:295–305
- Lightfoot DJ, Able AJ (2010) Growth of *Pyrenophora teres* in planta during barley net blotch disease. Australas Plant Pathol 39:499–507
- Lipka AE et al (2012) GAPIT: genome association and prediction integrated tool. Bioinformatics 28:2397–2399
- Liu Z, Ellwood SR, Oliver RP, Friesen TL (2011) *Pyrenophora teres*: profile of an increasingly damaging barley pathogen. Mol Plant Pathol 12:1–19. <https://doi.org/10.1111/j.1364-3703.2010.00649.x>
- Liu Z, Holmes DJ, Faris JD, Chao S, Brueggeman RS, Edwards MC, Friesen TL (2015) Necrotrophic effector-triggered susceptibility (NETS) underlies the barley-*Pyrenophora teres* f. *teres* interaction specific to chromosome 6H. Mol Plant Pathol 16:188–200. <https://doi.org/10.1111/mpp.12172>
- Ma Z, Lapitan NL, Steffenson B (2004) QTL mapping of net blotch resistance genes in a doubled-haploid population of six-rowed barley. Euphytica 137:291–296
- Manninen OM, Jalli M, Kalendar R, Schulman A, Afanasenko O, Robinson J (2006) Mapping of major spot-type and net-type net-blotch resistance genes in the Ethiopian barley line CI 9819. Genome 49:1564–1571. <https://doi.org/10.1139/g06-119>
- Martin A, Platz GJ, de Klerk D, Fowler RA, Smit F, Potgieter FG, Prins R (2018) Identification and mapping of net form of net blotch resistance in South African barley. Mol Breed 38:53. <https://doi.org/10.1007/s11032-018-0814-1>
- Mascher M et al (2017) A chromosome conformation capture ordered sequence of the barley genome. Nature 544:427–433. <https://doi.org/10.1038/nature22043>
- Massman J et al (2010) Genome-wide association mapping of Fusarium head blight resistance in contemporary barley breeding germplasm. Mol Breed 27:439–454. <https://doi.org/10.1007/s11032-010-9442-0>
- Mathre D (1997) Compendium of Barley Diseases. The American Phytopathological Society, St. Paul, MN
- Maurer A et al (2015) Modelling the genetic architecture of flowering time control in barley through nested association mapping. BMC Genom 16:290
- Mitterbauer E et al (2017) Growth response of 98 barley (*Hordeum vulgare* L.) genotypes to elevated CO₂ and identification of related quantitative trait loci using genome-wide association studies. Plant Breed 136:483–497. <https://doi.org/10.1111/pbr.12501>
- Mohammadi M et al (2015) A genome-wide association study of malting quality across eight US barley breeding programs. Theor Appl Genet 128:705–721. <https://doi.org/10.1007/s00122-015-2465-5>
- Moll E, Flath K, Tessenow I (2010) Assessment of resistance in cereal cultivars Design and analysis of experiments using the SAS-application RESI 2 Berichte aus dem Julius Kühn-Institut: 154
- Muqaddasi QH, Reif JC, Li Z, Basnet BR, Dreisigacker S, Röder MS (2017) Genome-wide association mapping and genome-wide prediction of anther extrusion in CIMMYT spring wheat. Euphytica 213:73. <https://doi.org/10.1007/s10681-017-1863-y>
- Murray GM, Brennan JP (2009) The current and potential costs from diseases of barley in Australia. Grains Research and Development Corporation, Barton
- Nordborg M et al (2002) The extent of linkage disequilibrium in Arabidopsis thaliana. Nat Genet 30:190–193. <https://doi.org/10.1038/ng813>
- O’Boyle P et al (2014) Mapping net blotch resistance in ‘Nomini’ and CIho 2291 barley. Crop Sci 54:2596–2602
- Poland JA, Brown PJ, Sorrells ME, Jannink JL (2012) Development of high-density genetic maps for barley and wheat using a novel two-enzyme genotyping-by-sequencing approach. PLoS ONE 7:e32253. <https://doi.org/10.1371/journal.pone.0032253>
- Pritchard JK, Stephens M, Donnelly P (2000) Inference of population structure using multilocus genotype data. Genetics 155:945–959
- Rafalski A, Morgante M (2004) Corn and humans: recombination and linkage disequilibrium in two genomes of similar size. Trends Genetics 20:103–111
- Raman H, Platz G, Chalmers K, Raman R, Read B, Barr A, Moody D (2003) Mapping of genomic regions associated with net form of net blotch resistance in barley. Aust J Agric Res 54:1359–1367
- Reif JC, Melchinger AE, Frisch M (2005) Genetical and mathematical properties of similarity and dissimilarity coefficients applied in plant breeding and seed bank management. Crop Sci 45:1–7
- Remington DL et al (2001) Structure of linkage disequilibrium and phenotypic associations in the maize genome. Proc Natl Acad Sci 98:11479–11484
- Richards J, Chao S, Friesen T, Brueggeman R (2016) Fine mapping of the barley chromosome 6H net form net blotch susceptibility locus. G3 (Bethesda) 6:1809–1818. <https://doi.org/10.1534/g3.116.028902>
- Richards JK, Friesen TL, Brueggeman RS (2017) Association mapping utilizing diverse barley lines reveals net form net blotch seedling resistance/susceptibility loci. Theor Appl Genet 130:915–927. <https://doi.org/10.1007/s00122-017-2860-1>
- Richter K, Schondelmaier J, Jung C (1998) Mapping of quantitative trait loci affecting *Drechslera teres* resistance in barley with molecular markers. Theor Appl Genet 97:1225–1234
- Robinson J, Jalli M (1997) Quantitative resistance to *Pyrenophora teres* in six Nordic spring barley accessions. Euphytica 94:201–208
- Rode J, Ahlemeyer J, Friedt W, Ordon F (2011) Identification of marker-trait associations in the German winter barley breeding gene pool (*Hordeum vulgare* L.). Mol Breed 30:831–843. <https://doi.org/10.1007/s11032-011-9667-6>
- Saari E, Prescott J (1975) Scale for appraising the foliar intensity of wheat diseases. Plant Disease Reporter 59:377–380
- Sannemann W, Huang BE, Mathew B, Léon J (2015) Multi-parent advanced generation inter-cross in barley: high-resolution quantitative trait locus mapping for flowering time as a proof of concept. Mol Breed 35:86

- Serenius M (2006) Population structure of *Pyrenophora teres*, the causal agent of net blotch of barley (Doctoral Dissertation). Agri-food Research Reports 78:60
- Shjerve RA, Faris JD, Brueggeman RS, Yan C, Zhu Y, Koladia V, Friesen TL (2014) Evaluation of a *Pyrenophora teres* f. *teres* mapping population reveals multiple independent interactions with a region of barley chromosome 6H. *Fungal Genet Biol* 70:104–112. <https://doi.org/10.1016/j.fgb.2014.07.012>
- Silvar C et al (2010) Screening the Spanish barley core collection for disease resistance. *Plant Breed* 129:45–52
- Simmonds J et al (2014) Identification and independent validation of a stable yield and thousand grain weight QTL on chromosome 6A of hexaploid wheat (*Triticum aestivum* L.). *BMC Plant Biol* 14:191
- Smedegård-Petersen V (1971) *Pyrenophora teres* f. *maculata* f. nov. and *Pyrenophora teres* f. *teres* on barley in Denmark. *Yearb R Vet Agric Univ (Copenhagen)* 1971:124–144
- Smedegård-Petersen V (1976) Pathogenesis and genetics of net-spot blotch and leaf stripe of barley caused by *Pyrenophora teres* and *Pyrenophora graminea* (Doctoral Dissertation) Copenhagen, p 176
- Steffenson BJ, Webster R (1992) Quantitative resistance to *Pyrenophora teres* f. *teres* in barley. *Phytopathology* 82:407–411
- Steffenson B, Hayes P, Kleinhofs A (1996) Genetics of seedling and adult plant resistance to net blotch (*Pyrenophora teres* f. *teres*) and spot blotch (*Cochliobolus sativus*) in barley. *Theor Appl Genet* 92:552–558
- Stein N, Herren G, Keller B (2001) A new DNA extraction method for high-throughput marker analysis in a large-genome species such as *Triticum aestivum*. *Plant Breed* 120:354–356
- Storey JD, Tibshirani R (2003) Statistical significance for genomewide studies. *Proc Natl Acad Sci* 100:9440–9445
- Tamang P, Neupane A, Mamidi S, Friesen T, Brueggeman R (2015) Association mapping of seedling resistance to spot form net blotch in a worldwide collection of barley. *Phytopathology* 105:500–508. <https://doi.org/10.1094/PHYTO-04-14-0106-R>
- Tekauz A (1985) A numerical scale to classify reactions of barley to *Pyrenophora teres*. *Can J Plant Pathol* 7:181–183
- Tekauz A (1990) Characterization and distribution of pathogenic variation in *Pyrenophora teres* f. *teres* and *P. teres* f. *maculata* from western Canada. *Can J Plant Pathol* 12:141–148
- Trofimovskaya AY, Afanasenko O, Levitin MM (1983) Sources of barley resistance to the causal agent of net blotch (*Drechslera teres*). *Rep Acad Agricu Sci* 3:19–21
- Vatter T, Maurer A, Kopahnke D, Perovic D, Ordon F, Pillen K (2017) A nested association mapping population identifies multiple small effect QTL conferring resistance against net blotch (*Pyrenophora teres* f. *teres*) in wild barley. *PLoS ONE* 12:e0186803. <https://doi.org/10.1371/journal.pone.0186803>
- Wallwork H, Butt M, Capio E (2016) Pathogen diversity and screening for minor gene resistance to *Pyrenophora teres* f. *teres* in barley and its use for plant breeding. *Australas Plant Pathol* 45:527–531
- Wang H, Smith KP, Combs E, Blake T, Horsley RD, Muehlbauer GJ (2012) Effect of population size and unbalanced data sets on QTL detection using genome-wide association mapping in barley breeding germplasm. *Theor Appl Genet* 124:111–124. <https://doi.org/10.1007/s00122-011-1691-8>
- Wehner GG, Balko CC, Enders MM, Humbeck KK, Ordon FF (2015) Identification of genomic regions involved in tolerance to drought stress and drought stress induced leaf senescence in juvenile barley. *BMC Plant Biol* 15:125
- Wonneberger R, Ficke A, Lillemo M (2017a) Identification of quantitative trait loci associated with resistance to net form net blotch in a collection of Nordic barley germplasm. *Theor Appl Genet* 130:2025–2043. <https://doi.org/10.1007/s00122-017-2940-2>
- Wonneberger R, Ficke A, Lillemo M (2017b) Mapping of quantitative trait loci associated with resistance to net form net blotch (*Pyrenophora teres* f. *teres*) in a doubled haploid Norwegian barley population. *PLoS ONE* 12:e0175773. <https://doi.org/10.1371/journal.pone.0175773>
- Yan J, Shah T, Warburton ML, Buckler ES, McMullen MD, Crouch JJ (2009) Genetic characterization and linkage disequilibrium estimation of a global maize collection using SNP markers. *PLoS ONE* 4:e8451
- Zhang Z et al (2010) Mixed linear model approach adapted for genome-wide association studies. *Nat Genet* 42:355
- Zhu C, Gore M, Buckler ES, Yu J (2008) Status and prospects of association mapping in plants. *Plant Genome J* 1:5–20. <https://doi.org/10.3835/plantgenome2008.02.0089>

Publisher's Note Springer Nature remains neutral with regard to jurisdictional claims in published maps and institutional affiliations.



5 Genome-wide association studies in a barley diversity set reveal a limited number of loci for resistance to spot blotch

Novakazi F, Afanasenko O, Lashina N, Platz GJ, Snowdon R, Loskutov I, Ordon F.

Plant Breeding, 00, 1-15

DOI: 10.1111/pbr.12792

Genome-wide association studies in a barley (*Hordeum vulgare*) diversity set reveal a limited number of loci for resistance to spot blotch (*Bipolaris sorokiniana*)

Fluturë Novakazi¹  | Olga Afanasenko² | Nina Lashina² | Gregory J. Platz³ | Rod Snowdon⁴  | Igor Loskutov⁵ | Frank Ordon¹

¹Institute for Resistance Research and Stress Tolerance, Julius Kuehn-Institute, Quedlinburg, Germany

²All-Russian Research Institute of Plant Protection, St. Petersburg, Russia

³Queensland Department of Agriculture and Fisheries, Hermitage Research Facility, Warwick, QLD, Australia

⁴Department of Plant Breeding, Land Use and Nutrition, IFZ Research Centre for Biosystems, Justus Liebig University, Giessen, Germany

⁵N. I. Vavilov Institute of Plant Genetic Resources, St. Petersburg, Russia

Correspondence

Frank Ordon, Julius Kuehn-Institute, Institute for Resistance Research and Stress Tolerance, Quedlinburg, Germany.
Email: frank.ordon@julius-kuehn.de

Funding information

Deutsche Forschungsgemeinschaft, Grant/Award Number: OR 72/11-1; Russian Foundation for Basic Research, Grant/Award Number: No 15-54-12365 NNIO_a

Communicated by: Thomas Miedaner

Abstract

Spot blotch caused by *Bipolaris sorokiniana* is an important disease in barley worldwide, causing considerable yield losses and reduced grain quality. In order to identify QTL conferring resistance to spot blotch, a highly diverse worldwide barley set comprising 449 accessions was phenotyped for seedling resistance with three isolates (No 31, SH 15 and SB 61) and for adult plant resistance at two locations (Russia and Australia) in two years. Genotyping with the 50 k iSelect barley SNP genotyping chip yielded 33,818 informative markers. Genome-wide association studies (GWAS) using a compressed mixed linear model, including population structure and kinship, revealed 38 significant marker-trait associations (MTA) for spot blotch resistance. The MTA corresponded to two major QTL on chromosomes 1H and 7H and a putative new minor QTL on chromosome 7H explaining between 2.79% and 13.67% of the phenotypic variance. A total of 10 and 14 high-confidence genes were identified in the respective major QTL regions, seven of which have a predicted involvement in pathogen recognition or defence.

KEYWORDS

Bipolaris sorokiniana, genetic diversity, Genome-wide Association Study, *Hordeum vulgare*, resistance, spot blotch

1 | INTRODUCTION

The fungal pathogen *Bipolaris sorokiniana* (Sacc.) Shoem. (teleomorph: *Cochliobolus sativus* (Ito & Kurib.) Drechs. ex Dastur) is present in all cereal growing regions with warm and humid conditions, but its importance is also increasing in the Americas and Europe (Gupta et al., 2018). *Bipolaris sorokiniana* is the causal agent of a number of diseases such as common root rot, seedling blight, black point and spot blotch (Kumar et al., 2002). This hemi-biotrophic

fungus has a wide host range and is pathogenic on a number of plant species, such as bread and durum wheat (*Triticum aestivum* and *T. durum*), barley (*Hordeum vulgare*), triticale (x *Triticosecale*), rye (*Secale cereal*), maize (*Zea mays*), rice (*Oryza sativa*), pearl and fox millet (*Pennisetum glaucum* and *Setaria italica*) and several other wild grasses (Acharya, Dutta, & Pradhan, 2011; Gupta et al., 2018; Kumar et al., 2002). First reported in 1914, it became an important pathogen mainly with the beginning of the Green Revolution when semi-dwarf wheat cultivars turned out to be highly susceptible

This is an open access article under the terms of the Creative Commons Attribution License, which permits use, distribution and reproduction in any medium, provided the original work is properly cited.

© 2019 The Authors. *Plant Breeding* published by Blackwell Verlag GmbH

(Gupta et al., 2018). Yield losses between 4% and 43% in South Asia, 18% to 22% in India and 10% to 20% in Scotland, Canada and Brazil have been reported (Murray et al., 1998; Sharma, Duveiller, & Sharma, 2006; Singh et al., 1998). In Nepal in wheat–rice growing systems, yield losses went up to 70% to 100% (Sharma & Duveiller, 2007), showing that short crop rotations or crop rotations with high proportions of cereal crops foster the disease. Apart from yield losses, the pathogen also has a negative effect on grain quality, which is of special importance with respect to malting barley. The disease severity is greatly affected by crop management practices, soil fertility, plant density and developmental stage, and abiotic conditions (Acharya et al., 2011; Gupta et al., 2018). Due to this and the wide host range, it is difficult to control the disease solely by agricultural practices.

In barley, the most important disease caused by *B. sorokiniana* is spot blotch. Symptoms appear on all aboveground plant parts as long, dark-brown necrotic blotches with chlorosis in later stages and are up to several centimetres in length (Acharya et al., 2011; Mathre, 1997). The fungus survives as conidia on plant debris and volunteer plants in the field as well as in soil and on seeds or as mycelium in infected plant tissue. Infected seeds are considered the primary source of inoculum. Primary infection starts with conidia germinating on the leaf (within 4 hr), formation of an appressorium (8 hr) and the penetration of the cuticle by infection hyphae (12 hr). The fungus multiplies and spreads into the intercellular space of the mesophyll from where further plant cells are infected. The hyphae eventually produce conidiophores, which appear through the stomata carrying new conidia. Under optimal conditions, a new generation of conidia is produced within 48h which makes it a highly epidemic disease with several infection cycles within one season (Acharya et al., 2011; Gupta et al., 2018). The sexual stage is of no importance in the disease cycle and has only been observed under natural conditions in Zambia (Raemaekers, 1988). Nonetheless, the existence of two mating types (A and a) was shown (Tinline, 1951) and isolates show high variability especially in the interaction with *H. vulgare* (Gupta et al., 2018).

The presence of pathotypes was first described by Valjavec-Gratian and Steffenson (1997). In their study, they evaluated the virulence patterns of 33 isolates from the United States, China and Japan on three barley genotypes, ND 5883, Bowman and ND B112, and found three pathotypes designated 0, 1 and 2. Leng, Wang, Ali, Zhao, and Zhong (2016) screened over 2000 barley accessions with isolate ND4008 from North Dakota and identified a new pathotype they designated pathotype 7. Arabi and Jawhar (2002, 2004) identified three different pathotypes among over 120 *B. sorokiniana* isolates from Syria. Meldrum, Platz, and Ogle (2004) identified six pathotypes among 34 Australian isolates and Ghazvini and Tekauz (2007) identified eight virulence groups among 92 Canadian isolates belonging to one of the three pathotypes (0, 1, 2) described by Valjavec-Gratian and Steffenson (1997).

Quantitative trait loci (QTL) for resistance against spot blotch have been identified on all seven barley chromosomes. Many have been identified via traditional bi-parental mapping (Bilgic, Steffenson, & Hayes, 2005, 2006; Bovill et al., 2010; Grewal, Rossnagel, & Scoles,

2012; Haas, Menke, Chao, & Steffenson, 2016; Steffenson, Hayes, & Kleinhofs, 1996; Yun et al., 2006, 2005) and others through the use of genome-wide association studies (GWAS) (Berger et al., 2013; Bykova, Lashina, Efimov, Afanasenko, & Khlestkina, 2017; Gutiérrez et al., 2015; Gyawali et al., 2018; Roy et al., 2010; Wang, Leng, Ali, Wang, & Zhong, 2017; Zhou & Steffenson, 2013). To date, three resistance genes have been fine-mapped. Resistance gene *Rcs 5* was initially described by Steffenson et al. (1996) and verified by Bilgic et al. (2005). Drader, Johnson, Brueggeman, Kudrna, and Kleinhofs (2009) narrowed the interval down to 2.8 cM located within bin 3 on chromosome 7H of the Morex genome. Bilgic et al. (2006) identified a resistance gene; they designated *Rcs 6* on chromosome 1H in a double-haploid population of Calicuchima-sib × Bowman-BC. Just recently, Leng et al. (2018) identified the corresponding susceptibility gene *Scs 6* and were able to anchor it to a 125 kb region on the short arm of chromosome 1H between 63,571 and 192,067 bp. Based on their data, Leng et al. (2018) postulated that *Rcs 6* and *Scs 6* are located at the same locus and that *Scs 6* is the dominant allele. In a GWAS study with 1,480 barley accessions, Wang et al. (2017) identified, among others, a QTL on the short arm of chromosome 6H for resistance against pathotype 7 using isolate ND4008. This was later anchored to an interval between 13,136,710 and 13,370,566 bp and designated *Rbs 7* (Wang, Leng, Zhao, & Zhong, 2019). This interval contains five low-confidence and ten high-confidence genes.

Resistant cultivars are pivotal for controlling this disease and the emergence of new pathotypes renders the identification of new resistance sources an ongoing task. Therefore, the aims of this study were (a) to screen a diverse barley set for resistance against *B. sorokiniana* under controlled and field conditions, (b) to identify QTL for resistance by employing genome-wide association studies and (c) to compare the detected regions with previously described QTL to identify putatively new loci and closely linked markers.

2 | MATERIAL AND METHODS

2.1 | Plant material

The association panel set comprised 449 *H. vulgare* (L.) accessions, including 277 barley landraces and 172 commercial cultivars, which were obtained from the N. I. Vavilov Research Institute of Plant Genetic Resources (VIR). The accessions are derived from different regions of the world and express different levels of resistance to *B. sorokiniana*. The panel includes 178 two-rowed and 271 six-rowed accessions. A total of 51 accessions have naked kernels, 28 have black kernels, and 20 are winter-types. For more detailed information on the accessions, see Novakazi et al. (2019).

2.2 | Fungal isolates

Four single-spore *B. sorokiniana* isolates were used in this study. Isolates No 31 and Cher 3 were collected in 2012 and 2015,

respectively, near Volosovo in the Leningrad region in the north-west of Russia. *Cher 3* was previously used by Bykova et al. (2017) for its high aggressiveness. Isolate *SH 15* was collected in 2015 on fields in Quedlinburg (JKI site) in Germany. Isolate *SB 61* was collected in 1998 from the fields in Monto, Queensland, Australia, and was used in glasshouse and field trials.

Spot blotch isolates *No 31* and *SH 15* were grown on SNA medium containing (g per 1L): 1 g KH_2PO_4 , 1 g KNO_3 , 0.5 g $\text{MgSO}_4 \cdot 7\text{H}_2\text{O}$, 0.5 g KCl, 0.5 g glucose, 0.5 g sucrose, 15 g phytoagar and 75 g cellulose. Isolates were grown at 23°C under UV-light (12 hr/day) for 12 to 14 days. The culture was then flooded with distilled water, and conidia were harvested with a sterile spatula and filtered through gauze to remove mycelial fragments. Conidia concentration was adjusted to 6,000 conidia/ml using a haemocytometer. Isolate *SB 61* was grown as described by Bovill et al. (2010), and conidial concentration was adjusted to 6,500 conidia/ml for phenotyping seedlings in the glasshouse.

The inoculum for the field trial with isolate *SB 61* was propagated in the laboratory and applied to blocks of very susceptible varieties in the field, which were sown in early to mid-April. When necessary infection was promoted by sprinkler irrigation at least twice a week, these blocks provided heavily infected plant material as inoculum for the subsequent field screening (Martin et al., 2018).

2.3 | Glasshouse experiments

Glasshouse trials with isolates *No 31* and *SH 15* were conducted at the Julius Kuehn-Institute in Quedlinburg, Germany, in 2016, and set up in four replications as complete randomized blocks. Accessions were grown in plastic pots (8 × 8 × 8 cm) with three seeds per accession at 16–18°C with alternating light/darkness periods of 12 hr (5,000 lux). When the second leaf was fully expanded (BBCH 12–13), the plants were spray-inoculated with approximately 1 ml spore suspension/pot and immediately covered with plastic foil for 48 hr to ensure 100% humidity. Inoculated plants were grown at 22–24°C and 70% humidity for another 7 to 10 days until symptoms were clearly developed.

Isolate *SB 61* was tested at the Hermitage Research Facility in Warwick, Queensland, Australia, in 2017, in two replications as incomplete blocks, with pots corresponding to blocks with three lines per block. Four to five seeds were sown at 0, 120 and 240° around the circumference of each pot (10 cm diameter, 17 cm tall) in commercial potting mix (Searles Premium Potting Mix) and grown at 15/25°C. At BBCH, 12–13 plants were inoculated from four directions using a WallWick® commercial spray gun applying an average 3 ml inoculum/pot. Inoculated plants were kept at 19°C in a dark fogging chamber for 24 hr. Incubated plants were moved to the glasshouse and grown at 15/25°C for another nine days.

Infection response type was assessed on the second leaf of each plant following the scale of Fetch and Steffenson (1999).

2.4 | Field experiments

Field experiments were conducted at two locations in Russia, that is Pushkin and Volosovo in 2016 and 2017, and at one location – Cleveland, in Queensland, Australia in 2017.

Experiments in Russia were conducted at the N. I. Vavilov Research Institute of Plant Industry (VIR) in Pushkin, Saint Petersburg, and at the Federal State Budget Institution “State Commission of the Russian Federation on Testing and Protection of Selection Achievements” in Volosovo, Leningrad Region, in 2016 and 2017. Accessions were sown in rows of 1 m with 15–20 seeds per row and a spacing of 0.3 m between rows. The trials were set up in a complete randomized block design with three replications. The susceptible cultivar ‘Cherio’ was sown around the trials as a border and after every 10th accession to support *B. sorokiniana* infection. To increase infection, all accessions were spray inoculated at the seedling stage with a mix of two spot blotch isolates (*No 31* and *Cher 3*) with a spore concentration of 20,000 conidia/ml. The percentage of leaf area infected was assessed at three time points during the growing period. The first assessment was conducted at BBCH 32–33, the second at BBCH 69–71 and the third at BBCH 83–85. The area under disease progress curve (AUDPC) and the average ordinate (AO) were calculated as described by Vatter et al. (2017).

Field experiments in Australia were conducted at the Redlands Research Facility, Cleveland, in 2017 with one distinct isolate (*SB 61*). Accessions were sown in hill plots with 0.5 m and 0.76 m in-row and between-row spacing. Spreaders were sown between every other plot-row about 2–3 weeks before the plots. Infected green plant material from the inoculum increase blocks was used as inoculum when the spreaders were at about BBCH 30. To ensure infection and enhance epidemics, overhead sprinkler irrigation was applied in the late afternoon and/or early evening two or more nights per week when conditions were favourable for infection; so that the nurseries remained wet overnight. Infection responses were taken on a whole plot basis using a variant of the scale by Saari and Prescott (1975) (0 to 9 scale) at BBCH stages 70–73. It takes into account the plant response (infection type; IT), and the amount of disease per plot and therefore correlates very well with the standard leaf area diseased measurement.

2.5 | Statistical analysis

Statistical analyses and analysis of variance (ANOVA) were performed using the software package SAS 9.4 (SAS Institute Inc.) using *proc glimmix* and *proc mixed*. For field trials in Pushkin and Volosovo, the least square means (lsmeans) of the average ordinates (AO) across years were calculated for each location separately. The genotype was treated as a fixed effect, the year and the year*genotype interaction were set as random effects. For glasshouse trials and the field trial in Cleveland, the means of the infection responses were calculated for each isolate separately. Lsmeans and means for each location and isolate, respectively, were used as phenotypic input data for subsequent genome-wide

association studies (GWAS). Broad sense heritability across years was calculated using the formula:

$$h^2 = V_G / (V_G + V_{GY}/y + (V_R/yr))$$

as described by Vatter et al. (2017), where V_G is genotypic variance, V_{GY} is genotype \times year variance, V_R is residual variance, and y and r are the number of years and replicates, respectively.

2.6 | Genotyping, population structure, kinship and linkage disequilibrium

Genomic DNA was extracted from 14-day-old plantlets according to Stein, Herren, and Keller (2001). Accessions were genotyped on the Illumina iSelect 50k Barley SNP Chip at Trait Genetics GmbH. SNPs with failure rates >10%, heterozygous calls >12.5% and a minor allele frequency (MAF) <5% were excluded from the analyses, as well as unmapped SNPs, leaving 33,818 SNPs for subsequent GWAS. Further filtering of the SNPs was done with the software PLINK 1.9 (www.cog-genomics.org/plink/1.9/) (Chang et al., 2015). The tool *LD prune* was used with the following parameters: indep pairwise window size 50, step 5 and r^2 threshold 0.5 (Campoy et al., 2016). The resulting 8,533 markers were used to calculate the kinship and population structure. With the web-based platform Galaxy (Afgan et al., 2016) using the tool *Kinship* and the Modified Roger's Distance, the kinship was calculated (Reif, Melchinger, & Frisch, 2005). Population structure was determined with the software STRUCTURE v2.3.4 (Pritchard, Stephens, & Donnelly, 2000) with a burn-in of 50,000, followed by 50,000 Monte Carlo Markov chain (MCMC) replications for $k = 1$ to $k = 10$ with 10 iterations. The optimal k was identified using STRUCTURE HARVESTER (Earl & vonHoldt, 2012), followed by a new STRUCTURE analysis with a burn-in of 100,000 and 100,000 MCMC iterations at the optimal k value. Accessions with membership probabilities <80% were considered as admixtures (Richards, Friesen, & Brueggeman, 2017). Physical positions of markers were obtained from Bayer et al. (2017), which is based on the barley pseudomolecule assembly by Mascher et al. (2017). The tool *linkage disequilibrium* in the web-based platform Galaxy was used to calculate the linkage disequilibrium (LD) as squared allele frequency correlations (R^2) between all intra-chromosomal marker pairs. Genome-wide LD decay was plotted as R^2 of a marker against the corresponding genetic distance, and a Loess regression was computed. For R^2 , the default settings were used (Novakazi et al., 2019; Sannemann, Huang, Mathew, & Léon, 2015).

2.7 | Association analyses

Genome-wide association studies (GWAS) were performed as described in Novakazi et al. (2019) using the Galaxy implemented tool GAPIIT, which uses the R package GAPIIT (Lipka et al., 2012). A compressed mixed linear model (CMLM) (Zhang et al., 2010) including the

population structure (Q) and kinship (K) was used. A Bonferroni corrected significance threshold was determined, based on the reduced marker set of 8,533 SNPs and a significance level of $p = .2$ (Muqaddasi et al., 2017; Storey & Tibshirani, 2003). This resulted in a threshold of logarithm of odds (LOD) ≥ 4.63 . GWAS for field trials in Pushkin, Russia, was conducted across years. GWAS for glasshouse trials and the field trial in Australia were conducted for each isolate separately. Manhattan plots were generated with the R v.3.4.4 package *qqman*.

The databases GrainGenes (<https://wheat.pw.usda.gov/GG3/>) and BARLEX (<https://apex.ipk-gatersleben.de/apex/f?p=284:10>) were used to identify physical positions of previously published QTL in order to compare them with QTL identified in the present study. If the previously described QTL were identified based on iSelect markers, the physical positions were obtained from Bayer et al. (2017).

Predicted genes, their locations and annotations were retrieved from the BARLEYMAP website (Cantalapiedra, Boudiar, Casas, Igartua, & Contreras-Moreira, 2015) (<http://floresta.eead.csic.es/barleymap/>).

3 | RESULTS

3.1 | Phenotypic evaluation

Analysis of variance (ANOVA) showed significant differences among the barley genotypes for all glasshouse and field experiments (Table 1). For field experiments in Volosovo, no significant differences among the barley genotypes were detected; hence, these data were excluded from further analyses.

Disease severity scores for field trials in Pushkin ranged between 3.09% and 16.77% (mean 9.67%), with seven accessions showing <5% and five accessions showing > 15% of leaf area diseased (Figure 1). The heritability for this location was $h^2 = 0.46$.

The infection response type (IRT) for isolate No 31 ranged between 3 and 8 (mean 4.89) (Figure 1). Most genotypes were moderately susceptible, with 204 and 164 accessions expressing IRT 5 and 6, respectively. Only two accessions showed IRT ≤ 3 and 22 accessions showed IRT ≥ 7 .

Isolate SH 15 showed IRT between 3 and 8 (mean 5.23), with 137 and 201 accessions expressing IRT 5 and 6, respectively (Figure 1).

TABLE 1 Analysis of variance (ANOVA) for spot blotch (*Bipolaris sorokiniana*) severity for 449 barley genotypes evaluated under glasshouse and field conditions

Isolate (glasshouse)	Effect	F-value	p-value	CV% ^a
No 31	Genotype	3.11	<.0001	14.71
SH 15	Genotype	3.67	<.0001	16.35
SB 61	Genotype	9.44	<.0001	27.16
Field location	Effect	F-value	p-value	CV%
Pushkin	Genotype	1.26	.0085	23.53
Volosovo	Genotype	0.89	.8829	55.80
Cleveland (SB 61)	Genotype	9.95	<.0001	20.07

^aCoefficient of variation.

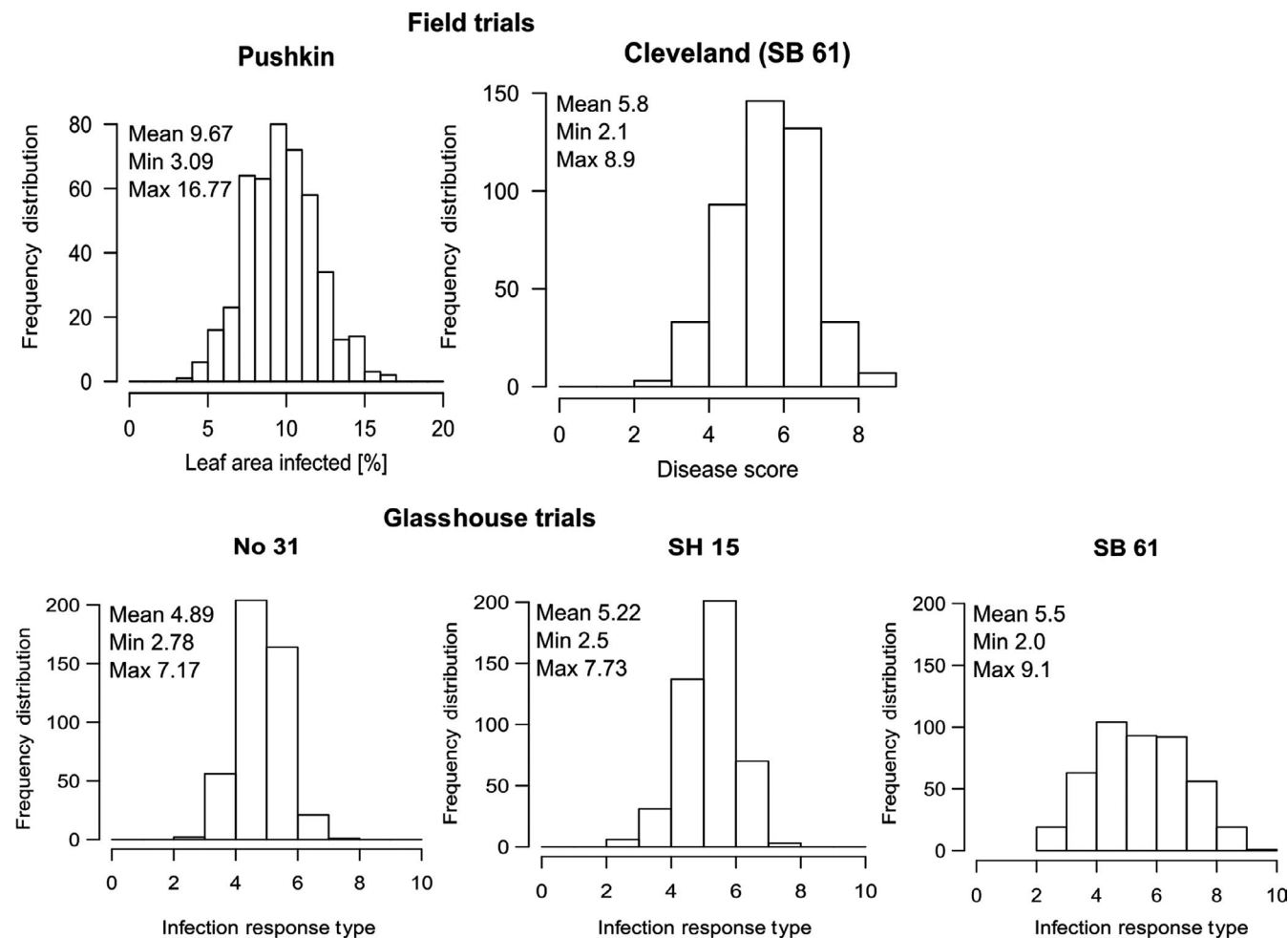


FIGURE 1 Frequency distribution of 449 barley accessions after inoculation with *Bipolaris sorokiniana* in field trials (Pushkin, Russia and Cleveland, Australia with isolate SB 61) and in glasshouse trials with three isolates (No 31, SH 15 and SB 61). Disease assessment in Pushkin was based on leaf area infected, in Cleveland on a 0–9 scale and in the glasshouse on the scale of Fetch and Steffenson (1999)

Six accessions were highly resistant ($IRT \leq 3$), and three accessions were highly susceptible ($IRT \geq 8$).

The IRT for isolate SB 61 tested under glasshouse conditions ranged between 3 and 10 (mean 5.55) (Figure 1). Twenty accessions were highly susceptible and showed $IRT \geq 9$; 19 accessions were highly resistant ($IRT \leq 3$). Most accessions expressed a moderately susceptible to susceptible reaction, with 104, 93 and 92 accessions expressing IRT of 5, 6 and 7, respectively.

Under field conditions, resistance to isolate SB 61 varied between disease scores of 3 and 9 (1 to 9 scale, mean 5.8), with only three accessions being highly resistant (disease score ≤ 3), 33 being moderately resistant (disease score ≤ 4) and 40 accessions being highly susceptible (disease scores ≥ 8) (Figure 1).

3.2 | Linkage disequilibrium and population structure

Genome-wide linkage disequilibrium (LD) decay was estimated at 167 kb. Analysis with the software STRUCTURE identified three

sub-populations. One-hundred and sixty-one accessions had membership probabilities of less than 80% and were considered admixtures, while 58, 139 and 91 individuals belonged to sub-population one, two and three, respectively. Sub-populations one and two comprised mainly 6-rowed accessions, whereas sub-population three comprised mainly 2-rowed accessions. For more information, see Novakazi et al. (2019).

3.3 | Genome-wide association studies

For isolate No 31, fifteen significant marker-trait associations (MTA) were detected—all located on chromosome 1H between 31 and 36 Mbp (40.63–41.02 cM) (Table 2, Figure 2). LOD scores ranged from 4.96 to 11.96. The two peak markers JHI-Hv50k-2016-17526 and SCRI_RS_153785 explained 10.22 and 9.49% of the phenotypic variance, respectively.

A total of seven MTA were detected for resistance to isolate SH 15 (Table 2, Figure 2). All markers were located on chromosome 7H between 26 and 28 Mbp (24.22 – 26.56 cM), with LOD scores

TABLE 2 Significant marker-trait associations identified for resistance to *Bipolaris sorokiniana* (spot blotch) in a set of 449 barley accessions

Marker	Chr	Position [MB] ^a	cM ^b	p-value	LOD	MAF	R ^{2b}
No 31							
JHI-Hv50k-2016-17275	1H	31.354357	N/A	1.09E-05	4.963	0.289	.0377
JHI-Hv50k-2016-17277	1H	31.354447	N/A	1.09E-05	4.963	0.289	.0377
JHI-Hv50k-2016-17526	1H	32.102667	40.63	1.09E-12	11.962	0.467	.1022
JHI-Hv50k-2016-17533	1H	32.178059	40.63	1.10E-09	8.959	0.392	.0738
JHI-Hv50k-2016-17683	1H	33.444712	N/A	5.36E-06	5.270	0.146	.0404
SCRI_RS_153785	1H	33.444893	40.63	6.39E-12	11.194	0.487	.0949
JHI-Hv50k-2016-17765	1H	34.086518	41.02	1.09E-06	5.964	0.219	.0465
BOPA1_5381-1950	1H	34.087694	41.02	1.47E-07	6.833	0.384	.0543
JHI-Hv50k-2016-17885	1H	35.724537	41.02	1.62E-06	5.790	0.220	.0450
SCRI_RS_189483	1H	35.725028	41.02	1.09E-06	5.964	0.219	.0465
JHI-Hv50k-2016-17892	1H	35.72625	41.02	1.62E-06	5.790	0.220	.0450
JHI-Hv50k-2016-17905	1H	35.728954	41.02	1.62E-06	5.790	0.220	.0450
JHI-Hv50k-2016-17907	1H	35.729187	41.02	1.94E-06	5.712	0.221	.0443
SCRI_RS_140837	1H	36.073804	41.02	4.08E-06	5.389	0.441	.0414
JHI-Hv50k-2016-17967	1H	36.074648	41.02	5.82E-06	5.235	0.483	.0401
SH 15							
BOPA1_8365-454	7H	26.44753	N/A	9.39E-06	5.027	0.446	.0363
JHI-Hv50k-2016-454168	7H	26.540553	N/A	3.28E-07	6.484	0.321	.0486
JHI-Hv50k-2016-454253	7H	26.737545	24.22	1.40E-06	5.854	0.489	.0433
JHI-Hv50k-2016-454328	7H	26.816315	N/A	1.77E-06	5.752	0.489	.0424
JHI-Hv50k-2016-454931	7H	27.770934	26.56	4.01E-06	5.397	0.273	.0394
JHI-Hv50k-2016-455261	7H	28.116204	N/A	1.14E-05	4.944	0.115	.0357
JHI-Hv50k-2016-455308	7H	28.146486	N/A	6.70E-06	5.174	0.110	.0376
SB 61 (seedling)							
SCRI_RS_139762	7H	26.541829	N/A	2.58E-06	5.588	0.132	.0346
JHI-Hv50k-2016-454253	7H	26.737545	24.22	2.83E-07	6.548	0.490	.0415
JHI-Hv50k-2016-454263	7H	26.738361	24.22	2.86E-06	5.543	0.133	.0343
JHI-Hv50k-2016-454328	7H	26.816315	N/A	1.04E-05	4.984	0.488	.0304
JHI-Hv50k-2016-454422	7H	27.122714	N/A	6.66E-06	5.177	0.267	.0317
JHI-Hv50k-2016-454931	7H	27.770934	26.56	1.13E-10	9.947	0.272	.0667
JHI-Hv50k-2016-454991	7H	27.775336	26.56	6.55E-10	9.184	0.125	.0609
JHI-Hv50k-2016-455015	7H	27.776943	26.56	6.36E-07	6.196	0.173	.0390
JHI-Hv50k-2016-455016	7H	27.777032	26.56	1.40E-09	8.853	0.139	.0584
JHI-Hv50k-2016-455041	7H	27.862823	26.56	3.06E-10	9.514	0.126	.0634
JHI-Hv50k-2016-455261	7H	28.116204	N/A	1.81E-19	18.742	0.115	.1367
JHI-Hv50k-2016-455308	7H	28.146486	N/A	2.38E-19	18.623	0.111	.1357
JHI-Hv50k-2016-455437	7H	28.772177	N/A	2.14E-05	4.671	0.200	.0282
SB 61 (adult plant)							
JHI-Hv50k-2016-455261	7H	28.116204	N/A	6.11E-06	5.2143	0.115	.0307
JHI-Hv50k-2016-455308	7H	28.146486	N/A	1.61E-05	4.7939	0.111	.0279
Pushkin							
JHI-Hv50k-2016-467659	7H	68.476333	N/A	8.96E-06	5.0478	0.490	.0395

Note: Adult plant resistance was tested in field experiments in Pushkin, Russia, and Cleveland, Australia (with isolate SB 61). Seedling resistance was tested under glasshouse conditions with isolates No 31, SH 15 and SB 61.

^aPhysical positions based on Bayer et al. (2017).

^bGenetic positions based on RIL population of Golden Promise × Morex by Bayer et al. (2017).

^cExplained phenotypic variance per marker.

between 4.94 and 6.48 explaining 3.57% to 4.86% of the phenotypic variance.

For glasshouse experiments with isolate SB 61, 13 significant MTAs were detected, which are located on chromosome 7H between 26 and 28 Mbp (24.22–26.56 cM) (Table 2, Figure 2). The two peak markers JHI-Hv50k-2016-455261 and JHI-Hv50k-2016-455308 with LOD scores of 18.74 and 18.62 explained 13.67 and 13.57% of the phenotypic variance, respectively. Under field conditions, two significant MTAs were detected for isolate SB 61 (Table 2, Figure 2). The two markers are the same as the peak markers under glasshouse conditions (JHI-Hv50k-2016-455261 and JHI-Hv50k-2016-455308) located on chromosome 7H at 28 Mbp and explaining 3.07% and 2.79% of the phenotypic variance in this case.

For field trials in Pushkin, only one significant MTA was detected on chromosome 7H at 68 Mbp, with a LOD score of 5.05 (Table 2, Figure 2). Marker JHI-Hv50k-2016-467659 explains 3.95% of the phenotypic variance.

In the interval identified on chromosome 1H between 31,354,357 bp and 36,074,648 bp, there are four low-confidence (LC) genes with undescribed protein annotations and ten high-confidence (HC) genes (Table 3). Of the ten HC genes, one (HORVU1Hr1G013490) has no designated function and three are directly involved in pathogen recognition or defence. They belong to the UDP-glycosyltransferase superfamily, tetraspanin family and lateral organ boundary (LOB) domain (HORVU1Hr1G012680, HORVU1Hr1G012690, HORVU1Hr1G012720). The remaining genes are a ribosome biogenesis regulatory protein homolog, magnesium-chelatase subunit, 4'-phosphopantetheinyl transferase, ubiquitin-conjugating enzyme, isoleucine-glutamine (IQ)-domain and a sugar transporter (Table 3).

In the detected regions on chromosome 7H, between 26,447,530 to 28,772,177 bp and at 68,476,333 bp, three LC genes and twenty-one HC genes are located (Table 3). Two of the LC genes have undescribed protein annotations, whereas the other is probably a transposon Ty1-PL Gag-Pol polyprotein. The 21 HC genes belong to different transporters (sulphate transporter, magnesium transporter), kinases (ATP-dependent 6-phosphofructokinase, receptor kinase, receptor-like protein kinase), oxidases (peroxidase superfamily, Fe superoxide dismutase), proteins (pentatricopeptide repeat-containing protein, DNA-repair protein, nodulin-related proteins), polygalacturonase-1 non-catalytic subunit β , coatomer subunit β , carbonic anhydrases, fatty acyl-CoA reductase, Cadmium tolerant, myosin-J heavy chain and protein arginine methyltransferase (Table 3).

4 | DISCUSSION

The fungal pathogen *B. sorokiniana* has a wide host range and induces a number of diseases, such as common root rot, seedling blight, black point and spot blotch (Acharya et al., 2011; Gupta et al., 2018; Kumar et al., 2002). One of the hosts of *B. sorokiniana* is barley (*H. vulgare*), a crop used worldwide for animal feed, human consumption and

malting. The most important disease in barley induced by *B. sorokiniana* is spot blotch. The symptoms are dark-brown, necrotic blotches that appear mostly on the leaves, but also on stems, awns and glumes (Acharya et al., 2011; Mathre, 1997). The damage is based on a reduced photosynthesis, which leads to reduced yields, but also to a decrease in grain quality. The pathogen prefers warm, humid conditions, which occur for example in South Asia, the Middle East, Upper Midwest of the USA and Central Canada (Acharya et al., 2011; Chatrath, Mishra, Ferrara, Singh, & Joshi, 2007; Fetch & Steffenson, 1999). However, with increasing temperatures in temperate climate zones due to climate change, the incidence of spot blotch infection and epidemics will increase. For example, in the north-west region of European Russia, epidemics of barley spot blotch have occurred every 2–3 years for the past two decades (Lashina & Afanasenko, 2019).

In the United States, resistance derived from the 6-rowed barley line ND B112 has provided effective control of spot blotch since the late 1950s. This resistance was effective against pathotypes 0, 1 and 2 (Valjavec-Gratian & Steffenson, 1997) and was used in the 6-rowed malting barley breeding programmes (Fetch & Steffenson, 1994; Wilcoxson, Rasmusson, & Miles, 1990). Meanwhile, two-rowed barleys generally remained susceptible. Eventually, the durable resistance of ND B112 was overcome by the emergence of a new pathotype identified by Leng et al. (2016) and designated pathotype 7. The occurrence of spot blotch pathotypes has been reported in several studies from different regions of the world (Arabi & Jawhar, 2002, 2004; Ghazvini & Tekauz, 2007; Meldrum et al., 2004). Breeding for resistance is an effective mean for controlling the disease and so far three major resistance loci have been mapped, namely *Rcs 6/Scs 6*, *Rbs 7* and *Rcs 5* located on chromosomes 1H, 6H and 7H, respectively (Drader et al., 2009; Leng et al., 2018; Wang et al., 2019). Additionally, several minor QTL have been identified on all seven barley chromosomes (Berger et al., 2013; Bilgic et al., 2005, 2006; Bovill et al., 2010; Bykova et al., 2017; Grewal et al., 2012; Gutiérrez et al., 2015; Gyawali et al., 2018; Haas et al., 2016; Roy et al., 2010; Steffenson et al., 1996; Wang et al., 2017; Yun et al., 2006, 2005; Zhou & Steffenson, 2013).

Overall, the barley accessions tested in our study revealed a large diversity in all experiments and phenotypic reactions varied from highly resistant to highly susceptible, with IRT ranging from three to 10. Disease levels in field trials in Pushkin ranged between 3% and 16.7%. However, these scores are AO values and based on AUDPC values of three scoring dates assessed during the growth period in two years (2016 and 2017). The AUDPC takes into account the development and intensity of the disease over time. The average ordinate (AO) describes the mean disease severity at every point in time. In our case, the unit of the curve is per cent. Disease severities in 2016 were quite high and ranged between 10% and 68% with some accessions occasionally expressing disease severities of 80%–100% (data not shown). Infection pressure and environmental conditions were less favourable for disease development in 2017. Mean disease severities ranged only between 4% and 38%. The variation

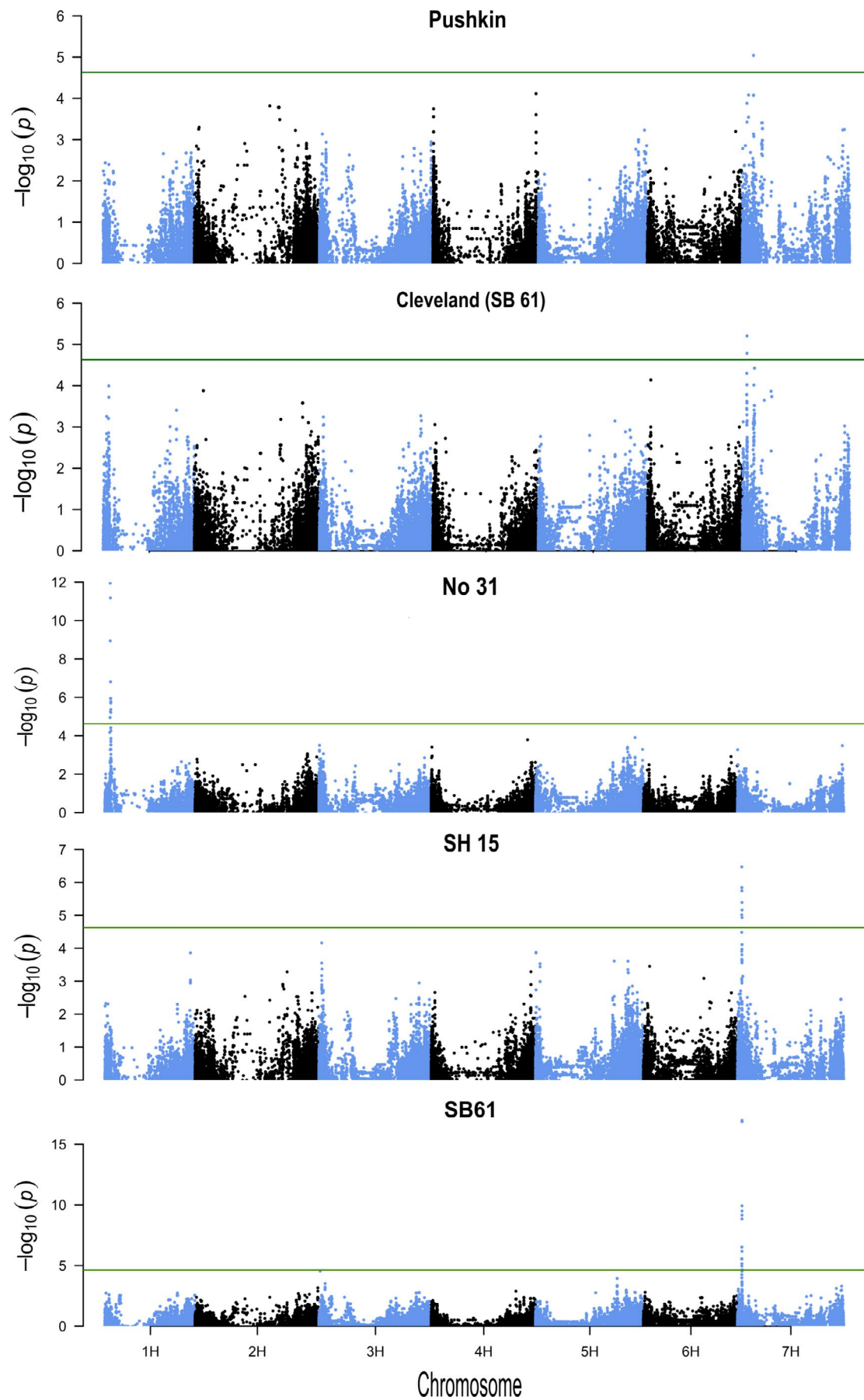


FIGURE 2 Genome-wide association analyses for resistance to *Bipolaris sorokiniana* in field trials (Pushkin, Russia and Cleveland, Australia with isolate SB 61) and in glasshouse trials with isolates No 31, SH 15 and SB 61. The x-axis shows the seven barley chromosomes, positions are based on the physical map, and the $-\log_{10}(p)$ value is displayed on the y-axis. The green horizontal line represents the significance threshold of $-\log_{10}(p) = 4.63$

of disease severity between the two years might explain the low heritability ($h^2 = 0.46$) for this location. Steffenson et al. (1996) and Grewal et al. (2012) reported heritabilities for spot blotch resistance in barley of 0.91 and 0.73–0.96, respectively. Heritability for spot blotch resistance in wheat was reported to be between 0.65 and 0.89 (Ayana et al., 2018; Kumar, Joshi, Kumar, Chand, & Röder, 2010; Lillemo, Joshi, Prasad, Chand, & Singh, 2013; Singh et al., 2016; Zhu et al., 2014).

A total of 38 marker-trait associations (MTA) were detected in the present study corresponding to two major QTL located on chromosome 1H and 7H, respectively, and one minor QTL on chromosome 7H. In several other studies, a major QTL was reported on the short arm of chromosome 3H for seedling and adult plant resistance (Bilgic et al., 2005, 2006; Bovill et al., 2010; Grewal et al., 2012; Haas et al., 2016; Roy et al., 2010; Wang et al., 2017; Zhou & Steffenson, 2013). This QTL explained phenotypic variations between 1% and 60% (Bilgic et al., 2005; Grewal et al., 2012; Zhou & Steffenson, 2013). However, most of those studies analysed germplasm from the USA and Canada. In the present study, the association panel was of diverse origin and out of 449 accessions only 19 originated from the USA and eleven from Canada. This emphasizes the importance of screening germplasm from a wide range of origins in order to identify new QTL for resistance.

The region detected on chromosome 1H is located between 31,354,357 bp (JHI-Hv50k-2016-17275) and 36,074,648 bp (JHI-Hv50k-2016-17967) and confers resistance in the seedling stage. Zhou and Steffenson (2013) screened 3,840 breeding lines and cultivars in glasshouse and field trials for spot blotch resistance with isolate ND85F (pathotype 1). On chromosome 1H, they identified a region conferring seedling and adult plant resistance located between 34 and 37 Mbp. One of their significant markers (11_10764) was also significantly associated with disease resistance in our study (BOPA1_5381-1950). This very same marker was identified as a peak marker in a bi-parental mapping study by Afanassenko et al. (2015). In their study, they tested a DH population of Ranniy 1 x Zernogradsky 813 for spot blotch resistance with several isolates. Finally, Wang et al. (2017) studied a barley set consisting of 621 two-rowed and 857 six-rowed accessions with three isolates (ND85F, ND90Pr and ND4008) representing the three pathotypes 1, 2 and 7, respectively. They detected a QTL for resistance against pathotype 1 on chromosome 1H named *QRcs-1H-P1*, which is located between 31 and 35 Mbp at a LOD score of up to 25.34 explaining between 17.3% and 24% of the phenotypic variance. Three of their peak markers (SCRI_RS_153785, SCRI_RS_189483 and BOPA1_5381-1950) were also significant in the present study. Bilgic et al. (2006) identified a region on the short arm of chromosome 1H conferring seedling and adult plant resistance to spot blotch pathotype 2 in a DH population of Calicuchima-sib x Bowman-BC (C/B).

Based on their results, the resistance was contributed by the resistant parent Calicuchima-sib based on a single gene they designated *Rcs 6*. In a more recent study, Leng et al. (2018) using the same DH population were able to show that the susceptible parent Bowman contributed a dominant susceptibility gene, *Scs 6*, which was located at the same locus as the resistance gene *Rcs 6*. Further fine mapping in F_2 recombinants of Bowman x ND 5,883 and Bowman x ND B112 narrowed the interval down to a 125 kb region physically located between 64 and 192 Mbp (Leng et al., 2018). Thus, the QTL detected in our study does not correspond to the resistance/ susceptibility locus *Rcs 6*/*Scs 6*, but represents another major resistance QTL against pathotype 1. In particular, marker BOPA1_5381-1950, located on chromosome 1H at 34,087,694 bp, may be of special importance as it turned out to be significantly associated with disease resistance in the present study as well as in the studies of Zhou and Steffenson (2013), Afanassenko et al. (2015) and Wang et al. (2017).

In the interval identified between 31,354,357 bp and 36,074,648 bp, there are four low-confidence (LC) genes with undescribed protein annotations and ten high-confidence (HC) genes (Table 3). Out of the ten HC genes, one has so far no designated function (HORVU1Hr1G013490) and three are involved in pathogen recognition or defence (HORVU1Hr1G012680, HORVU1Hr1G012690, HORVU1Hr1G012720). UDP-glycosyltransferase proteins (HORVU1Hr1G012680) are involved in the biosynthesis of, for example, phenolics and glucosinolates, but also in the glycosylation of phytohormones and other plant metabolites and have long been shown to be involved in plant defence against biotic stress (Vogt & Jones, 2000). Rehman et al. (2018) showed several UDP-glycosyltransferase genes to be upregulated in *Arabidopsis thaliana* after infection with fungal pathogens such as *Alternaria brassiciola*, *Blumeria graminis*, *E. coli*, *Rhizoctonia solani* and *Xanthomonas campestris*. Tetraspanins (HORVU1Hr1G012690) are a family of proteins found in all eukaryotic organisms located in the cell membrane and involved among others in cell adhesion, growth, fusion and migration (Reimann, Kost, & Dettmer, 2017). However, they also have been linked to be involved in pathogen recognition and to be upregulated in *A. thaliana* after treatment with pathogen elicitors (Wang et al., 2015). Lateral organ bounding (LOB) domains (LBD) are transcription factors with key roles in plant organ development, but have also been shown to be involved in plant regeneration, pollen development, nitrogen and anthocyanin metabolisms as well as pathogen response (Xu, Luo, & Hochholdinger, 2016). So far, 24 LBD genes have been described in barley located on all seven barley chromosomes, four of which are located on chromosome 1H (Guo et al., 2016). None of the barley LBDs have been linked to pathogen resistance or recognition yet; however, several LBD genes were identified to show differential expression levels after pathogen attack in, for example *Arabidopsis thaliana* (*Fusarium oxysporum*), *Vitis vinifera* (*Botrytis cinerea*, *Plasmopara viticola*) and *Malus domestica* (*Pseudomonas*

TABLE 3 Predicted genes located on chromosomes 1H and 7H at 31–36 Mbp and 26–28 Mbp and at 68 Mbp, respectively, and their respective functional annotations

Gene ID ^a	Gene class ^b	Chrom	Physical location [bp]		Annotation
HORVU1Hr1G012470	HC_G	1H	31,351,339	31,355,135	Ribosome biogenesis regulatory protein homolog
HORVU1Hr1G012600	HC_G	1H	31,622,380	31,623,341	Magnesium-chelatase subunit ChlH, chloroplastic
HORVU1Hr1G012620	LC_u	1H	31,630,058	31,630,407	Undescribed protein
HORVU1Hr1G012680^c	HC_G	1H	31,672,910	31,677,138	UDP-Glycosyltransferase superfamily protein
HORVU1Hr1G012690	HC_G	1H	31,684,461	31,688,423	Tetraspanin family protein
HORVU1Hr1G012720	HC_G	1H	32,101,798	32,102,986	Lateral organ boundary domain-containing protein 11
HORVU1Hr1G012730	HC_G	1H	32,173,373	32,186,590	4'-Phosphopantetheinyl transferase superfamily
HORVU1Hr1G012750	LC_u	1H	32,177,144	32,182,714	Undescribed protein
HORVU1Hr1G013040	HC_G	1H	33,441,856	33,445,024	Ubiquitin-conjugating enzyme 37
HORVU1Hr1G013210	HC_G	1H	34,083,562	34,088,731	Isoleucine–glutamine (IQ)-domain 2
HORVU1Hr1G013480	HC_G	1H	35,679,610	35,683,434	Sugar transporter 1
HORVU1Hr1G013490	HC_U	1H	35,723,711	35,729,110	Unknown function
HORVU1Hr1G013560	LC_u	1H	36,073,128	36,078,899	Undescribed protein
HORVU1Hr1G013570	LC_u	1H	36,073,270	36,074,655	Undescribed protein
HORVU7Hr1G019680	HC_G	7H	26,446,831	26,449,799	Polygalacturonase 1 non-catalytic β subunit
HORVU7Hr1G019720	LC_TE	7H	26,534,413	26,542,035	Transposon Ty1-PL Gag-Pol polyprotein
HORVU7Hr1G019730	HC_G	7H	26,546,229	26,549,975	Pentatricopeptide repeat-containing protein
HORVU7Hr1G019810	HC_G	7H	26,736,047	26,740,148	ATP-dependent 6-phosphofructokinase 7
HORVU7Hr1G019830	HC_G	7H	26,812,633	26,817,294	Acyl-ACP thioesterase
HORVU7Hr1G019880	LC_u	7H	26,920,657	26,921,300	Undescribed protein
HORVU7Hr1G019890	HC_G	7H	26,920,897	26,926,149	Sulphate transporter 3;4
HORVU7Hr1G019930	HC_G	7H	27,119,476	27,129,693	Coatomer, beta' subunit
HORVU7Hr1G019990	HC_G	7H	27,155,214	27,161,528	DNA-repair protein XRCC1
HORVU7Hr1G020190	HC_G	7H	27,478,173	27,480,352	Carbonic anhydrase
HORVU7Hr1G020270	HC_G	7H	27,505,060	27,507,837	Fatty acyl-CoA reductase 1
HORVU7Hr1G020300	HC_G	7H	27,546,603	27,556,612	Peroxidase superfamily protein
HORVU7Hr1G020370	HC_G	7H	27,657,951	27,659,978	Carbonic anhydrase
HORVU7Hr1G020580	HC_G	7H	27,768,879	27,774,101	Cadmium tolerant 1
HORVU7Hr1G020590	HC_G	7H	27,771,905	27,777,772	Fe superoxide dismutase 3
HORVU7Hr1G020610	HC_G	7H	27,775,540	27,775,880	Myosin-J heavy chain
HORVU7Hr1G020620	HC_G	7H	27,861,260	27,864,514	Protein arginine methyltransferase 10
HORVU7Hr1G020660	HC_G	7H	27,958,533	28,145,362	Receptor kinase 3
HORVU7Hr1G020720	HC_G	7H	27,986,777	27,992,005	Receptor-like protein kinase 4
HORVU7Hr1G020730	LC_u	7H	27,989,246	27,990,451	Undescribed protein
HORVU7Hr1G020770	HC_G	7H	28,104,777	28,112,667	Early nodulin-related
HORVU7Hr1G020780	HC_G	7H	28,111,982	28,112,637	Early nodulin-related
HORVU7Hr1G020830	HC_G	7H	28,203,216	28,204,125	Early nodulin-related
HORVU7Hr1G033370	HC_G	7H	68,395,174	68,477,165	Magnesium transporter protein 1

^aThe predicted genes and their respective annotations were obtained from BARLEYMAP (Cantalapiedra et al., 2015).
^bHC_G, high-confidence gene with predicted function, HC_U, high-confidence gene without predicted function, LC_u, low-confidence gene without predicted function.
^cGenes in bold are involved in pathogen defence or recognition.

syringae) (Grimplet, Pimentel, Agudelo-Romero, Martinez-Zapater, & Fortes, 2017; Thatcher, Kazan, & Manners, 2012; Wang, Zhang, Su, Liu, & Hao, 2013).

The second region identified in this study is located on chromosome 7H at 26,447,530 to 28,772,177 bp and was associated with seedling and adult plant resistance. Steffenson et al. (1996)

studied 150 DH lines of a cross of Steptoe \times Morex for spot blotch resistance using isolate ND85F and identified a major QTL on chromosome 7H active at the seedling and adult plant stage, which they designated *Rcs 5*. Bilgic et al. (2005) and Bovill et al. (2010) screened four DH populations each for seedling and adult plant resistance, and identified a QTL that co-located with the *Rcs 5* locus. In the former study, isolate ND85F was used and in the latter study isolate SB 61, which was also used in the present study. Yun et al. (2005) developed 104 recombinant inbred lines (RILs) and 98 advanced backcross lines (Yun et al., 2006) from a cross between OUH 602 (*H. vulgare* subsp. *spontaneum*) and barley cultivar Harrington, and as well identified the resistance locus *Rcs 5* using isolate ND85F. Furthermore, in GWA studies, Roy et al. (2010) screened 318 wild barley accessions with isolate ND85F and identified a QTL on chromosome 7H named *Rcs-qt1-7H-bPb-4584* located between 16 and 22Mbp that coincides with *Rcs 5*. Berger et al. (2013) studied 329 lines and cultivars from the Virginia Tech programme again with isolate ND85F and identified significant MTAs for seedling resistance on chromosome 7H located at 22 to 31 Mbp. Zhou and Steffenson (2013) identified a region located at 26 to 32 Mbp via GWAS. The BOPA marker 11_20162 was associated with resistance in all their trials. This marker was also significantly associated with disease resistance against pathotype 1 (isolate ND85F) in a GWA study by Wang et al. (2017). In an association study with 336 genotypes and an isolate mixture of 19 Moroccan isolates, Gyawali et al. (2018) identified a region associated with seedling and adult plant resistance located on chromosome 7H at 26 to 27 Mbp. Drader et al. (2009) developed a saturated map of the *Rcs 5* locus and postulated it to be flanked by markers BF263248 and BG414713 with a genetic interval of 2.8 cM. Drader et al. (2009) hypothesized that the spot blotch resistance on chromosome 7H in barley is similar or even the same gene as in wheat. This hypothesis was confirmed by Ayana et al. (2018), who conducted GWAS with 294 hard winter wheat accessions and identified a significant QTL (*Qsb.sdsu-7B.1*) on wheat chromosome 7B, which corresponded to the resistance QTL *Rcs 5* in barley.

The second region identified on chromosome 7H is located at 68,476,333 bp, where no overlapping QTL have yet been described in previous studies. Hence, based on the data available we presume this to be a new QTL.

In the region detected between 26,447,530 to 28,772,177 bp and at 68,476,333 bp, there are three low-confidence genes and twenty-one high-confidence genes located (Table 3). Polygalacturonase 1 non-catalytic β subunit (HORVU7Hr1G019680) is part of the polygalacturonase, which is involved in pectin degradation. Pectin is a macromolecule and is a major component of plant cell walls. It contributes to cell wall stability, surface charge, ion balance, porosity and pH (Voragen, Coenen, Verhoef, & Schols, 2009). Pectin degradation in plants is important for fruit ripening (Liu et al., 2014). Phytopathogenic fungi, bacteria and nematodes produce polygalacturonase in order to penetrate and colonize plant tissue (Gomathi & Gnanamanickam, 2004). It was shown that increased polygalacturonase levels, and in particular an increased

activity of the polygalacturonase 1 non-catalytic β subunit in plant tissue, lead to increased susceptibility towards abiotic and biotic stress in rice (Liu et al., 2014). In fact, markers SCRI_RS_139762, JHI-Hv50k-2016-454253, JHI-Hv50k-2016-454263 and JHI-Hv50k-2016-454328 showed positive allelic effects and therefore increased susceptibility (data not shown).

Sulphur is vital for plant growth and development, since it is essential for certain amino acids, hormones and secondary metabolites. Sulphate transporters (HORVU7Hr1G019890) are therefore important in every plant species (Gigolashvili & Kopriva, 2014; Takahashi, 2019). The role of glucosinolates in the *Brassicaceae* family against herbivorous and fungal pathogens has long been known (Bednarek et al., 2009; Radojčić Redovniković, Glivetić, Delonga, & Vorkapić-Furač, 2008). Glutathione is another sulphur containing essential molecule in every plant species, with vital roles in the primary metabolism, detoxification and redox signalling (Noctor et al., 2012). It was also shown to enhance susceptibility towards biotrophic and resistance towards necrotrophic fungal pathogens (Dubreuil-Maurizi & Poinssot, 2012; Gullner, Zechmann, Künstler, & Király, 2017; Noctor et al., 2012).

Besides catalysing the oxidoreduction between hydrogen peroxide and reductants, plant peroxidases are also involved in lignification, suberization, phytoalexin synthesis, the metabolism of auxin, reactive oxygen and nitrogen species, and cross-linkage of cell wall components (Almagro et al., 2008; Hiraga, Sasaki, Ito, Ohashi, & Matsui, 2001). Furthermore, it was demonstrated that peroxidases (HORVU7Hr1G020300) play a role in pathogen recognition and defence, by strengthening the cell wall through, for example, increased lignification, increasing levels of reactive oxygen species and levels of phytoalexin (Hiraga et al., 2001).

Nodules are root organs formed by legumes in order to go into symbiosis with nitrogen-fixing bacteria (Wagner, 2011). Nodulin genes were first described in soya bean (*Glycine max* L.) to be involved in the nodule formation (Legocki & Verma, 1980). However, nodulin-like proteins (HORVU7Hr1G020770, HORVU7Hr1G020780 and HORVU7Hr1G020830) were also described in non-nodulating plant species and classified into seven families (Denancé, Szurek, & Noël, 2014). They act as transporters among other functions for sugars, amino acids, auxin and nutrients or as virulence factors of pathogens (Chen et al., 2010; Denancé et al., 2014).

The aim of this study was to screen a diverse barley set for their response towards *B. sorokiniana*, the causal agent of the spot blotch disease in barley, and to identify QTL for resistance employing genome-wide association studies. The detected MTA corresponded to two major QTL located on chromosome 1H and 7H, respectively. Even though the two QTL on chromosome 1H (31 – 36 Mbp) and 7H (26 – 28 Mbp) have been described in previous studies, further research is necessary to narrow down and fine-map the intervals of interest and characterize the genes underlying resistance. Additionally, a putative new QTL identified on chromosome 7H at 68 Mbp represents a potentially interesting source of quantitative resistance for barley breeding.

ACKNOWLEDGEMENT

The authors thank the former "Pathogen-Stress Genomics" laboratory of the late Dr. Patrick Schweizer from the Department of Breeding Research at the Leibniz Institute of Plant Genetics and Crop Plant Research (IPK), Gatersleben, for the protocol on cultivation of *Bipolaris sorokiniana*. This research was supported by the German Research Society (DFG) (OR 72/11-1) and the Russian Foundation for Basic Research (RFBR) (No 15-54-12365 NNIO_a). Screening in Australia was jointly funded by the Queensland Department of Agriculture and Fisheries and the Grains Research and Development Corporation.

CONFLICT OF INTEREST

The authors declare that there are no conflicts of interest in the reported research.

AUTHOR CONTRIBUTION

OA and FO planned and managed the project. NL and IL conducted the field screenings in Russia. GJP was in charge of the screenings conducted in Australia (field and glasshouse). OA, FO, GJP and RS contributed to the interpretation and discussion of the results. FN conducted glasshouse screenings in Germany, analysed the data and wrote the manuscript.

ORCID

Fluturë Novakazi  <https://orcid.org/0000-0001-7151-6811>

Rod Snowdon  <https://orcid.org/0000-0001-5577-7616>

REFERENCES

- Acharya, K., Dutta, A. K., & Pradhan, P. (2011). 'Bipolaris sorokiniana'(Sacc.) Shoem.: The most destructive wheat fungal pathogen in the warmer areas. *Australian Journal of Crop Science*, 5, 1064.
- Afanasenkov, O., Koziakov, A., Hedlay, P., Lashina, N., Anisimova, A., Manninen, O., ... Potokina, E. (2015). Mapping of the loci controlling the resistance to *Pyrenophora teres* f. *terres* and *Cochliobolus sativus* in two double haploid barley populations. *Russian Journal of Genetics: Applied Research*, 5, 242–253.
- Afgan, E., Baker, D., van den Beek, M., Blankenberg, D., Bouvier, D., Cech, M., ... Goecks, J. (2016). The Galaxy platform for accessible, reproducible and collaborative biomedical analyses: 2016 update. *Nucleic Acids Research*, 44, 3–10. <https://doi.org/10.1093/nar/gkw343>
- Almagro, L., Gómez Ros, L., Belchi-Navarro, S., Bru, R., Ros Barceló, A., & Pedreno, M. (2008). Class III peroxidases in plant defence reactions. *Journal of Experimental Botany*, 60, 377–390. <https://doi.org/10.1093/jxb/ern277>
- Arabi, M., & Jawhar, M. (2002). Virulence spectrum to barley (*Hordeum vulgare* L.) in some isolates of *Cochliobolus sativus* from Syria. *Journal of Plant Pathology*, 84, 35–39.
- Arabi, M., & Jawhar, M. (2004). Identification of *Cochliobolus sativus* (spot blotch) isolates expressing differential virulence on barley genotypes in Syria. *Journal of Phytopathology*, 152, 461–464. <https://doi.org/10.1111/j.1439-0434.2004.00875.x>
- Ayana, G. T., Ali, S., Sidhu, J. S., Gonzalez Hernandez, J. L., Turnipseed, B., & Sehgal, S. K. (2018). Genome-Wide Association Study for Spot Blotch Resistance in Hard Winter Wheat. *Frontiers in Plant Science*, 9, 926. <https://doi.org/10.3389/fpls.2018.00926>
- Bayer, M. M., Rapazote-Flores, P., Ganai, M., Hedley, P. E., Macaulay, M., Plieske, J., ... Waugh, R. (2017). Development and Evaluation of a Barley 50k iSelect SNP Array. *Frontiers in Plant Science*, 8, 1792. <https://doi.org/10.3389/fpls.2017.01792>
- Bednarek, P., Pislewska-Bednarek, M., Svatos, A., Schneider, B., Doubek, J., Mansurova, M., ... Schulze-Lefert, P. (2009). A glucosinolate metabolism pathway in living plant cells mediates broad-spectrum antifungal defense. *Science*, 323, 101–106. <https://doi.org/10.1126/science.1163732>
- Berger, G. L., Liu, S., Hall, M. D., Brooks, W. S., Chao, S., Muehlbauer, G. J., ... Griffey, C. A. (2013). Marker-trait associations in Virginia Tech winter barley identified using genome-wide mapping. *Theoretical and Applied Genetics*, 126, 693–710. <https://doi.org/10.1007/s00122-012-2011-7>
- Bilgic, H., Steffenson, B., & Hayes, P. (2005). Comprehensive genetic analyses reveal differential expression of spot blotch resistance in four populations of barley. *Theoretical and Applied Genetics*, 111, 1238–1250. <https://doi.org/10.1007/s00122-005-0023-2>
- Bilgic, H., Steffenson, B., & Hayes, P. (2006). Molecular mapping of loci conferring resistance to different pathotypes of the spot blotch pathogen in barley. *Phytopathology*, 96, 699–708. <https://doi.org/10.1094/PHYTO-96-0699>
- Bovill, J., Lehmsiek, A., Sutherland, M. W., Platz, G. J., Usher, T., Franckowiak, J., & Mace, E. (2010). Mapping spot blotch resistance genes in four barley populations. *Molecular Breeding*, 26, 653–666. <https://doi.org/10.1007/s11032-010-9401-9>
- Bykova, I. V., Lashina, N. M., Efimov, V. M., Afanasenko, O. S., & Khlestkina, E. K. (2017). Identification of 50 K Illumina-chip SNPs associated with resistance to spot blotch in barley. *BMC Plant Biology*, 17, 250. <https://doi.org/10.1186/s12870-017-1198-9>
- Campoy, J. A., Lerigoleur-Balsemin, E., Christmann, H., Beauvieux, R., Girollet, N., Quero-Garcia, J., ... Barreneche, T. (2016). Genetic diversity, linkage disequilibrium, population structure and construction of a core collection of *Prunus avium* L. landraces and bred cultivars. *BMC Plant Biology*, 16, 49. <https://doi.org/10.1186/s12870-016-0712-9>
- Cantalapiedra, C. P., Boudiar, R., Casas, A. M., Igartua, E., & Contreras-Moreira, B. (2015). BARLEYMAP: Physical and genetic mapping of nucleotide sequences and annotation of surrounding loci in barley. *Molecular Breeding*, 35, 13. <https://doi.org/10.1007/s11032-015-0253-1>
- Chang, C. C., Chow, C. C., Tellier, L. C., Vattikuti, S., Purcell, S. M., & Lee, J. J. (2015). Second-generation PLINK: Rising to the challenge of larger and richer datasets. *Gigascience*, 4, 7. <https://doi.org/10.1186/s13742-015-0047-8>
- Chatrath, R., Mishra, B., Ferrara, G. O., Singh, S., & Joshi, A. (2007). Challenges to wheat production in South Asia. *Euphytica*, 157, 447–456. <https://doi.org/10.1007/s10681-007-9515-2>
- Chen, L.-Q., Hou, B.-H., Lalonde, S., Takanaga, H., Hartung, M. L., Qu, X.-Q., ... Frommer, W. B. (2010). Sugar transporters for intercellular exchange and nutrition of pathogens. *Nature*, 468, 527. <https://doi.org/10.1038/nature09606>
- Denancé, N., Szurek, B., & Noël, L. D. (2014). Emerging functions of nodulin-like proteins in non-nodulating plant species. *Plant and Cell Physiology*, 55, 469–474. <https://doi.org/10.1093/pcp/pct198>
- Drader, T., Johnson, K., Brueggeman, R., Kudrna, D., & Kleinhofs, A. (2009). Genetic and physical mapping of a high recombination region on chromosome 7H (1) in barley. *Theoretical and Applied Genetics*, 118, 811–820. <https://doi.org/10.1007/s00122-008-0941-x>
- Dubreuil-Maurizi, C., & Poinssot, B. (2012). Role of glutathione in plant signaling under biotic stress. *Plant Signaling & Behavior*, 7, 210–212. <https://doi.org/10.4161/psb.18831>

- Earl, D. A., & vonHoldt, B. M. (2012). STRUCTURE HARVESTER: A web-site and program for visualizing STRUCTURE output and implementing the Evanno method. *Conservation Genetics Resources*, 4, 359–361. <https://doi.org/10.1007/s12686-011-9548-7>
- Fetch, T., & Steffenson, B. (1994). Identification of *Cochliobolus sativus* isolates expressing differential virulence on two-row barley genotypes from North Dakota. *Canadian Journal of Plant Pathology*, 16, 202–206. <https://doi.org/10.1080/07060669409500754>
- Fetch, T. G., & Steffenson, B. J. (1999). Rating scales for assessing infection responses of barley infected with *Cochliobolus sativus*. *Plant Disease*, 83, 213–217.
- Ghazvini, H., & Tekauz, A. (2007). Virulence diversity in the population of *Bipolaris sorokiniana*. *Plant Disease*, 91, 814–821.
- Gigolashvili, T., & Kopriva, S. (2014). Transporters in plant sulfur metabolism. *Frontiers in Plant Science*, 5, 442. <https://doi.org/10.3389/fpls.2014.00442>
- Gomathi, V., & Gnanamanickam, S. (2004). Polygalacturonase-inhibiting proteins in plant defence. *Current Science*, 87, 1211–1217.
- Grewal, T. S., Rossnagel, B. G., & Scoles, G. J. (2012). Mapping quantitative trait loci associated with spot blotch and net blotch resistance in a doubled-haploid barley population. *Molecular Breeding*, 30, 267–279. <https://doi.org/10.1007/s11032-011-9616-4>
- Grimplet, J., Pimentel, D., Agudelo-Romero, P., Martinez-Zapater, J. M., & Fortes, A. M. (2017). The LATERAL ORGAN BOUNDARIES Domain gene family in grapevine: Genome-wide characterization and expression analyses during developmental processes and stress responses. *Scientific Reports*, 7, 15968. <https://doi.org/10.1038/s41598-017-16240-5>
- Gullner, G., Zechmann, B., Künstler, A., & Király, L. (2017). The signaling roles of glutathione in plant disease resistance. In: M. A. Hossain, M. G. Mostofa, P. Diaz-Vivancos, D. J. Burritt, M. Fujita, & L.-S. P. Tran (Eds.), *Glutathione in Plant Growth, Development, and Stress Tolerance* (pp. 331–357). Cham, Switzerland: Springer.
- Guo, B.-J., Wang, J., Lin, S., Tian, Z., Zhou, K., Luan, H.-Y., ... Xu, R.-G. (2016). A genome-wide analysis of the ASYMMETRIC LEAVES2/LATERAL ORGAN BOUNDARIES (AS2/LOB) gene family in barley (*Hordeum vulgare* L.). *Journal of Zhejiang University-Science B*, 17, 763–774. <https://doi.org/10.1631/jzus.B1500277>
- Gupta, P. K., Chand, R., Vasistha, N. K., Pandey, S. P., Kumar, U., Mishra, V. K., & Joshi, A. K. (2018). Spot blotch disease of wheat: The current status of research on genetics and breeding. *Plant Pathology*, 67, 508–531. <https://doi.org/10.1111/ppa.12781>
- Gutiérrez, L., German, S., Pereyra, S., Hayes, P. M., Perez, C. A., Capettini, F., ... Castro, A. J. (2015). Multi-environment multi-QTL association mapping identifies disease resistance QTL in barley germplasm from Latin America. *Theoretical and Applied Genetics*, 128, 501–516. <https://doi.org/10.1007/s00122-014-2448-y>
- Gyawali, S., Chao, S., Vaish, S. S., Singh, S. P., Rehman, S., Vishwakarma, S. R., & Verma, R. P. S. (2018). Genome wide association studies (GWAS) of spot blotch resistance at the seedling and the adult plant stages in a collection of spring barley. *Molecular Breeding*, 38, 1–14. <https://doi.org/10.1007/s11032-018-0815-0>
- Haas, M., Menke, J., Chao, S., & Steffenson, B. J. (2016). Mapping quantitative trait loci conferring resistance to a widely virulent isolate of *Cochliobolus sativus* in wild barley accession PI 466423. *Theoretical and Applied Genetics*, 129, 1831–1842. <https://doi.org/10.1007/s00122-016-2742-y>
- Hiraga, S., Sasaki, K., Ito, H., Ohashi, Y., & Matsui, H. (2001). A large family of class III plant peroxidases. *Plant and Cell Physiology*, 42, 462–468. <https://doi.org/10.1093/pcp/pce061>
- Kumar, J., Schäfer, P., Hüchelhoven, R., Langen, G., Baltruschat, H., Stein, E., ... Kogel, K. H. (2002). *Bipolaris sorokiniana*, a cereal pathogen of global concern: Cytological and molecular approaches towards better control. *Molecular Plant Pathology*, 3, 185–195. <https://doi.org/10.1046/j.1364-3703.2002.00120.x>
- Kumar, U., Joshi, A. K., Kumar, S., Chand, R., & Röder, M. S. (2010). Quantitative trait loci for resistance to spot blotch caused by *Bipolaris sorokiniana* in wheat (*T. aestivum* L.) lines 'Ning 8201' and 'Chirya 3'. *Molecular Breeding*, 26, 477–491. <https://doi.org/10.1007/s11032-009-9388-2>
- Lashina, N. M., & Afanasenko, O. S. (2019). Susceptibility of leaf blights of commercial barley cultivars in North-Western region of Russia. *Plant Protection News*, 2, 23–28. [https://doi.org/10.31993/2308-6459-2019-2\(100\)-23-28](https://doi.org/10.31993/2308-6459-2019-2(100)-23-28)
- Legocki, R. P., & Verma, D. P. S. (1980). Identification of "nodule-specific" host proteins (nodulins) involved in the development of *Rhizobium-legume* symbiosis. *Cell*, 20, 153–163. [https://doi.org/10.1016/0092-8674\(80\)90243-3](https://doi.org/10.1016/0092-8674(80)90243-3)
- Leng, Y., Wang, R., Ali, S., Zhao, M., & Zhong, S. (2016). Sources and Genetics of Spot Blotch Resistance to a New Pathotype of *Cochliobolus sativus* in the USDA National Small Grains Collection. *Plant Disease*, 100, 1988–1993. <https://doi.org/10.1094/pdis-02-16-0152-re>
- Leng, Y., Zhao, M., Wang, R., Steffenson, B. J., Brueggeman, R. S., & Zhong, S. (2018). The gene conferring susceptibility to spot blotch caused by *Cochliobolus sativus* is located at the *Mla* locus in barley cultivar Bowman. *Theoretical and Applied Genetics*, 131, 1531–1539. <https://doi.org/10.1007/s00122-018-3095-5>
- Lillemo, M., Joshi, A. K., Prasad, R., Chand, R., & Singh, R. P. (2013). QTL for spot blotch resistance in bread wheat line Saar co-locate to the biotrophic disease resistance loci *Lr34* and *Lr46*. *Theoretical and Applied Genetics*, 126, 711–719. <https://doi.org/10.1007/s00122-012-2012-6>
- Lipka, A. E., Tian, F., Wang, Q., Peiffer, J., Li, M., Bradbury, P. J., ... Zhang, Z. (2012). GAPIT: Genome association and prediction integrated tool. *Bioinformatics*, 28, 2397–2399. <https://doi.org/10.1093/bioinformatics/bts444>
- Liu, H., Ma, Y., Chen, N., Guo, S., Liu, H., Guo, X., ... Xu, Y. (2014). Overexpression of stress-inducible OsBURP16, the β subunit of polygalacturonase 1, decreases pectin content and cell adhesion and increases abiotic stress sensitivity in rice. *Plant, Cell & Environment*, 37, 1144–1158.
- Martin, A., Platz, G. J., de Klerk, D., Fowler, R. A., Smit, F., Potgieter, F. G., & Prins, R. (2018). Identification and mapping of net form of net blotch resistance in South African barley. *Molecular Breeding*, 38, <https://doi.org/10.1007/s11032-018-0814-1>
- Mascher, M., Gundlach, H., Himmelbach, A., Beier, S., Twardziok, S. O., Wicker, T., ... Stein, N. (2017). A chromosome conformation capture ordered sequence of the barley genome. *Nature*, 544, 427–433. <https://doi.org/10.1038/nature22043>
- Mathre, D. (1997). *Compendium of Barley Diseases*. The American Phytopathological Society. St. Paul, MN: APS Press.
- Meldrum, S., Platz, D., & Ogle, H. (2004). Pathotypes of *Cochliobolus sativus* on barley in Australia. *Australasian Plant Pathology*, 33, 109–114. <https://doi.org/10.1071/AP03088>
- Muqaddasi, Q. H., Reif, J. C., Li, Z., Basnet, B. R., Dreisigacker, S., & Röder, M. S. (2017). Genome-wide association mapping and genome-wide prediction of anther extrusion in CIMMYT spring wheat. *Euphytica*, 213, 1–7. <https://doi.org/10.1007/s10681-017-1863-y>
- Murray, T. D., Parry, D. W., & Cattlin, N. D. (1998). *A color handbook of diseases of small grain cereal crops*.
- Noctor, G., Mhamdi, A., Chaouch, S., Han, Y., Neukermans, J., Marquez-Garcia, B., ... Foyer, C. H. (2012). Glutathione in plants: An integrated overview. *Plant, Cell & Environment*, 35, 454–484. <https://doi.org/10.1111/j.1365-3040.2011.02400.x>
- Novakazi, F., Afanasenko, O., Anisimova, A., Platz, G. J., Snowdon, R., Kovaleva, O., ... Ordon, F. (2019). Genetic analysis of a worldwide barley collection for resistance to net form of net blotch disease (*Pyrenophora teres* f. *teres*). *Theoretical and Applied Genetics*, 132, 2633–2650. <https://doi.org/10.1007/s00122-019-03378-1>

- Pritchard, J. K., Stephens, M., & Donnelly, P. (2000). Inference of population structure using multilocus genotype data. *Genetics*, 155, 945–959.
- Radojčić Redovniković, I., Glivetić, T., Delonga, K., & Vorkapić-Furač, J. (2008). Glucosinolates and their potential role in plant. *Periodicum Biologorum*, 110, 297–309.
- Raemaekers, R. (1988). *Helminthosporium sativum*: disease complex on wheat and sources of resistance in Zambia. Paper presented at the Wheat Production Constraints in Tropical Environments. Chiang Mai, Thailand. 19–23 Jan 1987.
- Rehman, H. M., Nawaz, M. A., Shah, Z. H., Ludwig-Müller, J., Chung, G., Ahmad, M. Q., ... Lee, S. I. (2018). Comparative genomic and transcriptomic analyses of Family-1 UDP glycosyltransferase in three Brassica species and Arabidopsis indicates stress-responsive regulation. *Scientific Reports*, 8, 1875. <https://doi.org/10.1038/s41598-018-19535-3>
- Reif, J. C., Melchinger, A. E., & Frisch, M. (2005). Genetical and mathematical properties of similarity and dissimilarity coefficients applied in plant breeding and seed bank management. *Crop Science*, 45, 1–7. <https://doi.org/10.2135/cropsci2005.0001>
- Reimann, R., Kost, B., & Dettmer, J. (2017). Tetraspanins in plants. *Frontiers in Plant Science*, 8, 545. <https://doi.org/10.3389/fpls.2017.00545>
- Richards, J. K., Friesen, T. L., & Brueggeman, R. S. (2017). Association mapping utilizing diverse barley lines reveals net form net blotch seedling resistance/susceptibility loci. *Theoretical and Applied Genetics*, 130, 915–927. <https://doi.org/10.1007/s00122-017-2860-1>
- Roy, J. K., Smith, K. P., Muehlbauer, G. J., Chao, S., Close, T. J., & Steffenson, B. J. (2010). Association mapping of spot blotch resistance in wild barley. *Molecular Breeding*, 26, 243–256. <https://doi.org/10.1007/s11032-010-9402-8>
- Saari, E., & Prescott, J. (1975). Scale for appraising the foliar intensity of wheat diseases. *Plant Disease Reporter*, 56, 847–849.
- Sannemann, W., Huang, B. E., Mathew, B., & Léon, J. (2015). Multi-parent advanced generation inter-cross in barley: High-resolution quantitative trait locus mapping for flowering time as a proof of concept. *Molecular Breeding*, 35, 86. <https://doi.org/10.1007/s11032-015-0284-7>
- Sharma, P., Duveiller, E., & Sharma, R. C. (2006). Effect of mineral nutrients on spot blotch severity in wheat, and associated increases in grain yield. *Field Crops Research*, 95, 426–430. <https://doi.org/10.1016/j.fcr.2005.04.015>
- Sharma, R., & Duveiller, E. (2007). Advancement toward new spot blotch resistant wheats in South Asia. *Journal of Crop Science*, 47, 961–968. <https://doi.org/10.2135/cropsci2006.03.0201>
- Singh, R., Singh, A., & Singh, S. (1998). Distribution of pathogens causing foliar blights of wheat in India and neighboring countries. In E. Duveiller, H. Dubin, J. Reeves, & A. McNab (Eds.), *Helminthosporium blights of wheat: Spot blotch and Tan Spot* (pp. 59–62). Mexico, DF: Centro Internacional de Mejoramiento de Maíz y Trigo.
- Singh, V., Singh, G., Chaudhury, A., Ojha, A., Tyagi, B. S., Chowdhary, A. K., & Sheoran, S. (2016). Phenotyping at hot spots and tagging of QTLs conferring spot blotch resistance in bread wheat. *Molecular Biology Reports*, 43, 1293–1303. <https://doi.org/10.1007/s11033-016-4066-z>
- Steffenson, B., Hayes, P., & Kleinhofs, A. (1996). Genetics of seedling and adult plant resistance to net blotch (*Pyrenophora teres f. teres*) and spot blotch (*Cochliobolus sativus*) in barley. *Theoretical and Applied Genetics*, 92, 552–558. <https://doi.org/10.1007/BF00224557>
- Stein, N., Herren, G., & Keller, B. (2001). A new DNA extraction method for high-throughput marker analysis in a large-genome species such as *Triticum aestivum*. *Plant Breeding*, 120, 354–356. <https://doi.org/10.1046/j.1439-0523.2001.00615.x>
- Storey, J. D., & Tibshirani, R. (2003). Statistical significance for genome-wide studies. *Proceedings of the National Academy of Sciences*, 100, 9440–9445. <https://doi.org/10.1073/pnas.1530509100>
- Takahashi, H. (2019). Sulfate transport systems in plants: Functional diversity and molecular mechanisms underlying regulatory coordination. *Journal of Experimental Botany*, 70(16), 4075–4087. <https://doi.org/10.1093/jxb/erz132>
- Thatcher, L. F., Kazan, K., & Manners, J. M. (2012). Lateral organ boundaries domain transcription factors: New roles in plant defense. *Plant Signaling & Behavior*, 7, 1702–1704. <https://doi.org/10.4161/psb.22097>
- Tinline, R. (1951). Studies on the perfect stage of *Helminthosporium sativum*. *Canadian Journal of Botany*, 29, 467–478.
- Valjavec-Gratian, M., & Steffenson, B. (1997). Pathotypes of *Cochliobolus sativus* on barley in North Dakota. *Plant Disease*, 81, 1275–1278.
- Vatter, T., Maurer, A., Kopahnke, D., Perovic, D., Ordon, F., & Pillen, K. (2017). A nested association mapping population identifies multiple small effect QTL conferring resistance against net blotch (*Pyrenophora teres f. teres*) in wild barley. *PLoS ONE*, 12, e0186803. <https://doi.org/10.1371/journal.pone.0186803>
- Vogt, T., & Jones, P. (2000). Glycosyltransferases in plant natural product synthesis: Characterization of a supergene family. *Trends in Plant Science*, 5, 380–386. [https://doi.org/10.1016/S1360-1385\(00\)01720-9](https://doi.org/10.1016/S1360-1385(00)01720-9)
- Voragen, A. G., Coenen, G.-J., Verhoef, R. P., & Schols, H. A. (2009). Pectin, a versatile polysaccharide present in plant cell walls. *Structural Chemistry*, 20, 263. <https://doi.org/10.1007/s11224-009-9442-z>
- Wagner, S. (2011). *Biological Nitrogen Fixation*. Nature Education Knowledge 3 (10): 15. In (Vol. 3, pp. 15).
- Wang, F., Muto, A., Van de Velde, J., Neyt, P., Himanen, K., Vandepoele, K., & Van Lijsebettens, M. (2015). Functional analysis of the Arabidopsis TETRASPANIN gene family in plant growth and development. *Plant Physiology*, 169, 2200–2214.
- Wang, R., Leng, Y., Ali, S., Wang, M., & Zhong, S. (2017). Genome-wide association mapping of spot blotch resistance to three different pathotypes of *Cochliobolus sativus* in the USDA barley core collection. *Molecular Breeding*, 37, 1–14. <https://doi.org/10.1007/s11032-017-0626-8>
- Wang, R., Leng, Y., Zhao, M., & Zhong, S. (2019). Fine mapping of a dominant gene conferring resistance to spot blotch caused by a new pathotype of *Bipolaris sorokiniana* in barley. *Theoretical and Applied Genetics*, 132, 41–51. <https://doi.org/10.1007/s00122-018-3192-5>
- Wang, X., Zhang, S., Su, L., Liu, X., & Hao, Y. (2013). A genome-wide analysis of the LBD (LATERAL ORGAN BOUNDARIES domain) gene family in *Malus domestica* with a functional characterization of MdLBD11. *PLoS ONE*, 8, e57044. <https://doi.org/10.1371/journal.pone.0057044>
- Wilcoxson, R., Rasmusson, D., & Miles, M. (1990). Development of barley resistant to spot blotch and genetics of resistance. *Plant Disease*, 74, 207–210. <https://doi.org/10.1094/PD-74-0207>
- Xu, C., Luo, F., & Hochholdinger, F. (2016). LOB domain proteins: Beyond lateral organ boundaries. *Trends in Plant Science*, 21, 159–167. <https://doi.org/10.1016/j.tplants.2015.10.010>
- Yun, S., Gyenis, L., Bossolini, E., Hayes, P., Matus, I., Smith, K. P., ... Muehlbauer, G. J. (2006). Validation of quantitative trait loci for multiple disease resistance in barley using advanced backcross lines developed with a wild barley. *Crop Science*, 46, 1179–1186. <https://doi.org/10.2135/cropsci2005.08-0293>
- Yun, S. J., Gyenis, L., Hayes, P. M., Matus, I., Smith, K. P., Steffenson, B. J., & Muehlbauer, G. J. (2005). Quantitative Trait Loci for Multiple Disease Resistance in Wild Barley. *Crop Science*, 45, <https://doi.org/10.2135/cropsci2005.0236>
- Zhang, Z., Ersoz, E., Lai, C.-Q., Todhunter, R. J., Tiwari, H. K., Gore, M. A., ... Buckler, E. S. (2010). Mixed linear model approach adapted for genome-wide association studies. *Nature Genetics*, 42, 355. <https://doi.org/10.1038/ng.546>

- Zhou, H., & Steffenson, B. (2013). Genome-wide association mapping reveals genetic architecture of durable spot blotch resistance in US barley breeding germplasm. *Molecular Breeding*, 32, 139–154. <https://doi.org/10.1007/s11032-013-9858-4>
- Zhu, Z., Bonnett, D., Ellis, M., Singh, P., Heslot, N., Dreisigacker, S., ... Mujeeb-Kazi, A. (2014). Mapping resistance to spot blotch in a CIMMYT synthetic-derived bread wheat. *Molecular Breeding*, 34, 1215–1228. <https://doi.org/10.1007/s11032-014-0111-6>

How to cite this article: Novakazi F, Afanasenko O, Lashina N, et al. Genome-wide association studies in a barley (*Hordeum vulgare*) diversity set reveal a limited number of loci for resistance to spot blotch (*Bipolaris sorokiniana*). *Plant Breed.* 2019;00:1–15. <https://doi.org/10.1111/pbr.12792>

6 Discussion

6.1 Candidate genes located in regions identified for net blotch resistance

In the present study, a barley set comprising 449 accessions from all over the world was evaluated for resistance against the fungal pathogen *Pyrenophora teres* f. *teres*, the causal agent of the net form of net blotch. The accessions were phenotyped in field trials at three locations (Australia, Germany, Belarus) and under greenhouse conditions with three isolates (*NFNB 50*, *No 13*, *Hoehnstedt*). Subsequent genome-wide association studies revealed 15 distinct regions associated with resistance located on chromosomes 3H, 4H, 5H, 6H and 7H (Table 5.1) (Novakazi et al. 2019a). Predicted genes, their locations and annotations were retrieved from the BARLEYMAP pipeline (Cantalapiedra et al. 2015) (<http://floresta.eead.csic.es/barleymap/>). The number of predicted genes per identified QTL was between one and 363 genes (Table 5.1). In nine regions, promising candidate genes that are associated with disease resistance were identified (Table 5.2). The complete lists of predicted genes, and their annotated functions, located in the respective identified QTL can be found in the Annex in Table A.1 to Table A.12 .

Table 6.1 Number of high and low confidence genes located in QTL regions associated with resistance against *Pyrenophora teres* f. *teres*.

QTL ^a	Chromosome	Interval [Mb]	No of HC ^b	No of LC ^c	with unknown function
QRptt_3H-1	3H	58-101	38	9	9
QRptt_3H-2	3H	119-138	6	1	2
QRptt_3H-3	3H	233-350	88	29	24
QRptt_3H-4	3H	428-492	153	25	36
QRptt_3H-5	3H	621	3	1	1
QRptt_4H-1	4H	33-70	31	4	4
QRptt_4H-2	4H	352	1	-	-
QRptt_5H-1	5H	579	1	-	-
QRptt_5H-2	5H	634	1	-	-
QRptt_6H-1	6H	37-76	112	30	34
QRptt_6H-2	6H	123-344	279	84	80
QRptt_6H-3	6H	355-379	43	9	10
QRptt_6H-4	6H	406-410	10	4	2
QRptt_7H-1	7H	5	1	-	-
QRptt_7H-2	7H	645	5	3	1

^a QTL nomenclature follows Grewal et al. (2008) with a suffix to distinguish QTL on the same chromosome

^b HC – high confidence genes, ^c LC – low confidence genes

Discussion

Plants are constantly exposed to abiotic and biotic stresses. Abiotic factors include, e.g. cold and heat, drought and flooding, salinity, alkaline or acidic pH (Elmore et al. 2018). Biotic stress in plants is caused by vertebrates, insects, bacteria, viruses, and phytopathogenic fungi (Saade et al. 2018). Plants have different ways to defend themselves and react to biotic stress. The first barrier against pathogen attack is the plant cell wall. The cell wall is divided into the primary and secondary cell wall. The primary cell wall consists mainly of cellulose microfibrils, hemicellulose and pectin. In the secondary cell wall, pectin is mostly replaced by lignin, a phenolic compound that is insoluble, and hard to chew or penetrate for pathogens (Varner and Lin 1989). Monocotyledonous plants may have silicate in their epidermis, which gives strength to the leaves and makes it less attractive to chewing pests. The cuticle can be covered with a wax layer as protection against abiotic stress as well as against penetration by pathogens. Furthermore, the cuticle can be covered with trichomes that serve as mechanical or chemical repellents by secreting secondary plant metabolites (Freeman and Beattie 2008).

Next to the physical barrier, plants have several physiological pathways that are triggered by pathogen attack. The first level of plant defence is the pathogen unspecific basal resistance (horizontal resistance) that is recognized by pattern recognition receptors (PRR) anchored in the plant cell wall membrane, also called pattern triggered immunity (PTI) (Panstruga et al. 2009; Zipfel and Robatzek 2010). These PRR include leucine-rich repeat (LRR) receptor-like kinases, which bind to microbe-/ pathogen-associated molecular patterns (MAMPs/ PAMPs) (Panstruga et al. 2009). These patterns can be, for example pathogen cell wall fragments, extracellular proteins or lipopolysaccharides (Zipfel and Robatzek 2010). A pathogen or race specific (vertical resistance) pathway is the effector triggered immunity (ETI) (Panstruga et al. 2009). Receptors (*R* genes), like C-terminal LRR with nucleotide-binding (NB) domains located in the cytoplasm recognize pathogen specific proteins (*Avr* genes) and induce the defence pathway (Panstruga et al. 2009). PTI and ETI pathways are very similar and usually interact with each other in a zigzag model (Jones and Dangl 2006). However, ETI usually leads to a hypersensitive response (HR; programmed cell death) and is, therefore, associated with resistance to biotrophic and hemibiotrophic pathogens. PTI does not induce HR. Recognition of patterns or effectors leads to immediate activation of Ca^{2+} channels and activation of NADPH-oxidase complex producing reactive oxygen species (ROS) that are toxic to the pathogen (Almagro et al. 2008). Callose is deposited

Discussion

into the plant cell wall in order to hinder further pathogen penetration (Freeman and Beattie 2008). Through phosphorylation the mitogen-activated protein kinases (MAPK) cascade is activated, which transmits the signal to the nucleus and leads to transcription of defence genes (Asai et al. 2002; Panstruga et al. 2009). Recognition of patterns and effectors induce the biosynthesis of the plant hormones salicylic acid (SA), ethylene (ET) and jasmonic acid (JA), which are involved in intercellular signalling. Biosynthesis of ET and JA are coordinated, but in conflict with the SA pathway (Panstruga et al. 2009).

LRR are crucial proteins in plant defence. They are the first receptors to recognize MAMPs/PAMPs in PTI and Avr proteins in ETI (Bent et al. 1994; DeYoung and Innes 2006). In QRptt_6H-1, QRptt_6H-2 and QRptt_6H-4 four LRR receptor-like protein kinases are located (HORVU6Hr1G016710, HORVU6Hr1G038550, HORVU6Hr1G038700, HORVU6Hr1G061250; Table 5.2). LRRs activate the MAPK-cascade signalling pathway (Asai et al. 2002). Two MAPKs are located in QTL QRptt_3H-4 (HORVU3Hr1G057660, HORVU3Hr1G060390; Table 5.2). One of the first steps in early defence is the release of ROS (oxidative burst). Peroxidases (HORVU6Hr1G021520; QRptt_6H-1) are involved in the metabolism of ROS by catalysing hydrogen peroxide oxidoreduction, and have been shown to be involved in pathogen recognition and enhanced disease resistance (Almagro et al. 2008; Hiraga et al. 2001). Additionally, peroxidases are involved in lignin and suberin biosynthesis, which are well-described cell wall components (Almagro et al. 2008; Hiraga et al. 2001). Another enzyme involved in lignin and suberin biosynthesis is the O-methyltransferase, which is associated with increased cell wall strength and disease resistance (Lam et al. 2007; Wang et al. 2018). A family protein of this enzyme was identified to be located in QRptt_7H-2 (HORVU7Hr1G117710; Table 5.2). In the three identified regions QRptt_3H-3, QRptt_3H-4 and QRptt_6H-2 callose synthases are located (HORVU3Hr1G042540, HORVU3Hr1G061700 and HORVU6Hr1G031230; Table 5.2). Callose is a (1,3)- β -glucan polymer that is deposited between the plant cell wall and the cell membrane to form papillae after pathogen attack in order to hamper further cellular penetration (Freeman and Beattie 2008; Voigt 2014). It was shown that an early deposition of callose at sites of pathogen penetration can lead to complete resistance (Ellinger et al. 2013). Two glucan synthases, which are necessary for callose synthesis, are located in QRptt_3H-4 and QRptt_6H-2 (HORVU3Hr1G058470 and HORVU6Hr1G031200) in close proximity to the callose synthases (Table 5.2).

Table 6.2 Predicted genes that are associated with disease recognition or defence located in identified QTL regions on chromosomes 3H, 4H, 6H and 7H, and their respective functional annotations.

QTL	Gene ID ^a	Gene class ^b	Chr	Physical location [bp]		Annotation
QRptt_3H-1						
	HORVU3Hr1G021120	HC_G	3H	67,2667,34	67,272,759	WRKY DNA-binding protein 13
	HORVU3Hr1G021810	HC_G	3H	75,014,380	75,162,233	UDP-Glycosyltransferase superfamily protein
QRptt_3H-3						
	HORVU3Hr1G039500	HC_G	3H	233,580,657	233,585,235	WRKY family transcription factor
	HORVU3Hr1G039700	HC_G	3H	236,672,228	236,674,265	Chaperone protein DnaJ 1
	HORVU3Hr1G040040	HC_G	3H	239,983,665	239,989,000	Calmodulin 7
	HORVU3Hr1G042500	HC_G	3H	269,929,071	269,963,305	Chaperone protein DnaJ 15
	HORVU3Hr1G042540	HC_G	3H	270,264,122	270,269,601	Callose synthase 1
	HORVU3Hr1G049640	HC_G	3H	350,511,726	350,515,250	Calmodulin-binding family protein
QRptt_3H-4						
	HORVU3Hr1G057660	HC_G	3H	434,386,942	434,402,600	Mitogen-activated protein kinase 16
	HORVU3Hr1G058470	HC_G	3H	441,452,592	441,489,005	Glucan synthase-like 7
	HORVU3Hr1G059250	HC_G	3H	448,558,019	448,559,843	Ethylene-responsive transcription factor 3
	HORVU3Hr1G060390	HC_G	3H	460,310,395	460,316,427	Mitogen-activated protein kinase 18
	HORVU3Hr1G060500	HC_G	3H	460,762,240	460,768,227	WRKY DNA-binding protein 28
	HORVU3Hr1G061700	HC_G	3H	469,774,652	469,781,509	Callose synthase 5
	HORVU3Hr1G064470	HC_G	3H	491,894,156	491,895,847	Chitinase family protein
QRptt_4H-1						
	HORVU4Hr1G011160	HC_G	4H	33,953,501	33,958,081	Endoglucanase 10
	HORVU4Hr1G016010	HC_G	4H	64,247,694	64,252,294	Disease resistance protein
QRptt_6H-1						
	HORVU6Hr1G016710	HC_G	6H	37,818,242	37,819,918	Leucine-rich repeat receptor-like protein kinase family protein
	HORVU6Hr1G016750	HC_G	6H	38,138,862	38,155,102	Endoglucanase 11
	HORVU6Hr1G017680	HC_G	6H	42,338,523	42,350,309	E3 ubiquitin-protein ligase MARCH8
	HORVU6Hr1G018920	HC_G	6H	49,541,658	49,544,373	Disease resistance protein
	HORVU6Hr1G018960	HC_G	6H	49,777,455	49,792,561	Disease resistance protein
	HORVU6Hr1G019510	HC_G	6H	53,102,840	53,106,956	Calmodulin-binding family protein
	HORVU6Hr1G020960	HC_G	6H	61,216,573	61,218,634	UDP-Glycosyltransferase superfamily protein
	HORVU6Hr1G021340	HC_G	6H	64,214,424	64,223,510	Pathogenesis related homeodomain protein A
	HORVU6Hr1G021520	HC_G	6H	65,256,521	65,259,501	Peroxidase superfamily protein

Discussion

Table 6.2 continued

HORVU6Hr1G021780	HC_G	6H	67,713,930	67,718,653	Disease resistance protein
HORVU6Hr1G022270	HC_G	6H	70,238,436	70,243,944	Endoglucanase 5
QRptt_6H-2					
HORVU6Hr1G030270	HC_G	6H	125,731,730	125,739,064	Calmodulin-binding protein
HORVU6Hr1G030590	HC_G	6H	128,364,135	128,427,106	Calcium-transporting ATPase, putative
HORVU6Hr1G031200	HC_G	6H	131,470,904	131,488,669	Glucan synthase-like 4
HORVU6Hr1G031230	HC_G	6H	131,686,357	131,708,107	Callose synthase 1
HORVU6Hr1G031550	HC_G	6H	134,080,947	134,093,670	Disease resistance protein
HORVU6Hr1G032960	HC_G	6H	146,603,312	146,607,205	Calcium-binding protein 4
HORVU6Hr1G033290	HC_G	6H	151,122,430	151,129,124	MLO-like protein 1
HORVU6Hr1G035370	HC_G	6H	169,991,412	169,996,625	UDP-Glycosyltransferase superfamily protein
HORVU6Hr1G037080	HC_G	6H	185,162,825	185,164,404	Cytochrome c oxidase subunit 1
HORVU6Hr1G037680	HC_G	6H	190,084,075	190,088,684	Apoptotic protease-activating factor 1
HORVU6Hr1G038550	HC_G	6H	197,166,468	197,170,689	Leucine-rich receptor-like protein kinase family protein
HORVU6Hr1G038700	HC_G	6H	198,574,495	198,578,108	Leucine-rich receptor-like protein kinase family protein
HORVU6Hr1G040190	HC_G	6H	214,737,148	214,742,557	Calcium-binding EF hand family protein
HORVU6Hr1G042680	HC_G	6H	240,355,213	240,384,215	Ethylene-responsive transcription factor-like protein
HORVU6Hr1G046540	HC_G	6H	273,590,458	273,602,473	Calmodulin-binding protein
HORVU6Hr1G047770	HC_G	6H	286,130,856	286,133,131	Chaperone protein DnaJ-related
QRptt_6H-3					
HORVU6Hr1G057110	HC_G	6H	369,306,242	369,310,633	Disease resistance protein
HORVU6Hr1G058100	HC_G	6H	379,344,988	379,350,913	E3 ubiquitin-protein ligase PRT1
QRptt_6H-4					
HORVU6Hr1G061010	HC_G	6H	407,356,258	407,360,811	Hsp70-Hsp90 organizing protein
HORVU6Hr1G061250	HC_G	6H	410,038,393	410,040,206	Leucine-rich repeat receptor-like protein kinase family protein
QRptt_7H-2					
HORVU7Hr1G117570	HC_G	7H	645,373,486	645,381,646	Disease resistance protein
HORVU7Hr1G117710	HC_G	7H	645,731,921	645,733,781	O-methyltransferase family protein

^a The predicted genes and their respective annotations were obtained from the latest version of BARLEYMAP (Cantalapiedra et al. 2015)

^b HC_G - high confidence gene with predicted function

Discussion

Several calcium transporting and binding as well as calmodulin and calmodulin-binding proteins are located in the regions QRptt_3H-3, QRptt_6H-1 and QRptt_6H-2 (Table 5.2). Ca^{2+} is found in every cell and is the most important molecule for inter- and intracellular signal transduction and ion fluxes across the membrane (Cheval et al. 2013; Clapham 2007). Calcium concentration in the cytoplasm changes in reaction to environmental changes like light, temperature, abiotic stresses and after pathogen attack (Cheval et al. 2013). The change in Ca^{2+} concentration is sensed by proteins, from which calmodulin is perhaps the most famous (Cheval et al. 2013; Clapham 2007). Calmodulin binds 4 Ca^{2+} ions upon which calmodulin exposes binding sites for downstream proteins (Zhang et al. 2014). This way Ca^{2+} and calmodulin are involved in pathogen defence pathways like SA biosynthesis or nitric oxide (NO) production (Cheval et al. 2013; Zhang et al. 2014).

UDP-Glycosyltransferase superfamily proteins, HORVU3Hr1G021810, HORVU6Hr1G020960, and HORVU6Hr1G035370, are located in QTL QRptt_3H-1, QRptt_6H-1 and QRptt_6H-2, respectively (Table 5.2). UDP-Glycosyltransferases are involved in several biosynthesis pathways and glycosylation of phytohormones (Rehman et al. 2018; Vogt and Jones 2000). Phytohormones serve as signalling molecules in the cell but also over long distances (Heil and Ton 2008). Phytohormones associated with pathogen defence are SA, JA and gaseous ET (Panstruga et al. 2009). Increased levels of SA induce the expression of pathogenesis-related (PR) proteins and are associated with resistance against biotrophic pathogens and involved in systemic acquired resistance (SAR) (Heil and Ton 2008; Pieterse and Van Loon 1999). JA and ET biosynthesis are induced after attack of necrotrophic pathogens and trigger the transcription of pathogen defence genes (Adie et al. 2007; Bari and Jones 2009). Although, SA and ET/JA pathways are antagonistic, there is still some synergistic cross-talk between the pathways (Bari and Jones 2009; Panstruga et al. 2009). Ethylene responsive transcription factors are located in QTL QRptt_3H-4 and QRptt_6H-2 (HORVU3Hr1G059250, HORVU6Hr1G042680; Table 5.2). Ubiquitin proteins are a family of enzymes with a variety of mode of actions and can be divided into ubiquitin-activating (E1), ubiquitin-conjugating (E2) and ubiquitin ligase (E3) enzymes (Craig et al. 2009). E3 enzymes have been shown to regulate the JA pathway (Chini et al. 2007; Craig et al. 2009; Turner et al. 2002). Two E3 enzymes are located in QRptt_6H-1 and QRptt_6H-3, i.e. HORVU6Hr1G017680 and HORVU6Hr1G058100, respectively (Table 5.2). HORVU6Hr1G058100 is

Discussion

a PROTEOLYSIS 1 (PRT1) protein that was shown to confer resistance in *Arabidopsis thaliana* against the necrotrophic pathogen *Sclerotinia sclerotiorum*, but not the biotrophic pathogen *Botrytis cinerea* (De Marchi et al. 2016).

HSP70 and HSP90 (HORVU6Hr1G061010; QRptt_6H-4) belong to the family of heat shock proteins (HSPs) and are chaperones that are responsible for protein folding, translocation and degradation, but are also involved in response to abiotic and biotic stresses (Park and Seo 2015; Rajan and D'Silva 2009). In order to function properly some HSPs like HSP70 require the presence of and interaction with their co-chaperones, i.e. the J-proteins (DnaJ proteins) (Rajan and D'Silva 2009). In QRptt_3H-3 and QRptt_6H-2, two and one DnaJ proteins, respectively, were identified (HORVU3Hr1G039700, HORVU3Hr1G042500 and HORVU6Hr1G047770; Table 5.2). In soybean overexpression of DnaJ protein HSP40 resulted in enhanced cell death and disease resistance, while silencing had the opposite effect (Liu and Whitham 2013). In rice, however, silencing of DnaJ *OsDjA6* increased ROS levels and enhanced resistance towards the rice blast fungus *Magnaporthe oryzae* (Zhong et al. 2018).

A cytochrome c oxidase subunit (HORVU6Hr1G037080) and an apoptotic protease-activating factor 1 (Apaf1) (HORVU6Hr1G037680) are located in QRptt_6H-2, only 5 Mbp apart from each other (Table 5.2). Cytochrome c is involved in programmed cell death (PCD), an organised process necessary for animal and plant development and associated with hypersensitive response. Leaked cytochrome c from mitochondria into the cytoplasm binds Apaf1 and triggers PCD, also called apoptosis (Vianello et al. 2007).

One WRKY transcription factor (TF) (HORVU3Hr1G039500) and two WRKY DNA-binding proteins (HORVU3Hr1G021120, HORVU3Hr1G060500) are located in QRptt_3H-3 and QRptt_3H-1 and QRptt_3H-4, respectively (Table 5.2). The WRKY superfamily consists of many TFs. So far 74 in *Arabidopsis* (*Arabidopsis thaliana*), 109 in rice (*Oryza sativa*) and 45 in barley were identified (Mangelsen et al. 2008; Pandey and Somssich 2009). They can be distinguished into three subgroups (sucrose signalling, plant defence and temperature response) and form dense networks of TF that interact with each other (Bakshi and Oelmüller 2014; Mangelsen et al. 2008; Pandey and Somssich 2009). WRKY TFs are involved in regulating SA biosynthesis and expression of non-expressor of pathogen-

Discussion

related 1 (NPR1) (Eulgem and Somssich 2007; Panstruga et al. 2009). Induced by PAMPs and activated through phosphorylation by MAP-kinases WRKY proteins activate or repress the transcription of defence genes and can enhance or reduce resistance (Eulgem and Somssich 2007; Pandey and Somssich 2009). Shen et al. (2007) showed that the barley pathogen *Blumeria graminis* interacts with TFs *HvWRKY1/2* by activating their expression and thereby repressing basal defence mechanisms, leading to enhanced susceptibility of barley towards powdery mildew infection.

On chromosome 6H at 151,122,430 – 151,129,124 bp there is a MLO-like protein (QRptt_6H-2, Table 5.2). The first Mlo (mildew resistance locus o)-mediated resistant two-rowed spring barley cultivars were released in the late 1970s to early 1980s (Jørgensen 1992) and was since described in numerous plant species (Kusch and Panstruga 2017). The Mlo gene has numerous alleles and confers recessive (*mlo* genotype), broad resistance against almost all powdery mildew (*Blumeria graminis* f. sp. *hordei*) isolates (Acevedo-Garcia et al. 2014). The gene is located on the long arm of chromosome 4H and was cloned in the late 1990s (Büschges et al. 1997). The Mlo protein has seven transmembrane domains and is located in the lipid bilayer, with an intracellular carboxy terminus and an extracellular amino terminus (Devoto et al. 2003). The exact function of the *Mlo* gene still remains unclear (Acevedo-Garcia et al. 2014; Kusch and Panstruga 2017), however, in order to express full susceptibility, Mlo requires the binding of calmodulin and presence of Ca^{2+} (Bayles and Aist 1987; Kim et al. 2002). The *mlo* resistance is based on loss-of-function mutations and the early formation of papillae and callose deposition in the cell wall and the regulation of cell death, thereby inhibiting haustoria formation and pathogen development (Jørgensen 1992; Piffanelli et al. 2002; Skou 1985). It was suggested that *mlo* mutants confer resistance against biotrophic pathogens that colonize the epidermal cells (Jørgensen 1992), but show increased susceptibility towards hemibiotrophic, toxin releasing pathogens, like *Pyrenophora teres*, *Bipolaris sorokiniana* and *Rhynchosporium commune* (Jørgensen 1992; Kusch and Panstruga 2017).

The fungal cell wall consists mainly of mannoproteins (mannan), β -1,3-glucans, chitin and a phospholipid bilayer containing ergosterol (Bowman and Free 2006; Gow et al. 2017). Chitin and glucans are the main building blocks for fungal cell wall structure and integrity (Bowman and Free 2006), making both polymers easy targets for plant defence mechanisms. Plant chitinases, are located

Discussion

in region QRptt_3H-4 (HORVU3Hr1G064470, Table 5.2) and endoglucanases are located in regions QRptt_4H-1 and QRptt_6H-1 (HORVU4Hr1G011160, HORVU6Hr1G016750, HORVU6Hr1G022270; Table 5.2) They are directly involved in plant defence against fungal pathogens (Balasubramanian et al. 2012; Kumar et al. 2018; Punja and Zhang 1993). Chitinases hydrolyse the glycosidic bonds of chitin and endoglucanases degrade β -1,3- and β -1,6-glucans, thereby disrupting the cell wall, its formation and further fungal growth (Balasubramanian et al. 2012; Kumar et al. 2018).

The region QRptt_6H-1 harbours a pathogenesis related homeodomain protein A (HORVU6Hr1G021340, Table 5.2). Pathogenesis related (PR) proteins are triggered by abiotic and biotic stress and induced by the phytohormones SA, JA and ET (Al-Daoude et al. 2018; McGee et al. 2001; Muradov et al. 1993; van Loon et al. 2006). PR proteins can be classified into 17 families acting as glucanases (PR-2), chitinases (PR-3, PR-4, PR-8, PR-11), thaumatin-like (PR-5), proteinases and proteinase-inhibitors (PR-6, PR-7), peroxidases (PR-9), ribonuclease-like (PR-10), defensins (PR12), thionins (PR-13), lipid-transfer (PR-14) and oxalate oxidases (PR15, PR-16). Functions of PR-1 and PR-17 are still unknown (van Loon et al. 2006). Increased levels of PR-1, PR-2 and PR-5 were observed after infection with *Pyrenophora teres* in resistant barley lines (Al-Daoude et al. 2018; Reiss and Bryngelsson 1996; Reiss and Horstmann 2001).

In total, seven disease resistance (R) proteins were located in five of the identified QTL associated with *Ptt* resistance. Three are located in QRptt_6H-1 and one each in QRptt_4H-1, QRptt_6H-2, QRptt_6H-3 and QRptt_7H-2 (Table 5.2). *R* genes underlie the gene-for-gene concept proposed by Flor (1942; 1947; 1971), which states that each *R* gene in the plant matches a corresponding *Avr* gene in the pathogen. Plant *R* genes can be divided into eight major classes (Gururani et al. 2012). The largest groups are formed by toll interleukin receptor nucleotide binding site leucine-rich repeats (TIR-NBS-LRR or TNL) and coiled-coil NBS LRR (CC-NBS-LRR or CNL), but also TNL-nuclear localization signal amino acid domain (TNL-NLS-WRKY) form an important group (Gururani et al. 2012). The role and function of LRR in plant defence was discussed above.

In the nine regions associated with resistance/ susceptibility to *Ptt* a number of promising candidate genes coding for proteins that have long been known to be crucial in pathogen defence were detected (Table 5.2). Region QRptt_3H-4 harbours MAPKs, glucan and callose synthases, and

Discussion

chitinases (Table 5.2). This region was significantly associated with resistance in seedling and greenhouse trials in the present study (Novakazi et al. 2019a), but was also identified in a number of previous GWA studies, including a study for *Ptm* resistance (Burlakoti et al. 2017; Koladia et al. 2017; Wonneberger et al. 2017a).

QRptt_4H-1 was identified based on the data for field trials in Belarus and for greenhouse trials with isolate *No 13*, however, it was also identified by Islamovic et al. (2017), who tested four *Ptt* isolates on a RIL population derived from the cross Falcon x Azhul. In this region (4H, 33 – 70 Mbp) an endoglucanase and a disease resistance protein are located at 33 and 64 Mbp, respectively (Table 5.2, Table A.6).

The region QRptt_6H-1 is located on chromosome 6H between 37 and 76 Mbp (Table 5.1). This region was identified in numerous studies (Amezrou et al. 2018; Richards et al. 2017; Vatter et al. 2017; Wonneberger et al. 2017a) and corresponds to the necrotrophic effector-triggered susceptibility (NETS) locus *SPNI* identified by Liu et al. (2015). Liu et al. (2015) were able to show that in susceptible barley lines ROS levels increased compared to resistant lines. ROS induce programmed cell death, which is a resistant reaction to biotrophic pathogens. However, this mechanism is often exploited by hemibiotrophic and necrotrophic pathogens. Next to endoglucanases, PR and three disease resistance proteins, a peroxidase superfamily protein is located in the *SPNI* locus (Table 5.2). Therefore, the significant effect of this QTL on *Ptt* resistance/ susceptibility may probably be explained by an interaction of several genes located in this region.

The centromeric region of chromosome 6H is frequently associated with *Ptt* resistance (Abu Qamar et al. 2008; Cakir et al. 2003; Friesen et al. 2006a; Gupta et al. 2010; Gupta et al. 2011; Liu et al. 2015; Manninen et al. 2006; O’Boyle et al. 2014; Shjerve et al. 2014). Physically this region (QRptt_6H-2) spans from 123 – 344 Mbp in the present study (Table 5.1). The putative candidate genes located in QRptt_6H-2 encode for proteins like LRR-like protein kinases, proteins associated with calmodulin and calcium, glucan and callose synthases, apaf, MLO-like and disease resistance proteins (Table 5.2), allowing the assumption that a PAMP pathway might be triggered.

Richards et al. (2016) fine-mapped the susceptibility locus *Spt1* to barley contig_45181. This locus corresponds to QRptt_6H-3 (355 – 379 Mbp) and was identified in many previous studies

Discussion

(Amezrou et al. 2018; Islamovic et al. 2017; Koladia et al. 2017; Martin et al. 2018; Richards et al. 2017; Tamang et al. 2015; Vatter et al. 2017; Wonneberger et al. 2017a). Richards et al. (2016) postulated *Spt1* to be a dominant susceptibility locus that is triggered through necrotrophic effectors. One SNP that was highly associated with *Spt1* in the present and other studies was SCRI_RS_176650 located at 373,424,916 bp (Novakazi et al. 2019a). In close proximity to this SNP, a gene encoding for a disease resistance protein is located at 369,306,242 to 369,310,633 bp, making both the SNP and the gene interesting for marker assisted selection and candidate gene identification.

Regions QRptt_3H-3 and QRptt_6H-4 are putatively new QTL, since no overlaps with previously identified regions were determined (Novakazi et al. 2019a). QRptt_3H-3 is located in the centromeric region of chromosome 3H and spans a large physical interval from 233 to 350 Mbp (Table 5.1). This region contains 88 HC genes (Table 5.1; Table A.4). Six of those HC genes encode proteins involved in plant immune response, i.e. chaperone proteins DnaJ, calmodulin and calmodulin-binding protein, WRKY family TF and callose synthase. Although, this region was detected only for field trials in Belarus, it is possible that it confers resistance against several pathotypes, since the field trials were inoculated with infected barley straw that was harvested at the same location in the previous year (Novakazi et al. 2019a), and it cannot be ruled out that the inoculum was a mixture of different pathotypes. The same applies to region QRptt_6H-4, which was detected for field trials in Germany. This trial was also inoculated with infected straw from the previous years and pathotype mixtures most certainly occurred. QRptt_6H-4 is located on the long arm of chromosome 6H at 406 – 410 Mbp and contains ten HC genes (Table 5.1). Among those ten genes are a LRR-like protein kinase and Hsp70-Hsp90 organizing protein (Table 5.2).

All nine QTL contain genes that are directly involved in plant immunity and, therefore, represent promising candidate genes that are worth analyzing further.

6.2 Resistant accessions

Plant pathogens co-evolve with their hosts and selection pressure leads to virulent isolates overcoming disease resistance genes present in the host plant. This risk is especially high for sexually reproducing pathogens and pathogens with a high genetic variability within populations (McDonald and Linde 2002). Worldwide important foliar pathogens in barley are *Pyrenophora teres* f. *teres* (*Ptt*) and

Discussion

Bipolaris sorokiniana (*Bs*). Both pathogens show high variability and new virulent strains occur frequently, emphasizing the need for the continuous search for new resistant resources (Leng et al. 2016; Liu et al. 2011).

The barley set investigated in the present study consists of 449 accessions originating from different regions worldwide. The accessions were chosen for their diversity and differing resistance levels against *Ptt* and *Bs* (Novakazi et al. 2019a). The set was phenotyped under controlled greenhouse conditions and in field trials for seedling and adult plant resistance, respectively.

In order to identify which particular accessions showed enhanced resistance, haplotypes were formed based on one to three most significant MTAs per trial (environment) and identified QTL, and based on their phenotypic response (data not shown). A resistant phenotypic response was defined as infection response type ≤ 3 or disease severity $\leq 20\%$. *Ptt* was tested in eight environments (greenhouse: *No 13*, *Hoehnstedt*, *NFNB 50*; field: Quedlinburg (G), Zhodino (BLR), *NFNB 50*, *NFNB 73*, *NFNB 85* (AU)) and *Bs* was tested in five environments (greenhouse: *No 31*, *SH 15*, *SB 61*; field: Pushkin (RUS), *SB 61* (AU)).

For *Ptt*, this type of haplotype analysis revealed that 288 accessions expressed resistant phenotypic reactions in at least two environments (environment = isolate or location), i.e. more than half of the tested accessions were highly resistant (Table A.13). Of the resistant accessions, 102 were 2-rowed and 186 were 6-rowed, of which about 180 were landraces. The 288 resistant accessions originated from 41 different countries with number of entries between one and 32 (Russia), but still representing a wide range of regions (Table A.13). Almost all Ethiopian accessions, 26 out of 34, were resistant in at least two environments. Ethiopian landrace populations harbour large variation for plant morphological traits but also for disease resistance (Alemayehu and Parlevliet 1997; Yitbarek et al. 1998). In a PCA of the studied barley accessions, the Ethiopian accessions clearly clustered together and formed an own small subgroup (data not shown).

Two accessions were resistant against *Ptt* in six out of eight environments. “Omskij 82” (C.I. 29416) is a 2-rowed Russian line and was resistant in field trials with isolates *NFNB 50* and *NFNB 73*, field trials in Zhodino, and all greenhouse trials. C.I. 21538 is a 6-rowed Bolivian landrace and was resistant in all greenhouse trials, and field trials in Zhodino, Quedlinburg and Australian field

Discussion

trials with isolate *NFNB 50* (data not shown). Eleven landraces and six cultivars were resistant against *Ptt* in five environments. Two accessions are 2-rowed, one from Ethiopia and one from Ukraine; the other accessions were 6-rowed barleys from North America, Turkmenistan, Uzbekistan, Kyrgyzstan, Pakistan, and China (Table A.13). Line “Diamond” (C.I. 29192) from Canada and line “UC 603” (C.I. 30032) from the USA were also resistant against *Bs* in field trials in Pushkin; line “Virden” (C.I. 30408, USA) was resistant against *Bs* in field trials in Pushkin and Australia (isolate *SB 61*) (Table A.13, Table A.14). Seventy-six accessions, including 45 landraces, were resistant in four environments against *Ptt* (Table A.13). Among these accessions were breeding lines “Tifang” (C.I. 4407-1, VIR 18760b) and “NDB112” (C.I. 11531), which were resistant in trials with isolates *Hoehnstedt*, *NFNB 50* (greenhouse and field), and *NFNB 73* (data not shown). Both accessions were also resistant against *Bs* in field trials in Pushkin. “Tifang” is a 6-rowed US American line that shows resistant to susceptible reactions depending on the pathotype (Koladia et al. 2017) and was reported to harbour a resistance locus on chromosome 3H (Bockelman et al. 1977). “NDB112” is also a 6-rowed US American breeding line that is known to harbour resistance against both net and spot blotch (Steffenson et al. 1996) and provided a durable resistance against spot blotch for a long time until a new pathotype occurred and overcame this resistance (Leng et al. 2016; Valjavec-Gratian and Steffenson 1997).

The perhaps most interesting accession is “Ogalitsu” (C.I. 7152, VIR 18716), because it confers broad resistance against both pathogens (Table A.13, Table A.14). Dual resistance in spring barley accessions was already reported by Fetch et al. (2008), they, however, did not report this line to harbour dual resistance. “Ogalitsu” is a Canadian 6-row spring barley and was resistant in four (*NFNB 50* greenhouse and field, *NFNB 73* and *Zhodino*) and three (Pushkin, *No 13* and *SB 61* greenhouse) environments against *Ptt* and *Bs*, respectively. This line was also reported to be a source of resistance against covered and loose smuts (Stevenson and Jones 1953).

Eighty-six and 107 accessions were resistant in three and two environments against *Ptt* (Table A.13). The line “Morex” was resistant in three environments against *Ptt* (*NFNB 50* field and greenhouse, Quedlinburg) and in two environments against *Bs* (Pushkin, *SB 61* greenhouse) (Table A.13, Table A.14). “Morex” (VIR 26959) is an US American 6-row barley that is generally considered resistant against *Bs* and got its resistance from “NDB112” (Steffenson et al. 1996). The 2-rowed line “Bowman”

Discussion

(VIR 29676) was used in several studies as a standard for differentiating *Bs* pathotypes (Arabi and Jawhar 2010; Fetch and Steffenson 1999; Leng et al. 2018; Meldrum et al. 2004; Steffenson et al. 1996; Zhou and Steffenson 2013). “Bowman” expresses high susceptibility against *Bs* pathotype 2 and low susceptibility against pathotype 1 (Valjavec-Gratian and Steffenson 1997). In the present study, “Bowman” was resistant in three environments of each pathogen (*Ptt*: Quedlinburg, *NFNB 50* field, *Hoehnstedt*; *Bs*: *SB 61* greenhouse, *SH 15*, Pushkin).

For *Bs*, the haplotype analysis revealed that 113 accessions expressed resistant phenotypic reactions in at least one environment (Table A.14). The 113 accessions originated from 28 different countries with number of entries between 1 and 20 (Russia). Fifty-five out of 113 accessions were 2-rowed and 58 were 6-rowed, of which 61 are cultivars and 52 landraces (Table A.14).

Four accessions were resistant against *Bs* in three out of five environments. These were the already discussed lines “Bowman” and “Ogalitsu”, and the 6-rowed Indian cultivar “Naushera” (C.I. 5502) the 6-rowed landrace C.I. 5470 from Cyprus. “Naushera” and C.I. 5470 were resistant against *Bs* in trials with isolates *SB 61* (greenhouse and field) and *SH 15* and based on their haplotypes they both harbour favourable alleles of the QTL identified on chromosome 7H at 26 – 28 Mbp (data not shown). Ten accessions were resistant in two environments and nine of them were also resistant against *Ptt* (Table A.14). Five of the ten accessions are landraces from Ethiopia, Tajikistan, China, Mexico and Peru. Four and one of the cultivars are US American and Russian, respectively. The remaining 91 accessions were resistant in only one environment and 57 of them were resistant in field trials in Pushkin (Table A.14). GWAS for field trials in Pushkin revealed one significant MTA on chromosome 7H at 68,476,333 bp that was not described previously and not identified in other environments in the present study. Thus, making especially these 57 accessions interesting for testing with additional isolates.

The high number and high diversity of accessions resistant against *Ptt* reflects the high number of QTL regions identified in GWAS (Novakazi et al. 2019a). The comparably low number of resistant accessions against *Bs* reflects the low number of identified QTL associated with *Bs* resistance. Especially for *Ptt*, a high number of resistant landraces with diverse origins is available that confer resistance against a broad spectrum of isolates and are valuable sources for further testing and breeding

Discussion

purposes. Nonetheless, the Cyprian landrace C.I. 5470 is an interesting candidate for *Bs* resistance and the Canadian line “Ogalitsu” (C.I. 7152) confers dual resistance against *Ptt* and *Bs*.

The investigated germplasm set includes already known and established sources for resistance against the two pathogens *P. teres* f. *teres* and *B. sorokiniana*, but it also revealed putatively new QTL for resistance that were not described in previous studies, and includes many lesser-studied landraces that can be used for pre-breeding strategies and future breeding programmes.

References

- Abu Qamar M, Liu ZH, Faris JD, Chao S, Edwards MC, Lai Z, Franckowiak JD, Friesen TL (2008) A region of barley chromosome 6H harbors multiple major genes associated with net type net blotch resistance. *Theoretical and Applied Genetics* 117:1261-1270 doi:10.1007/s00122-008-0860-x
- Acevedo-Garcia J, Kusch S, Panstruga R (2014) Magical mystery tour: MLO proteins in plant immunity and beyond. *New Phytologist* 204:273-281
- Acharya K, Dutta AK, Pradhan P (2011) '*Bipolaris sorokiniana*'(Sacc.) Shoem.: The most destructive wheat fungal pathogen in the warmer areas. *Australian Journal of Crop Science* 5:1064
- Adie B, Chico JM, Rubio-Somoza I, Solano R (2007) Modulation of plant defenses by ethylene. *Journal of Plant Growth Regulation* 26:160-177
- Afanasenkov O, Koziakov A, Hedley P, Lashina N, Anisimova A, Manninen O, Jalli M, Potokina E (2015) Mapping of the loci controlling the resistance to *Pyrenophora teres* f. *teres* and *Cochliobolus sativus* in two double haploid barley populations. *Russian Journal of Genetics: Applied Research* 5:242-253
- Afonin A, Greene S, Dzyubenko N, Frolov A (2008) Interactive Agricultural Ecological Atlas of Russia and Neighboring Countries. Economic Plants and their Diseases, Pests and Weeds. [Online]. Available at: <http://www.wagroAtlas.ru>
- Agostinetto L, Casa RT, Bogo A, Sachs C, Souza CA, Reis EM, Cristina da Cunha I (2015) Barley spot blotch intensity, damage, and control response to foliar fungicide application in southern Brazil. *Crop Protection* 67:7-12 doi:10.1016/j.cropro.2014.09.012
- Åkesson H, Jansson H-B (1996) Prehelminthosporol, a phytotoxin from *Bipolaris sorokiniana*. In: *Monitoring Antagonistic Fungi Deliberately Released into the Environment*. Springer, pp 99-104
- Al-Daoude A, Jawhar M, Al-Shehadah E, Shoaib A, Orfi M, Arabi M (2018) Changes in salicylic acid content and pathogenesis-related (PR2) gene expression during barley-*Pyrenophora teres* interaction. *Hellenic Plant Protection Journal* 11:71-77
- Alemayehu F, Parlevliet J (1997) Variation between and within Ethiopian barley landraces. *Euphytica* 94:183
- Almagro L, Gómez Ros L, Belchi-Navarro S, Bru R, Ros Barceló A, Pedreno M (2008) Class III peroxidases in plant defence reactions. *Journal of Experimental Botany* 60:377-390
- Alqudah AM, Sallam A, Baenziger PS, Börner A (2019) GWAS: Fast-Forwarding Gene Identification in Temperate Cereals: Barley as a Case Study-A review. *Journal of Advanced Research*
- Amezrou R, Verma RPS, Chao S, Brueggeman RS, Belqadi L, Arbaoui M, Rehman S, Gyawali S (2018) Genome-wide association studies of net form of net blotch resistance at seedling and adult plant stages in spring barley collection. *Molecular Breeding* 38 doi:10.1007/s11032-018-0813-2
- Apoga D, Åkesson H, Jansson H-B, Odham G (2002) Relationship between production of the phytotoxin prehelminthosporol and virulence in isolates of the plant pathogenic fungus *Bipolaris sorokiniana*. *European Journal of Plant Pathology* 108:519-526
- Arabi M, Al-Safadi B, Charbaji T (2003) Pathogenic variation among isolates of *Pyrenophora teres*, the causal agent of barley net blotch. *Journal of Phytopathology* 151:376-382
- Arabi M, Jawhar M (2002) Virulence spectrum to barley (*Hordeum vulgare* L.) in some isolates of *Cochliobolus sativus* from Syria. *Journal of Plant Pathology* 84:35-39
- Arabi M, Jawhar M (2004) Identification of *Cochliobolus sativus* (spot blotch) isolates expressing differential virulence on barley genotypes in Syria. *Journal of Phytopathology* 152:461-464
- Arabi MIE, Jawhar M (2010) Greenhouse Method for Assessing Spot Blotch Resistance in Barley. *The Plant Pathology Journal* 26:421-423 doi:10.5423/ppj.2010.26.4.421
- Asai T, Tena G, Plotnikova J, Willmann MR, Chiu W-L, Gomez-Gomez L, Boller T, Ausubel FM, Sheen J (2002) MAP kinase signalling cascade in Arabidopsis innate immunity. *Nature* 415:977
- Bachlava E, Taylor CA, Tang S, Bowers JE, Mandel JR, Burke JM, Knapp SJ (2012) SNP discovery and development of a high-density genotyping array for sunflower. *PLoS One* 7:e29814
- Bakshi M, Oelmüller R (2014) WRKY transcription factors: Jack of many trades in plants. *Plant Signaling & Behavior* 9:e27700

References

- Balasubramanian V, Vashisht D, Cletus J, Sakthivel N (2012) Plant β -1, 3-glucanases: their biological functions and transgenic expression against phytopathogenic fungi. *Biotechnology Letters* 34:1983-1990
- Bari R, Jones JD (2009) Role of plant hormones in plant defence responses. *Plant Molecular Biology* 69:473-488
- Bayer MM, Rapazote-Flores P, Ganai M, Hedley PE, Macaulay M, Plieske J, Ramsay L, Russell J, Shaw PD, Thomas W, Waugh R (2017) Development and Evaluation of a Barley 50k iSelect SNP Array. *Frontiers in Plant Science* 8:1792 doi:10.3389/fpls.2017.01792
- Bayles CJ, Aist JR (1987) Apparent calcium mediation of resistance of an ml-o barley mutant to powdery mildew. *Physiological and Molecular Plant Pathology* 30:337-345
- Beckmann J, Soller M (1983) Restriction fragment length polymorphisms in genetic improvement: methodologies, mapping and costs. *Theoretical and Applied Genetics* 67:35-43
- Bengyella L, Yekwa EL, Nawaz K, Iftikhar S, Tambo E, Alisoltani A, Feto NA, Roy P (2018) Global invasive *Cochliobolus* species: cohort of destroyers with implications in food losses and insecurity in the twenty-first century. *Arch Microbiol* 200:119-135 doi:10.1007/s00203-017-1426-6
- Bent AF, Kunkel BN, Dahlbeck D, Brown KL, Schmidt R, Giraudat J, Leung J, Staskawicz BJ (1994) RPS2 of *Arabidopsis thaliana*: a leucine-rich repeat class of plant disease resistance genes. *Science* 265:1856-1860
- Berger GL, Liu S, Hall MD, Brooks WS, Chao S, Muehlbauer GJ, Baik B-K, Steffenson B, Griffey CA (2013) Marker-trait associations in Virginia Tech winter barley identified using genome-wide mapping. *Theoretical and Applied Genetics* 126:693-710 doi:10.1007/s00122-012-2011-7
- Bilgic H, Steffenson B, Hayes P (2005) Comprehensive genetic analyses reveal differential expression of spot blotch resistance in four populations of barley. *Theoretical and Applied Genetics* 111:1238-1250
- Bilgic H, Steffenson B, Hayes P (2006) Molecular mapping of loci conferring resistance to different pathotypes of the spot blotch pathogen in barley. *Phytopathology* 96:699-708
- Blattner FR (2018) Taxonomy of the genus *Hordeum* and barley (*Hordeum vulgare*). In: *The Barley Genome*. Springer, pp 11-23
- Bockelman H, Sharp E, Eslick R (1977) Trisomic analysis of genes for resistance to scald and net blotch in several barley cultivars. *Canadian Journal of Botany* 55:2142-2148
- Bovill J, Lehmensiek A, Sutherland MW, Platz GJ, Usher T, Franckowiak J, Mace E (2010) Mapping spot blotch resistance genes in four barley populations. *Molecular Breeding* 26:653-666 doi:10.1007/s11032-010-9401-9
- Bowman SM, Free SJ (2006) The structure and synthesis of the fungal cell wall. *Bioessays* 28:799-808
- Brandl F, Hoffmann G (1991) Differentiation of physiological races of *Drechslera teres* (Sacc.) Shoem., pathogen net blotch of barley. *Zeitschrift fuer Pflanzenkrankheiten und Pflanzenschutz*
- Burlakoti RR, Gyawali S, Chao S, Smith KP, Horsley RD, Cooper B, Muehlbauer GJ, Neate SM (2017) Genome-Wide Association Study of Spot Form of Net Blotch Resistance in the Upper Midwest Barley Breeding Programs. *Phytopathology* 107:100-108 doi:10.1094/PHYTO-03-16-0136-R
- Burleigh J, Tajani M, Seck M (1988) Effects of *Pyrenophora teres* and weeds on barley yield and yield components. *Phytopathology* 78:295-299
- Büschges R, Hollricher K, Panstruga R, Simons G, Wolter M, Frijters A, van Daelen R, van der Lee T, Diergaarde P, Groenendijk J (1997) The barley Mlo gene: a novel control element of plant pathogen resistance. *Cell* 88:695-705
- Bykova IV, Lashina NM, Efimov VM, Afanasenko OS, Khlestkina EK (2017) Identification of 50 K Illumina-chip SNPs associated with resistance to spot blotch in barley. *BMC Plant Biology* 17:250 doi:10.1186/s12870-017-1198-9
- Cakir M, Gupta S, Li C, Hayden M, Mather DE, Ablett GA, Platz GJ, Broughton S, Chalmers KJ, Loughman R (2011) Genetic mapping and QTL analysis of disease resistance traits in the barley population Baudin \times AC Metcalfe. *Crop and Pasture Science* 62:152-161
- Cakir M, Gupta S, Platz G, Ablett GA, Loughman R, Emebiri L, Poulsen D, Li C, Lance R, Galwey N (2003) Mapping and validation of the genes for resistance to *Pyrenophora teres* f. *teres* in barley (*Hordeum vulgare* L.). *Australian Journal of Agricultural Research* 54:1369-1377

References

- Cantalapiedra CP, Boudiar R, Casas AM, Igartua E, Contreras-Moreira B (2015) BARLEYMAP: physical and genetic mapping of nucleotide sequences and annotation of surrounding loci in barley. *Molecular Breeding* 35:13
- Carlson H, Nilsson P, Jansson H, Odham G (1991) Characterization and determination of prehelminthosporol, a toxin from the plant pathogenic fungus *Bipolaris sorokiniana*, using liquid chromatography/mass spectrometry. *Journal of Microbiological Methods* 13:259-269
- Chagné D, Crowhurst RN, Troggio M, Davey MW, Gilmore B, Lawley C, Vanderzande S, Hellens RP, Kumar S, Cestaro A (2012) Genome-wide SNP detection, validation, and development of an 8K SNP array for apple. *PLoS one* 7:e31745
- Cheval C, Aldon D, Galaud J-P, Ranty B (2013) Calcium/calmodulin-mediated regulation of plant immunity. *Biochimica et Biophysica Acta (BBA)-Molecular Cell Research* 1833:1766-1771
- Chini A, Fonseca S, Fernandez G, Adie B, Chico J, Lorenzo O, Garcia-Casado G, López-Vidriero I, Lozano F, Ponce M (2007) The JAZ family of repressors is the missing link in jasmonate signalling. *Nature* 448:666
- Clapham DE (2007) Calcium signaling. *Cell* 131:1047-1058
- Clarke WE, Higgins EE, Plieske J, Wieseke R, Sidebottom C, Khedkar Y, Batley J, Edwards D, Meng J, Li R (2016) A high-density SNP genotyping array for *Brassica napus* and its ancestral diploid species based on optimised selection of single-locus markers in the allotetraploid genome. *Theoretical and Applied Genetics* 129:1887-1899
- Collard BC, Mackill DJ (2008) Marker-assisted selection: an approach for precision plant breeding in the twenty-first century. *Philosophical Transactions of the Royal Society B: Biological Sciences* 363:557-572
- Comadran J, Kilian B, Russell J, Ramsay L, Stein N, Ganai M, Shaw P, Bayer M, Thomas W, Marshall D (2012) Natural variation in a homolog of *Antirrhinum CENTRORADIALIS* contributed to spring growth habit and environmental adaptation in cultivated barley. *Nature Genetics* 44:1388
- Craig A, Ewan R, Mesmar J, Gudipati V, Sadanandom A (2009) E3 ubiquitin ligases and plant innate immunity. *Journal of Experimental Botany* 60:1123-1132
- De Marchi R, Sorel M, Mooney B, Fudal I, Goslin K, Kwaśniewska K, Ryan PT, Pfalz M, Kroymann J, Pollmann S (2016) The N-end rule pathway regulates pathogen responses in plants. *Scientific Reports* 6:26020
- Deadman M, Cooke B (1989) An analysis of rain-mediated dispersal of *Drechslera teres* conidia in field plots of spring barley. *Annals of Applied Biology* 115:209-214
- Devaux P (2003) The *Hordeum bulbosum* (L.) method. In: *Doubled Haploid Production in Crop Plants*. Springer, pp 15-19
- Devoto A, Hartmann HA, Piffanelli P, Elliott C, Simmons C, Taramino G, Goh C-S, Cohen FE, Emerson BC, Schulze-Lefert P (2003) Molecular phylogeny and evolution of the plant-specific seven-transmembrane MLO family. *Journal of Molecular Evolution* 56:77-88
- DeYoung BJ, Innes RW (2006) Plant NBS-LRR proteins in pathogen sensing and host defense. *Nature Immunology* 7:1243
- Drader T, Johnson K, Brueggeman R, Kudrna D, Kleinhofs A (2009) Genetic and physical mapping of a high recombination region on chromosome 7H (1) in barley. *Theoretical and Applied Genetics* 118:811-820
- Earl DA, vonHoldt BM (2012) STRUCTURE HARVESTER: a website and program for visualizing STRUCTURE output and implementing the Evanno method. *Conservation Genetics Resources* 4:359-361 doi:10.1007/s12686-011-9548-7
- Ellinger D, Naumann M, Falter C, Zwikowics C, Jamrow T, Manisseri C, Somerville SC, Voigt CA (2013) Elevated early callose deposition results in complete penetration resistance to powdery mildew in *Arabidopsis*. *Plant Physiology* 161:1433-1444
- Elmore JM, Perovic D, Ordon F, Schweizer P, Wise RP (2018) A genomic view of biotic stress resistance. In: *The Barley Genome*. Springer, pp 233-257
- Elshire RJ, Glaubitz JC, Sun Q, Poland JA, Kawamoto K, Buckler ES, Mitchell SE (2011) A robust, simple genotyping-by-sequencing (GBS) approach for high diversity species. *PLoS One* 6:e19379 doi:10.1371/journal.pone.0019379
- Eulgem T, Somssich IE (2007) Networks of WRKY transcription factors in defense signaling. *Current opinion in plant biology* 10:366-371
- FAOSTAT (2019) <http://www.fao.org/faostat/en/#data>.

References

- Faure S, Turner AS, Gruszka D, Christodoulou V, Davis SJ, von Korff M, Laurie DA (2012) Mutation at the circadian clock gene EARLY MATURITY 8 adapts domesticated barley (*Hordeum vulgare*) to short growing seasons. *Proceedings of the National Academy of Sciences* 109:8328-8333
- Fetch TG, Steffenson BJ (1999) Rating scales for assessing infection responses of barley infected with *Cochliobolus sativus*. *Plant Disease* 83:213-217
- Fetch TG, Steffenson BJ, Bockelman HE, Wesenberg DM (2008) Spring barley accessions with dual spot blotch and net blotch resistance. *Canadian Journal of Plant Pathology* 30:534-542
- Flor H (1942) Inheritance of pathogenicity in *Melampsora lini*. *Phytopathology* 32:653-669
- Flor H (1947) Inheritance of reaction to rust in flax. *Journal Agricultural Research* 74:241-262
- Flor HH (1971) Current status of the gene-for-gene concept. *Annual Review of Phytopathology* 9:275-296
- Fowler RA, Platz GJ, Bell KL, Fletcher SEH, Franckowiak JD, Hickey LT (2017) Pathogenic variation of *Pyrenophora teres* f. *teres* in Australia. *Australasian Plant Pathology* 46:115-128 doi:10.1007/s13313-017-0468-1
- Freeman BC, Beattie GA (2008) An overview of plant defenses against pathogens and herbivores. *The Plant Health Instructor* doi:10.1094/PHI-I-2008-0226-01
- Friesen T, Holmes D, Bowden R, Faris J (2018) ToxA is present in the US *Bipolaris sorokiniana* population and is a significant virulence factor on wheat harboring Tsn1. *Plant Disease* 102:2446-2452
- Friesen TL, Faris JD, Lai Z, Steffenson BJ (2006a) Identification and chromosomal location of major genes for resistance to *Pyrenophora teres* in a doubled-haploid barley population. *Genome* 49:855-859 doi:10.1139/g06-024
- Friesen TL, Stukenbrock EH, Liu Z, Meinhardt S, Ling H, Faris JD, Rasmussen JB, Solomon PS, McDonald BA, Oliver RP (2006b) Emergence of a new disease as a result of interspecific virulence gene transfer. *Nature Genetics* 38:953
- Friis P, Olsen C, Møller B (1991) Toxin production in *Pyrenophora teres*, the ascomycete causing the net-spot blotch disease of barley (*Hordeum vulgare* L.). *Journal of Biological Chemistry* 266:13329-13335
- Ganal MW, Durstewitz G, Polley A, Bérard A, Buckler ES, Charcosset A, Clarke JD, Graner E-M, Hansen M, Joets J (2011) A large maize (*Zea mays* L.) SNP genotyping array: development and germplasm genotyping, and genetic mapping to compare with the B73 reference genome. *PloS one* 6:e28334
- Ghazvini H, Tekauz A (2007) Virulence diversity in the population of *Bipolaris sorokiniana*. *Plant Disease* 91:814-821
- Gow NA, Latge J-P, Munro CA (2017) The fungal cell wall: structure, biosynthesis, and function. *Microbiology Spectrum* 5 doi:10.1128/microbiolspec.FUNK-0035-2016
- Graner A, Foroughi-Wehr B, Tekauz A (1996) RFLP mapping of a gene in barley conferring resistance to net blotch (*Pyrenophora teres*). *Euphytica* 91:229-234
- Grewal TS, Rossnagel BG, Pozniak CJ, Scoles GJ (2008) Mapping quantitative trait loci associated with barley net blotch resistance. *Theoretical and Applied Genetics* 116:529-539 doi:10.1007/s00122-007-0688-9
- Grewal TS, Rossnagel BG, Scoles GJ (2012) Mapping quantitative trait loci associated with spot blotch and net blotch resistance in a doubled-haploid barley population. *Molecular Breeding* 30:267-279
- Gupta PK, Chand R, Vasistha NK, Pandey SP, Kumar U, Mishra VK, Joshi AK (2018) Spot blotch disease of wheat: the current status of research on genetics and breeding. *Plant Pathology* 67:508-531 doi:10.1111/ppa.12781
- Gupta S, Li C, Loughman R, Cakir M, Platz G, Westcott S, Bradley J, Broughton S, Lance R (2010) Quantitative trait loci and epistatic interactions in barley conferring resistance to net type net blotch (*Pyrenophora teres* f. *teres*) isolates. *Plant Breeding* 129:362-368
- Gupta S, Li C, Loughman R, Cakir M, Westcott S, Lance R (2011) Identifying genetic complexity of 6H locus in barley conferring resistance to *Pyrenophora teres* f. *teres*. *Plant Breeding* 130:423-429 doi:10.1111/j.1439-0523.2011.01854.x

References

- Gururani MA, Venkatesh J, Upadhyaya CP, Nookaraju A, Pandey SK, Park SW (2012) Plant disease resistance genes: current status and future directions. *Physiological and Molecular Plant Pathology* 78:51-65
- Gutiérrez L, German S, Pereyra S, Hayes PM, Perez CA, Capettini F, Locatelli A, Berberian NM, Falconi EE, Estrada R, Fros D, Gonza V, Altamirano H, Huerta-Espino J, Neyra E, Orjeda G, Sandoval-Islas S, Singh R, Turkington K, Castro AJ (2015) Multi-environment multi-QTL association mapping identifies disease resistance QTL in barley germplasm from Latin America. *Theoretical and Applied Genetics* 128:501-516 doi:10.1007/s00122-014-2448-y
- Gyawali S, Chao S, Vaish SS, Singh SP, Rehman S, Vishwakarma SR, Verma RPS (2018) Genome wide association studies (GWAS) of spot blotch resistance at the seedling and the adult plant stages in a collection of spring barley. *Molecular Breeding* 38 doi:10.1007/s11032-018-0815-0
- Haas M, Menke J, Chao S, Steffenson BJ (2016) Mapping quantitative trait loci conferring resistance to a widely virulent isolate of *Cochliobolus sativus* in wild barley accession PI 466423. *Theoretical and Applied Genetics* 129:1831-1842 doi:10.1007/s00122-016-2742-y
- Haas M, Schreiber M, Mascher M (2019) Domestication and crop evolution of wheat and barley: Genes, genomics, and future directions. *Journal of Integrative Plant Biology* 61:204-225
- He J, Zhao X, Laroche A, Lu Z-X, Liu H, Li Z (2014) Genotyping-by-sequencing (GBS), an ultimate marker-assisted selection (MAS) tool to accelerate plant breeding. *Frontiers in plant science* 5:484
- Heil M, Ton J (2008) Long-distance signalling in plant defence. *Trends in Plant Science* 13:264-272
- Hilmarsson HS, Göransson M, Lillemo M, Kristjánsdóttir ÞA, Hermannsson J, Hallsson J (2017) An overview of barley breeding and variety trials in Iceland in 1987-2014. *Icelandic Agricultural Sciences* 30:13-28 doi:http://dx.doi.org/10.16886/IAS.2017.02
- Hiraga S, Sasaki K, Ito H, Ohashi Y, Matsui H (2001) A large family of class III plant peroxidases. *Plant and Cell Physiology* 42:462-468
- Hrushovetz S (1956) Cytological studies of ascus development in *Cochliobolus sativus*. *Canadian Journal of Botany* 34:641-651
- Huang BE, Verbyla KL, Verbyla AP, Raghavan C, Singh VK, Gaur P, Leung H, Varshney RK, Cavanagh CR (2015) MAGIC populations in crops: current status and future prospects. *Theoretical and Applied Genetics* 128:999-1017
- Huang X, Han B (2014) Natural variations and genome-wide association studies in crop plants. *Annual review of plant biology* 65:531-551
- IBSC (2012) A physical, genetic and functional sequence assembly of the barley genome. *Nature* 491:711-716 doi:10.1038/nature11543
- Imelfort M, Duran C, Batley J, Edwards D (2009) Discovering genetic polymorphisms in next-generation sequencing data. *Plant Biotechnology Journal* 7:312-317
- Islamovic E, Bregitzer P, Friesen TL (2017) Barley 4H QTL confers NFNB resistance to a global set of *P. teres* f. *teres* isolates. *Molecular Breeding* 37 doi:10.1007/s11032-017-0621-0
- Jones JD, Dangl JL (2006) The plant immune system. *Nature* 444:323
- Jonsson R, Bryngelsson T, Gustafsson M (1997) Virulence studies of Swedish net blotch isolates (*Drechslera teres*) and identification of resistant barley lines. *Euphytica* 94:209-218
- Jørgensen IH (1992) Discovery, characterization and exploitation of Mlo powdery mildew resistance in barley. *Euphytica* 63:141-152
- Karov I, Mitrev S, Arsov E (2009) *Bipolaris sorokiniana* (teleomorph *Cochliobolus sativus*), causer of barley leaf lesions and root rot in Macedonia. *Proc Nat Sci Matica Srpska Novi sad*:167-174
- Keon J, Hargreaves J (1983) A cytological study of the net blotch disease of barley caused by *Pyrenophora teres*. *Physiological Plant Pathology* 22:321-329
- Khan T, Boyd W (1969) Physiologic specialization in *Drechslera teres*. *Australian Journal of Biological Sciences* 22:1229-1236
- Khlestkina E, Salina E (2006) SNP markers: methods of analysis, ways of development, and comparison on an example of common wheat. *Russian Journal of Genetics* 42:585-594
- Kim MC, Panstruga R, Elliott C, Müller J, Devoto A, Yoon HW, Park HC, Cho MJ, Schulze-Lefert P (2002) Calmodulin interacts with MLO protein to regulate defence against mildew in barley. *Nature* 416:447
- Koladia VM, Faris JD, Richards JK, Brueggeman RS, Chao S, Friesen TL (2017) Genetic analysis of net form net blotch resistance in barley lines CIho 5791 and Tifang against a global collection

References

- of *P. teres* f. *teres* isolates. Theoretical and Applied Genetics 130:163-173 doi:10.1007/s00122-016-2801-4
- Komatsuda T, Pourkheirandish M, He C, Azhaguvel P, Kanamori H, Perovic D, Stein N, Graner A, Wicker T, Tagiri A (2007) Six-rowed barley originated from a mutation in a homeodomain-leucine zipper I-class homeobox gene. Proceedings of the National Academy of Sciences 104:1424-1429
- König J, Perovic D, Kopahnke D, Ordon F (2013) Development of an efficient method for assessing resistance to the net type of net blotch (*Pyrenophora teres* f. *teres*) in winter barley and mapping of quantitative trait loci for resistance. Molecular Breeding 32:641-650 doi:10.1007/s11032-013-9897-x
- König J, Perovic D, Kopahnke D, Ordon F, Léon J (2014) Mapping seedling resistance to net form of net blotch (*Pyrenophora teres* f. *teres*) in barley using detached leaf assay. Plant Breeding 133:356-365 doi:10.1111/pbr.12147
- Kumar J, Schäfer P, Hückelhoven R, Langen G, Baltruschat H, Stein E, Nagarajan S, Kogel KH (2002) *Bipolaris sorokiniana*, a cereal pathogen of global concern: cytological and molecular approaches towards better control. Molecular Plant Pathology 3:185-195
- Kumar M, Brar A, Yadav M, Chawade A, Vivekanand V, Pareek N (2018) Chitinases—potential candidates for enhanced plant resistance towards fungal pathogens. Agriculture 8:88
- Kusch S, Panstruga R (2017) mlo-based resistance: an apparently universal “weapon” to defeat powdery mildew disease. Molecular Plant-Microbe Interactions 30:179-189
- Lam KC, Ibrahim RK, Behdad B, Dayanandan S (2007) Structure, function, and evolution of plant O-methyltransferases. Genome 50:1001-1013
- Langridge P (2018) Economic and Academic Importance of Barley. In: The Barley Genome. Springer, pp 1-10
- Lashina NM, Afanasenko OS (2019) Susceptibility of leaf blights of commercial barley cultivars in North-Western region of Russia. Plant Protection News 2:23-28 doi:doi.org/10.31993/2308-6459-2019-2(100)-23-28
- Leisova L, Kucera L, Minarikova V (2005) AFLP-based PCR markers that differentiate spot and net forms of *Pyrenophora teres*. Plant Pathology 54:66-73
- Leng Y, Wang R, Ali S, Zhao M, Zhong S (2016) Sources and Genetics of Spot Blotch Resistance to a New Pathotype of *Cochliobolus sativus* in the USDA National Small Grains Collection. Plant Disease 100:1988-1993 doi:10.1094/pdis-02-16-0152-re
- Leng Y, Zhao M, Wang R, Steffenson BJ, Brueggeman RS, Zhong S (2018) The gene conferring susceptibility to spot blotch caused by *Cochliobolus sativus* is located at the *Mla* locus in barley cultivar Bowman. Theoretical and Applied Genetics 131:1531-1539 doi:10.1007/s00122-018-3095-5
- Lightfoot DJ, Able AJ (2010) Growth of *Pyrenophora teres* in planta during barley net blotch disease. Australasian Plant Pathology 39:499-507
- Liu JZ, Whitham SA (2013) Overexpression of a soybean nuclear localized type-III DnaJ domain-containing HSP40 reveals its roles in cell death and disease resistance. The Plant Journal 74:110-121
- Liu Z, Ellwood SR, Oliver RP, Friesen TL (2011) *Pyrenophora teres*: profile of an increasingly damaging barley pathogen. Molecular Plant Pathology 12:1-19 doi:10.1111/j.1364-3703.2010.00649.x
- Liu Z, Holmes DJ, Faris JD, Chao S, Brueggeman RS, Edwards MC, Friesen TL (2015) Necrotrophic effector-triggered susceptibility (NETS) underlies the barley-*Pyrenophora teres* f. *teres* interaction specific to chromosome 6H. Molecular Plant Pathology 16:188-200 doi:10.1111/mpp.12172
- Ma Z, Lapitan NL, Steffenson B (2004) QTL mapping of net blotch resistance genes in a doubled-haploid population of six-rowed barley. Euphytica 137:291-296
- Manamgoda DS, Rossman AY, Castlebury LA, Crous PW, Madrid H, Chukeatirote E, Hyde KD (2014) The genus *Bipolaris*. Studies in Mycology 79:221-288 doi:10.1016/j.simyco.2014.10.002
- Mangelsen E, Kilian J, Berendzen KW, Kolukisaoglu ÜH, Harter K, Jansson C, Wanke D (2008) Phylogenetic and comparative gene expression analysis of barley (*Hordeum vulgare*) WRKY transcription factor family reveals putatively retained functions between monocots and dicots. BMC genomics 9:194

References

- Manninen OM, Jalli M, Kalendar R, Schulman A, Afanasenko O, Robinson J (2006) Mapping of major spot-type and net-type net-blotch resistance genes in the Ethiopian barley line CI 9819. *Genome* 49:1564-1571 doi:10.1139/g06-119
- Marenne G, Rodríguez-Santiago B, Closas MG, Pérez-Jurado L, Rothman N, Rico D, Pita G, Pisano DG, Kogevinas M, Silverman DT (2011) Assessment of copy number variation using the Illumina Infinium 1M SNP-array: a comparison of methodological approaches in the Spanish Bladder Cancer/EPICURO study. *Human Mutation* 32:240-248
- Martin A, Platz GJ, de Klerk D, Fowler RA, Smit F, Potgieter FG, Prins R (2018) Identification and mapping of net form of net blotch resistance in South African barley. *Molecular Breeding* 38 doi:10.1007/s11032-018-0814-1
- Mascher M, Gundlach H, Himmelbach A, Beier S, Twardziok SO, Wicker T, Radchuk V, Dockter C, Hedley PE, Russell J, Bayer M, Ramsay L, Liu H, Haberer G, Zhang XQ, Zhang Q, Barrero RA, Li L, Taudien S, Groth M, Felder M, Hastie A, Simkova H, Stankova H, Vrana J, Chan S, Munoz-Amatriain M, Ounit R, Wanamaker S, Bolser D, Colmsee C, Schmutzer T, Aliyeva-Schnorr L, Grasso S, Tanskanen J, Chailyan A, Sampath D, Heavens D, Clissold L, Cao S, Chapman B, Dai F, Han Y, Li H, Li X, Lin C, McCooke JK, Tan C, Wang P, Wang S, Yin S, Zhou G, Poland JA, Bellgard MI, Borisjuk L, Houben A, Dolezel J, Ayling S, Lonardi S, Kersey P, Langridge P, Muehlbauer GJ, Clark MD, Caccamo M, Schulman AH, Mayer KFX, Platzer M, Close TJ, Scholz U, Hansson M, Zhang G, Braumann I, Spannagl M, Li C, Waugh R, Stein N (2017) A chromosome conformation capture ordered sequence of the barley genome. *Nature* 544:427-433 doi:10.1038/nature22043
- Mason AS, Higgins EE, Snowdon RJ, Batley J, Stein A, Werner C, Parkin IA (2017) A user guide to the Brassica60K Illumina Infinium™ SNP genotyping array. *Theoretical and Applied Genetics* 130:621-633
- Mathre D (1997) *Compendium of Barley Diseases*. The American Phytopathological Society. APS Press, St. Paul, MN,
- Matukumalli LK, Lawley CT, Schnabel RD, Taylor JF, Allan MF, Heaton MP, O'Connell J, Moore SS, Smith TP, Sonstegard TS (2009) Development and characterization of a high density SNP genotyping assay for cattle. *PloS one* 4:e5350
- Maurer A, Draba V, Jiang Y, Schnaithmann F, Sharma R, Schumann E, Kilian B, Reif JC, Pillen K (2015) Modelling the genetic architecture of flowering time control in barley through nested association mapping. *BMC Genomics* 16:290
- McDonald BA, Linde C (2002) Pathogen population genetics, evolutionary potential, and durable resistance. *Annual Review of Phytopathology* 40:349-379
- McDonald MC, Ahren D, Simpfendorfer S, Milgate A, Solomon PS (2018) The discovery of the virulence gene ToxA in the wheat and barley pathogen *Bipolaris sorokiniana*. *Molecular Plant Pathology* 19:432-439 doi:10.1111/mpp.12535
- McGee JD, Hamer JE, Hodges TK (2001) Characterization of a PR-10 pathogenesis-related gene family induced in rice during infection with *Magnaporthe grisea*. *Molecular Plant-Microbe Interactions* 14:877-886
- McKevith B (2004) Nutritional aspects of cereals. *Nutrition Bulletin* 29:111-142
- McLean M, Howlett B, Hollaway G (2009) Epidemiology and control of spot form of net blotch (*Pyrenophora teres* f. *maculata*) of barley: A review. *Crop Pasture Science* 60:303-315
- Meldrum S, Platz D, Ogle H (2004) Pathotypes of *Cochliobolus sativus* on barley in Australia. *Australasian Plant Pathology* 33:109-114
- Muradov A, Petrasovits L, Davidson A, Scott K (1993) A cDNA clone for a pathogenesis-related protein 1 from barley. *Plant Molecular Biology* 23:439-442
- Murray G, Brennan J (2010) Estimating disease losses to the Australian barley industry. *Australasian Plant Pathology* 39:85-96
- Nakajima H, Isomi K, Hamasaki T, Ichinoe M (1994) Sorokinianin: a novel phytotoxin produced by the phytopathogenic fungus *Bipolaris sorokiniana*. *Tetrahedron Letters* 35:9597-9600
- Novakazi F, Afanasenko O, Anisimova A, Platz GJ, Snowdon R, Kovaleva O, Zubkovich A, Ordon F (2019a) Genetic analysis of a worldwide barley collection for resistance to net form of net blotch disease (*Pyrenophora teres* f. *teres*). *Theoretical and Applied Genetics* 132:2633–2650 doi:https://doi.org/10.1007/s00122-019-03378-1

References

- Novakazi F, Afanasenko O, Lashina NM, Platz GJ, Snowdon R, Loskutov I, Ordon F (2019b) Genome-wide association studies in a barley (*Hordeum vulgare*) diversity set reveal a limited number of loci for resistance to spot blotch (*Bipolaris sorokiniana*). Plant Breeding 00:1-15 doi:10.1111/pbr.12792
- Nutter F, Pederson V, Foster A (1985) Effect of inoculations with *Cochliobolus sativus* at specific growth stages on grain yield and quality of malting barley. Crop Science 25:933-938
- O'Boyle P, Brooks W, Barnett M, Berger G, Steffenson B, Stromberg E, Maroof M, Liu S, Griffey C (2014) Mapping net blotch resistance in 'Nomini' and CIho 2291 barley. Crop Science 54:2596-2602
- Obst A, Gehring K (2002) Getreide - Krankheiten, Schädlinge, Unkräuter. Verlag Thomas Mann, Gelsenkirchen-Buer, Germany, 1-256
- Olbe M, Sommarin M, Gustafsson M, Lundborg T (1995) Effect of the fungal pathogen *Bipolaris sorokiniana* toxin prehelminthosporol on barley root plasma membrane vesicles. Plant Pathology 44:625-635
- Pandey SP, Somssich IE (2009) The role of WRKY transcription factors in plant immunity. Plant Physiology 150:1648-1655
- Panstruga R, Parker JE, Schulze-Lefert P (2009) SnapShot: plant immune response pathways. Cell 136:978. e971-978. e973
- Park C-J, Seo Y-S (2015) Heat shock proteins: a review of the molecular chaperones for plant immunity. The Plant Pathology Journal 31:323
- Peace C, Bassil N, Main D, Ficklin S, Rosyara UR, Stegmeir T, Sebolt A, Gilmore B, Lawley C, Mockler TC (2012) Development and evaluation of a genome-wide 6K SNP array for diploid sweet cherry and tetraploid sour cherry. PLoS One 7:e48305
- Pieterse CM, Van Loon LC (1999) Salicylic acid-independent plant defence pathways. Trends in Plant Science 4:52-58
- Piffanelli P, Zhou F, Casais C, Orme J, Jarosch B, Schaffrath U, Collins NC, Panstruga R, Schulze-Lefert P (2002) The barley MLO modulator of defense and cell death is responsive to biotic and abiotic stress stimuli. Plant Physiology 129:1076-1085
- Pourkheirandish M, Hensel G, Kilian B, Senthil N, Chen G, Sameri M, Azhaguvel P, Sakuma S, Dhanagond S, Sharma R (2015) Evolution of the grain dispersal system in barley. Cell 162:527-539
- Price AL, Patterson NJ, Plenge RM, Weinblatt ME, Shadick NA, Reich D (2006) Principal components analysis corrects for stratification in genome-wide association studies. Nature Genetics 38:904
- Pritchard JK, Stephens M, Donnelly P (2000) Inference of population structure using multilocus genotype data. Genetics 155:945-959
- Punja ZK, Zhang Y-y (1993) Plant chitinases and their roles in resistance to fungal diseases. Journal of Nematology 25:526
- Rafalski JA (2010) Association genetics in crop improvement. Current Opinion in Plant Biology 13:174-180 doi:10.1016/j.pbi.2009.12.004
- Rajan VBV, D'Silva P (2009) *Arabidopsis thaliana* J-class heat shock proteins: cellular stress sensors. Functional & Integrative Genomics 9:433
- Raman H, Platz G, Chalmers K, Raman R, Read B, Barr A, Moody D (2003) Mapping of genomic regions associated with net form of netblotch resistance in barley. Australian Journal of Agricultural Research 54:1359-1367
- Ramsay L, Comadran J, Druka A, Marshall DF, Thomas WT, Macaulay M, MacKenzie K, Simpson C, Fuller J, Bonar N (2011) INTERMEDIUM-C, a modifier of lateral spikelet fertility in barley, is an ortholog of the maize domestication gene TEOSINTE BRANCHED 1. Nature Genetics 43:169
- Rau D, Brown AH, Brubaker CL, Attene G, Balmas V, Saba E, Papa R (2003) Population genetic structure of *Pyrenophora teres* Drechs. the causal agent of net blotch in Sardinian landraces of barley (*Hordeum vulgare* L.). Theoretical and Applied Genetics 106:947-959
- Rehman HM, Nawaz MA, Shah ZH, Ludwig-Müller J, Chung G, Ahmad MQ, Yang SH, Lee SI (2018) Comparative genomic and transcriptomic analyses of Family-1 UDP glycosyltransferase in three Brassica species and Arabidopsis indicates stress-responsive regulation. Scientific Reports 8:1875

References

- Reiss E, Bryngelsson T (1996) Pathogenesis-related proteins in barley leaves, induced by infection with *Drechslera teres* (Sacc.) Shoem. and by treatment with other biotic agents. *Physiological and Molecular Plant Pathology* 49:331-341
- Reiss E, Horstmann C (2001) *Drechslera teres*-infected barley (*Hordeum vulgare* L.) leaves accumulate eight isoforms of thaumatin-like proteins. *Physiological and Molecular Plant Pathology* 58:183-188
- Richards J, Chao S, Friesen T, Brueggeman R (2016) Fine Mapping of the Barley Chromosome 6H Net Form Net Blotch Susceptibility Locus. *G3 (Bethesda)* 6:1809-1818 doi:10.1534/g3.116.028902
- Richards JK, Friesen TL, Brueggeman RS (2017) Association mapping utilizing diverse barley lines reveals net form net blotch seedling resistance/susceptibility loci. *Theoretical and Applied Genetics* 130:915-927 doi:10.1007/s00122-017-2860-1
- Richter K, Schondelmaier J, Jung C (1998) Mapping of quantitative trait loci affecting *Drechslera teres* resistance in barley with molecular markers. *Theoretical and Applied Genetics* 97:1225-1234
- Robinson J, Jalli M (1996) Diversity among Finnish net blotch isolates and resistance in barley. *Euphytica* 92:81-87
- Roy JK, Smith KP, Muehlbauer GJ, Chao S, Close TJ, Steffenson BJ (2010) Association mapping of spot blotch resistance in wild barley. *Molecular Breeding* 26:243-256 doi:10.1007/s11032-010-9402-8
- Saade S, Negrão S, Plett D, Garnett T, Tester M (2018) Genomic and Genetic Studies of Abiotic Stress Tolerance in Barley. In: *The Barley Genome*. Springer, pp 259-286
- Sannemann W, Huang BE, Mathew B, Léon J (2015) Multi-parent advanced generation inter-cross in barley: high-resolution quantitative trait locus mapping for flowering time as a proof of concept. *Molecular Breeding* 35:86
- Sarpeleh A, Wallwork H, Catcheside DE, Tate ME, Able AJ (2007) Proteinaceous metabolites from *Pyrenophora teres* contribute to symptom development of barley net blotch. *Phytopathology* 97:907-915
- Schmalenbach I, March TJ, Bringezu T, Waugh R, Pillen K (2011) High-resolution genotyping of wild barley introgression lines and fine-mapping of the threshability locus thresh-1 using the Illumina GoldenGate assay. *G3: Genes, Genomes, Genetics* 1:187-196
- Shen Q-H, Saijo Y, Mauch S, Biskup C, Bieri S, Keller B, Seki H, Ülker B, Somssich IE, Schulze-Lefert P (2007) Nuclear activity of MLA immune receptors links isolate-specific and basal disease-resistance responses. *Science* 315:1098-1103
- Shjerve RA, Faris JD, Brueggeman RS, Yan C, Zhu Y, Koladia V, Friesen TL (2014) Evaluation of a *Pyrenophora teres* f. *teres* mapping population reveals multiple independent interactions with a region of barley chromosome 6H. *Fungal Genetics and Biology* 70:104-112 doi:10.1016/j.fgb.2014.07.012
- Shoemaker R (1955) Biology, cytology, and taxonomy of *Cochliobolus sativus*. *Canadian Journal of Botany* 33:562-576
- Sierotzki H, Frey R, Wulschleger J, Palermo S, Karlin S, Godwin J, Gisi U (2007) Cytochrome b gene sequence and structure of *Pyrenophora teres* and *P. tritici-repentis* and implications for QoI resistance. *Pest Management Science* 63:225-233
- Sim S-C, Durstewitz G, Plieske J, Wieseke R, Ganai MW, Van Deynze A, Hamilton JP, Buell CR, Causse M, Wijeratne S (2012) Development of a large SNP genotyping array and generation of high-density genetic maps in tomato. *PloS one* 7:e40563
- Skou J-P (1985) On the enhanced callose deposition in barley with ml-o powdery mildew resistance genes. *Journal of Phytopathology* 112:207-216
- Smedegård-Petersen V (1971) *Pyrenophora teres* f. *maculata* f. *nov.* and *Pyrenophora teres* f. *teres* on barley in Denmark. Yearbook of the Royal Veterinary and Agricultural University (Copenhagen) 1971:124-144
- Smedegård-Petersen V (1977) Isolation of two toxins produced by *Pyrenophora teres* and their significance in disease development of net-spot blotch of barley. *Physiological Plant Pathology* 10:203-211
- Sprague R (1950) Diseases of cereals and grasses in North America. The Ronald Press Company, New York, 538
- Statkevičiūtė G, Brazauskas G, Semaškienė R, Leistrumaitė A, Dabkevičius Z (2010) *Pyrenophora teres* genetic diversity as detected by ISSR analysis. *Agriculture* 97:91-98

References

- Stefansson TS, Serenius M, Hallsson JH (2012) The genetic diversity of Icelandic populations of two barley leaf pathogens, *Rhynchosporium commune* and *Pyrenophora teres*. *European Journal of Plant Pathology* 134:167-180
- Steffenson B, Hayes P, Kleinhofs A (1996) Genetics of seedling and adult plant resistance to net blotch (*Pyrenophora teres* f. *teres*) and spot blotch (*Cochliobolus sativus*) in barley. *Theoretical and Applied Genetics* 92:552-558
- Steffenson BJ, Webster R (1992a) Pathotype diversity of *Pyrenophora teres* f. *teres* on barley. *Phytopathology* 82:170-177
- Steffenson BJ, Webster R (1992b) Quantitative resistance to *Pyrenophora teres* f. *teres* in barley. *Phytopathology* 82:407-411
- Stein N, Mascher M (2018) Barley genome sequencing and assembly—a first version reference sequence. In: *The Barley Genome*. Springer, pp 57-71
- Stevenson FJ, Jones HA (1953) Some Sources of Resistance in Crop Plants. In: Stefferud A (ed) *Yearbook of Agriculture*. United States Department of Agriculture, Washington, D.C., pp 192-193
- Taketa S, Amano S, Tsujino Y, Sato T, Saisho D, Kakeda K, Nomura M, Suzuki T, Matsumoto T, Sato K (2008) Barley grain with adhering hulls is controlled by an ERF family transcription factor gene regulating a lipid biosynthesis pathway. *Proceedings of the National Academy of Sciences* 105:4062-4067
- Tamang P, Neupane A, Mamidi S, Friesen T, Brueggeman R (2015) Association mapping of seedling resistance to spot form net blotch in a worldwide collection of barley. *Phytopathology* 105:500-508 doi:10.1094/PHYTO-04-14-0106-R
- Tekauz A (1990) Characterization and distribution of pathogenic variation in *Pyrenophora teres* f. *teres* and *P. teres* f. *maculata* from western Canada. *Canadian Journal of Plant Pathology* 12:141-148
- Tinline R (1951) Studies on the perfect stage of *Helminthosporium sativum*. *Canadian Journal of Botany* 29:467-478
- Tuohy J, Jalli M, Cooke B, O'Sullivan E (2006) Pathogenic variation in populations of *Drechslera teres* f. *teres* and *D. teres* f. *maculata* and differences in host cultivar responses. *European journal of plant pathology* 116:177-185
- Tuori R, Wolpert T, Ciuffetti L (1995) Purification and immunological characterization of toxic components from cultures of *Pyrenophora tritici-repentis*. *Ile* 9:10.13
- Turner A, Beales J, Faure S, Dunford RP, Laurie DA (2005) The pseudo-response regulator Ppd-H1 provides adaptation to photoperiod in barley. *Science* 310:1031-1034
- Turner JG, Ellis C, Devoto A (2002) The jasmonate signal pathway. *The Plant Cell* 14:S153-S164
- Valjavec-Gratian M, Steffenson B (1997) Pathotypes of *Cochliobolus sativus* on barley in North Dakota. *Plant Disease* 81:1275-1278
- van Loon LC, Rep M, Pieterse CM (2006) Significance of inducible defense-related proteins in infected plants. *Annual Review of Phytopathology* 44:135-162
- Varner JE, Lin L-S (1989) Plant cell wall architecture. *Cell* 56:231-239
- Vatter T, Maurer A, Kopahnke D, Perovic D, Ordon F, Pillen K (2017) A nested association mapping population identifies multiple small effect QTL conferring resistance against net blotch (*Pyrenophora teres* f. *teres*) in wild barley. *PLoS One* 12:e0186803 doi:10.1371/journal.pone.0186803
- Verde I, Bassil N, Scalabrin S, Gilmore B, Lawley CT, Gasic K, Micheletti D, Rosyara UR, Cattonaro F, Vendramin E (2012) Development and evaluation of a 9K SNP array for peach by internationally coordinated SNP detection and validation in breeding germplasm. *PloS one* 7:e35668
- Vianello A, Zancani M, Peresson C, Petrusa E, Casolo V, Krajňáková J, Patui S, Braidot E, Macrì F (2007) Plant mitochondrial pathway leading to programmed cell death. *Physiologia plantarum* 129:242-252
- Vieira MLC, Santini L, Diniz AL, Munhoz CdF (2016) Microsatellite markers: what they mean and why they are so useful. *Genetics and Molecular Biology* 39:312-328
- Vogt T, Jones P (2000) Glycosyltransferases in plant natural product synthesis: characterization of a supergene family. *Trends in Plant Science* 5:380-386
- Voigt CA (2014) Callose-mediated resistance to pathogenic intruders in plant defense-related papillae. *Frontiers in Plant Science* 5:168

References

- von Bothmer R, Sato K, Komatsuda T, Yasuda S, Fischbeck G (2003) The domestication of cultivated barley. In: Diversity in barley (*Hordeum vulgare*). Elsevier Science, pp 9-27
- von Zitzewitz J, Szűcs P, Dubcovsky J, Yan L, Francia E, Pecchioni N, Casas A, Chen TH, Hayes PM, Skinner JS (2005) Molecular and structural characterization of barley vernalization genes. *Plant Molecular Biology* 59:449-467
- Vos P, Hogers R, Bleeker M, Reijans M, Lee Tvd, Hornes M, Friters A, Pot J, Paleman J, Kuiper M (1995) AFLP: a new technique for DNA fingerprinting. *Nucleic Acids Research* 23:4407-4414
- Voss-Fels K, Snowden RJ (2016) Understanding and utilizing crop genome diversity via high-resolution genotyping. *Plant biotechnology journal* 14:1086-1094
- Wallwork H, Butt M, Capio E (2016) Pathogen diversity and screening for minor gene resistance to *Pyrenophora teres* f. *teres* in barley and its use for plant breeding. *Australasian Plant Pathology* 45:527-531
- Wang H, Smith KP, Combs E, Blake T, Horsley RD, Muehlbauer GJ (2012) Effect of population size and unbalanced data sets on QTL detection using genome-wide association mapping in barley breeding germplasm. *Theoretical and Applied Genetics* 124:111-124 doi:10.1007/s00122-011-1691-8
- Wang M, Zhu X, Wang K, Lu C, Luo M, Shan T, Zhang Z (2018) A wheat caffeic acid 3-O-methyltransferase TaCOMT-3D positively contributes to both resistance to sharp eyespot disease and stem mechanical strength. *Scientific Reports* 8:6543
- Wang R, Leng Y, Ali S, Wang M, Zhong S (2017) Genome-wide association mapping of spot blotch resistance to three different pathotypes of *Cochliobolus sativus* in the USDA barley core collection. *Molecular Breeding* 37 doi:10.1007/s11032-017-0626-8
- Wang R, Leng Y, Zhao M, Zhong S (2019) Fine mapping of a dominant gene conferring resistance to spot blotch caused by a new pathotype of *Bipolaris sorokiniana* in barley. *Theoretical and Applied Genetics* 132:41-51
- Wang S, Wong D, Forrest K, Allen A, Chao S, Huang BE, Maccaferri M, Salvi S, Milner SG, Cattivelli L (2014) Characterization of polyploid wheat genomic diversity using a high-density 90 000 single nucleotide polymorphism array. *Plant Biotechnology Journal* 12:787-796
- Waugh R, Power W (1992) Using RAPD markers for crop improvement. *Trends in Biotechnology* 10:186-191
- Weiergang I, Lyngs Jørgensen HJ, Møller IM, Friis P, Smedegaard-Petersen V (2002) Optimization of in vitro growth conditions of *Pyrenophora teres* for production of the phytotoxin aspergillomarasmine A. *Physiological and Molecular Plant Pathology* 60:131-140 doi:10.1006/pmpp.2002.0383
- Williams K, Smyl C, Lichon A, Wong K, Wallwork H (2001) Development and use of an assay based on the polymerase chain reaction that differentiates the pathogens causing spot form and net form of net blotch of barley. *Australasian Plant Pathology* 30:37-44
- Wonneberger R, Ficke A, Lillemo M (2017a) Identification of quantitative trait loci associated with resistance to net form net blotch in a collection of Nordic barley germplasm. *Theoretical and Applied Genetics* 130:2025-2043 doi:10.1007/s00122-017-2940-2
- Wonneberger R, Ficke A, Lillemo M (2017b) Mapping of quantitative trait loci associated with resistance to net form net blotch (*Pyrenophora teres* f. *teres*) in a doubled haploid Norwegian barley population. *PLoS One* 12:e0175773 doi:10.1371/journal.pone.0175773
- Wu H-L, Steffenson B, Zhong S, Li Y, Oleson A (2003) Genetic variation for virulence and RFLP markers in *Pyrenophora teres*. *Canadian Journal of Plant Pathology* 25:82-90
- Yan L, Fu D, Li C, Blechl A, Tranquilli G, Bonafede M, Sanchez A, Valarik M, Yasuda S, Dubcovsky J (2006) The wheat and barley vernalization gene VRN3 is an orthologue of FT. *Proceedings of the National Academy of Sciences* 103:19581-19586
- Yan L, Loukoianov A, Blechl A, Tranquilli G, Ramakrishna W, SanMiguel P, Bennetzen JL, Echenique V, Dubcovsky J (2004) The wheat VRN2 gene is a flowering repressor down-regulated by vernalization. *Science* 303:1640-1644
- Yitbarek S, Berhane L, Fikadu A, Van Leur J, Grando S, Ceccarelli S (1998) Variation in Ethiopian barley landrace populations for resistance to barley leaf scald and net blotch. *Plant Breeding* 117:419-423
- Yu J, Pressoir G, Briggs WH, Vroh Bi I, Yamasaki M, Doebley JF, McMullen MD, Gaut BS, Nielsen DM, Holland JB, Kresovich S, Buckler ES (2006) A unified mixed-model method for

References

- association mapping that accounts for multiple levels of relatedness. *Nature Genetics* 38:203-208 doi:10.1038/ng1702
- Yun S, Gyenis L, Bossolini E, Hayes P, Matus I, Smith KP, Steffenson BJ, Tuberosa R, Muehlbauer GJ (2006) Validation of quantitative trait loci for multiple disease resistance in barley using advanced backcross lines developed with a wild barley. *Crop Science* 46:1179-1186
- Yun SJ, Gyenis L, Hayes PM, Matus I, Smith KP, Steffenson BJ, Muehlbauer GJ (2005) Quantitative Trait Loci for Multiple Disease Resistance in Wild Barley. *Crop Science* 45 doi:10.2135/cropsci2005.0236
- Zakhrabekova S, Gough SP, Braumann I, Müller AH, Lundqvist J, Ahmann K, Dockter C, Matyszczyk I, Kurowska M, Druka A (2012) Induced mutations in circadian clock regulator *Mat-a* facilitated short-season adaptation and range extension in cultivated barley. *Proceedings of the National Academy of Sciences* 109:4326-4331
- Zeng X, Guo Y, Xu Q, Mascher M, Guo G, Li S, Mao L, Liu Q, Xia Z, Zhou J (2018) Origin and evolution of qingke barley in Tibet. *Nature Communications* 9:5433
- Zhang L, Du L, Poovaiah B (2014) Calcium signaling and biotic defense responses in plants. *Plant Signaling & Behavior* 9:e973818
- Zhong X, Yang J, Shi Y, Wang X, Wang GL (2018) The DnaJ protein OsDjA6 negatively regulates rice innate immunity to the blast fungus *Magnaporthe oryzae*. *Molecular Plant Pathology* 19:607-614
- Zhou H, Steffenson B (2013) Genome-wide association mapping reveals genetic architecture of durable spot blotch resistance in US barley breeding germplasm. *Molecular Breeding* 32:139-154 doi:10.1007/s11032-013-9858-4
- Zhou M (2009) Barley production and consumption. In: *Genetics and improvement of barley malt quality*. Springer, Berlin, Heidelberg, pp 1-17. doi:10.1007/978-3-642-01279-2_1
- Zipfel C, Robatzek S (2010) Pathogen-associated molecular pattern-triggered immunity: *veni, vidi...?* *Plant Physiology* 154:551-554

Appendix

Table A.1 Predicted genes located on chromosomes 3H at 58-101 Mbp and their respective functional annotations.

Gene ID ^a	Gene class ^b	Chr	Physical location [bp]		Annotation
HORVU3Hr1G019900	HC_G	3H	58,919,635	58,924,049	Pentatricopeptide repeat-containing protein
HORVU3Hr1G019920	HC_G	3H	59,142,152	59,154,811	glycine-rich protein
HORVU3Hr1G020200	HC_G	3H	62,101,338	62,106,035	FAR1-related sequence 5
HORVU3Hr1G020230	HC_G	3H	62,321,474	62,325,343	HXXXD-type acyl-transferase family protein
HORVU3Hr1G020310	HC_G	3H	63,224,095	63,240,854	Homeodomain-like transcriptional regulator
HORVU3Hr1G020420	LC_TE?	3H	63,618,522	63,627,039	DEAD-box ATP-dependent RNA helicase 39
HORVU3Hr1G020470	HC_G	3H	63,800,868	63,807,891	ubiquitin-conjugating enzyme 3
HORVU3Hr1G020660	LC_TE?	3H	64,617,802	64,621,872	Chromosome 3B, cultivar Chinese Spring
HORVU3Hr1G020690	HC_G	3H	64,666,810	64,675,469	Ribosomal protein L18ae family
HORVU3Hr1G021050	HC_U	3H	66,760,126	66,838,408	unknown protein
HORVU3Hr1G021120	HC_G	3H	67,266,734	67,272,759	WRKY DNA-binding protein 13
HORVU3Hr1G021140	HC_G	3H	67,421,435	67,430,123	gigantea protein (GI)
HORVU3Hr1G021150	HC_G	3H	67,560,410	67,562,131	gigantea protein (GI)
HORVU3Hr1G021310	HC_G	3H	68,834,975	68,838,931	TSL-kinase interacting protein 1
HORVU3Hr1G021470	HC_G	3H	70,774,675	70,781,561	DDT domain superfamily
HORVU3Hr1G021520	LC_u	3H	71,727,416	71,740,865	undescribed protein
HORVU3Hr1G021650	HC_TE?	3H	73,222,982	73,225,235	Protein of unknown function (DUF581)
HORVU3Hr1G021660	HC_G	3H	73,423,323	73,433,832	MAR binding filament-like protein 1
HORVU3Hr1G021730	HC_G	3H	73,918,529	73,925,361	BTB/POZ/Kelch-associated protein
HORVU3Hr1G021750	HC_G	3H	74,784,620	74,790,194	Serine incorporator 1
HORVU3Hr1G021810	HC_G	3H	75,014,380	75,162,233	UDP-Glycosyltransferase superfamily protein
HORVU3Hr1G021820	HC_G	3H	75,101,169	75,107,041	DNA polymerase epsilon subunit B2
HORVU3Hr1G021830	LC_TE	3H	75,133,326	75,137,811	unknown function
HORVU3Hr1G021910	HC_G	3H	75,453,803	75,458,618	tetratricopeptide repeat (TPR)-containing protein
HORVU3Hr1G021930	LC_u	3H	75,512,365	75,516,595	undescribed protein
HORVU3Hr1G021940	LC_u	3H	75,512,379	75,516,586	undescribed protein
HORVU3Hr1G021970	HC_G	3H	76,044,757	76,052,955	Transcription initiation factor IIA subunit 2
HORVU3Hr1G022000	HC_G	3H	76,054,288	76,087,672	embryo defective 2410
HORVU3Hr1G022020	HC_u	3H	76,087,869	76,091,394	undescribed protein
HORVU3Hr1G022030	HC_G	3H	76,091,634	76,095,793	Syntaxin-32
HORVU3Hr1G022040	LC_u	3H	76,092,113	76,092,505	undescribed protein
HORVU3Hr1G022270	HC_G	3H	78,241,796	78,243,136	pentatricopeptide repeat 336
HORVU3Hr1G022350	HC_G	3H	78,933,679	79,045,801	Valine--tRNA ligase
HORVU3Hr1G022370	HC_G	3H	78,988,727	78,990,642	ROTUNDIFOLIA like 12

Appendix

Table A.1 continued

HORVU3Hr1G022380	HC_G	3H	78,994,165	78,996,747	Chromosome 3B, cultivar Chinese Spring
HORVU3Hr1G022500	HC_G	3H	80,216,668	80,226,652	Zinc transporter ZIP13 homolog
HORVU3Hr1G022620	HC_TE?	3H	81,047,235	81,050,688	Zinc-finger domain of monoamine-oxidase A repressor R1
HORVU3Hr1G022780	HC_G	3H	82,280,121	82,287,713	Protein kinase family protein
HORVU3Hr1G022800	HC_G	3H	82,838,259	82,850,099	ABC transporter G family member 31
BAK52288.1	ncbi EIBI1	3H	82,838,566	82,849,750	EIBI1 protein
HORVU3Hr1G022890	HC_U	3H	83,675,968	83,677,172	unknown protein
HORVU3Hr1G023020	LC_U	3H	84,971,122	84,974,818	Chromosome 3B, cultivar Chinese Spring
HORVU3Hr1G023220	HC_G	3H	86,137,493	86,150,517	chloride channel C
HORVU3Hr1G023790	HC_G	3H	88,695,007	88,701,431	O-fucosyltransferase family protein
HORVU3Hr1G024610	HC_TE?	3H	95,702,928	95,710,058	ATP-dependent RNA helicase DBP2
HORVU3Hr1G025510	HC_G	3H	101,18,0815	101,185,063	Mitochondrial import inner membrane translocase subunit TIM14-3
HORVU3Hr1G025520	HC_G	3H	101,183,879	101,186,196	Glycosyltransferase

^a The predicted genes and their respective annotations were obtained from BARLEYMAP (Cantalapiedra et al. 2015)

^b HC_G high confidence gene with predicted function, HC_U high confidence gene without predicted function, LC_u low-confidence gene without predicted function

Table A.2 Predicted genes located on chromosomes 3H at 119-128 Mbp and their respective functional annotations.

Gene ID ^a	Gene class ^b	Chr	Physical location [bp]		Annotation
HORVU3Hr1G027610	HC_G	3H	119,622,755	119,628,066	Class I glutamine amidotransferase-like superfamily protein
HORVU3Hr1G027730	HC_G	3H	120,303,710	120,307,660	Protein transport protein SEC13 homolog B
HORVU3Hr1G027990	HC_G	3H	122,465,365	122,467,535	GDSL esterase/lipase
HORVU3Hr1G028210	HC_G	3H	124,052,960	124,058,809	GDSL esterase/lipase
HORVU3Hr1G028220	LC_u	3H	124,057,218	124,057,686	undescribed protein
HORVU3Hr1G028240	HC_G	3H	124,687,267	124,690,324	Transcription factor TCP4
HORVU3Hr1G029730	HC_G	3H	138,755,766	138,759,783	unknown function

^a The predicted genes and their respective annotations were obtained from BARLEYMAP (Cantalapiedra et al. 2015)

^b HC_G high confidence gene with predicted function, HC_U high confidence gene without predicted function, LC_u low-confidence gene without predicted function

Appendix

Table A.3 Predicted genes located on chromosomes 3H at 233-350 Mbp and their respective functional annotations.

Gene ID ^a	Gene class ^b	Chr	Physical location [bp]		Annotation
HORVU3Hr1G039480	HC_G	3H	233,010,935	233,012,321	arginine/serine-rich splicing factor 35
HORVU3Hr1G039500	HC_G	3H	233,580,657	233,585,235	WRKY family transcription factor
HORVU3Hr1G039530	LC_u	3H	233,878,473	233,880,175	undescribed protein
HORVU3Hr1G039540	HC_G	3H	233,988,385	234,000,622	Phospholipid-transporting ATPase 1
HORVU3Hr1G039550	LC_TE?	3H	233,988,485	233,995,600	DOF zinc finger protein 1
HORVU3Hr1G039570	LC_TE	3H	234,982,822	234,993,041	unknown function
HORVU3Hr1G039600	HC_G	3H	235,267,245	235,286,946	Ran-binding protein 17
HORVU3Hr1G039680	HC_G	3H	236,508,938	236,509,937	GRAM domain-containing protein / ABA-responsive protein-related
HORVU3Hr1G039700	HC_G	3H	236,672,228	236,674,265	Chaperone protein DnaJ 1
HORVU3Hr1G039710	LC_u	3H	236,673,771	236,674,305	undescribed protein
HORVU3Hr1G039760	HC_G	3H	236,991,561	237,011,307	Lipase class 3-related protein
HORVU3Hr1G039800	HC_G	3H	237,231,212	237,234,793	Subtilisin-like protease
HORVU3Hr1G039810	LC_u	3H	237,232,598	237,234,536	undescribed protein
HORVU3Hr1G039930	HC_G	3H	238,598,524	238,601,525	Magnesium-protoporphyrin IX monomethyl ester [oxidative] cyclase 3
HORVU3Hr1G039980	HC_G	3H	239,240,252	239,247,230	COP9 signalosome complex subunit 2
HORVU3Hr1G040040	HC_G	3H	239,983,665	239,989,000	calmodulin 7
HORVU3Hr1G040270	HC_G	3H	241,775,085	241,780,591	Coatomer, beta subunit
HORVU3Hr1G040350	HC_G	3H	244,048,158	244,055,241	Coatomer, beta subunit
HORVU3Hr1G040360	HC_G	3H	244,136,880	244,329,433	ATP-citrate synthase subunit 1
HORVU3Hr1G040420	HC_G	3H	245,083,227	245,086,831	CCR4-NOT transcription complex subunit 3
HORVU3Hr1G040960	LC_TE	3H	254,116,193	254,121,841	unknown function
HORVU3Hr1G040990	HC_G	3H	254,456,729	254,460,078	Cyclin family protein
HORVU3Hr1G041160	HC_G	3H	256,194,419	256,233,445	Protein translocase subunit SecA
HORVU3Hr1G041250	HC_G	3H	256,251,311	256,281,939	Protein translocase subunit SecA
HORVU3Hr1G041440	HC_G	3H	258,119,732	258,123,019	2-oxoglutarate (2OG) and Fe(II)-dependent oxygenase superfamily protein
HORVU3Hr1G041450	LC_u	3H	258,120,352	258,120,777	undescribed protein
HORVU3Hr1G041500	LC_TE	3H	259,668,011	259,756,581	Gag-pol polyprotein
HORVU3Hr1G041530	LC_TE	3H	260,144,552	260,153,224	Retrotransposon protein, putative, unclassified
HORVU3Hr1G041540	LC_TE	3H	260,144,585	260,153,241	Ribonuclease H-like superfamily protein
HORVU3Hr1G041560	HC_G	3H	260,272,034	260,285,532	Phospholipid/glycerol acyltransferase family protein
HORVU3Hr1G041640	HC_G	3H	260,673,495	260,698,557	lipase class 3 family protein
HORVU3Hr1G041670	LC_u	3H	260,678,938	260,679,416	undescribed protein
HORVU3Hr1G041810	HC_G	3H	261,009,541	261,028,057	receptor-like protein kinase 1
HORVU3Hr1G041820	HC_G	3H	261,022,546	261,028,057	Protein kinase superfamily protein
HORVU3Hr1G041990	HC_G	3H	264,936,592	264,952,027	alpha/beta-Hydrolases superfamily protein

Appendix

Table A.3 continued

HORVU3Hr1G042140	HC_G	3H	267,285,420	267,302,003	fimbrin 1
HORVU3Hr1G042210	LC_u	3H	267,677,843	267,705,424	undescribed protein
HORVU3Hr1G042290	HC_G	3H	268,461,072	268,473,269	lipase 1
HORVU3Hr1G042330	HC_G	3H	268,906,906	268,955,150	Kinesin-related protein 6
HORVU3Hr1G042440	HC_G	3H	269,272,858	269,328,719	Divalent metal cation transporter MntH
HORVU3Hr1G042500	HC_G	3H	269,929,071	269,963,305	Chaperone protein dnaJ 15
HORVU3Hr1G042540	HC_G	3H	270,264,122	270,269,601	Callose synthase 1
HORVU3Hr1G042680	HC_G	3H	271,527,268	271,564,536	dentin sialophosphoprotein-related .
HORVU3Hr1G042770	HC_G	3H	271,757,175	271,770,306	phosphate transporter 4;1
HORVU3Hr1G042890	HC_G	3H	273,462,159	273,470,735	ERI1 exoribonuclease 2
HORVU3Hr1G042920	HC_U	3H	274,853,155	274,873,957	Protein of unknown function (DUF630 and DUF632)
HORVU3Hr1G043180	LC_u	3H	278,326,322	278,331,499	undescribed protein
HORVU3Hr1G043190	LC_u	3H	278,326,322	278,331,637	undescribed protein
HORVU3Hr1G043300	HC_G	3H	279,060,588	279,078,489	zinc induced facilitator-like 2
HORVU3Hr1G043380	HC_G	3H	279,755,871	279,759,438	Mitochondrial uncoupling protein 1
HORVU3Hr1G043390	HC_G	3H	280,115,534	280,144,231	Carbohydrate-binding-like fold
HORVU3Hr1G043440	HC_G	3H	280,310,298	280,339,871	AMSH-like ubiquitin thioesterase 3
HORVU3Hr1G043510	HC_G	3H	280,495,354	280,501,135	Ubiquitin-like-specific protease 1A
HORVU3Hr1G043530	HC_G	3H	280,711,035	280,766,862	Tetratricopeptide repeat protein 5
HORVU3Hr1G043730	HC_U	3H	282,624,697	282,648,576	unknown protein
HORVU3Hr1G043760	LC_u	3H	282,645,490	282,646,382	undescribed protein
HORVU3Hr1G043800	HC_G	3H	283,265,910	283,328,168	Mitochondrial substrate carrier family protein
HORVU3Hr1G043930	HC_G	3H	284,718,272	284,752,061	Sec-independent protein translocase protein TatC
HORVU3Hr1G044440	HC_U	3H	286,334,362	286,351,670	Protein of unknown function (DUF789)
HORVU3Hr1G044530	HC_G	3H	286,946,652	286,996,901	ATP-dependent Clp protease proteolytic subunit 1
HORVU3Hr1G044550	HC_G	3H	287839512	287,852,891	serine/threonine protein phosphatase 2A
HORVU3Hr1G044880	HC_G	3H	292,079,971	292,106,641	Serine/threonine-protein phosphatase 4 regulatory subunit 3
HORVU3Hr1G045150	HC_G	3H	294,750,254	294,757,389	ADP-ribosylation factor 3
HORVU3Hr1G045270	HC_G	3H	296,7088,18	296,740,420	ERD (early-responsive to dehydration stress) family protein
HORVU3Hr1G045310	LC_TE	3H	296,730,239	296,740,477	Transposon Ty1-BR Gag-Pol polypeptide
HORVU3Hr1G045410	HC_G	3H	298,534,266	298,552,049	2-oxoglutarate (2OG) and Fe(II)-dependent oxygenase superfamily protein
HORVU3Hr1G045480	HC_G	3H	299,420,640	299,478,444	dehydroquinase dehydratase, putative / shikimate dehydrogenase, putative
HORVU3Hr1G045490	HC_G	3H	299,446,023	299,455,323	Phosphatidic acid phosphatase (PAP2) family protein
HORVU3Hr1G045890	HC_G	3H	302,784,705	302,789,786	evolutionarily conserved C-terminal region 7
HORVU3Hr1G045900	HC_G	3H	303,219,666	303,249,986	bromo-adjacent homology (BAH) domain-containing protein

Appendix

Table A.3 continued

HORVU3Hr1G046180	HC_G	3H	306,942,033	306,970,001	Protein FAM91A1
HORVU3Hr1G046280	HC_G	3H	307,953,328	308,000,422	MORC family CW-type zinc finger protein 3
HORVU3Hr1G046500	LC_TE?	3H	309,690,344	309,695,060	ATP-dependent RNA helicase DBP2
HORVU3Hr1G046530	LC_U	3H	310,581,877	310,594,914	unknown function
HORVU3Hr1G046570	HC_G	3H	311,867,465	311,876,945	Piezo-type mechanosensitive ion channel component 2
HORVU3Hr1G046680	HC_U	3H	312,174,280	312,179,139	omosome 3B, genomic scaffold, cultivar Chinese Spring
HORVU3Hr1G046690	LC_u	3H	312,174,307	312,179,093	undescribed protein
HORVU3Hr1G046970	HC_G	3H	315,704,288	315,728,138	Condensin complex subunit 2
HORVU3Hr1G047030	HC_G	3H	316,865,974	316,870,925	Ferredoxin-thioredoxin reductase, catalytic chain
HORVU3Hr1G047040	HC_G	3H	317,316,276	317,372,733	Protein HASTY 1
HORVU3Hr1G047110	HC_G	3H	318,463,541	318,488,458	Ell-associated factor Eaf
HORVU3Hr1G047150	LC_TE	3H	319,206,689	319,228,498	unknown function
HORVU3Hr1G047160	HC_G	3H	319,229,273	319,270,456	protein kinase family protein / protein phosphatase 2C (PP2C) family protein
HORVU3Hr1G047180	HC_G	3H	319,541,939	319,544,354	omosome 3B, genomic scaffold, cultivar Chinese Spring
HORVU3Hr1G047230	HC_G	3H	320,765,132	320,770,250	DNA replication licensing factor MCM4
HORVU3Hr1G047320	HC_G	3H	321,716,731	321,718,108	Peptide-N4-(N-acetyl-beta-glucosaminy)asparagine amidase A protein
HORVU3Hr1G047330	LC_u	3H	321,716,787	321,719,667	undescribed protein
HORVU3Hr1G047350	LC_TE?	3H	322,160,843	322,166,394	ATP-dependent RNA helicase DeaD
HORVU3Hr1G047440	HC_TE?	3H	322,725,918	322,729,816	F-box protein SKIP8
HORVU3Hr1G047510	HC_G	3H	323,644,309	323,646,954	V-type proton ATPase subunit F
HORVU3Hr1G047530	HC_G	3H	324,426,411	324,475,195	transducin family protein / WD-40 repeat family protein
HORVU3Hr1G047710	LC_TE	3H	326,704,245	326,777,477	Transposon Ty1-OR Gag-Pol polyprotein
HORVU3Hr1G047750	HC_G	3H	327,138,843	327,142,950	Tudor/PWWP/MBT superfamily protein
HORVU3Hr1G047910	LC_TE	3H	329,231,623	329,289,312	Retrotransposon protein, putative, unclassified
HORVU3Hr1G047980	HC_G	3H	329,253,524	329,290,599	Mitochondrial ATP synthase
HORVU3Hr1G048090	HC_G	3H	330,287,509	330,291,124	Ras-related protein Rab-1A
HORVU3Hr1G048100	LC_u	3H	330,288,424	330,290,495	undescribed protein
HORVU3Hr1G048210	HC_G	3H	331,630,521	331,636,707	Oxidoreductase/transition metal ion-binding protein
HORVU3Hr1G048240	HC_G	3H	331,935,314	331,961,017	Peptidase M16 family
HORVU3Hr1G048310	HC_G	3H	332,578,608	332,595,447	PITH domain-containing protein 1
HORVU3Hr1G048340	HC_G	3H	333,545,208	333,550,599	PHAX RNA-binding domain protein
HORVU3Hr1G048440	LC_TE?	3H	334,487,237	334,552,981	pentatricopeptide repeat 336
HORVU3Hr1G048620	HC_U	3H	336,497,321	336,501,282	UPF0587 protein C1orf123 homolog
HORVU3Hr1G048660	HC_G	3H	336,951,370	336,954,300	Hypoxia-responsive family protein

Appendix

Table A.3 continued

HORVU3Hr1G048690	LC_U	3H	337,028,119	337,035,325	unknown function
HORVU3Hr1G048770	HC_G	3H	338,004,044	338,006,390	Transcription factor bHLH87
HORVU3Hr1G048870	HC_G	3H	339,064,182	339,071,356	Glutamate dehydrogenase
HORVU3Hr1G048890	HC_G	3H	339,513,481	339,517,258	RWD domain-containing protein 1
HORVU3Hr1G049060	HC_G	3H	341,212,476	341,217,436	Vacuolar cation/proton exchanger 1a
HORVU3Hr1G049120	HC_G	3H	341,852,142	341,864,197	Ubiquitin carboxyl-terminal hydrolase 7
HORVU3Hr1G049240	LC_U	3H	344,076,913	344,081,359	Protein of Unknown Function (DUF239)
HORVU3Hr1G049360	HC_G	3H	345,384,179	345,394,373	Pentatricopeptide repeat-containing protein
HORVU3Hr1G049390	HC_TE?	3H	346,271,410	346,273,078	zinc finger (Ran-binding) family protein
HORVU3Hr1G049480	HC_G	3H	348,705,427	348,709,946	Protein kinase superfamily protein
HORVU3Hr1G049490	LC_u	3H	348,709,173	348,710,012	undescribed protein
HORVU3Hr1G049610	HC_G	3H	350,097,931	350,103,029	Carbamoyl-phosphate synthase large chain
HORVU3Hr1G049640	HC_G	3H	350,511,726	350,515,250	calmodulin-binding family protein

^aThe predicted genes and their respective annotations were obtained from BARLEYMAP (Cantalapiedra et al. 2015)

^bHC_G high confidence gene with predicted function, HC_U high confidence gene without predicted function, LC_u low-confidence gene without predicted function

Table A.4 Predicted genes located on chromosomes 3H at 428-492 Mbp and their respective functional annotations.

Gene ID ^a	Gene class ^b	Chr	Physical location [bp]		Annotation
HORVU3Hr1G057180	HC_U	3H	428,369,322	428,371,199	unknown function
HORVU3Hr1G057240	HC_G	3H	429,177,580	429,179,365	Glutaredoxin family protein
HORVU3Hr1G057270	HC_G	3H	429,449,626	429,456,332	RNA-binding KH domain-containing protein
HORVU3Hr1G057390	HC_G	3H	430,729,579	430,797,169	defective in meristem silencing 3
HORVU3Hr1G057440	HC_G	3H	431,180,711	431,184,807	Protein kinase superfamily protein
HORVU3Hr1G057470	LC_U	3H	431,379,478	431,385,068	Chromosome 3B, cultivar Chinese Spring
HORVU3Hr1G057480	LC_u	3H	431,385,444	431,393,245	undescribed protein
HORVU3Hr1G057520	LC_TE	3H	432,096,804	432,108,322	Retrotransposon protein, putative, Ty1-copia subclass
HORVU3Hr1G057530	HC_G	3H	432,097,070	432,118,808	Isoprenylcysteine alpha-carbonyl methylesterase ICME
HORVU3Hr1G057540	HC_G	3H	432,121,828	432,158,965	ATP-dependent zinc metalloprotease FtsH
HORVU3Hr1G057560	HC_U	3H	432,948,452	432,949,918	Protein of unknown function, DUF617
HORVU3Hr1G057660	HC_G	3H	434,386,942	434,402,600	mitogen-activated protein kinase 16
HORVU3Hr1G057840	HC_TE?	3H	435,389,419	435,402,515	Zinc finger protein ZPR1
HORVU3Hr1G057860	HC_u	3H	435,525,690	435,526,990	undescribed protein
HORVU3Hr1G057920	HC_TE?	3H	435,882,426	435,884,362	Zinc finger CCCH domain-containing protein 9

Appendix

Table A.4 continued

HORVU3Hr1G057940	HC_U	3H	435,976,291	435,979,905	Chromosome 3B, cultivar Chinese Spring
HORVU3Hr1G057970	LC_u	3H	436,616,436	436,623,248	undescribed protein
HORVU3Hr1G058070	HC_G	3H	437,234,289	437,237,989	Pentatricopeptide repeat-containing protein
HORVU3Hr1G058150	HC_TE?	3H	438,233,271	438,235,842	unknown protein
HORVU3Hr1G058170	HC_G	3H	438,361,859	438,366,708	ADP,ATP carrier protein 1
HORVU3Hr1G058300	HC_G	3H	439,321,823	439,329,111	Potassium channel AKT1
HORVU3Hr1G058320	HC_G	3H	439,331,534	439,335,887	alpha/beta-Hydrolases superfamily protein
HORVU3Hr1G058380	HC_G	3H	440,008,876	440,016,836	Transcription initiation factor TFIID subunit 7
HORVU3Hr1G058390	HC_G	3H	440,013,000	440,017,152	Bromodomain-containing factor 1
HORVU3Hr1G058410	HC_G	3H	440,562,247	440,570,858	transducin family protein / WD-40 repeat family protein
HORVU3Hr1G058440	HC_G	3H	441,083,231	441,091,930	GDSL esterase/lipase
HORVU3Hr1G058460	HC_G	3H	441,092,714	441,096,307	malate dehydrogenase
HORVU3Hr1G058470	HC_G	3H	441,452,592	441,489,005	glucan synthase-like 7
HORVU3Hr1G058580	HC_G	3H	442,153,604	442,156,619	Phospholipase A1-II 1
HORVU3Hr1G058590	HC_G	3H	442,171,432	442,174,231	Pentatricopeptide repeat-containing protein
HORVU3Hr1G058600	HC_G	3H	442,287,002	442,289,786	Phospholipase A1-II 2
HORVU3Hr1G058610	HC_G	3H	442,444,217	442,456,027	GDSL esterase/lipase
HORVU3Hr1G058700	HC_G	3H	442,861,665	442,864,199	Phospholipase A1-II 3
HORVU3Hr1G058740	HC_G	3H	443,657,431	443,665,585	Protein CHUP1, chloroplastic
HORVU3Hr1G058810	HC_G	3H	444,112,630	444,136,353	TRICHOME BIREFRINGENCE-LIKE 38
HORVU3Hr1G058830	HC_G	3H	444,736,432	444,738,710	TRICHOME BIREFRINGENCE-LIKE 19
HORVU3Hr1G058850	LC_U	3H	444,742,105	444,752,719	Chromosome 3B, cultivar Chinese Spring
HORVU3Hr1G058910	HC_G	3H	445,382,766	445,407,511	Transducin/WD40 repeat-like superfamily protein
HORVU3Hr1G058990	HC_G	3H	445,916,873	445,924,321	CTP synthase family protein
HORVU3Hr1G059010	HC_G	3H	445,928,632	445,933,760	Actin-related protein 2/3 complex subunit 2A
HORVU3Hr1G059060	HC_G	3H	446,058,318	446,062,780	Isocitrate dehydrogenase [NADP]
HORVU3Hr1G059080	HC_G	3H	446,230,541	446,240,517	Histone-lysine N-methyltransferase 2A
HORVU3Hr1G059120	HC_U	3H	446,912,069	446,922,626	Chromosome 3B, cultivar Chinese Spring
HORVU3Hr1G059130	HC_G	3H	447,064,974	447,070,639	OBP3-responsive gene 1
HORVU3Hr1G059140	HC_G	3H	447,236,706	447,245,971	Long-chain-fatty-acid--CoA ligase 1
HORVU3Hr1G059160	LC_u	3H	447,515,469	447,520,906	undescribed protein
HORVU3Hr1G059170	HC_G	3H	447,515,469	447,521,381	Protein phosphatase 2C family protein
HORVU3Hr1G059250	HC_G	3H	448,558,019	448,559,843	Ethylene-responsive transcription factor 3
HORVU3Hr1G059290	HC_G	3H	449,074,317	449,092,625	ubiquitin conjugating enzyme 9
HORVU3Hr1G059320	HC_G	3H	449,662,700	449,666,771	V-type proton ATPase subunit E

Appendix

Table A.4 continued

HORVU3Hr1G059390	HC_G	3H	450,590,313	450,708,634	GDP-D-mannose 3',5'-epimerase
HORVU3Hr1G059420	LC_u	3H	450,705,488	450,708,230	undescribed protein
HORVU3Hr1G059440	HC_G	3H	450,886,623	450,890,677	Calcium-dependent lipid-binding (CaLB domain) family protein
HORVU3Hr1G059460	HC_TE?	3H	451,374,074	451,376,950	F-box/kelch-repeat protein
HORVU3Hr1G059550	HC_U	3H	452,338,718	452,342,853	unknown function
HORVU3Hr1G059580	LC_U	3H	452,688,480	452,689,883	Chromosome 3B, cultivar Chinese Spring
HORVU3Hr1G059610	HC_G	3H	452,750,506	452,752,730	Phosphoglycerate mutase family protein
HORVU3Hr1G059700	HC_G	3H	453,794,588	453,802,210	AMSH-like ubiquitin thioesterase 2
HORVU3Hr1G059720	HC_U	3H	454,048,620	454,050,261	unknown function
HORVU3Hr1G059810	HC_G	3H	454,648,283	454,651,819	50S ribosomal protein L7/L12
HORVU3Hr1G059830	HC_G	3H	454,709,586	454,712,489	Iron-sulfur cluster assembly protein 1
HORVU3Hr1G059840	HC_G	3H	455,067,404	455,071,814	1,4-dihydroxy-2-naphthoyl-CoA synthase
HORVU3Hr1G059980	HC_G	3H	456,193,967	456,206,202	Cyclin family protein
HORVU3Hr1G059990	LC_TE	3H	456,194,431	456,203,020	Retrotransposon protein, putative, unclassified
HORVU3Hr1G060040	HC_G	3H	457,544,221	457,550,673	Pterin-4- α -carbinolamine dehydratase
HORVU3Hr1G060060	HC_G	3H	457,635,793	457,638,653	Mannan endo-1,4- β -mannosidase 1
HORVU3Hr1G060080	HC_U	3H	457,705,107	457,725,109	Kinase-related protein of unknown function (DUF1296)
HORVU3Hr1G060150	HC_G	3H	457,986,299	458,011,664	Carboxyl-terminal-processing protease
HORVU3Hr1G060220	LC_TE?	3H	458,363,058	458,376,618	ATP-dependent RNA helicase, putative
HORVU3Hr1G060290	HC_G	3H	458,581,457	458,586,776	Magnesium transporter CorA-like family protein
HORVU3Hr1G060390	HC_G	3H	460,310,395	460,316,427	mitogen-activated protein kinase 18
HORVU3Hr1G060410	LC_u	3H	460,315,493	460,316,135	undescribed protein
HORVU3Hr1G060430	HC_G	3H	460,556,342	460,562,698	CTD small phosphatase-like protein 2
HORVU3Hr1G060480	HC_G	3H	460,696,501	460,706,729	Bifunctional protein HldE
HORVU3Hr1G060500	HC_G	3H	460,762,240	460,768,227	WRKY DNA-binding protein 28
HORVU3Hr1G060570	HC_U	3H	461,387,020	461,388,031	unknown protein
HORVU3Hr1G060620	HC_G	3H	461,614,998	461,617,980	high mobility group B1
HORVU3Hr1G060640	HC_G	3H	461,625,275	461,715,159	Coiled-coil domain-containing protein 174
HORVU3Hr1G060720	HC_G	3H	461,802,887	461,804,879	Cytochrome b561 domain-containing protein
HORVU3Hr1G060730	HC_U	3H	461,805,212	461,806,944	unknown function
HORVU3Hr1G060780	HC_G	3H	463,228,096	463,238,155	Vacuolar protein sorting-associated protein 16 homolog

Appendix

Table A.4 continued

HORVU3Hr1G060800	HC_G	3H	463,293,949	463,295,719	60S ribosomal protein L18A-1
HORVU3Hr1G060960	LC_TE	3H	464,542,290	464,543,457	unknown function
HORVU3Hr1G061000	HC_G	3H	464,904,627	464,906,838	Ras-related protein Rab-25
HORVU3Hr1G061010	HC_G	3H	464,906,865	464,916,887	RING/U-box superfamily protein
HORVU3Hr1G061060	HC_G	3H	465,070,198	465,073,788	Splicing factor U2af small subunit B
HORVU3Hr1G061140	HC_G	3H	466,272,307	466,275,053	Queuine tRNA-ribosyltransferase
HORVU3Hr1G061190	HC_G	3H	466,704,614	466,707,325	Organic cation/carnitine transporter 4
HORVU3Hr1G061240	HC_G	3H	467,039,497	467,052,567	26S protease regulatory subunit 4 homolog
HORVU3Hr1G061400	HC_G	3H	467,088,836	467,091,961	Serine/threonine-protein kinase
HORVU3Hr1G061410	HC_G	3H	467,237,359	467,240,913	Serine/threonine-protein kinase
HORVU3Hr1G061470	HC_G	3H	467,888,483	467,891,073	Beta-1,3-galactosyltransferase 15
HORVU3Hr1G061560	HC_G	3H	468,266,163	468,274,680	NAC domain containing protein 73
HORVU3Hr1G061620	HC_G	3H	468,795,699	468,799,286	Pentatricopeptide repeat-containing protein
HORVU3Hr1G061630	LC_u	3H	468,798,300	468,799,470	undescribed protein
HORVU3Hr1G061690	HC_G	3H	469,768,135	469,772,099	Protein DEHYDRATION-INDUCED 19 homolog 3
HORVU3Hr1G061700	HC_G	3H	469,774,652	469,781,509	callose synthase 5
HORVU3Hr1G061750	HC_G	3H	470,317,876	470,329,068	Poly(A) RNA polymerase protein 2
HORVU3Hr1G061770	LC_U	3H	470,329,569	470,349,981	Chromosome 3B, cultivar Chinese Spring
HORVU3Hr1G061790	HC_G	3H	470,477,288	470,480,401	ubiquitin-conjugating enzyme 35
HORVU3Hr1G061800	HC_G	3H	470,539,593	470,583,534	Katanin p60 ATPase-containing subunit A-like 2
HORVU3Hr1G061850	HC_G	3H	470,811,385	470,820,244	RING/U-box superfamily protein
HORVU3Hr1G061950	HC_G	3H	472,717,190	472,723,894	pentatricopeptide repeat 336
HORVU3Hr1G061970	HC_G	3H	472,842,156	472,844,347	Ectonucleoside triphosphate diphosphohydrolase 4
HORVU3Hr1G061980	HC_G	3H	472,877,264	472,884,590	Receptor-like protein kinase 5
HORVU3Hr1G062030	HC_G	3H	473,170,069	473,175,037	ROP guanine nucleotide exchange factor 5
HORVU3Hr1G062040	HC_G	3H	473,172,169	473,175,042	Peroxiredoxin-2C
HORVU3Hr1G062130	HC_G	3H	474,423,476	474,428,164	Galactosylgalactosylxylosylp
HORVU3Hr1G062150	HC_G	3H	474,827,697	474,833,035	rotein 3-beta-glucuronosyltransferase 2
HORVU3Hr1G062160	HC_G	3H	474,827,701	474,830,632	NAC domain containing protein 2
HORVU3Hr1G062320	HC_U	3H	475,576,335	475,578,315	Auxin-responsive protein IAA5
HORVU3Hr1G062350	HC_G	3H	476,138,786	476,141,218	unknown function
					unknown protein

Appendix

Table A.4 continued

HORVU3Hr1G062370	HC_G	3H	476,380,758	476,388,549	Ubiquitin-conjugating enzyme family protein
HORVU3Hr1G062460	HC_G	3H	476,714,198	476,732,026	Two pore calcium channel protein 1
HORVU3Hr1G062470	HC_G	3H	476,991,168	476,994,816	Transcription factor-like protein DPB
HORVU3Hr1G062500	HC_G	3H	477,180,998	477,196,766	DNA-directed RNA polymerase III subunit RPC3
HORVU3Hr1G062510	HC_G	3H	477,189,428	477,196,766	Ribosomal protein L18e/L15 superfamily protein
HORVU3Hr1G062570	HC_G	3H	477,538,592	477,543,029	Eukaryotic aspartyl protease family protein
HORVU3Hr1G062590	HC_G	3H	477,737,855	477,739,885	60S ribosomal protein L37a
HORVU3Hr1G062620	HC_G	3H	477,765,260	477,771,440	YTH domain-containing family protein 2
HORVU3Hr1G062710	HC_G	3H	479,845,073	479,848,007	Transcription initiation factor TFIID subunit 11
HORVU3Hr1G062730	HC_TE?	3H	479,966,771	479,969,420	unknown function
HORVU3Hr1G062740	HC_U	3H	479,976,250	479,983,057	Protein of unknown function (DUF1639)
HORVU3Hr1G062750	LC_u	3H	479,981,171	479,982,088	undescribed protein
HORVU3Hr1G062890	HC_G	3H	481,143,734	481,147,139	Homeodomain-like superfamily protein
HORVU3Hr1G062950	LC_U	3H	481,477,980	481,482,046	unknown function
HORVU3Hr1G062970	HC_G	3H	481,649,627	481,658,031	Beclin-1-like protein
HORVU3Hr1G062980	HC_G	3H	481,654,902	481,661,297	Chromosome 3B, cultivar Chinese Spring
HORVU3Hr1G063050	HC_G	3H	482,165,393	482,176,766	glutamate synthase 2
HORVU3Hr1G063220	HC_G	3H	482,724,652	482,734,251	Splicing factor 3A subunit 3
HORVU3Hr1G063250	HC_G	3H	482,884,414	482,889,270	GPI transamidase component family protein / Gaa1-like family protein
HORVU3Hr1G063280	HC_G	3H	482,926,372	482,930,965	D-glycerate 3-kinase, chloroplastic
HORVU3Hr1G063300	HC_G	3H	483,294,229	483,300,059	Katanin p60 ATPase-containing subunit A1
HORVU3Hr1G063310	HC_u	3H	483,532,390	483,533,984	undescribed protein
HORVU3Hr1G063320	HC_G	3H	483,896,856	483,903,545	origin recognition complex subunit 4
HORVU3Hr1G063340	LC_u	3H	483,902,202	483,902,488	undescribed protein
HORVU3Hr1G063450	HC_G	3H	484,360,015	484,366,966	ASF1 like histone chaperone
HORVU3Hr1G063460	HC_G	3H	484,556,539	484,558,457	myb domain protein 36
HORVU3Hr1G063470	HC_G	3H	484,905,436	484,923,457	DNA LIGASE 6
HORVU3Hr1G063580	LC_TE?	3H	485,565,149	485,569,096	Pre-mRNA-splicing factor ATP-dependent RNA helicase PRP16
HORVU3Hr1G063630	HC_G	3H	485,950,089	485,951,352	N-terminal protein myristoylation
HORVU3Hr1G063680	HC_TE?	3H	486,903,528	486,908,477	RING/FYVE/PHD zinc finger superfamily protein
HORVU3Hr1G063690	HC_G	3H	486,905,451	486,913,155	Chromosome 3B, cultivar Chinese Spring
HORVU3Hr1G063700	LC_U	3H	487,066,193	487,074,573	Chromosome 3B, cultivar Chinese Spring

Appendix

Table A.4 continued

HORVU3Hr1G063710	HC_G	3H	487,257,411	487,261,483	Methionyl-tRNA formyltransferase
HORVU3Hr1G063720	HC_G	3H	487,310,257	487,317,106	Methionyl-tRNA formyltransferase
HORVU3Hr1G063730	HC_G	3H	487,310,261	487,316,859	Pco129446
HORVU3Hr1G063790	HC_G	3H	487,378,087	487,380,549	Methionyl-tRNA formyltransferase
HORVU3Hr1G063840	HC_G	3H	487,514,842	487,518,781	alpha/beta-Hydrolases superfamily protein
HORVU3Hr1G063850	LC_u	3H	487,516,871	487,517,418	undescribed protein
HORVU3Hr1G063860	HC_G	3H	487,521,134	487,529,379	Regulator of Vps4 activity in the MVB pathway protein
HORVU3Hr1G063900	LC_u	3H	487,526,559	487,527,555	undescribed protein
HORVU3Hr1G064040	HC_U	3H	489,113,573	489,115,813	Chromosome 3B, genomic scaffold, cultivar Chinese Spring
HORVU3Hr1G064050	LC_u	3H	489,114,323	489,114,997	undescribed protein
HORVU3Hr1G064070	HC_U	3H	489,393,734	489,396,105	Protein of unknown function (DUF1639)
HORVU3Hr1G064080	HC_TE?	3H	489,630,358	489,643,914	zinc finger protein-related
HORVU3Hr1G064110	HC_G	3H	489,987,777	490,003,929	Receptor-like protein kinase- like
HORVU3Hr1G064120	HC_G	3H	489,987,828	490,006,022	Alpha/beta hydrolase domain-containing protein 13
HORVU3Hr1G064130	HC_G	3H	490,134,505	490,244,622	Chromosome 3B, cultivar Chinese Spring
HORVU3Hr1G064180	HC_G	3H	490,222,327	490,226,751	Protein kinase superfamily protein
HORVU3Hr1G064190	HC_TE?	3H	490,224,965	490,228,637	Zinc finger MYM-type protein
HORVU3Hr1G064200	HC_G	3H	490,244,656	490,248,080	receptor-like protein kinase 4
HORVU3Hr1G064230	HC_G	3H	490,250,334	490,258,624	Nucleotidyl transferase superfamily protein
HORVU3Hr1G064240	HC_G	3H	490,251,881	490,254,637	Reticulon family protein
HORVU3Hr1G064290	HC_G	3H	490,788,416	490,795,983	serine/threonine protein phosphatase 2A
HORVU3Hr1G064300	HC_TE?	3H	490,796,655	490,805,716	TFIIH basal transcription factor complex helicase XPB subunit
HORVU3Hr1G064320	HC_G	3H	491,037,145	491,038,491	Glutathione S-transferase family protein
HORVU3Hr1G064330	LC_U	3H	491,037,152	491,037,818	unknown function
HORVU3Hr1G064340	HC_G	3H	491,084,331	491,087,583	Protein PLASTID MOVEMENT IMPAIRED 2
HORVU3Hr1G064370	HC_G	3H	491,370,347	491,374,436	RING/U-box superfamily protein
HORVU3Hr1G064390	HC_G	3H	491,376,493	491,383,628	Alpha/beta fold hydrolase
HORVU3Hr1G064410	HC_G	3H	491,428,834	491,434,720	Clathrin assembly protein
HORVU3Hr1G064420	HC_G	3H	491,486,104	491,487,212	hydroxyproline-rich glycoprotein family protein
HORVU3Hr1G064450	HC_G	3H	491,848,618	491,851,335	lipid phosphate phosphatase 2
HORVU3Hr1G064460	LC_u	3H	491,850,523	491,851,103	undescribed protein
HORVU3Hr1G064470	HC_G	3H	491,894,156	491,895,847	Chitinase family protein

Appendix

Tale A.4 continued

HORVU3Hr1G064550	HC_G	3H	492,772,813	492,777,682	Serine/arginine-rich splicing factor 1
HORVU3Hr1G064560	LC_u	3H	492,772,986	492,774,153	undescribed protein

^a The predicted genes and their respective annotations were obtained from BARLEYMAP (Cantalapiedra et al. 2015)

^b HC_G high confidence gene with predicted function, HC_U high confidence gene without predicted function, LC_u low-confidence gene without predicted function

Table A.5 Predicted genes located on chromosomes 3H at 621 Mbp and their respective functional annotations.

Gene ID ^a	Gene class ^b	Chr	Physical location [bp]		Annotation
HORVU3Hr1G087380	HC_G	3H	621,112,310	621,113,950	30S ribosomal protein S12
HORVU3Hr1G087390	HC_G	3H	621,114,775	621,118,012	Nuclear transcription factor Y subunit B
AGL39456.1	ncbi	3H	621,115,147	621,116,788	NF-YB1

^a The predicted genes and their respective annotations were obtained from BARLEYMAP (Cantalapiedra et al. 2015)

^b HC_G high confidence gene with predicted function, HC_U high confidence gene without predicted function, LC_u low-confidence gene without predicted function

Table A.6 Predicted genes located on chromosomes 4H at 33-70 Mbp and at 352 Mbp and their respective functional annotations.

Gene ID ^a	Gene class ^b	Chr	Physical location [bp]		Annotation
HORVU4Hr1G010910	HC_G	4H	33,034,985	33,040,285	Transducin family protein / WD-40 repeat family protein
HORVU4Hr1G010940	HC_G	4H	33,365,816	33,368,037	Eukaryotic translation initiation factor 3 subunit G
HORVU4Hr1G010970	HC_G	4H	33,375,678	33,377,992	Pentatricopeptide repeat-containing protein
HORVU4Hr1G010980	HC_TE?	4H	33,378,648	33,381,751	CHY-type/CTCHY-type/RING-type Zinc finger protein
HORVU4Hr1G011020	HC_G	4H	33,501,236	33,505,267	Alba DNA/RNA-binding protein
HORVU4Hr1G011040	HC_U	4H	33,659,188	33,661,446	Plant protein of unknown function (DUF247)
HORVU4Hr1G011060	HC_G	4H	33,734,316	33,739,796	zinc induced facilitator-like 1
HORVU4Hr1G011090	HC_G	4H	33,845,151	33,847,975	ATP synthase delta-subunit gene
HORVU4Hr1G011100	HC_G	4H	33,845,639	33,848,016	GRAM domain-containing protein / ABA-responsive protein-related
HORVU4Hr1G011110	HC_G	4H	33,860,747	33,863,194	glycerol-3-phosphate acyltransferase 6
HORVU4Hr1G011120	HC_U	4H	33,946,411	33,950,658	unknown function
HORVU4Hr1G011160	HC_G	4H	33,953,501	33,958,081	Endoglucanase 10
HORVU4Hr1G011170	HC_G	4H	33,954,343	33,967,727	Pentatricopeptide repeat-containing protein
HORVU4Hr1G015950	LC_TE	4H	64,200,347	64,252,218	Transposon Ty1-BR Gag-Pol polyprotein
HORVU4Hr1G016000	LC_TE?	4H	64,212,768	64,213,579	Glucan endo-1,3-beta-glucosidase 14

Appendix

Table A.6 continued

HORVU4Hr1G016010	HC_G	4H	64,247,694	64,252,294	Disease resistance protein
HORVU4Hr1G016160	HC_G	4H	65,195,751	65,201,030	Auxin-responsive protein IAA27
HORVU4Hr1G016180	LC_u	4H	65,200,714	65,201,048	undescribed protein
HORVU4Hr1G016200	HC_G	4H	65,346,751	65,353,640	ATP-dependent zinc metalloprotease FtsH
HORVU4Hr1G016210	HC_G	4H	65,649,263	65,650,382	unknown function
HORVU4Hr1G016260	HC_G	4H	66,255,311	66,265,148	ATP-dependent protease La (LON) domain protein
HORVU4Hr1G016350	HC_G	4H	66,861,420	66,864,859	DNA-directed RNA polymerases II, IV and V subunit 11
HORVU4Hr1G016400	HC_G	4H	67,308,884	67,331,805	mRNA capping enzyme family protein
HORVU4Hr1G016410	HC_G	4H	67,332,377	67,336,900	Methylthioribose-1-phosphate isomerase
HORVU4Hr1G016430	LC_u	4H	67,413,846	67,415,439	undescribed protein
HORVU4Hr1G016440	HC_G	4H	67,512,572	67,517,399	Multiple organellar RNA editing factor 1, mitochondrial
HORVU4Hr1G016470	HC_G	4H	68,264,236	68,273,338	Protein kinase superfamily protein
HORVU4Hr1G016500	HC_G	4H	68,389,078	68,390,101	tapetum determinant 1
HORVU4Hr1G016510	HC_G	4H	68,421,004	68,425,862	Chaperone protein DnaJ
HORVU4Hr1G016520	HC_G	4H	68,421,046	68,429,324	Pyruvate kinase family protein
HORVU4Hr1G016620	HC_G	4H	69,299,031	69,304,742	Ubiquitin-like-specific protease 1D
HORVU4Hr1G016640	HC_G	4H	69,379,505	69,383,521	Protein transport protein Sec24-like
HORVU4Hr1G016730	HC_G	4H	70,428,911	70,434,990	Carboxypeptidase Y
HORVU4Hr1G016770	HC_G	4H	70,810,518	70,813,853	alcohol dehydrogenase 1
HORVU4Hr1G016810	HC_G	4H	70,912,804	70,929,994	alcohol dehydrogenase 1
HORVU4Hr1G044140	HC_G	4H	352,904,030	352,906,956	Processive diacylglycerol beta-glucosyltransferase

^a The predicted genes and their respective annotations were obtained from BARLEYMAP (Cantalapiedra et al. 2015)

^b HC_G high confidence gene with predicted function, HC_U high confidence gene without predicted function, LC_u low-confidence gene without predicted function

Table A.7 Predicted genes located on chromosomes 5H at 579 Mbp and at 634 Mbp and their respective functional annotations.

Gene ID ^a	Gene class ^b	Chr	Physical location [bp]		Annotation
HORVU5Hr1G087690	HC_G	5H	579,066,160	579,069,438	Protein kinase superfamily protein
HORVU5Hr1G110970	LC_TE?	5H	634,732,673	634,736,696	F-box protein PP2-A13

^a The predicted genes and their respective annotations were obtained from BARLEYMAP (Cantalapiedra et al. 2015)

^b HC_G high confidence gene with predicted function, HC_U high confidence gene without predicted function, LC_u low-confidence gene without predicted function

Appendix

Table A.8 Predicted genes located on chromosomes 6H at 37-74 Mbp and their respective functional annotations.

Gene ID ^a	Gene class ^b	Chr	Physical location [bp]		Annotation
HORVU6Hr1G016590	LC_u	6H	37,570,783	37,572,032	undescribed protein
HORVU6Hr1G016600	LC_u	6H	37,570,785	37,571,989	undescribed protein
HORVU6Hr1G016610	HC_G	6H	37,673,566	37,712,468	unknown function
HORVU6Hr1G016700	HC_TE?	6H	37,776,360	37,780,060	Chromosome 3B, cultivar Chinese Spring
HORVU6Hr1G016710	HC_G	6H	37,818,242	37,819,918	Leucine-rich repeat receptor-like protein kinase family protein
HORVU6Hr1G016750	HC_G	6H	38,138,862	38,155,102	Endoglucanase 11
HORVU6Hr1G016810	HC_G	6H	38,242,530	38,247,432	anthranilate phosphoribosyltransferase, putative
HORVU6Hr1G016860	LC_u	6H	38,406,437	38,409,057	undescribed protein
HORVU6Hr1G016940	HC_G	6H	38,571,660	38,575,557	Chlorophyll a-b binding protein, chloroplastic
HORVU6Hr1G016980	HC_G	6H	39,064,977	39,066,288	NAC domain containing protein 46
HORVU6Hr1G017000	HC_G	6H	39,218,173	39,220,987	Pyruvate dehydrogenase E1 component subunit beta
HORVU6Hr1G017020	LC_u	6H	39,431,245	39,443,368	undescribed protein
HORVU6Hr1G017030	LC_u	6H	39,431,344	39,435,095	undescribed protein
HORVU6Hr1G017040	LC_u	6H	39,466,381	39,467,270	undescribed protein
HORVU6Hr1G017050	LC_u	6H	39,467,461	39,471,388	undescribed protein
HORVU6Hr1G017060	LC_u	6H	39,467,464	39,471,495	undescribed protein
HORVU6Hr1G017080	HC_G	6H	39,690,170	39,696,697	Pentatricopeptide repeat-containing protein
HORVU6Hr1G017100	HC_U	6H	39,761,654	39,767,122	Uncharacterised conserved protein (UCP030365)
HORVU6Hr1G017220	HC_G	6H	40,408,681	40,420,893	P-loop containing nucleoside triphosphate hydrolases superfamily protein
HORVU6Hr1G017270	LC_u	6H	40,455,237	40,457,287	undescribed protein
HORVU6Hr1G017280	LC_u	6H	40,455,292	40,457,287	undescribed protein
HORVU6Hr1G017340	HC_G	6H	40,873,990	40,882,404	BRCT domain-containing protein
HORVU6Hr1G017370	HC_U	6H	41,033,121	41,036,229	unknown function
HORVU6Hr1G017390	HC_G	6H	41,136,972	41,139,753	4-phosphopantetheine adenylyltransferase
HORVU6Hr1G017440	LC_u	6H	41,151,892	41,157,195	undescribed protein
HORVU6Hr1G017480	HC_G	6H	41,293,323	41,298,409	Transmembrane protein 53
HORVU6Hr1G017500	HC_G	6H	41,299,028	41,302,263	Proteasome subunit alpha type-1
HORVU6Hr1G017570	HC_G	6H	41,706,341	41,712,129	Sec14p-like phosphatidylinositol transfer family protein
HORVU6Hr1G017590	HC_G	6H	41,763,797	41,768,997	Protoheme IX farnesyltransferase
HORVU6Hr1G017620	HC_G	6H	41,917,497	41,920,546	F-box/LRR-repeat protein 14
HORVU6Hr1G017670	LC_u	6H	42,336,913	42,343,099	undescribed protein
HORVU6Hr1G017680	HC_G	6H	42,338,523	42,350,309	E3 ubiquitin-protein ligase MARCH8
HORVU6Hr1G017700	LC_u	6H	42,367,710	42,371,944	undescribed protein
HORVU6Hr1G017710	HC_u	6H	42,378,405	42,380,249	undescribed protein

Appendix

Table A.8 continued

HORVU6Hr1G017720	HC_G	6H	42,541,276	42,573,258	pentatricopeptide repeat 336
HORVU6Hr1G017850	HC_G	6H	43,318,375	43,321,786	CASP-like protein 4A2
HORVU6Hr1G017860	HC_G	6H	43,352,934	43,363,219	L-aspartate oxidase
HORVU6Hr1G017870	HC_G	6H	43,355,845	43,365,934	pentatricopeptide repeat 336
HORVU6Hr1G017900	HC_G	6H	43,584,600	43,594,461	Synaptotagmin-5
HORVU6Hr1G017920	HC_G	6H	43,736,669	44,019,971	chloride channel B
HORVU6Hr1G018030	HC_TE?	6H	44,178,474	44,182,431	Chromosome 3B, cultivar Chinese Spring
HORVU6Hr1G018050	HC_G	6H	44,243,132	44,248,596	Esterase/lipase/thioesterase family protein
HORVU6Hr1G018060	HC_G	6H	44,278,176	44,282,939	Protein kinase superfamily protein
HORVU6Hr1G018070	HC_G	6H	44,280,074	44,296,135	Zinc transporter 2
HORVU6Hr1G018090	HC_u	6H	44,534,875	44,537,763	undescribed protein
HORVU6Hr1G018150	HC_G	6H	44,783,157	44,786,871	BURP domain-containing protein 4
HORVU6Hr1G018160	HC_G	6H	45,201,262	45,204,098	Subtilisin-like protease
HORVU6Hr1G018280	HC_G	6H	45,740,054	45,742,230	Signal recognition particle protein
HORVU6Hr1G018330	HC_G	6H	46,298,799	46,306,137	DNA polymerase V family
HORVU6Hr1G018340	LC_U	6H	46,305,744	46,309,505	unknown function
HORVU6Hr1G018410	LC_u	6H	46,515,995	46,516,494	undescribed protein
HORVU6Hr1G018420	HC_G	6H	46,538,711	46,542,489	calnexin 1
HORVU6Hr1G018460	LC_TE	6H	46,930,826	46,947,121	unknown function
HORVU6Hr1G018480	HC_G	6H	47,259,651	47,263,375	unknown function
HORVU6Hr1G018500	HC_G	6H	47,266,223	47,273,978	5'-AMP-activated protein kinase-related
HORVU6Hr1G018510	HC_G	6H	47,266,293	47,273,984	Plant regulator RWP-RK family protein
HORVU6Hr1G018520	HC_G	6H	47,359,727	47,366,647	Prolyl endopeptidase
HORVU6Hr1G018530	HC_U	6H	47,369,617	47,373,389	unknown protein
HORVU6Hr1G018600	HC_G	6H	47,513,054	47,519,115	kinesin-like protein 1
HORVU6Hr1G018610	HC_G	6H	47,627,027	47,629,896	Protein FLUORESCENT IN BLUE LIGHT, chloroplastic
HORVU6Hr1G018710	HC_G	6H	48,053,907	48,059,055	unknown function
HORVU6Hr1G018740	HC_TE?	6H	48,209,759	48,212,903	F-box domain containing protein
HORVU6Hr1G018760	LC_u	6H	48,592,502	48,593,615	undescribed protein
HORVU6Hr1G018770	HC_U	6H	48,592,558	48,598,170	Plant protein 1589 of unknown function
HORVU6Hr1G018790	HC_G	6H	48,641,559	48,654,549	Transducin family protein / WD-40 repeat family protein
HORVU6Hr1G018810	HC_G	6H	48,709,146	48,710,618	unknown function
HORVU6Hr1G018890	HC_G	6H	49,428,968	49,433,401	Ectonucleoside triphosphate diphosphohydrolase 1
HORVU6Hr1G018920	HC_G	6H	49,541,658	49,544,373	Disease resistance protein
HORVU6Hr1G018960	HC_G	6H	49,777,455	49,792,561	Disease resistance protein
HORVU6Hr1G019080	HC_G	6H	50,166,476	50,175,300	ABC transporter G family member 36
HORVU6Hr1G019130	HC_G	6H	50,346,680	50,352,247	Splicing factor 3B subunit 3
HORVU6Hr1G019170	LC_u	6H	50,782,521	50,783,024	undescribed protein
HORVU6Hr1G019190	HC_G	6H	50,788,664	50,801,649	Histone acetyltransferase HAC12
HORVU6Hr1G019230	HC_G	6H	50,943,212	50,950,053	Ribosomal RNA small subunit methyltransferase H

Appendix

Table A.8 continued

HORVU6Hr1G019240	LC_u	6H	50,943,570	50,944,136	undescribed protein
HORVU6Hr1G019280	HC_G	6H	51,403,982	51,411,556	Tetratricopeptide repeat (TPR)-like superfamily protein
HORVU6Hr1G019300	HC_G	6H	51,816,998	51,827,137	Delta-aminolevulinic acid dehydratase
HORVU6Hr1G019320	HC_G	6H	52,051,618	52,053,510	pentatricopeptide repeat 336
HORVU6Hr1G019510	HC_G	6H	53,102,840	53,106,956	calmodulin-binding family protein
HORVU6Hr1G019930	HC_G	6H	55,137,978	55,142,780	Protein kinase superfamily protein
HORVU6Hr1G020120	HC_G	6H	55,787,019	55,796,014	Subtilisin-like protease
HORVU6Hr1G020140	HC_G	6H	55,807,794	55,811,551	ubiquitin 11
HORVU6Hr1G020210	HC_G	6H	55,997,579	56,000,034	receptor kinase 3
HORVU6Hr1G020220	HC_G	6H	56,115,879	56,118,047	Chromosome 3B, cultivar Chinese Spring
HORVU6Hr1G020230	LC_u	6H	56,162,219	56,242,273	undescribed protein
HORVU6Hr1G020310	HC_G	6H	56,936,938	56,940,517	2,3-bisphosphoglycerate-dependent phosphoglycerate mutase
HORVU6Hr1G020330	HC_G	6H	56,978,027	56,988,192	auxin response factor 19
HORVU6Hr1G020380	HC_G	6H	57,291,641	57,300,927	Galactokinase
HORVU6Hr1G020400	HC_G	6H	57,483,469	57,492,342	CAAX amino terminal protease family protein
HORVU6Hr1G020420	HC_G	6H	57,820,194	57,839,311	Nuclear pore complex protein NUP160
HORVU6Hr1G020570	HC_TE?	6H	58,731,625	58,738,221	ATP-dependent RNA helicase DeaD
HORVU6Hr1G020580	LC_u	6H	58,731,692	58,732,934	undescribed protein
HORVU6Hr1G020600	HC_G	6H	58,810,893	58,814,136	Acyl-coenzyme A oxidase 2
HORVU6Hr1G020680	LC_TE	6H	59,069,441	59,073,945	Zinc finger BED domain-containing protein RICESLEEPER 2
HORVU6Hr1G020720	HC_G	6H	59,555,539	59,559,020	purple acid phosphatase 18
HORVU6Hr1G020790	HC_G	6H	60,181,991	60,188,824	Protein EFR3 homolog B
HORVU6Hr1G020820	HC_G	6H	60,465,739	60,472,251	DNA/RNA-binding protein KIN17
HORVU6Hr1G020850	HC_G	6H	60,815,668	60,821,608	Splicing factor 3B subunit 1
HORVU6Hr1G020880	LC_TE?	6H	60,835,556	60,838,217	unknown function
HORVU6Hr1G020910	HC_TE?	6H	61,014,054	61,018,527	ATP-dependent RNA helicase eIF4A
HORVU6Hr1G020960	HC_G	6H	61,216,573	61,218,634	UDP-Glycosyltransferase superfamily protein
HORVU6Hr1G020970	LC_U	6H	61,309,401	61,311,884	unknown function
HORVU6Hr1G020980	HC_G	6H	61,309,520	61,317,032	Polynucleotide 5'-hydroxyl-kinase NOL9
HORVU6Hr1G021020	HC_G	6H	61,352,928	61,360,430	26S proteasome regulatory subunit S2 1A
HORVU6Hr1G021040	HC_G	6H	61,368,296	61,372,366	auxin signaling F-box 3
HORVU6Hr1G021050	LC_U	6H	61,431,408	61,434,175	unknown function
HORVU6Hr1G021150	HC_G	6H	61,736,740	61,742,738	Kinetochore protein NUF2
HORVU6Hr1G021170	HC_G	6H	61,758,669	61,764,048	DNA-binding protein BIN4
HORVU6Hr1G021260	HC_G	6H	63,082,575	63,333,071	histone H2A 6
HORVU6Hr1G021320	HC_G	6H	64,007,359	64,016,549	Lipid A export ATP-binding/permease protein MsbA

Appendix

Table A.8 continued

HORVU6Hr1G021340	HC_G	6H	64,214,424	64,223,510	pathogenesis related homeodomain protein A
HORVU6Hr1G021450	LC_TE?	6H	64,623,901	64,637,830	DNA/RNA helicase protein
HORVU6Hr1G021460	HC_G	6H	64,743,116	64,747,390	Zinc finger protein CONSTANS-LIKE 7
HORVU6Hr1G021520	HC_G	6H	65,256,521	65,259,501	Peroxidase superfamily protein
HORVU6Hr1G021550	HC_U	6H	65,592,126	65,602,913	BnaA01g34800D protein
HORVU6Hr1G021570	HC_G	6H	66,009,913	66,013,732	GATA transcription factor 17
HORVU6Hr1G021610	HC_G	6H	66,186,638	66,189,914	4/1 protein short form
HORVU6Hr1G021620	HC_G	6H	66,191,452	66,196,574	Serrate RNA effector molecule
HORVU6Hr1G021630	HC_G	6H	66,484,961	66,488,498	Eukaryotic translation initiation factor 5
HORVU6Hr1G021650	HC_G	6H	67,050,979	67,052,153	Sec14p-like phosphatidylinositol transfer family protein
HORVU6Hr1G021670	HC_G	6H	67,131,227	67,138,591	Aleurone layer morphogenesis protein
HORVU6Hr1G021690	HC_G	6H	67,344,422	67,346,958	exocyst subunit exo70 family protein G1
HORVU6Hr1G021730	HC_G	6H	67,386,980	67,387,900	OTU-like cysteine protease family protein, putative, expressed
HORVU6Hr1G021750	HC_G	6H	67,703,547	67,706,602	Protein phosphatase 2C family protein
HORVU6Hr1G021780	HC_G	6H	67,713,930	67,718,653	Disease resistance protein
HORVU6Hr1G021920	HC_G	6H	68,136,350	68,138,879	tRNA modification GTPase MnmE
HORVU6Hr1G022180	LC_u	6H	69,634,390	69,634,877	undescribed protein
HORVU6Hr1G022220	HC_G	6H	69,831,033	69,834,896	Diaminopimelate decarboxylase
HORVU6Hr1G022270	HC_G	6H	70,238,436	70,243,944	Endoglucanase 5
HORVU6Hr1G022330	HC_G	6H	70,576,254	70,582,507	Adagio-like protein 1
HORVU6Hr1G022340	HC_TE?	6H	70,582,694	70,586,344	Protein of unknown function (DUF1644)
HORVU6Hr1G022360	HC_G	6H	70,645,069	70,652,474	protein kinase family protein
HORVU6Hr1G022370	HC_G	6H	70,907,608	70,913,391	RING/U-box superfamily protein
HORVU6Hr1G022480	LC_u	6H	71,733,176	71,755,554	undescribed protein
HORVU6Hr1G022500	HC_G	6H	71,744,568	71,747,330	BTB/POZ domain-containing protein
HORVU6Hr1G022510	LC_u	6H	71,744,618	71,747,207	undescribed protein
HORVU6Hr1G022570	HC_G	6H	71,970,183	71,976,558	Protein kinase superfamily protein
HORVU6Hr1G022580	HC_G	6H	72,037,607	72,039,602	Electron transfer flavoprotein subunit alpha
HORVU6Hr1G022680	HC_G	6H	72,704,084	72,705,374	Late embryogenesis abundant (LEA) hydroxyproline-rich glycoprotein family
HORVU6Hr1G022690	LC_TE	6H	72,705,942	72,708,283	Integrase-type DNA-binding superfamily protein
HORVU6Hr1G022770	HC_G	6H	72,968,401	72,973,495	Protein VERNALIZATION INSENSITIVE 3
HORVU6Hr1G023100	HC_G	6H	74,453,579	74,491,625	receptor-like protein kinase 1

^a The predicted genes and their respective annotations were obtained from BARLEYMAP (Cantalapiedra et al. 2015)

^b HC_G high confidence gene with predicted function, HC_U high confidence gene without predicted function, LC_u low-confidence gene without predicted function

Appendix

Table A.9 Predicted genes located on chromosomes 6H at 123-344 Mbp and their respective functional annotations.

Gene ID ^a	Gene class ^b	Chr	Physical location [bp]		Annotation
HORVU6Hr1G029840	LC_u	6H	123,046,351	123,048,900	undescribed protein
HORVU6Hr1G029850	LC_u	6H	123,190,429	123,193,892	undescribed protein
HORVU6Hr1G029860	LC_u	6H	123,190,438	123,193,896	undescribed protein
HORVU6Hr1G029880	HC_G	6H	123,561,863	123,588,687	DNA-directed RNA polymerase family protein
HORVU6Hr1G029930	HC_G	6H	123,757,017	123,759,582	Protein CYP4
HORVU6Hr1G030000	HC_G	6H	123,871,388	123,873,835	Protein transport protein Sec61 subunit gamma
HORVU6Hr1G030140	HC_G	6H	124,983,916	124,992,158	Glycerol kinase
HORVU6Hr1G030150	HC_G	6H	124,983,933	124,992,048	serine/threonine protein kinase 1
HORVU6Hr1G030180	LC_u	6H	125,172,695	125,177,798	undescribed protein
HORVU6Hr1G030190	LC_TE?	6H	125,172,700	125,177,806	Zinc finger MYM-type protein 5
HORVU6Hr1G030270	HC_G	6H	125,731,730	125,739,064	Calmodulin-binding protein
HORVU6Hr1G030310	HC_G	6H	125,740,538	125,753,711	CASP-like protein
HORVU6Hr1G030340	LC_u	6H	125,752,716	125,753,716	undescribed protein
HORVU6Hr1G030390	HC_G	6H	126,211,480	126,217,428	4-coumarate:CoA ligase 1
HORVU6Hr1G030590	HC_G	6H	128,364,135	128,427,106	calcium-transporting ATPase, putative
HORVU6Hr1G030600	HC_G	6H	128,976,797	128,985,368	Regulator of chromosome condensation (RCC1) family protein
HORVU6Hr1G030690	LC_u	6H	129,177,207	129,183,177	undescribed protein
HORVU6Hr1G030780	HC_TE?	6H	129,590,069	129,593,798	F-box family protein
HORVU6Hr1G030800	HC_G	6H	129,836,908	129,838,797	Transmembrane protein 230
HORVU6Hr1G030880	HC_G	6H	130,232,824	130,240,252	Receptor-like protein kinase 5
HORVU6Hr1G030990	HC_G	6H	130,981,717	130,988,856	Core-2/I-branching beta-1,6-N-acetylglucosaminyltransferase family protein
HORVU6Hr1G031080	HC_G	6H	131,357,502	131,402,773	3beta-hydroxysteroid-dehydrogenase/decarboxylase isoform 1
HORVU6Hr1G031110	LC_u	6H	131,370,965	131,371,755	undescribed protein
HORVU6Hr1G031200	HC_G	6H	131,470,904	131,488,669	glucan synthase-like 4
HORVU6Hr1G031230	HC_G	6H	131,686,357	131,708,107	callose synthase 1
HORVU6Hr1G031330	HC_G	6H	132,098,828	132,101,303	Basic-leucine zipper (bZIP) transcription factor family protein
HORVU6Hr1G031370	HC_G	6H	132,298,367	132,308,405	Calcineurin-like metallo-phosphoesterase superfamily protein
HORVU6Hr1G031440	HC_G	6H	133,165,442	133,168,534	Protein kinase superfamily protein
HORVU6Hr1G031450	HC_G	6H	133,169,150	133,173,306	squamosa promoter binding protein-like 2
HORVU6Hr1G031480	HC_G	6H	133,923,890	133,933,249	Aldehyde dehydrogenase family 2 member C4
HORVU6Hr1G031520	HC_G	6H	134,060,662	134,068,268	Ribosomal RNA large subunit methyltransferase I
HORVU6Hr1G031530	HC_G	6H	134,063,087	134,068,659	Cell cycle control protein 50A

Appendix

Table A.9 continued

HORVU6Hr1G031550	HC_G	6H	134,080,947	134,093,670	Disease resistance protein
HORVU6Hr1G031600	HC_G	6H	134,411,844	134,416,896	receptor-like protein kinase 2
HORVU6Hr1G031610	HC_G	6H	134,748,518	134,751,978	Urease accessory protein UreD
HORVU6Hr1G031650	HC_G	6H	135,372,894	135,379,576	Cytochrome P450 superfamily protein
HORVU6Hr1G031750	LC_U	6H	136,464,714	136,484,004	Plant protein of unknown function (DUF247)
HORVU6Hr1G031830	HC_G	6H	136,923,800	136,927,448	phosphoglycerate kinase
HORVU6Hr1G031850	LC_u	6H	137,377,542	137,384,111	undescribed protein
HORVU6Hr1G031920	HC_G	6H	137,590,678	137,595,370	50S ribosomal protein L14
HORVU6Hr1G031960	HC_G	6H	137,850,548	137,856,341	Copper-transporting ATPase 2
HORVU6Hr1G032070	HC_G	6H	138,553,867	138,559,578	glyceraldehyde-3-phosphate dehydrogenase C2
HORVU6Hr1G032150	LC_U	6H	139,453,549	139,456,411	unknown function
HORVU6Hr1G032200	HC_G	6H	139,749,583	139,755,576	Nuclear transcription factor Y subunit C-2
HORVU6Hr1G032270	HC_G	6H	140,840,171	140,847,599	Pentatricopeptide repeat-containing protein
HORVU6Hr1G032400	HC_G	6H	141,736,694	141,753,366	rRNA N-glycosidase
HORVU6Hr1G032490	HC_G	6H	142,400,821	142,402,935	Glucan endo-1,3-beta-glucosidase 14
HORVU6Hr1G032510	HC_G	6H	142,508,498	142,514,885	SEC14 cytosolic factor
HORVU6Hr1G032570	HC_G	6H	143,256,473	143,261,264	26S protease regulatory subunit 8
HORVU6Hr1G032610	HC_G	6H	143,703,137	143,712,206	actin-related protein 4
HORVU6Hr1G032630	LC_u	6H	143,704,138	143,704,920	undescribed protein
HORVU6Hr1G032680	HC_G	6H	144,014,447	144,018,437	FKBP-like peptidyl-prolyl cis-trans isomerase family protein
HORVU6Hr1G032690	HC_u	6H	144,014,493	144,018,437	undescribed protein
HORVU6Hr1G032770	HC_G	6H	144,672,084	144,677,900	Subtilisin-like protease
HORVU6Hr1G032790	LC_TE	6H	144,738,900	144,739,721	Transposon protein, putative, Mariner sub-class
HORVU6Hr1G032800	HC_G	6H	145,009,197	145,015,294	DNA damage-inducible protein 1
HORVU6Hr1G032840	HC_G	6H	145,770,320	145,773,842	Transcription initiation factor TFIID subunit A
HORVU6Hr1G032920	LC_u	6H	146,115,221	146,134,193	undescribed protein
HORVU6Hr1G032930	HC_U	6H	146,370,366	146,374,003	unknown protein
HORVU6Hr1G032940	HC_G	6H	146,581,719	146,584,641	ADP-ribosylation factor GTPase-activating protein 1
HORVU6Hr1G032960	HC_G	6H	146,603,312	146,607,205	Calcium-binding protein 4
HORVU6Hr1G033000	LC_u	6H	147,869,541	147,878,563	undescribed protein
HORVU6Hr1G033060	HC_G	6H	148,634,736	148,641,484	alpha/beta-Hydrolases superfamily protein
HORVU6Hr1G033070	HC_G	6H	148,640,914	148,649,196	alpha/beta-Hydrolases superfamily protein
HORVU6Hr1G033150	LC_u	6H	149,601,845	149,605,573	undescribed protein
HORVU6Hr1G033160	HC_G	6H	149,856,196	149,868,725	chlorophyll A/B binding protein 3
HORVU6Hr1G033170	LC_u	6H	149,858,578	149,859,544	undescribed protein
HORVU6Hr1G033180	LC_u	6H	149,859,626	149,861,590	undescribed protein
HORVU6Hr1G033200	HC_G	6H	150,130,273	150,133,211	Regulator of chromosome condensation (RCC1) family protein
HORVU6Hr1G033210	LC_U	6H	150,490,617	150,491,339	unknown function

Appendix

Table A.9 continued

HORVU6Hr1G033280	HC_G	6H	151,045,446	151,050,318	GRAS family transcription factor
HORVU6Hr1G033290	HC_G	6H	151,122,430	151,129,124	MLO-like protein 1
HORVU6Hr1G033310	HC_G	6H	151,493,024	151,497,957	BEST Arabidopsis thaliana protein match is: TPX2 (targeting protein for Xklp2) protein family
HORVU6Hr1G033320	HC_G	6H	151,591,309	151,599,611	3-oxoacyl-[acyl-carrier-protein] synthase 2
HORVU6Hr1G033350	HC_G	6H	151,844,423	151,850,686	fumarylacetoacetase, putative
HORVU6Hr1G033380	HC_G	6H	151,875,761	151,881,885	Copper-transporting ATPase 1
HORVU6Hr1G033420	HC_G	6H	152,357,561	152,364,886	Zinc transporter ZupT
HORVU6Hr1G033430	HC_G	6H	152,360,805	152,371,719	Outer envelope protein 80, chloroplastic
HORVU6Hr1G033490	HC_G	6H	153,218,179	153,237,647	T-complex protein 11
HORVU6Hr1G033540	HC_G	6H	153,412,332	153,418,308	Putative glycosyl hydrolase of unknown function (DUF1680)
HORVU6Hr1G033550	LC_TE?	6H	153,418,362	153,489,254	Zinc finger A20 and AN1 domain-containing stress-associated protein 4
HORVU6Hr1G033630	HC_G	6H	154,896,919	154,905,352	Glucose-1-phosphate adenyltransferase family protein
HORVU6Hr1G033670	HC_G	6H	155,477,941	155,487,662	receptor-like protein kinase 2
HORVU6Hr1G033690	HC_U	6H	155,694,068	155,704,922	unknown protein
HORVU6Hr1G033750	HC_G	6H	155,946,837	155,951,409	Non-structural maintenance of chromosomes element 4 homolog A
HORVU6Hr1G033930	HC_G	6H	156,757,372	156,759,984	Phosphoethanolamine N-methyltransferase 1
HORVU6Hr1G033970	HC_G	6H	156,947,809	156,950,890	glycerol dehydrogenase
HORVU6Hr1G033980	HC_G	6H	156,951,444	156,958,616	Citrate synthase family protein
HORVU6Hr1G034030	HC_G	6H	157,298,248	157,301,181	Integral membrane HRF1 family protein
HORVU6Hr1G034070	HC_G	6H	157,614,488	157,620,275	SWI/SNF complex subunit SWI3B
HORVU6Hr1G034130	HC_G	6H	158,180,327	158,192,604	Brefeldin A-inhibited guanine nucleotide-exchange protein 1
HORVU6Hr1G034140	HC_G	6H	158,188,672	158,192,287	Mediator of RNA polymerase II transcription subunit 18
HORVU6Hr1G034150	HC_U	6H	158,524,294	158,526,001	unknown function
HORVU6Hr1G034180	HC_G	6H	158,745,594	158,750,674	Cytokinin-O-glucosyltransferase 2
HORVU6Hr1G034380	HC_G	6H	160,509,375	160,511,083	N-terminal protein myristoylation
HORVU6Hr1G034450	HC_G	6H	161,086,292	161,095,713	Pentatricopeptide repeat-containing protein
HORVU6Hr1G034480	LC_TE	6H	161,098,181	161,102,139	unknown function
HORVU6Hr1G034570	HC_G	6H	161,983,863	161,986,530	receptor kinase 2
HORVU6Hr1G034630	HC_G	6H	162,670,510	162,676,836	cellulose synthase-like A3
HORVU6Hr1G034660	HC_G	6H	163,337,648	163,351,394	autophagy 2
HORVU6Hr1G034680	HC_G	6H	163,562,102	163,587,494	methyl-CPG-binding domain 9
HORVU6Hr1G034720	HC_U	6H	164,364,821	164,375,074	unknown protein
HORVU6Hr1G034760	HC_G	6H	164,748,458	164,749,418	glutamine dumper 4

Appendix

Table A.9 continued

HORVU6Hr1G034840	HC_G	6H	165,333,047	165,337,831	Serine/threonine protein phosphatase 2A regulatory subunit B"alpha
HORVU6Hr1G034870	HC_G	6H	165,680,948	165,685,875	Alpha/beta hydrolase domain-containing protein 13
HORVU6Hr1G034900	HC_G	6H	165,691,829	165,697,779	Transmembrane amino acid transporter family protein
HORVU6Hr1G034960	HC_U	6H	165,732,619	165,733,505	unknown function
HORVU6Hr1G034990	HC_G	6H	165,912,283	165,921,196	receptor kinase 2
HORVU6Hr1G035000	HC_G	6H	165,917,648	165,920,609	Lycopene beta cyclase
HORVU6Hr1G035040	HC_G	6H	166,230,581	166,244,401	Lipid A export ATP-binding/permease protein MsbA
HORVU6Hr1G035160	HC_G	6H	167,230,141	167,234,230	Branched-chain-amino-acid aminotransferase
HORVU6Hr1G035190	HC_G	6H	167,631,175	167,663,939	Branched-chain-amino-acid aminotransferase-like protein 1
HORVU6Hr1G035210	HC_G	6H	168,139,234	168,144,424	GDSL esterase/lipase
HORVU6Hr1G035260	HC_G	6H	168,603,691	168,605,046	30S ribosomal protein S21
HORVU6Hr1G035280	HC_G	6H	168,843,833	168,848,734	Subtilisin-like protease
HORVU6Hr1G035370	HC_G	6H	169,991,412	169,996,625	UDP-Glycosyltransferase superfamily protein
HORVU6Hr1G035430	LC_u	6H	171,043,806	171,044,193	undescribed protein
HORVU6Hr1G035470	HC_G	6H	171,520,645	171,523,251	myb domain protein r1
HORVU6Hr1G035550	HC_G	6H	172,471,009	172,480,478	Glycerophosphodiester phosphodiesterase GDPDL7
HORVU6Hr1G035560	LC_U	6H	172,480,666	172,483,662	unknown protein
HORVU6Hr1G035570	LC_u	6H	172,482,831	172,483,651	undescribed protein
HORVU6Hr1G035600	HC_G	6H	172,639,588	172,647,145	Exostosin family protein
HORVU6Hr1G035610	HC_G	6H	172,640,474	172,659,999	Kynurenine formamidase
HORVU6Hr1G035690	LC_TE?	6H	173,438,381	173,440,799	FAR1-related sequence 3
HORVU6Hr1G035730	HC_G	6H	174,233,445	174,236,150	Cytochrome P450 superfamily protein
HORVU6Hr1G035750	LC_u	6H	174,384,026	174,399,974	undescribed protein
HORVU6Hr1G035790	LC_u	6H	174,394,033	174,400,040	undescribed protein
HORVU6Hr1G035880	HC_G	6H	174,769,173	174,773,122	receptor kinase 2
HORVU6Hr1G035950	HC_G	6H	175,606,147	175,610,656	glycine-rich RNA-binding protein 3
HORVU6Hr1G035970	HC_G	6H	175,818,336	175,824,999	respiratory burst oxidase protein F
HORVU6Hr1G036010	HC_G	6H	176,034,942	176,040,422	TOPLESS-related 1
HORVU6Hr1G036020	HC_G	6H	176,038,676	176,043,556	Myosin heavy chain-related protein
HORVU6Hr1G036060	HC_G	6H	176,354,967	176,365,203	tRNA(Ile)-lysidine synthase
HORVU6Hr1G036320	LC_u	6H	178,970,596	179,064,884	undescribed protein
HORVU6Hr1G036330	LC_u	6H	178,971,380	179,060,516	undescribed protein
HORVU6Hr1G036510	HC_G	6H	179,054,685	179,059,367	Carboxypeptidase Y homolog A
HORVU6Hr1G036640	HC_G	6H	180,781,902	180,789,590	ARF-GAP domain 5
HORVU6Hr1G036660	HC_G	6H	181,328,904	181,340,273	Coatomer, beta' subunit
HORVU6Hr1G036720	HC_G	6H	181,988,302	181,993,310	MOB kinase activator-like 1A
HORVU6Hr1G036760	HC_u	6H	182,667,165	182,668,715	undescribed protein
HORVU6Hr1G036770	HC_G	6H	182,690,966	182,692,781	Mannan endo-1,4-beta-mannosidase 7

Appendix

Table A.9 continued

HORVU6Hr1G036790	LC_TE	6H	182,804,586	182,813,153	Transposon protein, putative, CACTA, En/Spm sub-class
HORVU6Hr1G036800	HC_G	6H	182,926,207	182,933,284	ABC transporter G family member 39
HORVU6Hr1G036810	HC_G	6H	182,972,837	182,978,618	RNA-binding protein 39
HORVU6Hr1G036840	HC_TE?	6H	183,574,870	183,587,426	Argonaute family protein
HORVU6Hr1G036950	HC_G	6H	184,751,830	184,815,469	3-ketoacyl-CoA synthase 11
HORVU6Hr1G036990	HC_G	6H	184,920,624	184,925,002	26S protease regulatory subunit 8 homolog A
HORVU6Hr1G037080	HC_G	6H	185,162,825	185,164,404	Cytochrome c oxidase subunit 1
HORVU6Hr1G037140	HC_G	6H	185,893,356	185,896,701	Cytochrome P450 superfamily protein
HORVU6Hr1G037420	HC_G	6H	187,527,184	187,535,354	Plant Tudor-like RNA-binding protein
HORVU6Hr1G037460	HC_G	6H	187,823,771	187,837,262	Cryptochrome-1
HORVU6Hr1G037500	HC_G	6H	187,971,793	187,979,293	Peptidyl-prolyl cis-trans isomerase G
HORVU6Hr1G037610	HC_TE?	6H	189,312,796	189,321,121	zinc finger (Ran-binding) family protein
HORVU6Hr1G037620	LC_u	6H	189,312,851	189,313,125	undescribed protein
HORVU6Hr1G037680	HC_G	6H	190,084,075	190,088,684	Apoptotic protease-activating factor 1
HORVU6Hr1G037750	LC_TE	6H	190,805,787	190,818,947	Retrotransposon protein, putative, Ty1-copia subclass
HORVU6Hr1G037760	HC_G	6H	190,806,898	190,818,846	Transcription factor HY5
HORVU6Hr1G037810	LC_TE	6H	190,811,622	190,811,821	Retrotransposon protein, putative, unclassified
HORVU6Hr1G038010	HC_G	6H	192,933,895	192,937,786	histone deacetylase 6
HORVU6Hr1G038030	HC_TE?	6H	192,942,939	192,947,889	ATP-dependent RNA helicase DED1
HORVU6Hr1G038160	LC_U	6H	193,427,671	193,460,808	unknown function
HORVU6Hr1G038390	HC_G	6H	195,134,370	195,140,247	Lipid binding protein
HORVU6Hr1G038430	HC_TE?	6H	195,454,650	195,458,148	F-box family protein
HORVU6Hr1G038460	HC_G	6H	196,098,697	196,100,431	Protein kinase family protein
HORVU6Hr1G038500	HC_G	6H	196,590,434	196,596,364	Sterol 3-beta-glucosyltransferase
HORVU6Hr1G038520	HC_G	6H	197,017,139	197,029,001	ABC transporter ATP-binding protein NatA
HORVU6Hr1G038540	HC_G	6H	197,162,493	197,178,321	Pentatricopeptide repeat-containing protein
HORVU6Hr1G038550	HC_G	6H	197,166,468	197,170,689	Leucine-rich receptor-like protein kinase family protein
HORVU6Hr1G038590	HC_G	6H	197,684,169	197,698,753	P-loop containing nucleoside triphosphate hydrolases superfamily protein
HORVU6Hr1G038620	HC_G	6H	197,867,357	197,871,749	Ribonuclease Z
HORVU6Hr1G038700	HC_G	6H	198,574,495	198,578,108	Leucine-rich receptor-like protein kinase family protein
HORVU6Hr1G038710	HC_G	6H	198,579,213	198,588,416	histone deacetylase 1
HORVU6Hr1G038750	HC_G	6H	199,022,602	199,234,331	Cytochrome P450 superfamily protein
HORVU6Hr1G038770	HC_G	6H	199,135,228	199,275,141	serine/threonine protein phosphatase 2A
HORVU6Hr1G038870	HC_G	6H	200,044,289	200,050,317	Ribosomal RNA small subunit methyltransferase B

Appendix

Table A.9 continued

HORVU6Hr1G038970	LC_TE	6H	200,815,428	200,818,935	Retrotransposon protein, putative, unclassified
HORVU6Hr1G039140	HC_G	6H	201,946,715	201,955,008	aminopeptidase M1
HORVU6Hr1G039200	HC_U	6H	202,950,929	202,960,409	Plant protein of unknown function
HORVU6Hr1G039260	LC_U	6H	203,505,728	203,511,120	unknown function
HORVU6Hr1G039270	HC_G	6H	203,505,734	203,512,226	protein kinase family protein
HORVU6Hr1G039490	HC_G	6H	205,453,551	205,458,670	beta galactosidase 1
HORVU6Hr1G039510	HC_G	6H	205,697,776	205,700,545	Mahogunin, ring finger 1-like protein
HORVU6Hr1G039550	HC_G	6H	206,107,320	206,118,438	GPI-anchor transamidase
HORVU6Hr1G039590	LC_u	6H	206,535,576	206,538,509	undescribed protein
HORVU6Hr1G039610	HC_G	6H	206,677,485	206,682,932	Tetraspanin family protein
HORVU6Hr1G039680	HC_G	6H	207,624,576	207,626,177	cytokinin oxidase/dehydrogenase 1
HORVU6Hr1G039720	HC_G	6H	207,778,968	207,792,235	GATA transcription factor 23
HORVU6Hr1G039740	HC_G	6H	208,330,742	208,343,377	Protein kinase superfamily protein
HORVU6Hr1G039890	HC_G	6H	210,031,609	210,037,717	V-type ATP synthase beta chain
HORVU6Hr1G039910	HC_G	6H	210,470,020	210,497,833	Serine/threonine protein phosphatase 2A 55 kDa regulatory subunit B beta isoform
HORVU6Hr1G039940	HC_G	6H	210,762,786	210,767,184	Protein phosphatase 2C family protein
HORVU6Hr1G040140	LC_u	6H	214,259,662	214,261,831	undescribed protein
HORVU6Hr1G040150	LC_u	6H	214,259,716	214,261,032	undescribed protein
HORVU6Hr1G040190	HC_G	6H	214,737,148	214,742,557	Calcium-binding EF hand family protein
HORVU6Hr1G040220	HC_G	6H	215,060,284	215,064,497	RNA-binding protein Musashi homolog 2
HORVU6Hr1G040310	HC_G	6H	216,425,459	216,431,780	Far upstream element-binding protein 2
HORVU6Hr1G040480	HC_G	6H	218,526,299	218,538,144	Peroxisomal membrane protein PMP22
HORVU6Hr1G040530	LC_TE	6H	219,260,091	219,263,635	Polyprotein
HORVU6Hr1G040890	LC_u	6H	221,552,577	221,562,874	undescribed protein
HORVU6Hr1G040900	HC_G	6H	221,552,713	221,564,703	early nodulin-related
HORVU6Hr1G041020	HC_G	6H	223,064,500	223,076,215	50S ribosomal protein L21
HORVU6Hr1G041140	HC_G	6H	224,523,951	224,581,349	Copine-3
HORVU6Hr1G041230	HC_G	6H	224,658,059	224,671,068	pentatricopeptide repeat 336
HORVU6Hr1G041310	HC_G	6H	226,904,154	226,906,004	Acid phosphatase 1
HORVU6Hr1G041330	LC_TE?	6H	226,980,141	226,987,357	DNA helicase
HORVU6Hr1G041430	HC_G	6H	228,200,647	228,211,681	U-box domain-containing protein 4
HORVU6Hr1G041610	HC_G	6H	229,187,455	229,193,473	ROP guanine nucleotide exchange factor 5
HORVU6Hr1G041650	HC_G	6H	229,632,667	229,646,774	Protein phosphatase 1 regulatory subunit 7
HORVU6Hr1G041750	HC_G	6H	230,689,821	230,691,864	60S ribosomal protein L6
HORVU6Hr1G041840	LC_TE	6H	231,525,643	231,563,982	unknown function
HORVU6Hr1G042060	LC_u	6H	233,291,335	233,294,395	undescribed protein
HORVU6Hr1G042070	LC_u	6H	233,291,488	233,294,491	undescribed protein

Appendix

Table A.9 continued

HORVU6Hr1G042080	HC_G	6H	233,583,049	233,587,434	Mitochondrial substrate carrier family protein
HORVU6Hr1G042160	HC_G	6H	235,104,666	235,109,164	Aldehyde dehydrogenase
HORVU6Hr1G042320	HC_G	6H	237,514,415	237,519,460	eukaryotic translation initiation factor SUI1 family protein
HORVU6Hr1G042410	HC_G	6H	238,434,956	238,488,883	Magnesium transporter NIPA2
HORVU6Hr1G042550	HC_G	6H	238,807,727	238,815,870	GDSL esterase/lipase
HORVU6Hr1G042680	HC_G	6H	240,355,213	240,384,215	Ethylene-responsive transcription factor-like protein
HORVU6Hr1G042890	HC_G	6H	241,392,275	241,424,824	SPla/RYanodine receptor (SPRY) domain-containing protein
HORVU6Hr1G043010	HC_G	6H	242,333,277	242,338,210	alkaline/neutral invertase
HORVU6Hr1G043170	LC_TE?	6H	244,114,867	244,123,161	FAR1-related sequence 5
HORVU6Hr1G043180	LC_u	6H	244,121,867	244,133,770	undescribed protein
HORVU6Hr1G043190	HC_U	6H	244,129,783	244,130,439	unknown function
HORVU6Hr1G043230	HC_G	6H	245,235,550	245,240,219	Ankyrin repeat family protein
HORVU6Hr1G043280	HC_G	6H	245,289,045	245,292,485	AAA-type ATPase family protein / ankyrin repeat family protein
HORVU6Hr1G043290	LC_TE	6H	245,289,348	245,297,621	Retrotransposon gag protein, putative
HORVU6Hr1G043690	HC_G	6H	247,611,657	247,626,033	Ubiquitin carboxyl-terminal hydrolase 15
HORVU6Hr1G043710	HC_G	6H	247,797,776	247,798,957	alpha/beta-Hydrolases superfamily protein
HORVU6Hr1G043740	HC_G	6H	248,085,716	248,085,931	U-box domain-containing protein 11
HORVU6Hr1G043770	LC_u	6H	248,517,795	248,526,202	undescribed protein
HORVU6Hr1G043780	LC_u	6H	248,522,872	248,526,140	undescribed protein
HORVU6Hr1G043930	HC_G	6H	249,811,096	249,812,410	Ubiquinone/menaquinone biosynthesis C-methyltransferase UbiE
HORVU6Hr1G043940	LC_u	6H	249,829,961	249,839,799	undescribed protein
HORVU6Hr1G043950	LC_u	6H	249,836,036	249,839,713	undescribed protein
HORVU6Hr1G043960	LC_u	6H	250,061,630	250,063,406	undescribed protein
HORVU6Hr1G044030	HC_G	6H	250,540,657	250,575,265	ATP-dependent Clp protease ATP-binding subunit ClpX
HORVU6Hr1G044080	HC_G	6H	251,136,039	251,161,167	Protein SIP5
HORVU6Hr1G044300	HC_G	6H	253,510,064	253,556,229	cyclic nucleotide gated channel 1
HORVU6Hr1G044360	HC_G	6H	254,320,621	254,325,910	Transducin/WD40 repeat-like superfamily protein
HORVU6Hr1G044590	HC_G	6H	256,477,282	256,482,953	Transcription factor jumonji domain-containing protein, putative isoform 9
HORVU6Hr1G044600	HC_G	6H	256,478,174	256,482,901	P-loop NTPase domain-containing protein LPA1
HORVU6Hr1G044820	HC_G	6H	258,340,240	258,343,668	Isoprenylcysteine alpha-carbonyl methylesterase ICME
HORVU6Hr1G045130	HC_G	6H	262,165,882	262,180,506	eukaryotic translation initiation factor 4B1
HORVU6Hr1G045140	HC_G	6H	262,199,868	262,201,205	P0696G06.27 protein
HORVU6Hr1G045170	HC_G	6H	262,222,240	262,223,968	Crt homolog 1

Appendix

Table A.9 continued

HORVU6Hr1G045460	HC_G	6H	264,583,441	264,585,392	YELLOW STRIPE like 2
HORVU6Hr1G045520	LC_U	6H	264,915,778	264,967,163	Plant protein of unknown function
HORVU6Hr1G045720	LC_TE	6H	265,498,373	265,500,890	Retrotransposon protein, putative, unclassified
HORVU6Hr1G045800	HC_G	6H	265,913,201	265,931,571	lipase class 3 family protein
HORVU6Hr1G045820	HC_G	6H	265,933,083	265,950,760	lipase class 3 family protein
HORVU6Hr1G045970	HC_G	6H	267,733,725	267,836,428	NHL domain-containing protein
HORVU6Hr1G046160	HC_G	6H	269,408,680	269,412,934	cyclin-dependent kinase C;1
HORVU6Hr1G046290	HC_G	6H	269,994,312	270,027,620	DNA repair protein XRCC3 homolog
HORVU6Hr1G046390	LC_U	6H	270,969,327	270,970,565	Chromosome 3B, cultivar Chinese Spring
HORVU6Hr1G046490	HC_G	6H	272,451,988	272,453,330	Protein kinase superfamily protein
HORVU6Hr1G046540	HC_G	6H	273,590,458	273,602,473	Calmodulin-binding protein
HORVU6Hr1G046900	LC_U	6H	276,294,208	276,312,068	unknown function
HORVU6Hr1G046910	HC_G	6H	276,405,772	276,433,163	NIPA-like protein 3
HORVU6Hr1G047040	HC_G	6H	278,389,884	278,433,658	Iron-sulphur cluster biosynthesis family protein
HORVU6Hr1G047100	LC_TE	6H	278,400,888	278,410,762	RNA-directed DNA polymerase (Reverse transcriptase) domain containing protein
HORVU6Hr1G047300	HC_G	6H	280,273,656	280,275,177	prohibitin 3
HORVU6Hr1G047360	HC_G	6H	281,189,641	281,201,691	Isocitrate dehydrogenase [NAD] subunit 2, mitochondrial
HORVU6Hr1G047440	HC_G	6H	281,976,025	281,979,732	CDT1-like protein b
HORVU6Hr1G047560	HC_G	6H	284,363,911	284,444,769	calcium-dependent lipid-binding family protein
HORVU6Hr1G047650	HC_G	6H	284,488,010	284,553,958	calcium-dependent lipid-binding family protein
HORVU6Hr1G047770	HC_G	6H	286,130,856	286,133,131	chaperone protein dnaJ-related
HORVU6Hr1G047810	HC_G	6H	286,866,883	286,868,011	Ubiquinone/menaquinone biosynthesis C-methyltransferase UbiE
HORVU6Hr1G047830	LC_TE	6H	287,514,875	287,524,641	unknown function
HORVU6Hr1G047840	LC_U	6H	287,514,965	287,524,598	unknown function
HORVU6Hr1G047890	LC_TE	6H	287,835,360	287,838,219	Transposon protein, putative, CACTA, En/Spm sub-class
HORVU6Hr1G048080	HC_G	6H	288,949,367	288,963,484	Cytochrome b-c1 complex subunit 6
HORVU6Hr1G048370	LC_u	6H	291,624,235	291,627,626	undescribed protein
HORVU6Hr1G048390	HC_G	6H	291,973,141	291,980,709	Polyadenylate-binding protein 2
HORVU6Hr1G048410	HC_G	6H	293,085,821	293,112,209	phosphoenolpyruvate carboxylase 3
HORVU6Hr1G048600	HC_G	6H	295,125,066	295,144,984	Transmembrane 9 superfamily member 1
HORVU6Hr1G048650	HC_G	6H	296,869,908	296,871,099	dihydroflavonol 4-reductase
HORVU6Hr1G048780	HC_G	6H	297,226,460	297,257,555	Vacuolar protein sorting-associated protein 29
HORVU6Hr1G048810	LC_TE	6H	297,239,480	297,240,586	Reverse transcriptase
HORVU6Hr1G049000	HC_G	6H	297,891,207	297,891,699	Vacuolar ATPase assembly integral membrane protein VMA21-like domain

Appendix

Table A.9 continued

HORVU6Hr1G049050	HC_G	6H	298,340,921	298,369,596	Protein kinase superfamily protein
HORVU6Hr1G049080	HC_G	6H	298,924,989	298,937,642	Galactosyltransferase family protein
HORVU6Hr1G049790	HC_G	6H	301,614,309	301,620,239	acyl carrier protein 1
HORVU6Hr1G049950	HC_G	6H	302,446,931	302,451,004	cryptochrome 1
HORVU6Hr1G050090	HC_G	6H	303,846,578	303,859,594	Ubiquitin carboxyl-terminal hydrolase 4
HORVU6Hr1G050370	HC_G	6H	304,527,897	304,564,996	DNA binding protein-like
HORVU6Hr1G050440	HC_G	6H	305,085,225	305,120,660	senescence-associated family protein
HORVU6Hr1G050490	HC_G	6H	306,378,344	306,383,446	RING/U-box superfamily protein
HORVU6Hr1G050550	HC_G	6H	306,989,820	306,991,098	cellulose synthase like E1
HORVU6Hr1G051110	HC_G	6H	311,131,284	311,145,486	bZIP protein
HORVU6Hr1G051210	HC_G	6H	311,582,412	311,591,902	Cytochrome b-c1 complex subunit Rieske, mitochondrial
HORVU6Hr1G051450	HC_G	6H	313,371,489	313,376,703	Small nuclear ribonucleoprotein family protein
HORVU6Hr1G051560	HC_G	6H	313,918,343	313,922,405	3,4-dihydroxy-2-butanone 4-phosphate synthase
HORVU6Hr1G051700	LC_U	6H	316,340,461	316,349,155	unknown function
HORVU6Hr1G051760	HC_G	6H	316,930,406	316,953,097	GPI ethanolamine phosphate transferase 1
HORVU6Hr1G051990	HC_G	6H	319,245,725	319,255,953	Papain-like cysteine proteinase
HORVU6Hr1G052000	LC_u	6H	319,250,537	319,252,167	undescribed protein
HORVU6Hr1G052010	HC_G	6H	319,428,413	319,430,914	Kelch-like protein 21
HORVU6Hr1G052140	HC_G	6H	320,288,530	320,327,024	Beta-1,3-galactosyltransferase 7
HORVU6Hr1G052230	HC_u	6H	320,935,516	320,939,382	undescribed protein
HORVU6Hr1G052310	LC_TE	6H	321,886,576	321,892,576	Zinc finger protein 1 homolog
HORVU6Hr1G052330	LC_U	6H	322,066,426	322,077,626	unknown function
HORVU6Hr1G052360	HC_G	6H	322,112,886	322,123,282	fimbrin-like protein 2
HORVU6Hr1G052370	LC_u	6H	322,114,513	322,116,248	undescribed protein
HORVU6Hr1G052420	HC_G	6H	322,881,760	322,887,916	Glycerophosphodiester phosphodiesterase GDPDL4
HORVU6Hr1G052520	HC_G	6H	323,780,724	323,786,310	Protein kinase superfamily protein
HORVU6Hr1G052560	HC_G	6H	324,406,830	324,410,254	Ribosome biogenesis protein BRX1 homolog
HORVU6Hr1G052600	HC_G	6H	325,194,452	325,196,297	60S ribosomal protein L6
HORVU6Hr1G052620	HC_U	6H	325,367,294	325,372,518	unknown function
HORVU6Hr1G052630	LC_u	6H	325,371,636	325,372,483	undescribed protein
HORVU6Hr1G052660	HC_G	6H	325,501,576	325,521,458	Transducin/WD40 repeat-like superfamily protein
HORVU6Hr1G052670	LC_u	6H	325,503,198	325,508,539	undescribed protein
HORVU6Hr1G052800	LC_u	6H	325,650,097	325,651,127	undescribed protein
HORVU6Hr1G052810	HC_U	6H	325,650,100	325,653,250	unknown function
HORVU6Hr1G052850	HC_G	6H	326,399,000	326,409,497	Alkaline phosphatase D
HORVU6Hr1G052890	HC_G	6H	326,570,277	326,574,985	Armadillo repeat-containing protein LFR
HORVU6Hr1G052920	HC_G	6H	326,690,420	326,697,081	DNA mismatch repair protein PMS1

Appendix

Table A.9 continued

HORVU6Hr1G052930	LC_TE	6H	326,917,295	326,940,304	Transposon protein, putative, CACTA, En/Spm sub-class
HORVU6Hr1G052940	LC_u	6H	327,234,616	327,240,258	undescribed protein
HORVU6Hr1G052970	HC_G	6H	327,819,592	327,822,851	BnaA09g03880D protein
HORVU6Hr1G053080	LC_TE	6H	328,522,640	328,523,843	unknown function
HORVU6Hr1G053090	HC_G	6H	328,630,264	328,632,697	receptor lectin kinase
HORVU6Hr1G053100	HC_G	6H	328,930,020	328,936,372	phosphate transporter 2;1
HORVU6Hr1G053110	HC_G	6H	328,930,052	328,934,927	unknown protein
HORVU6Hr1G053120	HC_G	6H	328,938,304	328,940,712	receptor kinase 2
HORVU6Hr1G053290	HC_G	6H	331,157,769	331,168,323	Ribosomal RNA-processing protein 8
HORVU6Hr1G053310	HC_G	6H	331,583,539	331,590,126	Protein kinase superfamily protein
HORVU6Hr1G053330	HC_G	6H	331,591,956	331,599,040	Serine/threonine-protein kinase
HORVU6Hr1G053340	LC_TE	6H	331,592,109	331,595,566	unknown function
HORVU6Hr1G053490	HC_G	6H	333,319,137	333,322,130	BTB/POZ domain-containing protein
HORVU6Hr1G053540	HC_G	6H	334,190,358	334,194,662	NAC domain protein,
HORVU6Hr1G053600	LC_U	6H	335,351,554	335,359,276	unknown protein
HORVU6Hr1G053640	HC_G	6H	335,729,021	335,739,569	unknown protein
HORVU6Hr1G053650	HC_G	6H	335,741,592	335,746,045	isocitrate dehydrogenase 1
HORVU6Hr1G053680	HC_G	6H	336,377,047	336,380,003	Elongation factor Tu
HORVU6Hr1G053730	HC_G	6H	337,167,990	337,183,017	Protein GLE1
HORVU6Hr1G053760	HC_G	6H	337,183,377	337,254,568	Protein kinase superfamily protein
HORVU6Hr1G053830	HC_G	6H	338,281,545	338,287,347	Charged multivesicular body protein 6
HORVU6Hr1G053850	HC_u	6H	338,666,208	338,666,976	undescribed protein
HORVU6Hr1G053890	HC_G	6H	338,780,019	338,797,047	CCAAT/enhancer-binding protein zeta
HORVU6Hr1G053900	LC_u	6H	338,796,895	338,797,255	undescribed protein
HORVU6Hr1G053910	HC_G	6H	339,076,120	339,088,374	Actin-related protein 3
HORVU6Hr1G053940	LC_u	6H	339,453,884	339,461,922	undescribed protein
HORVU6Hr1G053960	HC_G	6H	339,459,880	339,461,905	GDSL esterase/lipase
HORVU6Hr1G053970	HC_G	6H	339,684,526	339,687,349	Ribosomal RNA small subunit methyltransferase NEP1
HORVU6Hr1G053980	HC_G	6H	339,761,366	339,764,358	BAG family molecular chaperone regulator 1
HORVU6Hr1G054000	HC_G	6H	340,035,170	340,039,929	Very-long-chain 3-oxoacyl-CoA reductase 1
HORVU6Hr1G054010	HC_U	6H	340,035,303	340,043,270	unknown function
HORVU6Hr1G054050	HC_G	6H	340,300,408	340,307,065	B3 domain-containing protein
HORVU6Hr1G054060	HC_G	6H	340,591,782	340,605,332	TGN-localized SYP41-interacting protein
HORVU6Hr1G054070	HC_G	6H	340,819,594	340,830,213	Telomere length regulation protein TEL2 homolog
HORVU6Hr1G054100	HC_G	6H	341,709,382	341,714,812	26S proteasome non-ATPase regulatory subunit 6
HORVU6Hr1G054110	HC_G	6H	341,710,988	341,714,779	Protein HHL1, chloroplastic
HORVU6Hr1G054120	LC_U	6H	341,724,096	341,733,973	Chromosome 3B, cultivar Chinese Spring
HORVU6Hr1G054190	LC_u	6H	342,275,278	342,293,644	undescribed protein

Appendix

Table A.9 continued

HORVU6Hr1G054200	LC_u	6H	342,599,033	342,604,051	undescribed protein
HORVU6Hr1G054280	HC_G	6H	342,867,863	342,871,364	Cytosolic Fe-S cluster assembly factor NBP35
HORVU6Hr1G054310	LC_U	6H	343,185,716	343,204,327	unknown function
HORVU6Hr1G054320	LC_u	6H	343,187,700	343,189,452	undescribed protein
HORVU6Hr1G054340	HC_G	6H	343,247,875	343,250,060	negative regulator of systemic acquired resistance (SNI1)
HORVU6Hr1G054420	HC_G	6H	344,112,304	344,117,621	Oxygen-dependent coproporphyrinogen-III oxidase
HORVU6Hr1G054430	HC_G	6H	344,112,322	344,119,107	methionine aminopeptidase 1B
HORVU6Hr1G054520	HC_G	6H	344,797,185	344,800,499	glyceraldehyde-3-phosphate dehydrogenase C2

^a The predicted genes and their respective annotations were obtained from BARLEYMAP (Cantalapiedra et al. 2015)

^b HC_G high confidence gene with predicted function, HC_U high confidence gene without predicted function, LC_u low-confidence gene without predicted function

Table A.10 Predicted genes located on chromosomes 6H at 355-379 Mbp and their respective functional annotations.

Gene ID ^a	Gene class ^b	Chr	Physical location [bp]		Annotation
HORVU6Hr1G055740	HC_TE?	6H	355,014,413	355,020,602	FAR1-related sequence 6
HORVU6Hr1G055750	HC_G	6H	355,019,832	355,029,490	LETM1 and EF-hand domain-containing protein 1, mitochondrial
HORVU6Hr1G055820	HC_G	6H	355,516,468	355,521,532	Ankyrin repeat family protein
HORVU6Hr1G055830	HC_TE?	6H	355,853,928	355,855,079	Zinc finger protein, putative
HORVU6Hr1G055870	HC_G	6H	356,023,662	356,027,552	Outer envelope pore protein 37, chloroplastic
HORVU6Hr1G055910	HC_U	6H	356,233,321	356,240,924	unknown function
HORVU6Hr1G055960	HC_G	6H	356,677,679	356,682,060	Bidirectional sugar transporter N3
HORVU6Hr1G056000	HC_G	6H	357,490,863	357,492,603	CONSTANS-like 3
HORVU6Hr1G056090	LC_u	6H	359,349,893	359,350,867	undescribed protein
HORVU6Hr1G056110	HC_G	6H	359,587,382	359,590,244	S-adenosylmethionine decarboxylase proenzyme
HORVU6Hr1G056130	LC_u	6H	359,690,569	359,705,948	undescribed protein
HORVU6Hr1G056140	HC_G	6H	359,700,138	359,701,528	SDG905
HORVU6Hr1G056180	HC_G	6H	360,335,318	360,339,964	Pentatricopeptide repeat-containing protein
HORVU6Hr1G056200	HC_G	6H	360,467,304	360,471,738	enhancer of rudimentary protein, putative
HORVU6Hr1G056230	HC_G	6H	361,061,379	361,066,837	hydroxycinnamoyl-CoA shikimate/quinic acid hydroxycinnamoyl transferase
HORVU6Hr1G056260	HC_G	6H	361,523,074	361,530,287	Nuclear cap-binding protein subunit 2
HORVU6Hr1G056280	HC_G	6H	361,528,654	361,534,239	Protein GrpE
HORVU6Hr1G056400	LC_TE	6H	362,942,357	362,948,608	Transposon protein, putative, CACTA, En/Spm sub-class
HORVU6Hr1G056440	HC_G	6H	363,543,259	363,543,836	40S ribosomal protein S20
HORVU6Hr1G056460	HC_G	6H	363,827,265	363,828,984	BTB/POZ domain-containing protein

Appendix

Table A.10 continued

HORVU6Hr1G056490	HC_G	6H	364,354,426	364,362,218	Sister chromatid cohesion protein PDS5 homolog B
HORVU6Hr1G056500	HC_u	6H	364,361,658	364,361,906	undescribed protein
HORVU6Hr1G056570	HC_G	6H	365,305,405	365,306,903	temperature-induced lipocalin
HORVU6Hr1G056610	HC_G	6H	365,341,314	365,344,671	40S ribosomal protein S11
HORVU6Hr1G056720	HC_G	6H	365,643,300	365,648,939	Calcium-binding mitochondrial carrier protein
HORVU6Hr1G056760	LC_u	6H	365,878,587	365,883,167	undescribed protein
HORVU6Hr1G056850	HC_G	6H	366,312,255	366,316,126	H/ACA ribonucleoprotein complex non-core subunit NAF1
HORVU6Hr1G056860	HC_G	6H	366,398,977	366,404,290	Trafficking protein particle complex subunit 2
HORVU6Hr1G056910	HC_G	6H	367,334,216	367,339,730	adenine phosphoribosyltransferase 5
HORVU6Hr1G056930	LC_u	6H	367,948,322	367,951,416	undescribed protein
HORVU6Hr1G057090	HC_G	6H	368,964,871	368,968,449	Nucleotide-sugar transporter family protein
HORVU6Hr1G057110	HC_G	6H	369,306,242	369,310,633	Disease resistance protein
AGZ89626.1	ncbi	6H	369,308,674	369,308,961	MLOC_36552-like protein
HORVU6Hr1G057140	HC_G	6H	370,396,139	370,400,943	Filament-like plant protein 7
HORVU6Hr1G057170	HC_G	6H	370,428,133	370,430,644	SPLa/Ryanodine receptor (SPRY) domain-containing protein
HORVU6Hr1G057500	HC_G	6H	373,418,735	373,425,452	rRNA N-glycosidase
HORVU6Hr1G057520	HC_u	6H	373,611,651	373,617,369	undescribed protein
HORVU6Hr1G057550	HC_G	6H	373,920,972	373,948,299	CLIP-associating protein 1-B
HORVU6Hr1G057560	HC_G	6H	374,242,958	374,272,688	Prolyl oligopeptidase family protein
HORVU6Hr1G057570	HC_G	6H	374,488,067	374,526,780	polyribonucleotide nucleotidyltransferase, putative
HORVU6Hr1G057610	LC_u	6H	374,644,032	374,647,018	undescribed protein
HORVU6Hr1G057630	HC_G	6H	374,866,561	374,869,556	Two-component response regulator-like PRR1
HORVU6Hr1G057640	HC_G	6H	374,875,965	374,877,962	H/ACA ribonucleoprotein complex subunit 3-like protein
HORVU6Hr1G057770	HC_G	6H	376,635,036	376,646,010	Protein ROOT HAIR DEFECTIVE 3 homolog 2
HORVU6Hr1G057780	HC_G	6H	376,800,081	376,803,528	Protein ROOT HAIR DEFECTIVE 3 homolog 2
HORVU6Hr1G057800	HC_U	6H	376,967,244	376,969,706	unknown function
HORVU6Hr1G057990	HC_G	6H	378,157,250	378,165,681	Histone-lysine N-methyltransferase 2A
HORVU6Hr1G058000	HC_G	6H	378,204,288	378,211,731	Fatty acid hydroxylase superfamily
HORVU6Hr1G058090	HC_G	6H	378,973,093	378,977,271	Pre-mRNA-processing factor 40-like protein A
HORVU6Hr1G058100	HC_G	6H	379,344,988	379,350,913	E3 ubiquitin-protein ligase PRT1
HORVU6Hr1G058110	LC_u	6H	379,348,484	379,348,938	undescribed protein

^a The predicted genes and their respective annotations were obtained from BARLEYMAP (Cantalapiedra et al. 2015)

^b HC_G high confidence gene with predicted function, HC_U high confidence gene without predicted function, LC_u low-confidence gene without predicted function

Appendix

Table A.11 Predicted genes located on chromosomes 6H at 406-410 Mbp and their respective functional annotations.

Gene ID ^a	Gene class ^b	Chr	Physical location [bp]		Annotation
HORVU6Hr1G060850	HC_G	6H	406,692,607	406,694,443	SAUR-like auxin-responsive protein family
HORVU6Hr1G060870	HC_G	6H	406,806,340	406,810,509	Reticulon-like protein
HORVU6Hr1G060900	LC_u	6H	406,912,979	406,916,668	undescribed protein
HORVU6Hr1G060910	LC_u	6H	406,912,979	406,917,340	undescribed protein
HORVU6Hr1G060990	HC_G	6H	407,203,000	407,209,104	Vacuolar-processing enzyme
CBX26636.1	ncbi vpe1	6H	407,203,590	407,208,801	vacuolar processing enzyme 1
HORVU6Hr1G061010	HC_G	6H	407,356,258	407,360,811	Hsp70-Hsp90 organizing protein
HORVU6Hr1G061020	HC_G	6H	407,801,004	407,805,826	Autophagy-related protein 13
HORVU6Hr1G061060	HC_G	6H	408,529,067	408,535,256	kinesin 4
HORVU6Hr1G061170	LC_TE?	6H	409,522,738	409,528,917	B-box zinc finger family protein
HORVU6Hr1G061200	HC_G	6H	409,612,569	409,615,105	Glutaredoxin family protein
HORVU6Hr1G061220	HC_G	6H	409,799,423	409,829,174	Aldehyde dehydrogenase family 3 member F1
HORVU6Hr1G061250	HC_G	6H	410,038,393	410,040,206	Leucine-rich repeat receptor-like protein kinase family protein
HORVU6Hr1G061270	HC_G	6H	410,500,503	410,506,247	Aldehyde dehydrogenase family 3 member F1

^a The predicted genes and their respective annotations were obtained from BARLEYMAP (Cantalapiedra et al. 2015)

^b HC_G high confidence gene with predicted function, HC_U high confidence gene without predicted function, LC_u low-confidence gene without predicted function

Table A.12 Predicted genes located on chromosomes 7H at 5 Mbp and 645 Mbp, and their respective functional annotations.

Gene ID ^a	Gene class ^b	Chr	Physical location [bp]		Annotation
HORVU7Hr1G002810	LC_TE	7H	5,164,462	5,169,538	RNase H family protein
HORVU7Hr1G117540	HC_G	7H	645,343,641	645,347,149	Pseudouridine synthase family protein
HORVU7Hr1G117560	LC_u	7H	645,367,664	645,370,887	undescribed protein
HORVU7Hr1G117570	HC_G	7H	645,373,486	645,381,646	Disease resistance protein
HORVU7Hr1G117640	HC_G	7H	645,487,552	645,490,971	RING/U-box superfamily protein
HORVU7Hr1G117650	LC_U	7H	645,488,573	645,490,975	unknown function
HORVU7Hr1G117660	LC_u	7H	645,489,425	645,489,554	undescribed protein
HORVU7Hr1G117710	HC_G	7H	645,731,921	645,733,781	O-methyltransferase family protein
HORVU7Hr1G117780	HC_G	7H	645,815,374	645,825,726	Pleckstrin homology (PH) domain-containing protein / lipid-binding START domain-containing protein

^a The predicted genes and their respective annotations were obtained from BARLEYMAP (Cantalapiedra et al. 2015)

^b HC_G high confidence gene with predicted function, HC_U high confidence gene without predicted function, LC_u low-confidence gene without predicted function

Appendix

Table A.13 List of barley accessions resistant against *Pyrenophora teres* f. *teres* in at least two environments (isolate or location), sorted in descending order.

VIR or CI No ^a	No of environments	Accession name	Landrace	Origin	Row- Type	Growth habit	Notes
21538	6	Omskij 82	Landrace	Bolivia	6	spring	naked
29416	6		Cultivar	Russia	2	spring	
3108	5		Landrace	Turkmenistan	6	spring	
5909	5		Landrace	Turkmenistan	6	spring	
11625	5		Landrace	Uzbekistan	6	spring	
11987	5		Landrace	Kyrgystan	6	spring	
11993	5		Landrace	Kyrgystan	6	spring	
12070	5		Landrace	Kyrgystan	6	spring	
16293	5		Landrace	China	6	spring	
16320	5		Landrace	China	6	spring	
17934	5	Husky	Landrace	Uzbekistan	6	spring	naked
18506	5		Cultivar	Canada	6	spring	
21115	5		Landrace	Ethiopia	2	spring	
26664	5	DZ02-570	Landrace	Pakistan	6	spring	naked
29192	5	Diamond	Cultivar	Canada	6	spring	
29548	5	Khar`kovskij 99	Cultivar	Ukraine	2	spring	
30029	5	Noble	Cultivar	Canada	6	spring	
30032	5	UC 603	Cultivar	USA	6	spring	
30408	5	Virden	Cultivar	USA	6	spring	black
1030	4	Coruva 37	Landrace	Russia	6	spring	
2589	4		Landrace	Ukraine	6	spring	
2893	4		Landrace	Turkmenistan	6	spring	
3175	4		Landrace	Tajikistan	6	spring	
5208	4		Cultivar	Australia	2	spring	
6827	4		Landrace	Turkey	2	spring	
7420	4		Landrace	Israel	6	spring	
7471	4		Landrace	Mexico	6	spring	
7599	4		Landrace	Palestine	6	spring	
8726	4		Landrace	Ethiopia	6	spring	
8759	4	Venez	Landrace	Ethiopia	2	spring	naked, black
8780	4		Cultivar	Italy	6	spring	
8789	4		Landrace	Italy	6	spring	
8835	4		Landrace	Italy	6	spring	
8869	4		Landrace	Spain	6	spring	
8877	4		Landrace	Spain	6	spring	
9004	4		Landrace	Turkey	2	spring	
9308	4		Landrace	Turkmenistan	6	spring	
9846	4		Landrace	Russia	2	spring	
10583	4		Landrace	Tajikistan	6	spring	
10625	4	Japonicum	Landrace	Tajikistan	6	spring	naked, black
11011	4		Cultivar	Japan	6	winter	
11139	4		Cultivar	Japan	6	spring	

Appendix

Table A.13 continued

11169	4	Muisaki purple	Cultivar	Japan	6	winter	black
11996	4		Landrace	Kyrgystan	6	spring	
12023	4		Landrace	Kyrgystan	6	spring	
14679	4		Landrace	Russia	6	spring	
14900	4		Landrace	Tajikistan	6	spring	
14936	4		Landrace	Tajikistan	6	spring	
14945	4		Landrace	Tajikistan	6	spring	
14958	4		Landrace	Tajikistan	6	spring	
14959	4		Landrace	Tajikistan	6	spring	
14961	4		Landrace	Tajikistan	6	spring	
14970	4		Landrace	Tajikistan	6	spring	
14974	4		Landrace	Tajikistan	6	spring	
15429	4	Early Challenger	Cultivar	Australia	2	spring	
16165	4		Landrace	China	6	winter	
16468	4		Landrace	Turkmenistan	6	spring	black
16924	4		Landrace	Turkmenistan	2	spring	
17819	4		Landrace	China	6	spring	
18505	4	Fort	Cultivar	Canada	6	spring	
18542	4	Taktehark anyi Hanna	Cultivar	Australia	6	spring	
18552	4	Zolo	Cultivar	Australia	2	spring	
18716	4	Ogalitsu C.I.7152	Cultivar	Canada	6	spring	
18728	4	Ricardo C.I.6306	Cultivar	Uruguay	6	spring	
19182	4	Fox	Cultivar	USA	6	spring	
19393	4	Prior	Cultivar	Australia	2	spring	
20249	4	Kaikei N 22	Cultivar	Japan	6	winter	
20497	4	Saga hadaka n3	Cultivar	Japan	6	spring	naked
21112	4	DZ02-458	Landrace	Ethiopia	6	spring	
21576	4		Landrace	Ecuador	6	spring	
21578	4		Landrace	Ecuador	6	spring	
21579	4		Landrace	Ecuador	6	spring	
21849	4	DZ02-547	Landrace	Ethiopia	2	spring	
22022	4	Celinnyi 5	Cultivar	Kazakhstan	2	spring	
23351	4	Australische zweizeilige	Cultivar	Australia	2	spring	
24709	4	Obskij	Cultivar	Russia	2	spring	
25078	4	Tlaxcala	Cultivar	Mexico	6	spring	
25811	4	Estate C.I.3410 [AHOR 2476/74]	Cultivar	USA	6	spring	
26110	4	-705	Landrace	Uzbekistan	6	spring	
26260	4	Olimpiets	Cultivar	Russia	2	spring	
27926	4	Primorskij	Cultivar	Russia	2	spring	
28232	4		Landrace	Uzbekistan	6	spring	
28235	4		Landrace	Uzbekistan	6	spring	
28239	4		Landrace	Uzbekistan	6	spring	
28241	4		Landrace	Uzbekistan	6	spring	
28906	4	Covmestnyi	Cultivar	Russia	2	spring	
29040	4	Bagan	Cultivar	Russia	2	spring	
29709	4	EH532/F2-5B-4	Cultivar	Mexico	2	spring	

Appendix

Table A.13 continued

30035	4	Excel	Cultivar	USA	6	spring	
30351	4	C.I. 11104 Lan	Landrace	Peru	6	spring	
30776	4	Ubagan	Cultivar	Russia	2	spring	
30796	4	C-99-2837	Cultivar	Russia	2	spring	naked
18760b	4	C.I.4407-1,Tifang	Landrace	USA	6	spring	black
NDB112	4	C.I. 11531 NDB 112	Landrace	USA	6	spring	
	4	C.I. 4207	Landrace	USA	6	spring	
2710	3		Landrace	Kazakhstan	6	spring	naked
2894	3		Landrace	Turkmenistan	6	spring	
2946	3		Landrace	Russia	2	spring	naked
2959	3		Landrace	Mongolia	6	spring	black
4355	3	USA	Landrace	USA	6	spring	
4719	3		Landrace	Uzbekistan	6	spring	
5059	3		Landrace	Turkmenistan	2	spring	naked
5900	3		Landrace	Turkmenistan	6	spring	
6814	3		Landrace	Turkey	2	spring	
6855	3		Landrace	Turkey	2	spring	black
6906	3		Landrace	Turkey	6	spring	
7623	3		Landrace	Syria	2	spring	
7747	3		Landrace	Turkey	2	spring	
8332	3		Landrace	Mongolia	6	spring	
8725	3		Landrace	Ethiopia	6	spring	
8727	3		Landrace	Ethiopia	2	spring	black
8829	3		Landrace	Italy	6	spring	
9257	3		Landrace	Uzbekistan	2	spring	
9264	3		Landrace	Uzbekistan	6	spring	
10095	3		Landrace	Turkmenistan	6	winter	
10106	3		Landrace	Turkmenistan	6	winter	
11031	3	Kosaba N2 (Jamagushi-ken)	Cultivar	Japan	6	winter	naked
11162	3		Landrace	Japan	6	winter	
11189	3		Landrace	Japan	6	spring	
11777	3		Landrace	Kyrgystan	2	spring	naked
12611	3		Landrace	Moldova	6	spring	
14957	3		Landrace	Tajikistan	6	spring	
15402	3	Manchuria	Cultivar	USA	6	spring	
15430	3	Pryor	Cultivar	Australia	2	spring	
15431	3	Short Head	Cultivar	Australia	6	spring	
15432	3	Roseworthy Crossbred	Cultivar	Australia	6	spring	half naked
15811	3		Landrace	China	6	spring	
15812	3		Landrace	China	6	spring	
15823	3		Landrace	China	6	spring	
15864	3		Landrace	China	6	winter	naked
16340	3		Landrace	China	6	winter	
17507	3	Golden Archer	Cultivar	Australia	6	spring	
17820	3		Landrace	China	6	spring	
17939	3		Landrace	China	2	spring	

Appendix

Table A.13 continued

18268	3	Fu-shuey	Cultivar	China	6	spring	naked
18614	3	Aurore	Cultivar	France	2	spring	
18636	3		Cultivar	Portugal	6	spring	
18755	3	C.I.1227 Benton	Cultivar	Canada	6	spring	
19395	3	Skinless	Cultivar	Australia	6	spring	naked
19646	3	Quinn	Cultivar	India	2	spring	
20127	3	AHOR 3582/63	Landrace	Ethiopia	6	spring	
20165	3	AHOR 3613/63	Landrace	Ethiopia	2	spring	black
20169	3	AHOR 3617/63	Landrace	Ethiopia	2	spring	black
20179	3	AHOR 3863/64	Landrace	Ethiopia	2	spring	black
20185	3	AHOR3284/66	Landrace	Ethiopia	2	spring	
20921	3	Abyssinian 1102=194	Cultivar	Ethiopia	2	spring	black, naked
20928	3	Nackta	Cultivar	Germany	2	spring	naked
21413	3	Chugokuhadaka N 3	Cultivar	Japan	6	spring	naked
21462	3	Shiromugi	Cultivar	China	6	spring	
21472	3	Hosogara	Cultivar	Sardinia	6	spring	
21567	3		Landrace	Bolivia	2	spring	black
21770	3		Landrace	Russia	2	spring	
21772	3		Landrace	Russia	2	spring	
21850	3	DZ02-744	Landrace	Ethiopia	6	spring	black
21856	3	KM 1192	Cultivar	Czech	2	spring	
23874	3	WGA 148-3	Cultivar	Ethiopia	6	spring	
24723	3	Prishimskij	Cultivar	Kazakhstan	2	spring	
25274	3	C.I.9819	Landrace	Ethiopia	2	spring	
25283	3	C.I.4922	Landrace	USA	6	spring	
26092	3	-437	Landrace	Uzbekistan	2	spring	
26403	3		Landrace	Uzbekistan	6	spring	
26959	3	Morex	Cultivar	USA	6	spring	
28664	3	S-301	Landrace	Mexico	6	spring	naked
29268	3	Altan-Bulag	Cultivar	Russia	2	spring	
29352	3	Risk	Cultivar	Russia	2	spring	
29576	3	Bowman	Cultivar	USA	2	spring	
29595	3	Waranga	Cultivar	Australia	2	spring	
29651	3	3170 1/21H5/2/7	Cultivar	Russia	2	spring	
30012	3	C.I.11034	Landrace	Peru	6	spring	
30120	3	Omskii 88	Cultivar	Russia	2	spring	
30174	3	El'f	Cultivar	Russia	2	spring	
30320	3	Obruk 86	Cultivar	Turkey	2	spring	
30329	3	C.I. 10985 Lan	Landrace	Peru	6	spring	
30341	3	C.I. 11025 Lan	Landrace	Peru	6	spring	black
30350	3	C.I. 11091 Lan	Landrace	Peru	6	spring	
30471	3	Viking	Cultivar	Germany	2	spring	
30479	3	Novosadski 501	Cultivar	Yugoslavia	2	winter	
30491	3	Akta Abed	Cultivar	Denmark	2	spring	
30617	3	KM-1485-1475	Cultivar	Czech	2	spring	naked
18760a	3	C.I.4407-1,Tifang	Landrace	USA	2	spring	
	3	C.I. 9820	Landrace	Ethiopia	6	spring	

Appendix

Table A.13 continued

838	2		Landrace	Georgia	2	spring	naked
2186	2		Landrace	Russia	6	spring	black
3114	2		Landrace	Tajikistan	6	spring	
3132	2		Landrace	Tajikistan	6	spring	
3945	2		Landrace	China	6	spring	naked
3952	2		Landrace	Mongolia	6	spring	
5094	2		Landrace	Uzbekistan	2	spring	naked
5211	2	Reka	Cultivar	Australia	6	spring	
6685	2		Landrace	Armenia	6	spring	
6816	2		Landrace	Turkey	6	spring	
6864	2		Landrace	Turkey	2	spring	
6880	2		Landrace	Turkey	2	spring	black
6913	2		Landrace	Turkey	6	spring	
7683	2		Landrace	Tunisia	6	winter	
7688	2		Landrace	Turkey	6	spring	
7694	2		Landrace	Turkey	6	spring	naked
7713	2		Landrace	Turkey	6	spring	
7751	2		Landrace	Turkey	2	spring	
7765	2		Landrace	Turkey	6	spring	
7766	2		Landrace	Turkey	2	spring	
8080	2		Landrace	Palestine	6	spring	black
8383	2		Landrace	Cyprus	6	spring	
8632	2		Landrace	Russia	6	spring	
8639	2		Landrace	Italy	6	spring	
8695	2		Landrace	Ethiopia	6	spring	
8706	2		Landrace	Ethiopia	6	spring	
8715	2		Landrace	Ethiopia	2	spring	
8801	2		Landrace	Italy	6	spring	
8812	2		Landrace	Italy	6	spring	
8984	2		Landrace	Turkey	6	spring	
9003	2		Landrace	Turkey	6	spring	
9148	2		Landrace	Italy	6	spring	
9254	2		Landrace	Tajikistan	6	spring	
10161	2		Landrace	Japan	6	spring	
10562	2		Landrace	Pakistan	6	spring	
11025	2	Miho N22 (Ehime-ken)	Cultivar	Japan	6	spring	naked
11188	2		Landrace	Japan	6	spring	naked
11653	2		Landrace	China	6	spring	naked
11916	2		Landrace	Kyrgystan	2	spring	
12291	2		Landrace	China	6	spring	
12647	2		Landrace	Moldova	6	spring	
12728	2		Landrace	Moldova	6	spring	
14249	2		Landrace	Tajikistan	6	spring	
15849	2		Landrace	China	6	spring	half naked
15872	2		Landrace	China	6	spring	
15912	2		Landrace	China	6	spring	
16114	2		Landrace	China	6	winter	

Appendix

Table A.13 continued

16164	2		Landrace	China	6	winter	
18269	2	Gyuvy-may	Cultivar	China	2	spring	
18677	2	Bolivia C.I.1257	Cultivar	Canada	6	spring	
18890	2		Landrace	India	6	spring	
19304	2	Keystone	Cultivar	Canada	2	spring	
19357	2	Australsky rani	Cultivar	Australia	2	spring	
19643	2	Sudan C.I. 6489	Cultivar	India	6	spring	
19975	2	AHOR 1635/66	Landrace	Ethiopia	2	spring	
19979	2	AHOR 40/65	Landrace	Ethiopia	6	spring	naked
20001	2	AHOR 3526/63	Landrace	Ethiopia	6	spring	black
20008	2	AHOR 3279/63	Landrace	Ethiopia	2	spring	
20533	2	DZ02-398	Landrace	Ethiopia	6	spring	black
21272	2	DZ02-610	Landrace	Ethiopia	6	spring	
21873	2	Effendi	Cultivar	Netherlands	2	spring	
22292	2		Landrace	Bolivia	6	spring	black
23384	2		Landrace	Bolivia	6	spring	
26926	2	Hora	Cultivar	Netherlands	2	spring	naked
27737	2	Rannij 1	Cultivar	Russia	2	spring	
28673	2	S-330	Landrace	Mexico	2	spring	naked
29002	2	Medicum 85	Cultivar	Kazakhstan	2	spring	
29216	2	Dina	Cultivar	Russia	2	spring	
29277	2	Perun	Cultivar	Czech	2	spring	
29334	2	Line 2-242	Cultivar	Russia	2	spring	naked
29345	2		Landrace	Russia	2	spring	
29434	2	Stirling	Cultivar	Australia	2	spring	
29438	2	Prejiya	Cultivar	Ukraine	2	spring	
29577	2	Cantala	Cultivar	Australia	2	spring	
29591	2	Schooner	Cultivar	Australia	2	spring	
29614	2	Britta	Cultivar	Sweden	2	spring	
29718	2	Sobotka	Cultivar	Poland	2	spring	
29723	2	Rus'	Cultivar	Russia	2	spring	
29830	2	Orenburgskij 15	Cultivar	Russia	2	spring	
30008	2	C.I.11001	Landrace	Peru	6	spring	
30014	2	C.I.11072	Landrace	Peru	6	spring	
30162	2	Belaris	Cultivar	France	2	spring	
30167	2	CDC Richard	Cultivar	Canada	2	spring	naked
30248	2	Mironovskij 86	Cultivar	Ukraine	2	spring	
30311	2	Povolgsskij 86	Cultivar	Russia	2	spring	
30327	2	C.I. 10972 Lan	Landrace	Peru	6	spring	
30328	2	C.I. 10974 Lan	Landrace	Peru	6	spring	
30330	2	C.I. 10986 Lan	Landrace	Peru	6	spring	
30340	2	C.I. 11024 Lan	Landrace	Peru	6	spring	
30342	2	C.I. 11030 Lan	Landrace	Peru	6	spring	black
30343	2	C.I. 11035 Lan	Landrace	Peru	6	spring	
30345	2	C.I. 11051 Lan	Landrace	Peru	6	spring	
30347	2	C.I. 11058 Lan	Landrace	Peru	6	spring	
30349	2	C.I. 11084 Lan	Landrace	Peru	6	spring	black, naked

Appendix

Table A.13 continued

30352	2	C.I. 11108 Lan	Landrace	Peru	6	spring
30353	2	Pallidum	Landrace	Peru	6	spring
30366	2	Galaktika	Cultivar	Ukraine	2	spring
30390	2	C.I. 11093 Lan	Landrace	Peru	6	spring
30453	2	Zernogradskij 813	Cultivar	Russia	2	spring
30562	2	Chelyabinskij 96	Cultivar	Russia	2	spring
30591	2	Rahat	Cultivar	Russia	2	spring
30634	2	C.I. 11010	Landrace	Peru	6	spring
30650	2	C.I. 11056	Landrace	Peru	6	spring
30670	2	C.I. 11092	Landrace	Peru	6	spring
30721	2	Omskij 90	Cultivar	Russia	2	spring
30927	2	Pejas	Cultivar	Czech	2	spring
	2	C.I. 9214	Landrace	Korea	6	spring

^a Accessions in bold were resistant against *P. teres* f. *teres* and *B. sorokiniana*

Table A.14 List of barley accessions resistant against *Bipolaris sorokiniana* in at least one environment (isolate or location), sorted in descending order.

VIR or CI No ^a	No of environments	Accession name	Landrace	Origin	Row- Type	Growth habit	Notes
5470	3		Landrace	Cyprus	6	spring	
5502	3	Naushera	Cultivar	India	6	spring	
18716	3	Ogalitsu C.I.7152	Cultivar	Canada	6	spring	
29576	3	Bowman	Cultivar	USA	2	spring	
8723	2		Landrace	Ethiopia	6	spring	
14936	2		Landrace	Tajikistan	6	spring	
15402	2	Manchuria	Cultivar	USA	6	spring	
15823	2		Landrace	China	6	spring	
26959	2	Morex	Cultivar	USA	6	spring	
28664	2	S-301	Landrace	Mexico	6	spring	naked
29216	2	Dina	Cultivar	Russia	2	spring	
30035	2	Excel	Cultivar	USA	6	spring	
30327	2	C.I. 10972 Lan	Landrace	Peru	6	spring	
30408	2	Virden	Cultivar	USA	6	spring	
1030	1		Landrace	Russia	6	spring	
2710	1		Landrace	Kazakhstan	6	spring	naked
2959	1		Landrace	Mongolia	6	spring	black
3114	1		Landrace	Tajikistan	6	spring	
4355	1	USA	Landrace	USA	6	spring	
6850	1		Landrace	Turkey	2	spring	
6874	1		Landrace	Turkey	2	spring	
6932	1		Landrace	Turkey	6	spring	
7683	1		Landrace	Tunisia	6	winter	
8332	1		Landrace	Mongolia	6	spring	
8632	1		Landrace	Russia	6	spring	

Appendix

Table A.14 continued

8695	1		Landrace	Ethiopia	6	spring	
8715	1		Landrace	Ethiopia	2	spring	
8726	1		Landrace	Ethiopia	6	spring	naked, black
8812	1		Landrace	Italy	6	spring	
8977	1		Landrace	Turkey	2	spring	
9015	1		Landrace	Turkey	6	spring	
10583	1		Landrace	Tajikistan	6	spring	
10843	1	Dzshov Buchary	Cultivar	Turkmenistan	6	spring	
11653	1		Landrace	China	6	spring	naked
12611	1		Landrace	Moldova	6	spring	
14931	1		Landrace	Tajikistan	6	spring	
15185	1		Landrace	Russia	6	spring	
15355	1	Bore	Cultivar	Australia	6	spring	
15811	1		Landrace	China	6	spring	
15812	1		Landrace	China	6	spring	
15912	1		Landrace	China	6	spring	
17507	1	Golden Archer	Cultivar	Australia	6	spring	
18267	1	Che-vomay n 1	Cultivar	China	6	spring	
18268	1	Fu-shuey	Cultivar	China	6	spring	naked
18269	1	Gyuvy-may	Cultivar	China	2	spring	
18505	1	Fort	Cultivar	Canada	6	spring	
18552	1	Zolo	Cultivar	Australia	2	spring	
18755	1	C.I.1227 Benton	Cultivar	Canada	6	spring	
18973	1	Tsi-lun-tsin-ko 190	Cultivar	China	6	spring	
19182	1	Fox	Cultivar	USA	6	spring	
19304	1	Keystone	Cultivar	Canada	2	spring	
19643	1	Sudan C.I. 6489	Cultivar	India	6	spring	
19646	1	Quinn	Cultivar	India	2	spring	
19924	1		Landrace	Tajikistan	2	winter	
19979	1	AHOR 40/65	Landrace	Ethiopia	6	spring	naked
20019	1	AHOR 2541/63	Landrace	Ethiopia	6	spring	
20130	1	AHOR 3585/63	Landrace	Ethiopia	2	spring	
20165	1	AHOR 3613/63	Landrace	Ethiopia	2	spring	black
20179	1	AHOR 3863/64	Landrace	Ethiopia	2	spring	black
20921	1	Abyssinian 1102=I94	Cultivar	Ethiopia	2	spring	black, naked
21272	1	DZ02-610	Landrace	Ethiopia	6	spring	
21462	1	Shiromugi	Cultivar	China	6	spring	
21578	1		Landrace	Ecuador	6	spring	
21763	1		Landrace	Russia	2	spring	
21772	1		Landrace	Russia	2	spring	
21849	1	DZ02-547	Landrace	Ethiopia	2	spring	
21873	1	Effendi	Cultivar	Netherlands	2	spring	
22336	1	Dempiar	Cultivar	Australia	2	spring	
24723	1	Prishimskij	Cultivar	Kazakhstan	2	spring	
25078	1	Tlaxcala	Cultivar	Mexico	6	spring	
25274	1	C.I.9819	Landrace	Ethiopia	2	spring	

Appendix

Table A.14 continued

25283	1	C.I.4922	Landrace	USA	6	spring	
26092	1	-437	Landrace	Uzbekistan	2	spring	
26180	1	Prikumskiy	Cultivar	Russia	2	spring	
26260	1	Olimpiets	Cultivar	Russia	2	spring	
26338	1	Druzhba	Cultivar	Ukraine	2	spring	
26926	1	Hora	Cultivar	Netherlands	2	spring	naked
27594	1	Moskovsii 3	Cultivar	Russia	2	spring	
27880	1	Orenburgskij 11	Cultivar	Russia	2	spring	
28239	1		Landrace	Uzbekistan	6	spring	
29192	1	Diamond	Cultivar	Canada	6	spring	naked
29277	1	Perun	Cultivar	Czech	2	spring	
29345	1		Landrace	Russia	2	spring	
29438	1	Prejiya	Cultivar	Ukraine	2	spring	
29496	1	Nutans	Cultivar	Russia	2	spring	
29614	1	Britta	Cultivar	Sweden	2	spring	
29651	1	3170 1/21H5/2/7	Cultivar	Russia	2	spring	
29696	1	Jennifer	Cultivar	France	2	winter	
29723	1	Rus'	Cultivar	Russia	2	spring	
29967	1	Kira	Cultivar	Germany	2	winter	
29977	1	Moskovskii 3/125	Cultivar	Russia	2	spring	
30013	1	C.I.11046	Landrace	Peru	6	spring	
30032	1	UC 603	Cultivar	USA	6	spring	
30120	1	Omskii 88	Cultivar	Russia	2	spring	
30162	1	Belaris	Cultivar	France	2	spring	
30163	1	Dominique	Cultivar	France	2	spring	
30292	1	Onslow	Cultivar	Australia	2	spring	
30313	1	Ethiopia AB-9	Cultivar	Ethiopia	2	spring	naked
30320	1	Obruk 86	Cultivar	Turkey	2	spring	
30351	1	C.I. 11104 Lan	Landrace	Peru	6	spring	
30353	1	Pallidum	Landrace	Peru	6	spring	
30366	1	Galaktika	Cultivar	Ukraine	2	spring	
30432	1	WW-7201	Cultivar	Sweden	2	spring	
30453	1	Zernogradskij 813	Cultivar	Russia	2	spring	
30461	1	Viiivi	Cultivar	Finland	2	spring	
30479	1	Novosadski 501	Cultivar	Yugoslavia	2	winter	
30562	1	Chelyabinskij 96	Cultivar	Russia	2	spring	
30591	1	Rahat	Cultivar	Russia	2	spring	
30617	1	KM-1485-1475	Cultivar	Czech	2	spring	naked
30721	1	Omskij 90	Cultivar	Russia	2	spring	
30927	1	Pejas	Cultivar	Czech	2	spring	
18760b	1	C.I.4407-1,Tifang	Landrace	USA	6	spring	black
NDB112	1	C.I. 11531 NDB 112	Landrace	USA	6	spring	

^a Accessions in bold were resistant against *P. teres* f. *teres* and *B. sorokiniana*

Contributions to meetings and conferences

Oral presentations

Novakazi F, Anisimova A, Afanasenko O, Kopahnke D, Ordon F, 2017. **Identification of QTL for resistance to *Pyrenophora teres f. teres* and *Cochliobolus sativus* in Barley employing Genome Wide Association Studies**. In: Book of Abstracts: 2nd International Workshop on Barley Leaf Diseases, April 5-7, 2017, Institut Agronomique et Vétérinaire Hassan-II, Rabat, Morocco, 3.

Novakazi F, Anisimova A, Afanasenko O, Kopahnke D, Ordon F, 2016. **Identification of genes for resistance against *Pyrenophora teres f. teres* and *Cochliobolus sativus* employing genome-wide association studies**. In: JKI (Hrsg.): 9th Young Scientists Meeting 2016, 9th – 11th November in Quedlinburg - Abstracts - (Berichte aus dem Julius Kühn-Institut 186), Quedlinburg, 18.

Novakazi F, Anisimova A, Afanasenko O, Kopahnke D, Ordon F, 2016. **Genome wide association studies for resistance to *Pyrenophora teres f. teres* and *Cochliobolus sativus* in barley (*Hordeum vulgare*)**. The IV International Conference on Plant Resistance to Diseases, October 11-13, 2016, St. Petersburg, Pushkin, Russia.

Novakazi F, Kopahnke D, Anisimova A, Afanasenko O, Ordon F, 2016. **Genomweite Assoziationsstudien zur Resistenz gegenüber *Pyrenophora teres f. teres* in Gerste (*Hordeum vulgare*)**. In: JKI (Hrsg.): 60. Deutsche Pflanzenschutztagung: 20. - 23. September 2016, Martin-Luther-Universität Halle-Wittenberg ; Kurzfassungen der Beiträge (Julius-Kühn-Archiv 454), Quedlinburg, 91-92.

Poster presentations

Novakazi F, Anisimova A, Afanasenko O, Kopahnke D, Ordon F, 2018. **Association mapping for resistance to the net form of net blotch in a diverse barley set**. In: Graner, A. (ed.): Book of Abstracts: GPBC 2018 - German Plant Breeding Conference, 28.02.-02.03.2018, HKK Hotel, Wernigerode - Leveraging the value of genomic information, 88.

Novakazi F, Anisimova A, Afanasenko O, Kopahnke D, Ordon F, 2017. **Genome wide association studies for resistance to *Pyrenophora teres f. teres* and *Cochliobolus sativus* in barley (*Hordeum vulgare*)**. In: Stein, N. (Ed.): Book of Abstracts - 5th Quedlinburger Pflanzenzüchtungstage, 18th Kurt von Rümker Vorträge, GPZ Meeting of AG Genomanalyse - Status of translating genomics into application, 32.

Novakazi F, Anisimova A, Afanasenko O, Kopahnke D, Ordon F, 2017. **Employing GWAS for identifying QTL for resistance to *Pyrenophora teres f. teres* and *Cochliobolus sativus* in barley (*Hordeum vulgare*)**. 4th International Symposium on Genomics of Plant Genetic Resources (GPGR4), Giessen, Germany, Sept. 3-7, 2017, P42.

Novakazi F, Anisimova A, Afanasenko O, Kopahnke D, Ordon F, 2017. **Association mapping for resistance to Net Form of Net Blotch (*Pyrenophora teres f. teres*) and Spot Blotch (*Cochliobolus sativus*) in a diverse barley set**. In: JKI (ed.): 10th Young Scientists Meeting 2017, 8th – 10th November in Siebeldingen - Abstracts (Berichte aus dem Julius Kühn-Institut 192), 62.

Ordon F, Novakazi F, Anisimova A, Afanasenko O, Kopahnke D, 2016. **Genome wide association studies for resistance to *Pyrenophora teres f. teres* and *Cochliobolus sativus* in barley (*Hordeum vulgare*)**. The 12th International Barley Genetics Symposium, June 26-30, 2016, Minneapolis-St. Paul, Minnesota, United States of America, Poster: 138.

Novakazi F, Anisimova A, Afanasenko O, Kopahnke D, Ordon F, 2015. **Resistance of *Hordeum vulgare* against *Pyrenophora teres f. teres***. XVIII. International Plant Protection Congress - Mission possible: food for all through appropriate plant protection, 24-27 August 2015, Berlin, Germany - Abstracts, 413.

Acknowledgement

This project was part of a cooperation between the Institute of Resistance Research and Stress Tolerance at the Julius Kuehn-Institute and the All-Russian Research Institute of Plant Protection and was funded by the Deutsche Forschungsgemeinschaft (DFG; OR 72/11-1) and the Russian Foundation for Basic Research (15-54-12365 NNIO_a).

I would like to thank Prof. Frank Ordon for giving me the opportunity to pursue my PhD on this subject, for his guidance and support and the many opportunities to attend national and international conferences and meetings, which have greatly contributed to expanding my knowledge and professional network.

I would also like to thank my project partner Prof. Olga Afanasenko, who was in charge of field trials in Russia and provided not only important data, but also support, knowledge and valuable comments to the manuscripts. The same gratitude goes towards Dr. Gregory Platz, who agreed to join the collaboration and conduct field and greenhouse trials in Australia, which greatly improved the quality of the research.

My thanks go to Prof. Rod Snowdon for the supervision at the Justus-Liebig-University in Gießen, and the valuable input to the manuscripts.

Many thanks go to Tanja Zahn for the technical assistance and conduction of the KASP analysis, even though most of the data she generated were not used for this thesis. I always enjoyed working with you and especially our breakfast “group meetings” on the terrace of the JKI.

My deepest gratitude goes to Heike Lehnert, without whom, I feel, I would not have been able to conduct the statistical analysis as well as the GWAS. At least it would have been much harder without your help. Thank you so much for always taking the time, being so patient and explaining for the tenth time that my GWAS run is not working because of errors in the input files. I cannot thank you enough!

I would also like to thank Kai Voss-Fels for explaining LD decay and how to calculate it, as well as for taking the time to answer all my questions, which at times popped up almost every day.

Many thanks go to Britta, Caroline, Sandra and Sarah. I am very glad we all ended up in the same office! Thank you all for your friendship and support.

I would like to thank Helge for being there for me, and providing board and lodge during the writing process of this thesis.

Lastly, a big thank you goes to my parents for always supporting and being there for me whenever I need them!

Erklärung

gemäß der Promotionsordnung des Fachbereichs 09 vom 07. Juli 2004 § 17 (2)

„Ich erkläre: Ich habe die vorgelegte Dissertation selbständig und ohne unerlaubte fremde Hilfe und nur mit den Hilfen angefertigt, die ich in der Dissertation angegeben habe.

Alle Textstellen, die wörtlich oder sinngemäß aus veröffentlichten Schriften entnommen sind, und alle Angaben, die auf mündlichen Auskünften beruhen, sind als solche kenntlich gemacht.

Bei den von mir durchgeführten und in der Dissertation erwähnten Untersuchungen habe ich die Grundsätze guter wissenschaftlicher Praxis, wie sie in der „Satzung der Justus-Liebig-Universität Gießen zur Sicherung guter wissenschaftlicher Praxis“ niedergelegt sind, eingehalten.“

Rostock, den

